

CARMENES input catalogue of M dwarfs

I. Low-resolution spectroscopy with CAFOS

F. J. Alonso-Floriano¹, J. C. Morales^{2,3}, J. A. Caballero⁴, D. Montes¹, A. Klutsch^{5,1}, R. Mundt⁶, M. Cortés-Contreras¹, I. Ribas², A. Reiners⁷, P. J. Amado⁸, A. Quirrenbach⁹, and S. V. Jeffers⁷

¹ Departamento de Astrofísica y Ciencias de la Atmósfera, Facultad de Ciencias Físicas, Universidad Complutense de Madrid, 28040 Madrid, Spain, e-mail: fjalonso@fis.ucm.es

² Institut de Ciències de l’Espai (CSIC-IEEC), Campus UAB, Facultat Ciències, Torre C5 - parell - 2^a, 08193 Bellaterra, Barcelona, Spain

³ LESIA-Observatoire de Paris, CNRS, UPMC Univ. Paris 06, Univ. Paris-Diderot, 5 Pl. Jules Janssen, 92195 Meudon Cedex, France

⁴ Departamento de Astrofísica, Centro de Astrobiología (CSIC-INTA), PO Box 78, 28691 Villanueva de la Cañada, Madrid, Spain

⁵ INAF - Osservatorio Astrofisico di Catania, via S. Sofia 78, 95123 Catania, Italy

⁶ Max-Planck-Institut für Astronomie, Königstuhl 17, 69117 Heidelberg, Germany

⁷ Institut für Astrophysik, Friedrich-Hund-Platz 1, 37077 Göttingen, Germany

⁸ Instituto de Astrofísica de Andalucía (CSIC), Glorieta de la Astronomía s/n, 18008 Granada, Spain

⁹ Landessternwarte, Zentrum für Astronomie der Universität Heidelberg, Königstuhl 12, 69117 Heidelberg, Germany

Received 4 February 2015; accepted 18 February 2015

ABSTRACT

Context. CARMENES is a stabilised, high-resolution, double-channel spectrograph at the 3.5 m Calar Alto telescope. It is optimally designed for radial-velocity surveys of M dwarfs with potentially habitable Earth-mass planets.

Aims. We prepare a list of the brightest, single M dwarfs in each spectral subtype observable from the northern hemisphere, from which we will select the best planet-hunting targets for CARMENES.

Methods. In this first paper on the preparation of our input catalogue, we compiled a large amount of public data and collected low-resolution optical spectroscopy with CAFOS at the 2.2 m Calar Alto telescope for 753 stars. We derived accurate spectral types using a dense grid of standard stars, a double least-squares minimisation technique, and 31 spectral indices previously defined by other authors. Additionally, we quantified surface gravity, metallicity, and chromospheric activity for all the stars in our sample.

Results. We calculated spectral types for all 753 stars, of which 305 are new and 448 are revised. We measured pseudo-equivalent widths of H α for all the stars in our sample, concluded that chromospheric activity does not affect spectral typing from our indices, and tabulated 49 stars that had been reported to be young stars in open clusters, moving groups, and stellar associations. Of the 753 stars, two are new subdwarf candidates, three are T Tauri stars, 25 are giants, 44 are K dwarfs, and 679 are M dwarfs. Many of the 261 investigated dwarfs in the range M4.0–8.0 V are among the brightest stars known in their spectral subtype.

Conclusions. This collection of low-resolution spectroscopic data serves as a candidate target list for the CARMENES survey and can be highly valuable for other radial-velocity surveys of M dwarfs and for studies of cool dwarfs in the solar neighbourhood.

Key words. stars: activity – stars: late-type – stars: low-mass

1. Introduction

The *Calar Alto high-Resolution search for M dwarfs with Exoearths with Near-infrared and optical Échelle Spectrographs* (hereafter CARMENES¹) is a next-generation instrument close to completion for the Zeiss 3.5 m Calar Alto telescope, which is located in the Sierra de Los Filabres, Almería, in southern Spain, at a height of about 2200 m (Sánchez et al. 2007, 2008). CARMENES is the name of used for the instrument, the consortium of 11 German and Spanish institutions that builds it, and of the scientific project to be carried out during guaranteed time observations. The instrument consists of two separated, highly stable, fibre-fed spectrographs covering the wavelength ranges from 0.55 to 0.95 μm and from 0.95 to 1.70 μm at spectral resolution $R \approx 82\,000$, each of which shall perform high-accuracy radial-velocity measurements with long-term stability of $\sim 1 \text{ m s}^{-1}$ (Quirrenbach et al. 2010, 2012, 2014, and references therein; Amado et al. 2013). First light is scheduled for the sum-

mer of 2015, followed by the commission of the instrument in the second half of that year.

The main scientific objective for CARMENES is the search for very low-mass planets (i.e., super- and exo-earths) orbiting mid- to late-M dwarfs, including a sample of moderately active M-dwarf stars. Dwarf stars of M spectral type have effective temperatures between 2300 and 3900 K (Kirkpatrick et al. 2005; Rajpurohit et al. 2013). For stars with ages greater than that of the Hyades, of about 0.6 Ga, these effective temperatures translate in the main sequence into a mass interval from 0.09 to 0.55 M_{\odot} , approximately (Baraffe et al. 1998; Chabrier et al. 2000; Allard et al. 2011). Of particular interest is the detection of very low-mass planets in the stellar habitable zone, the region around the star within which a planet can support liquid water (Kasting et al. 1993; Joshi et al. 1997; Lammer et al. 2007; Tarter et al. 2007; Scalo et al. 2007). In principle, the lower the mass of a host star, the higher the radial-velocity amplitude velocity induced (i.e., K_{star} is proportional to $M_{\text{planet}} a^{-1/2} (M_{\text{star}} + M_{\text{planet}})^{-1/2} \approx (a M_{\text{star}})^{-1/2}$ when $M_{\text{star}} \gg$

¹ <http://carmenes.caha.es> – Pronunciation: /kar’-men-es/

M_{planet}). In addition, the lower luminosity of an M dwarf with respect to a star of earlier spectral type causes its habitable zone to be located very close to the host star, which makes detecting habitable planets around M dwarfs (at ~ 0.1 au) easier than detections around solar-like stars (at ~ 1 au).

From transit surveys with the NASA 0.95 m *Kepler* space observatory, very small planet candidates are found to be relatively more abundant than Jupiter-type candidates as the host stellar mass decreases (Howard et al. 2012; Dressing & Charbonneau 2013, 2015; Kopparapu 2013; Kopparapu et al. 2013). For early-M dwarf stars in the field, some radial-velocity studies have already been carried out (ESO CES, UVES and HARPS by Zechmeister et al. 2009, 2013; CRIRES by Bean et al. 2010; HARPS by Bonfils et al. 2013), but the much-sought value of η_{\oplus} , that is, the relative abundance of Earth-type planets in the habitable zone, is as yet only poorly constrained from radial-velocity data (e.g., $\eta_{\oplus} = 0.41^{+0.54}_{-0.13}$ from Bonfils et al. 2013).

Highly stable, high-resolution spectrographs in the near-infrared currently under construction, such as SPIRou (Artigau et al. 2014), IRD (Kotani et al. 2014), HPF (Mahadevan et al. 2014), and CARMENES, are preferable over visible for targets with spectral types M4 V or later (see Table 1 in Crossfield 2014). This is because the spectral energy distribution of late-M dwarfs approximately peaks at $1.0\text{--}1.2\mu\text{m}$ (Reiners et al. 2010), while HARPS and its copy in the northern hemisphere, HARPS-N, cover the wavelength interval from 0.38 to $0.69\mu\text{m}$. That faintness in the optical is quantitatively illustrated with the tabulated V magnitudes of the brightest M dwarfs in the northern hemisphere (HD 79210/GJ 338 A, HD 79211/GJ 338 B, and HD 95735/GJ 411) at 7.5–7.7 mag, far from the limit of the naked human eye.

The specific advantage of CARMENES is the wide wavelength coverage and high spectral resolution in both visible and near-infrared channels. Simultaneous observation from 0.5 to $1.7\mu\text{m}$ is a powerful tool for distinguishing between genuine planet detections and false positives caused by stellar activity, which have plagued planet searches employing spectrographs with a smaller wavelength coverage, especially in the M-type spectral domain (Reiners et al. 2010; Barnes et al. 2011). A substantial amount of guaranteed time for the completion of the key project is also an asset.

A precise knowledge of the targets is critical to ensure that most of the CARMENES guaranteed time is spent on the most promising targets. This selection involves not only a comprehensive data compilation from the literature, but also summarises our observational effort to achieve new low- and high-resolution optical spectroscopy and high-resolution imaging. The present publication on low-resolution spectroscopy is the first paper of a series aimed at describing the selection and characterisation of the CARMENES sample. We have shown some preliminary results at conferences before that described the input catalogue description and selection (Caballero et al. 2013; Morales et al. 2013), low-resolution spectroscopy (Klutsch et al. 2012; Alonso-Floriano et al. 2013a), high-resolution spectroscopy (Alonso-Floriano et al. 2013b; Passegger et al. 2014), resolved multiplicity (Béjar et al. 2012; Cortés-Contreras et al. 2013), X-rays (Lalitha et al. 2012), exploitation of public databases (Montes et al. 2015), or synergies with *Kepler* K2 (Rodríguez-López et al. 2014). This first item of the CARMENES science-preparation series details the low-resolution optical spectroscopy of M dwarfs with the CAFOS spectrograph at the Zeiss 2.2 m Calar Alto telescope.

Table 1. Completeness and limiting J -band magnitudes per spectral type for the CARMENES input catalogue.

Spectral type	J [mag]	
	Completeness	Limiting
M0.0–0.5 V	7.3	8.5
M1.0–1.5 V	7.8	9.0
M2.0–2.5 V	8.3	9.5
M3.0–3.5 V	8.8	10.0
M4.0–4.5 V	9.3	10.5
M5.0–5.5 V	9.8	11.0
M6.0–6.5 V	10.3	11.5
M7.0–7.5 V	10.8	11.5
M8.0–9.5 V	11.3	11.5

2. CARMENES sample

To prepare the CARMENES input catalogue with the best targets, we systematically collected all published M dwarfs in the literature that fulfilled two simple criteria:

- They had to be observable from Calar Alto with target declinations $\delta > -23$ deg (i.e., zenith distances < 60 deg, air masses at culmination < 2.0).
- They were selected according to late spectral type and brightness. We only catalogued confirmed dwarf stars with an accurate spectral type determination from spectroscopic data (i.e., not from photometry) between M0.0 V and M9.5 V. Additionally, we only compiled the brightest stars of each spectral type. Our database contains virtually all known M dwarfs that are brighter than the completeness magnitudes shown in Table 1, and most of them brighter than the limiting magnitudes. No target fainter than $J = 11.5$ mag is in our catalogue.

We started to fill the CARMENES database with the M dwarfs from the Research Consortium on Nearby Stars at <http://www.recons.org>, which catalogues all known stars with measured astrometric parallaxes that place them within 10 pc (e.g., Henry et al. 1994; Kirkpatrick et al. 1995; Riedel et al. 2014; Winters et al. 2015). The RECONS stellar compilation was next completed with the Palomar/Michigan State University survey catalogue of nearby stars (PMSU – Reid et al. 1995, 2002; Hawley et al. 1996; Gizis et al. 2002). Afterwards, we gave special attention to the comprehensive proper-motion catalogues of Lépine et al. (2003, 2009, 2013) and Lépine & Gaidos (2011), and the “Meeting the Cool Neighbors” series of papers (Cruz & Reid 2002; Cruz et al. 2003, 2007; Reid et al. 2003, 2004, 2008). Table 2 provides the sources of our information on M dwarfs. Until we start our survey at the end of 2015, we will still include some new, particularly bright, late, single, M dwarfs².

As of February 2015, our input catalogue, dubbed CARMENCITA (CARMENES Cool dwarf Information and daTa Archive), contains approximately 2200 M dwarfs. For each target star, we tabulate a number of parameters compiled from the literature or measured by us with new data: accurate astrometry and distance, spectral type, photometry in 20 bands from the ultraviolet to the mid-infrared, rotational, radial, and Galactocentric velocities, H α emission, X-ray count rates and

² Please contribute to the comprehensiveness of our input catalogue by sending an e-mail with suggestions to José A. Caballero, e-mail: caballero@cab.inta-csic.es.

Table 2. Sources of the CARMENES input catalogue.

Source	Reference ^a	Number of stars
The Palomar/MSU nearby star spectroscopic survey	PMSU ^b	676
A spectroscopic catalog of the brightest ($J < 9$) M dwarfs in the northern sky	Lépine et al. 2013	446
G. P. Kuiper's spectral classifications of proper-motion stars	Bidelman 1985	285
An all-sky catalog of bright M dwarfs ^c	Lépine & Gaidos 2011	248
Spectral types of M dwarf stars	Joy & Abt 1974	223
Spectral classification of high-proper-motion stars	Lee 1984	118
Meeting the cool neighbors	RECONS ^d	22
Search for nearby stars among proper... III. Spectroscopic distances of 322 NLTT stars	Scholz et al. 2005	19
New neighbors: parallaxes of 18 nearby stars selected from the LSPM-North catalog	Lépine et al. 2009	13
Near-infrared metallicities, radial velocities and spectral types for 447 nearby M dwarfs	Newton et al. 2014	10

^a Some other publications and meta-archives that we have searched for potential CARMENES targets are Kirkpatrick et al. (1991), Gizis (1997), Gizis & Reid (1997), Gizis et al. (2000b), Henry et al. (2002, 2006), Mochnaki et al. (2002), Gray et al. (2003), Bochanski et al. (2005), Crifo et al. (2005), Lodieu et al. (2005), Scholz et al. (2005), Phan-Bao & Bessell (2006), Reylé et al. (2006), Riaz et al. (2006), Caballero (2007, 2009, 2012), Gatewood & Coban (2009), Shkolnik et al. (2009, 2012), Bergfors et al. (2010), Johnson et al. (2010), Boyd et al. (2011), Irwin et al. (2011), West et al. (2011), Avenhaus et al. (2012), Deacon et al. (2012), Janson et al. (2012, 2014), Frith et al. (2013), Jódar et al. (2013), Malo et al. (2013), Aberasturi et al. (2014), Dieterich et al. (2014), Riedel et al. (2014), Yi et al. (2014), Gaidos et al. (2014), and the DwarfArchive at <http://dwarfarchive.org>.

^b PMSU: Reid et al. 1995, 2002; Hawley et al. 1996; Gizis et al. 2002.

^c With spectral types derived from spectroscopy in this work.

^d RECONS: Henry et al. 1994; Kirkpatrick et al. 1995; Henry et al. 2006; Jao et al. 2011; Riedel et al. 2014; Winters et al. 2015 and references therein.

hardness ratios, close and wide multiplicity data, membership in open clusters and young moving groups, target in other radial-velocity surveys, and exoplanet candidacy (Caballero et al. 2013). The private on-line catalogue, including preparatory science observations (i.e., low- and high-resolution spectroscopy, high-resolution imaging), will become public as a CARMENES legacy.

Of the 2200 stars, we discard all spectroscopic binaries and multiples, and resolved systems with physical or visual companions at less than 5 arcsec to our targets. The size of the CARMENES optical fibres projected on the sky is 1.5 arcsec (Seifert et al. 2012; Quirrenbach et al. 2014), and consequently any companion at less than 5 arcsec may induce real or artificial radial-velocity variations that would contaminate our measurements (Guenther & Wuchterl 2003; Ehrenreich et al. 2010; Guenther & Tal-Or 2010). About 1900 single stars currently remain after discarding all multiple systems.

2.1. CAFOS sample

The aim of our low-resolution spectroscopic observations is twofold: (i) to increase the number of bright, late-M dwarfs in CARMENCITA and (ii) to ensure that the compiled spectral types used for the selection and pre-cleaning are correct. With this double objective in mind, we observed the following:

- High proper-motion M-dwarf candidates from Lépine & Shara (2005) and Lépine & Gaidos (2011) with spectral types with large uncertainties or derived only from photometric colours. Spectral types from $V^* - J$ colours are not suitable for our purposes (Alonso-Floriano et al. 2013a; Mundt et al. 2013; Lépine et al. 2013 – V^* is an average of photographic magnitudes B_J and R_F from the Digital Sky Survey; cf. Lépine & Gaidos 2011). In collaboration with Sébastien Lépine, we observed and analysed an extension of the Lépine & Gaidos (2011) catalogue of high proper-motion candidates brighter than $J = 10.5$ mag. The spectra of stars

brighter than $J = 9.0$ mag were published by Lépine et al. (2013), while most of the remaining fainter ones are published here.

- M dwarf candidates in nearby young moving groups (e.g., Montes et al. 2001; Zuckermann & Song 2004; da Silva et al. 2009; Shkolnik et al. 2012; Gagné et al. 2014; Klutsch et al. 2014), in multiple systems containing FGK-type primaries that are subjects of metallicity studies (Gliese & Jahreiss 1991; Poveda et al. 1994; Gould & Chanamé 2004; Rojas-Ayala et al. 2012; Terrien et al. 2012; Mann et al. 2013; Montes et al. 2013), in fragile binary systems at the point of disruption by the Galactic gravitational field (Caballero 2012 and references therein), and resulting from new massive virtual-observatory searches (Jiménez-Esteban et al. 2012; Aberasturi et al. 2014). Such a broad diversity of sources allowed us to widen the investigated intervals of age, activity, multiplicity, metallicity, and dynamical evolution.
- Known M dwarfs with well-determined spectral types from PMSU (see above) and Lépine et al. (2013). The comparison of these two samples with ours was a sanity check for determining the spectral types (see Sect. 4.1).
- M dwarfs in our input catalogue with uncertain or probably incorrect spectral types based on apparent magnitudes, $r' - J$ colours, and heliocentric distances, including resolved physical binaries. See some examples in Cortés-Contreras et al. (2014).
- Numerous standard stars. For an accurate determination of spectral type and class, we also included approximately 50 stars with well-determined spectral types from K3 to M8 for both dwarf (Johnson & Morgan 1953; Kirkpatrick et al. 1991; PMSU) and giant classes (e.g., Moore & Paddock 1950; Ridgway et al. 1980; Jacoby et al. 1984; García 1989; Keenan & McNeil 1989; Kirkpatrick et al. 1991; Sánchez-Blázquez et al. 2006; Jiménez-Esteban et al. 2012).

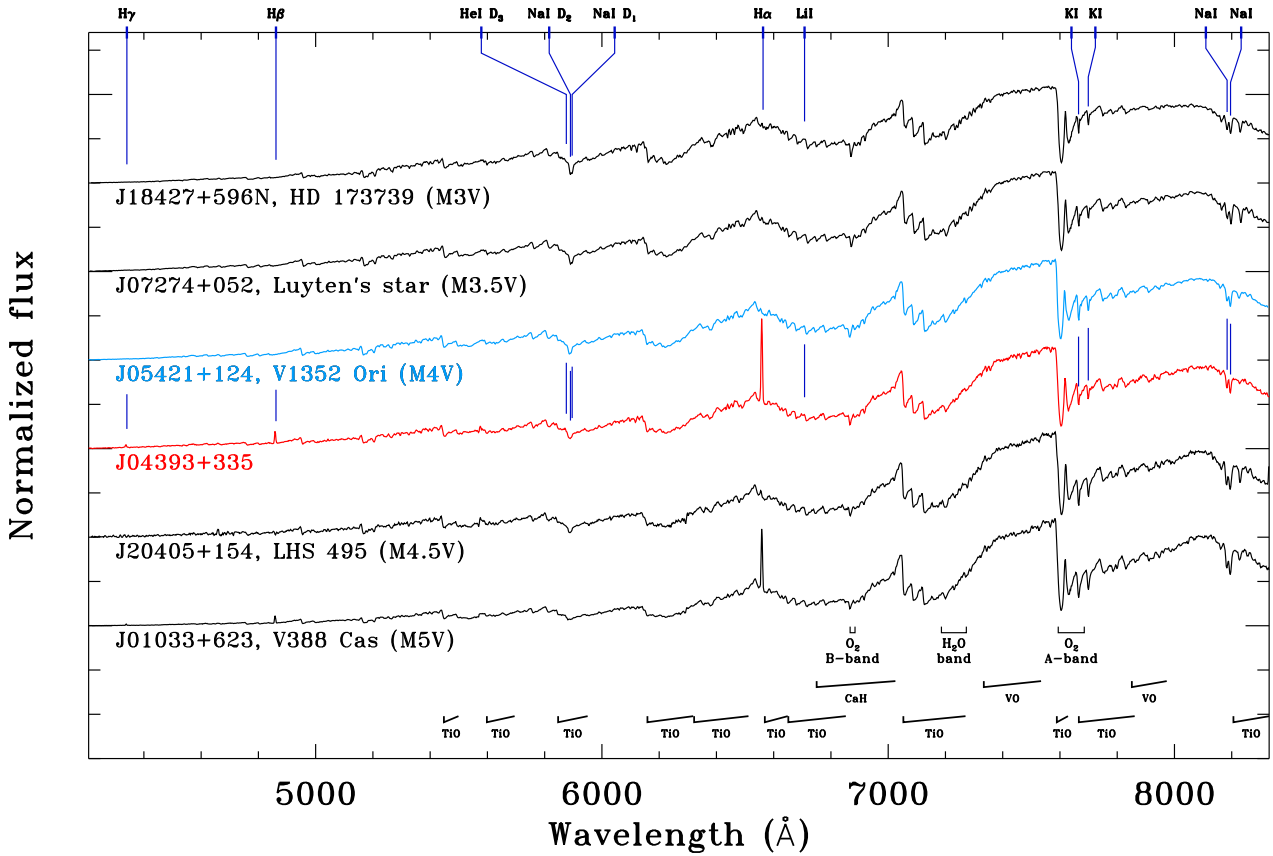


Fig. 1. Six representative CAFOS spectra. From top to bottom, spectra of standard stars with spectral type 1.0 and 0.5 subtypes earlier than the target (black), standard star with the same spectral type as the target (cyan), the target star (red; in this case, J04393+335 – M4.0 V, Simbad name: V583 Aur B), and standard stars with spectral type 0.5 and 1.0 subtypes later than the target (black). We mark activity-, gravity-, and youth-sensitive lines and doublets at the top of the figure ($H\gamma$, $H\beta$, $He\text{ I }D_3$, $Na\text{ I }D_2$ and D_1 , $H\alpha$, $Li\text{ I}$, $K\text{ I}$, and $Na\text{ I}$, from left to right) and molecular absorption bands at the bottom. Note the three first lines of the Balmer series in emission of the target star.

3. Observations and analysis

3.1. Low-resolution spectroscopic data

Observations were secured with the Calar Alto Focal reductor and Spectrograph (CAFOS) mounted on the Ritchey-Chrétien focus of the Zeiss 2.2 m Calar Alto telescope (Meisenheimer 1994). We obtained more than 900 spectra of 745 targets during 38 nights over four semesters from 2011 November to 2013 April. All observations were carried out in service mode with the G-100 grism, which resulted in a useful wavelength coverage of 4200–8300 Å at a resolution $\mathcal{R} \sim 1500$. Exposure times ranged from shorter than 1 s to 1 h. The longest exposures were split into up to four sub-exposures. On some occasions, another star fell in the slit aperture (usually the primary of a close multiple system containing our M-dwarf candidate main target). We also added the 13 red dwarfs and giants observed in 2011 March by Jiménez-Esteban et al. (2012), which made a total of 758 targets.

We reduced the spectra using typical tasks within the IRAF environment. The reduction included bias subtraction, flat fielding, removal of sky background, optimal aperture extraction, wavelength calibration (with Hg-Cd-Ar, He, and Rb lamps), and instrumental response correction. For the latter, we repeatedly observed the spectrophotometric standards G 191–B2B (DA0.8), HD 84937 (sdF5), Feige 34 (sdO), BD+25 3941 (B1.5 V), and BD+28 421 (sdO) at different air masses. In the end, we only

used the spectra with the highest signal-to-noise ratio of the hot subdwarf Feige 34, which gave the best-behaved instrumental response correction. We extracted all traces in the spectra, including those of other stars in the slit aperture. We did not remove telluric absorption lines from the spectra that were due to the variable meteorological conditions during two years of observation (see Sect. 3.2.2). All our spectra had a signal-to-noise ratio higher than 50 near the $H\alpha \lambda 6562.8$ Å line, which together with the wide wavelength coverage allowed us to make a comprehensive analysis and to measure numerous spectral indices and activity indicators.

We list in Table A.1 the 753 observed K and M dwarf and giant candidates according to identification number, our CARMENCITA identifier, discovery name, Gliese or Gliese & Jahreß number, J2000.0 coordinates and J -band magnitude from the Two-Micron All-Sky Survey (Skrutskie et al. 2006), observation date, and exposure time. The five stars not tabulated are the spectrophotometric standards.

In Table A.1, our CARMENCITA identifier follows the nomenclature format ‘Karmn JHHMMm±DDd(X)’, where ‘Karmn’ is the acronym, ‘m’ and ‘d’ in the sequence are the truncated decimal parts of a minute or degree of the corresponding equatorial coordinates for the standard equinox of J2000.0 (*IRAS* style for right ascension, PKS quasar style for declination), and X is an optional letter (N, S, E, W) to distinguish be-

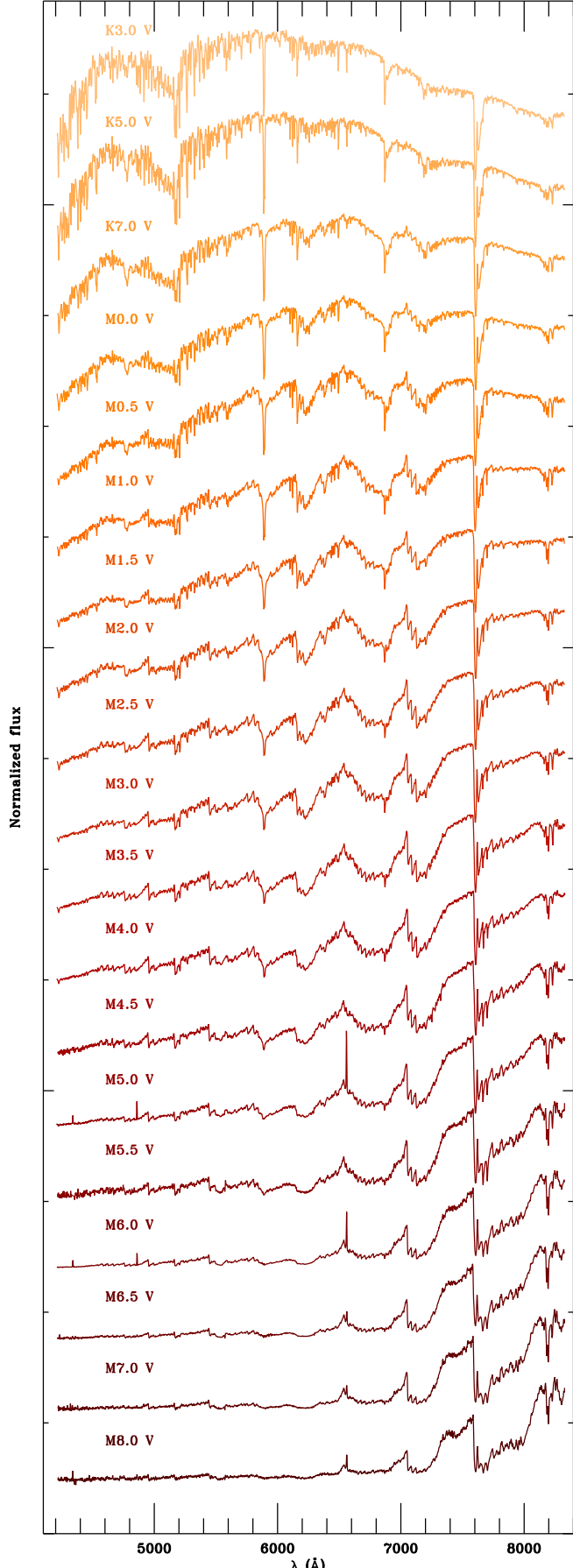


Fig. 2. CAFOS spectra of our prototype stars. From top to bottom, K3 V, K5 V, K7 V, M0.0–7.0 V in steps of 0.5 subtypes, and M8.0 V.

Table 3. Standard and prototype stars^a.

SpT	Karmn	Name
M0.0 V	J09143+526	HD 79210
	J07195+328	BD+33 1505
	J09144+526	HD 79211
	J18353+457	BD+45 2743
M0.5 V	J04329+001S	LP 595–023
	J22021+014	HD 209290
	J00183+440	GX And
	J05151–073	LHS 1747
M1.0 V	J11054+435	BD+44 2051A
	J05314–036	HD 36395
	J00136+806	G 242–048
	J01026+623	BD+61 195
M1.5 V	J11511+352	BD+36 2219
	J08161+013	GJ 2066
	J03162+581N	Ross 370 B
	J03162+581S	Ross 370 A
M2.0 V	J11421+267	Ross 905
	J10120–026 AB	LP 609–071
	J19169+051N	V1428 Aql
	J21019–063	Wolf 906
M2.5 V	J18427+596N	HD 173739
	J17364+683	BD+68 946
	J22524+099	σ Peg B
	J07274+052	Luyten's star
M3.0 V	J17199+265	V647 Her
	J17578+046	Barnard's star
	J18427+596S	HD 173740
	J05421+124	V1352 Ori
M3.5 V	J04308–088	Koenigstuhl 2 A
	J06246+234	Ross 64
	J10508+068	EE Leo
	J20405+154	G 144–025
M4.0 V	J04153–076	o² Eri C
	J16528+610	GJ 625
	J17198+265	V639 Her
	J01033+623	V388 Cas
M4.5 V	J16042+235	LSPM J1604+2331
	J23419+441	HH And
	J02022+103	LP 469–067
	J21245+400	LSR J2124+4003
M5.0 V	J10564+070	CN Leo
	J07523+162	LP 423–031
	J16465+345	LP 276–022
	J08298+267	DX Cnc
M5.5 V	J09003+218	LP 368–128
	J10482–113	LP 731–058
	J16555–083	V1054 Oph D (vB 8)
	J02530+168	Teegarden's star
M6.0 V	J19169+051S	V1298 Aql (vB 10)

^a Prototype stars are marked with an asterisk.

tween physical or visual pairs with the same HHMMm±DDd sequence within CARMENCITA. We use the discovery name for every target, except for M dwarfs with variable names (e.g., EZ PSc, GX And, V428 And) or those that are physical companions to bright stars (e.g., BD–00 109 B, η Cas B, HD 6440 B). We associate for the first time many X-ray events with active M dwarfs (e.g., Lalitha et al. 2012; Montes et al. 2015). In these cases, we use the precovery³ Einstein 2E or ROSAT RX/1RXS

³ “Pre-discovery recovery”.

event identifications instead of the names given by the proper-motion survey that recovered the stars.

Additionally, we always indicate whether the star is a known close binary or triple unresolved in our spectroscopic data (with ‘AB’, ‘BC’, ‘ABC’). There are 75 such close multiple systems in our sample (70 double and 5 triple), of which the widest unresolved pair is J09045+164 AB (BD+16 1895), with $\rho \approx 4.1$ arcsec. A comprehensive study on the multiplicity of M dwarfs in CARMENCITA, including spectral-type estimate of companions from magnitude differences in high-resolution imaging data, will appear in a forthcoming paper of this series (preliminary data were presented in Cortés-Contreras et al. 2015).

3.2. Spectral typing

We followed two widely used spectral classification schemes that require an accurate, wide grid of reference stars. The first strategy relies on least-squares minimisation and best-fitting to spectra of the standard stars, while the second scheme uses spectral indices that quantify the strength of the main spectral features in M dwarfs, notably molecular absorption bands (again, preliminary data were presented in Klutsch et al. 2012 –least-squares minimisation– and Alonso-Floriano et al. 2013a –spectral indices).

Before applying the two spectral-typing strategies, we normalised our spectra by dividing by the observed flux at 7400 Å. We also corrected for spatial distortions at the reddest wavelengths (with $R \sim 1500$, there is no need for a stellar radial-velocity correction). For that, we shifted our spectra until the K I $\lambda\lambda 7664.9, 7699.0$ Å doublet was placed at the laboratory wavelengths. This correction, often of 1–2 Å, was critical for the definition of spectral indices, some of which are very narrow.

3.2.1. Spectral standard and prototype stars

We list the used standard stars in Table 3 (see also Sect. 3.2.4), most of which were taken from Kirkpatrick et al. (1991) and PMSU (Table 2). Our intention was to provide one prototype star and up to four reference stars per half subtype, but this was not always possible, especially at the latest spectral types. The prototype stars, shown in Fig. 2, are the brightest, least active reference stars that have spectra with the highest signal-to-noise ratio, and that do not deviate significantly from the general trend during fitting. In Table 3, the first star of each subtype is the prototype for that subtype. In the case of standard stars with different reported spectral types in the bibliography (with maximum differences of 0.5 subtypes), we chose the value that gave us less scatter in our fits.

We also used three K dwarfs from Kirkpatrick et al. (1991), not listed in Table 3, to extend our grid of standard stars towards warmer effective temperatures. The three K-dwarf standard stars are HD 50281 (K3 V), 61 Cyg A (K5 V), and η Cas B (K7 V). The standard star LP 609–071 AB is a close binary composed of an M2.5 V star and a faint companion separated by $\rho = 0.18 \pm 0.02$ arcsec (Delfosse et al. 1999). With $\Delta K = 0.95 \pm 0.05$ mag, the faint companion flux barely affects the primary spectrum in the optical.

3.2.2. Best-match and χ^2_{\min} methods

Before any least-squares minimisation, we discarded five narrow (20–30 Å) wavelength ranges influenced by activity indicar-

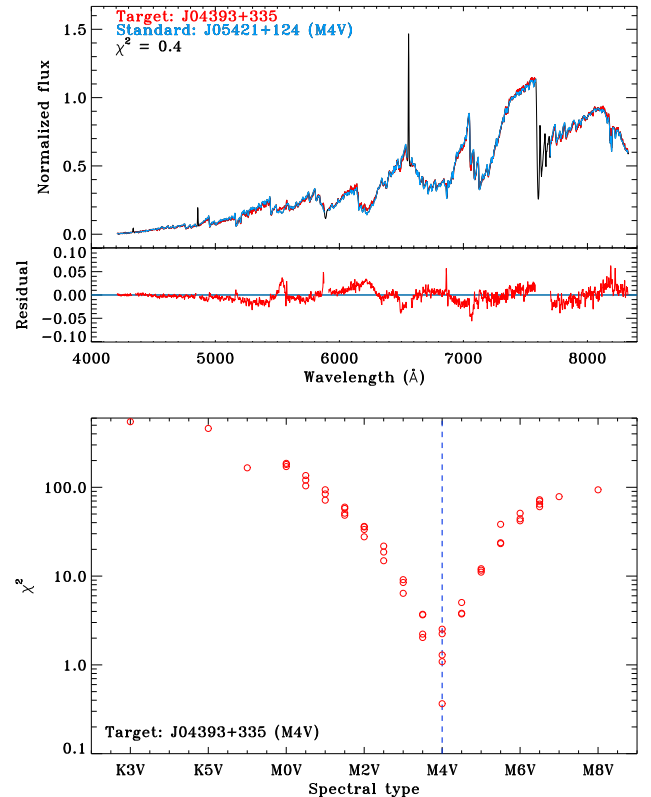


Fig. 3. Spectral typing of J04393+335 with best-match and χ^2_{\min} methods. *Top panel:* best-match. CAFOS normalised spectra of the target star and of the standard star that fits best (top) and the difference (bottom). *Bottom panel:* χ^2_{\min} . Values of χ^2 as a function of the spectral type (open red circles). The vertical dashed line marks the spectral type at the lowest χ^2 value. Note the logarithmic scale in the Y axis.

tors ($H\alpha$, $H\beta$, $H\gamma$, and the Na I doublet – Fraunhofer C, F, and G’ lines) and by strong telluric lines (O₂ band around 7594 Å –Fraunhofer A line). Next, in the full remaining spectral range, we compared the normalised spectrum of every target star with those of all our standard stars in Table 3 and computed a χ^2 value for each fit. In the best-match method, we assigned the spectral type of the standard star that best fitted our target spectrum (i.e., with the lowest χ^2 value); in the χ^2_{\min} method, we assigned the spectral type that corresponded to the minimum of the curve resulting from the (sixth-order) polynomial fit of all the χ^2 –spectral type pairs. As expected, the best-match and χ^2_{\min} methods give the same result in most cases. In the representative case shown in Figs. 1 and 3, the target dwarf has an M4.0 V spectral type using both the best match and χ^2_{\min} methods.

3.2.3. Spectral indices

The spectral indices methodology for spectral typing is based on computing flux ratios at certain wavelength intervals in low-resolution spectra (e.g., Kirkpatrick et al. 1991; Reid et al. 1994; Martín et al. 1996, 1999). In the present analysis, we compiled 31 spectral indices defined in the literature to determine spectral types of late-K dwarfs and M dwarfs that occur in the useable wavelength interval of our CAFOS spectra. In general, a spectral index I_i is defined by the ratio of numerator and denominator fluxes (i.e., $I_i = F_{i,\text{num}} / F_{i,\text{den}}$). Table 4 lists the 31 wavelength

Table 4. Spectral indices used in this work.

Index	$\Delta\lambda_{\text{num}}$ [Å]	$\Delta\lambda_{\text{den}}$ [Å]	Reference
CaOH	6230:6240	6345:6354	Reid et al. 1995
CaH 1	6380:6390	Σ 6345:6355, 6410:6420	Reid et al. 1995
I2 (CaH)	6510:6540	6370:6400	Martín & Kun 1996
I3 (TiO)	6510:6540	6660:6690	Martín & Kun 1996
H α	6560:6566	6545:6555	Reid et al. 1995
TiO 1	6718:6723	6703:6708	Reid et al. 1995
CaH 2	6814:6846	7042:7046	Reid et al. 1995
CaH 3	6960:6990	7042:7046	Reid et al. 1995
TiO-7053	7000:7040	7060:7100	Martín et al. 1999
Ratio A (CaH)	7020:7050	6960:6990	Kirkpatrick et al. 1991
TiO-7140	7015:7045	7125:7155	Wilking et al. 2005
PC1	7030:7050	6525:6550	Martín et al. 1996
CaH Narr	7044:7049	6972.5:6977.5	Shkolnik et al. 2009
TiO 2	7058:7061	7043:7046	Reid et al. 1995
TiO 3	7092:7097	7079:7084	Reid et al. 1995
TiO 5	7126:7135	7042:7046	Reid et al. 1995
TiO 4	7130:7135	7115:7120	Reid et al. 1995
VO-a	Σ 7350:7370, 7550:7570	7430:7470	Kirkpatrick et al. 1999
VO	Σ α 7350:7400, β 7510:7560 ^a	7420:7470	Kirkpatrick et al. 1995
Ratio B (Ti 1)	7375:7385	7353:7363	Kirkpatrick et al. 1991
VO-7434	7430:7470	7550:7570	Hawley et al. 2002
PC2	7540:7580	7030:7050	Martín et al. 1996
VO 1	7540:7580	7420:7460	Martín et al. 1999
TiO 6	7550:7570	7745:7765	Lépine et al. 2003
VO-b	Σ 7860:7880, 8080:8100	7960:8000	Kirkpatrick et al. 1999
VO 2	7920:7960	8130:8150	Lépine et al. 2003
VO-7912	7990:8030	7900:7940	Martín et al. 1999
Ratio C (Na 1)	8100:8130	8174:8204	Kirkpatrick et al. 1991
Color-M	8105:8155	6510:6560	Lépine et al. 2003
Na-8190	8140:8165	8173:8210	Hawley et al. 2002
PC3	8235:8265	7540:7580	Martín et al. 1996

^a $\alpha = 0.5625$, $\beta = 0.4375$.

intervals of fluxes in the numerator and denominator, $\Delta\lambda_{\text{num}}$ and $\Delta\lambda_{\text{den}}$, and corresponding reference for each index. Some flux wavelength intervals are the linear combination of two subintervals (CaH 1, VO-a, VO-b) or, in the case of the VO index, a nonlinear combination. Additionally, there are wavelength intervals of fluxes in the numerator that are either redder and bluer than the one in the denominator, which translates into different slopes in the index–spectral type relations. Of the 31 tabulated indices, nine are related to TiO features, seven to VO, six to CaH, three to the “pseudo-continuum” (i.e., relative absence of features), and the rest to H and neutral metallic lines (Ti, Na).

For every star observed with CAFOS, we computed the stellar numerator and denominator fluxes using an automatic trapezoidal integration procedure. When all indices were available, we plotted all spectral index vs. spectral type diagrams for the standard stars listed in Table 3 and fitted low-order polynomials to the data points. Although some spectral indices allowed linear (e.g., I2, Ratio B) or parabolic fits, most of the fits were to cubic polynomials of the form $\text{SpT}(i) = a + b i + c i^2 + d i^3$, where i was the index. In all cases, we checked our diagrams and fits with those in the original papers and found no significant differences (of less than 0.5 subtypes). We also took special care in defining the range of application of our fits in spectral type. The different shapes of fitting curves, ranges of application, and internal dispersion of the data points are illustrated in Fig. 4.

Some indices are sensitive not only to spectral type (i.e., effective temperature), but also to surface gravity (e.g., I2, Ratio A, CaH Narr, Ratio C, Na-8190 – Sect. 4.2), metallicity (e.g., CaOH, CaH 1, CaH 2, CaH 3 – Sect. 4.3), or activity (H α – Sect. 4.4). We identified the spectral indices with the widest range of application and least scatter. Table 5 lists the coefficients of the cubic polynomial fits of the five spectral indices that we eventually chose for spectral typing (note the logarithmic scale of the Color-M index). The spectral index vs. spectral type diagrams of VO-7912 and Color-M are very similar to those of PC, TiO 2, and TiO 5, shown in Fig. 4. All of them are valid from K7 V to M7 V (to M8 V in the case of PC1 and Color-M), while the dispersion of the fits is of about 0.5 subtypes. The TiO 5 has been a widely used index for spectral typing (Reid et al. 1995; Gizis 1997; Seeliger et al. 2011; Lépine et al. 2013) but, to our knowledge, we propose here for the first time to use it with a nonlinear fit.

In Table A.2, we list the values of the five spectral-typing indices of all CAFOS stars together with the CaH 2 and CaH 3 indices that are used to compute the ζ metallicity index (Sect. 4.3) and the pseudo-equivalent width of the H α line (Sect. 4.4).

3.2.4. Adopted spectral types

After applying the best-match and χ^2_{min} methods and using the five spectral-index-type relations in Table 5, we obtained seven

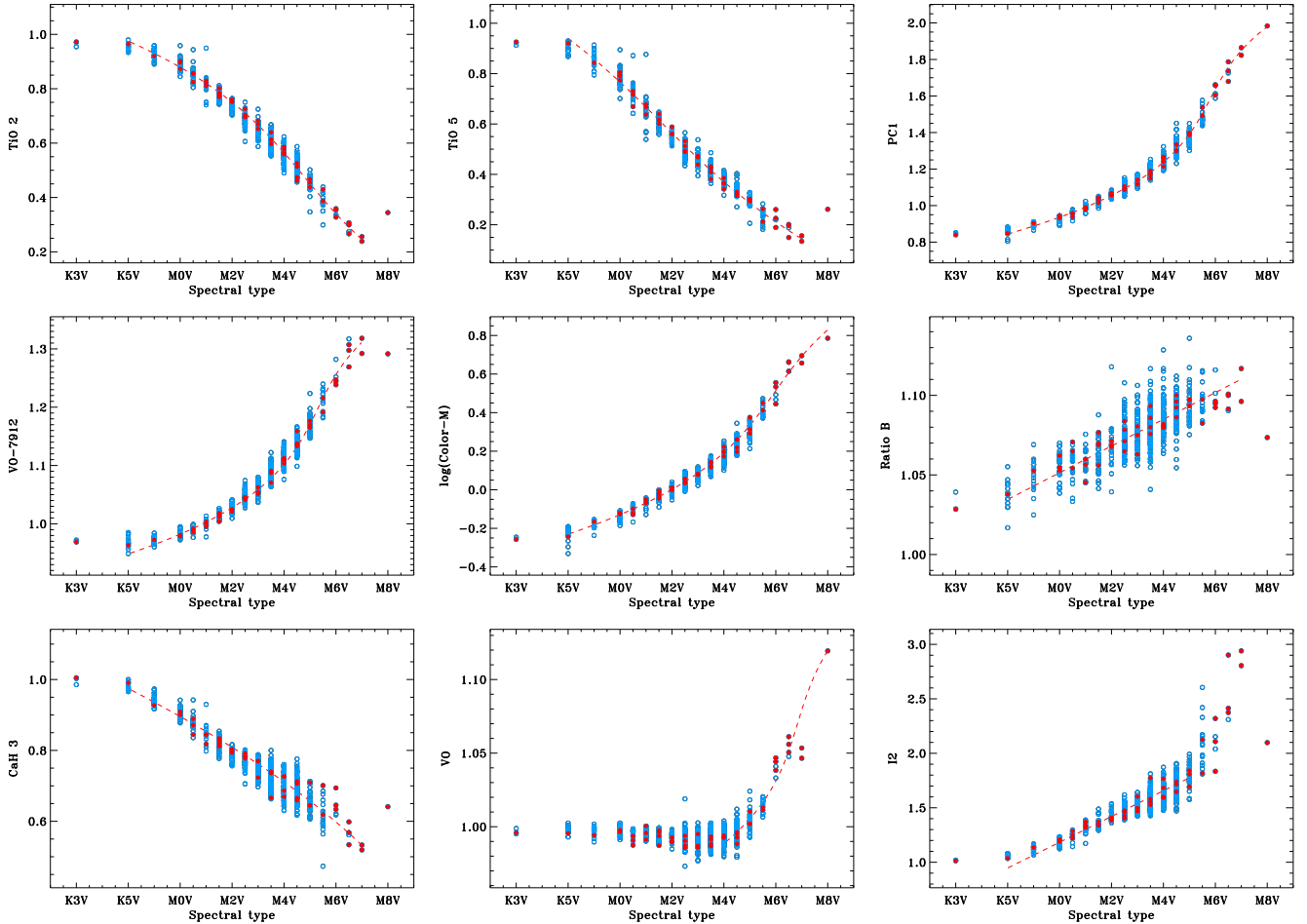


Fig. 4. Nine representative spectral indices as a function of spectral type. Filled (red) circles: standard stars. Open (blue) circles: remaining target stars. Dashed (red) line: fit to straight line, parabola, or cubic polynomial, drawn only in the range of application of the fit. *Top left and middle*: TiO 2 and TiO 5 (Reid et al. 1995), with negative slopes and useable up to M7 V; *top right*: PC1 (Martín et al. 1996), a monotonous spectral indicator from K5 V to M8 V; *centre left and middle*: VO-7912 (Martín et al. 1999) and Color-M (Lépine et al. 2003), two indices very similar to the PC1. Note the logarithmic scale in Color-M; *centre right*: ratio B (Kirkpatrick et al. 1991), sensitive to several stellar parameters and, thus, with a large scatter in the spectral type relation; *bottom left*: CaH 3 (Reid et al. 1995), with a slightly larger scatter than pseudo-continuum or titanium oxide indices, due to metallicity; *bottom middle*: VO (Kirkpatrick et al. 1995), useable only for determining spectral types later than M4 V; *bottom right*: I2 (Martín & Kun 1996), with a linear range of variation from mid-K to mid-M and a sudden increase (or high dispersion) at late-M.

Table 5. Coefficients and standard deviation (in spectral subtypes) of the cubic polynomial fits of the five spectral-typing indices^a.

Index	<i>a</i>	<i>b</i>	<i>c</i>	<i>d</i>	σ
TiO 2	+11.0	-22	+28	-20	0.83
TiO 5	+9.6	-20	+17.0	-9.0	0.57
PC1	-50	+97	-59	+12.4	0.52
VO-7912	-520	+1300	-1070	+300	0.59
Color-M	+1.98	+13.1	-15.6	+10.3	0.53

^a We used the relation $\text{SpT}(i) = a + b i + c i^2 + d i^3$ for the cubic fits. For the Color-M index we used the relation $\text{SpT}(i) = a + b \log i + c (\log i)^2 + d (\log i)^3$.

complementary spectral-type determinations for each star. In Table A.3, we assigned a value between 0.0 and 8.0 in steps of 0.5 to each M spectral subtype for all stars of dwarf luminosity

class (there are no stars later than M8.0 V in our CAFOS sample). In addition, we used the values -2.0 and -1.0 for referring to K5 V and K7 V spectral types (there are no K6, 8, 9 spectral types in the standard K-dwarf classification – Johnson & Morgan 1953; Keenan & McNeil 1989). In some cases, we were able to identify dwarfs earlier than K5 V with the best-match and χ^2_{\min} methods. For giant stars, we only provide a visual estimation (K III, M III) based on the spectral types of well-known giant stars observed with CAFOS.

For all late-K and M dwarfs, we calculated one single spectral type per star based on the information provided by the seven individually determined spectral indices. We used a median of the seven values for cases where they were identical within 0.5 subtypes. To avoid any bias, we carefully checked the original spectra if the spectral types from the best-match and χ^2_{\min} methods and from the spectral indices were different by 0.5 subtypes, or if any spectral type deviated by 1.0 subtypes or more (which occurred very rarely). In these cases, we adopted the spectral type of the closest (visually and in χ^2) standard star. The uncertainty of the adopted spectral types is 0.5 subtype, except for

some odd spectra indicated with a colon (probably young dwarfs or low gravity or subdwarfs of low metallicity; see below).

4. Results and discussion

4.1. Spectral types

Among the 753 investigated stars with adopted spectral types from CAFOS data, there were 23 late-K dwarfs at the K/M boundary (K7 V), 21 early- and intermediate-K dwarfs (K0–5 V), 22 M-type giants (M III), three K-type giants (K III), and one star without class determination (i.e., J04313+241 AB). This left 683 M-type dwarfs (and subdwarfs) in our CAFOS sample.

As shown in Table A.3, we searched for previous spectral type determinations in the literature for the 753 investigated stars (small ‘m’ and ‘k’ denote spectral types estimated from photometry). Taking previous determinations and estimations into account, we derived spectral types from spectra for the first time for 305 stars, and revised typing for most of the remaining 448 stars.

The agreement in spectral typing with previous large spectroscopic surveys of M dwarfs is shown in Fig. 5. The standard deviations of the differences between the spectral types derived by us and by PMSU (with a narrower wavelength interval; 100 stars in common) and by Lépine et al. (2013; 95 stars in common) were 0.55 and 0.38 subtypes, respectively, which are of the order of our internal uncertainty (0.5 subtypes). The standard deviation of the differences between our spectral types and those estimated from photometry by Lépine & Gaidos (2011; 576 stars in common) is larger, of up to 1.32 subtypes. The bias towards later spectral types in Lépine & Gaidos (2011) and the scatter of the spectral type differences is obvious from the bottom panel in Fig. 5. In particular, we measured maximum differences of up to 7 subtypes, by which some late-M dwarf candidates become actual K dwarfs (probably due to the use by Lépine & Gaidos of B_J and R_F from photographic plates for the spectral type estimation; see references in Sect. 2). However, over 93 % of the compared stars have disagreements lower than or equal to 2 subtypes. We emphasize that our CARMENCITA data base is very homogeneous because more than 95 % of the spectral type determinations come from either PMSU, Lépine et al. (2013), or our CAFOS data, which are consistent with each other, as shown above.

Of the 683 CAFOS M-type dwarfs (and subdwarfs), 414 and 106 M dwarfs satisfy our criteria in Table 1 of restrictive J -band spectral type limiting and completeness, respectively. In total, 261 dwarfs have spectral type M4.0 V or later. The brightest, latest of them are being followed-up with high-resolution spectrographs and imagers and with data from the bibliography to identify the most suitable targets for CARMENES (no physical or visual companions at less than 5 arcsec, low $v \sin i$; see forthcoming papers of this series). Furthermore, there are 61 relatively bright ($J < 10.9$ mag) CAFOS stars with spectral types between M5.0 V and M8.0 V that are also suitable targets for any other near-infrared radial-velocity monitoring programmes with the instruments mentioned above (i.e., HPF, SPIRou, IRD).

4.2. Gravity

Table 6 lists the 25 giants observed with CAFOS. Of these, 17 stars have previously been tabulated as M giant standard stars (e.g., Keenan & McNeil 1989; García 1989; Kirkpatrick et al. 1991; Sánchez-Blázquez et al. 2006). They are bright ($J \lesssim 5.0$ mag; down to –1.0 mag in the case of Mirach, β And)

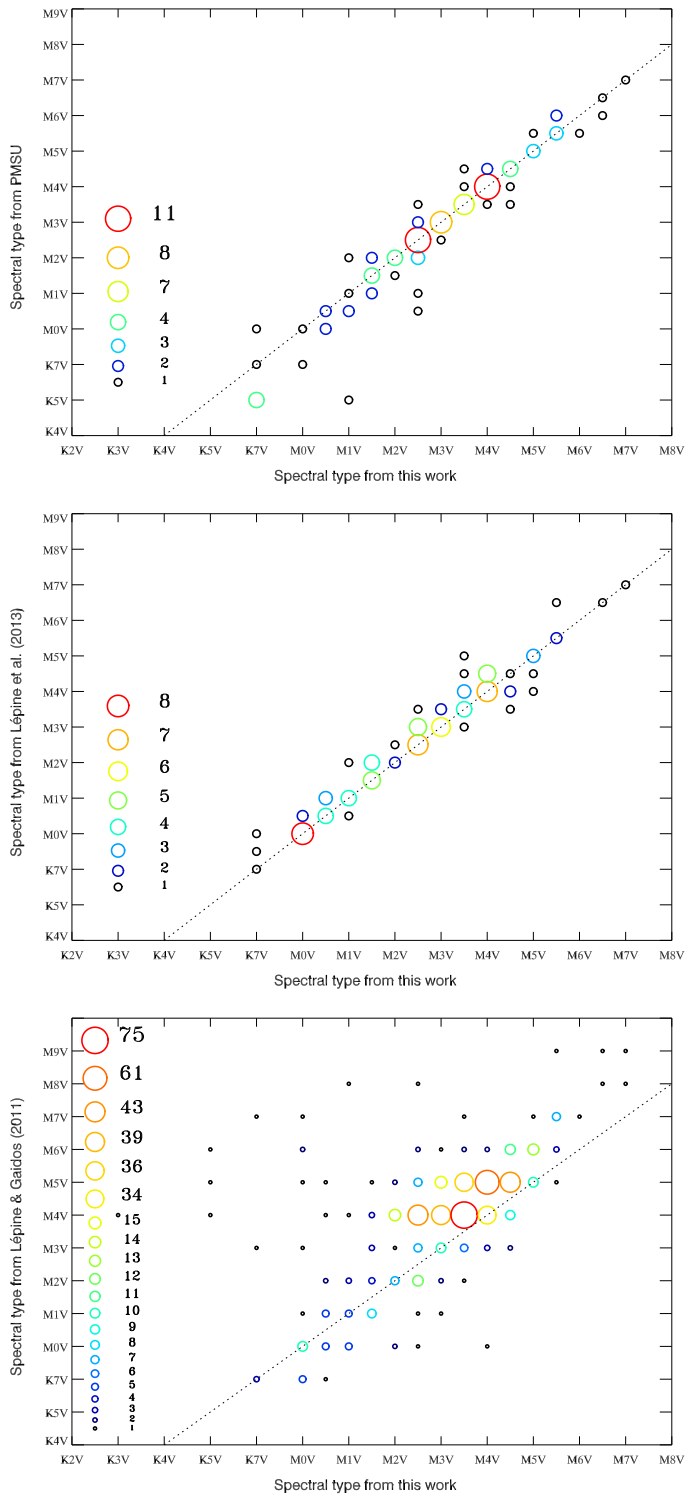


Fig. 5. Spectral type comparison between our results and those from PMSU (top panel), Lépine et al. (2013; middle panel), and Lépine & Gaidos (2011; from $V^* - J$ photometry, bottom panel). The larger a circle, the greater the number of stars on a data point. Dotted lines indicate the one-to-one relationship.

and show the low-gravity spectral features typically found in M giants: faint alkali lines ($K_1 \lambda\lambda 7665, 7699 \text{ \AA}$ and $Na_1 \lambda\lambda 8183, 8195 \text{ \AA}$), a tooth-shaped feature produced by MgH/TiO blend near 4770 Å, and a decrease of CaH in the A-band at

Table 6. Giant stars observed with CAFOS.

Karmn	Name	Giant
J00146+202	χ Peg	Standard
J00367+444	V428 And	Standard
J00502+601	HD 236547	Standard
J01012+571	1RXS J010112.8+570839	New
J01097+356	Mirach	Standard
J02479-124	Z Eri	Standard
J02558+183	ρ^2 Ari	Standard
J03319+492	TYC 3320-337-1	LG11 ^a
J04206-168	DG Eri	Standard
J07420+142	NZ Gem	Standard
J10560+061	56 Leo	Standard
J11018-024	p^2 Leo	Standard
J11201+301	HD 98500	Standard
J11458+065	ν Vir	Standard
J12322+454	BW CVn	Standard
J12456+271	HD 110964	Standard
J12533+466	BZ CVn	Standard
J13587+465	HD 122132	Standard
J17126-099	Ruber 7	JE12 ^b
J17216-171	TYC 6238-480-1	JE12 ^b
J18423-013	Ruber 8	JE12 ^b
J22386+567	V416 Lac	Standard
J23070+094	55 Peg	Standard
J23177+490	8 And	Standard
J23266+453	2MASS J23263798+4521054	Background

^a LG11: Lépine & Gaidos (2011).

^b JE12: Jiménez-Esteban et al. (2012).

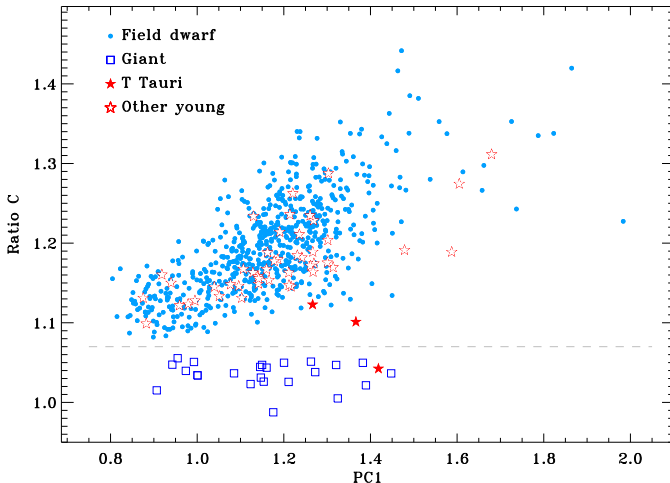


Fig. 6. Ratio C vs. PC1 index-index diagram. The different symbols represent field dwarfs (small dots, blue), giants (open squares, dark blue), Taurus stars (filled stars, red), and other young stars (open stars, red). All giants are below the dashed line at Ratio C = 1.07. The dashed line is the empirical border of the giant star region.

6908–6946 Å with the increase of luminosity (Kirkpatrick et al. 1991; Martín et al. 1999; Riddick et al. 2007; Gray & Corbally 2009). Two other stars, V428 And and HD 236547, are well-known K giant standard stars (Jacoby et al. 1984; García 1989; Kirkpatrick et al. 1991).

Of the other six giant stars in Table 6, three have *J*-band magnitudes of 6.1–6.2 mag and were identified by Jiménez-Esteban et al. (2012) as some of the reddest Tycho-2 stars with proper motions $\mu > 50$ mas a⁻¹, namely Ruber 7, TYC 6238-480-1, and Ruber 8 (which seems to be also one of the brightest metal-poor M giants ever identified). The remaining three giant stars, with faint *J*-band magnitudes between 8.2 and 10.0 mag, are listed below.

- J01012+571 (1RXS J010112.8+570839). It is a previously unknown distant M giant close to the Galactic plane ($b = -5.7$ deg). It was serendipitously identified in an unpublished photometric survey by one of us (J.A.C.), and was observed with CAFOS because of its very red optical and near-infrared colours and possible association with an X-ray event catalogued by *ROSAT* at a separation of only 6.4 arcsec.
- J03319+492 (TYC 3320-337-1). From photographic magnitudes, Pickles & Depagne (2010) and Lépine & Gaidos (2011) classified it as an M1.9 and M3 dwarf, respectively. However, it appears to be an early-K giant with a significant proper motion of 56 mas a⁻¹. It is not possible to separate it from the main sequence in a reduced proper-motion diagram.
- J23266+453 (2MASS J23263798+4521054). Our intention was to observe BD+44 4419 B (G 216-43), an M4.5 dwarf of roughly the same *V*-band magnitude (10.3 vs. 10.9 mag). Unfortunately, we incorrectly observed instead a background giant at a separation of about 20 arcsec.

In a Ratio C vs. PC1 index-index diagram as the one shown in Fig. 6, where Ratio C is highly sensitive to gravity and PC1 is an effective temperature proxy (PC1 was indeed one of the five indices used for deriving spectral types), all giants are below the dashed line at Ratio C = 1.07. There is only one star not classified as a giant that lies below that empirical boundary. It is J04313+241 (V927 Tau AB), a T Tauri star for which we did not provide a luminosity class in Sect. 4.1. We discuss this in detail in Sect. 4.4. Ratio C, which contains the sodium doublet at 8193,8195 Å, can also be used as a youth indicator (e.g., Schlieder et al. 2012b).

4.3. Metallicity

In F-, G-, and K-type stars whose photospheric continua are well-defined in high-resolution spectra, stellar metallicity is computed through spectral synthesis (McWilliam 1990; Valenti & Piskunov 1996; González 1997; González Hernández et al. 2004; Valenti & Fischer 2005; Recio-Blanco et al. 2006) or measuring equivalent widths, especially of iron lines (Sousa et al. 2008, 2011; Magrini et al. 2010; Adibekyan et al. 2012; Tabernero et al. 2012; Bensby et al. 2014). However, it is not possible to measure a photospheric continuum in M-type stars and, thus, their metallicity is studied through other techniques. Since the first determinations from broad-band photometry by Stauffer & Hartmann (1986), there have been three main observational techniques employed to determine metallicity in M dwarfs:

- Photometry calibrated with M dwarfs in physical double and multiple systems with warmer companions, typically F, G, K dwarfs, of known metallicity (Bonfils et al. 2005; Casagrande et al. 2008; Schlaufman & Laughlin 2010; Neves et al. 2012).
- Low-resolution spectroscopy, also calibrated with M dwarfs with earlier primaries, in the optical (Dhital et al. 2012), in the near infrared (Rojas-Ayala et al. 2010, 2012; Terrien et al.

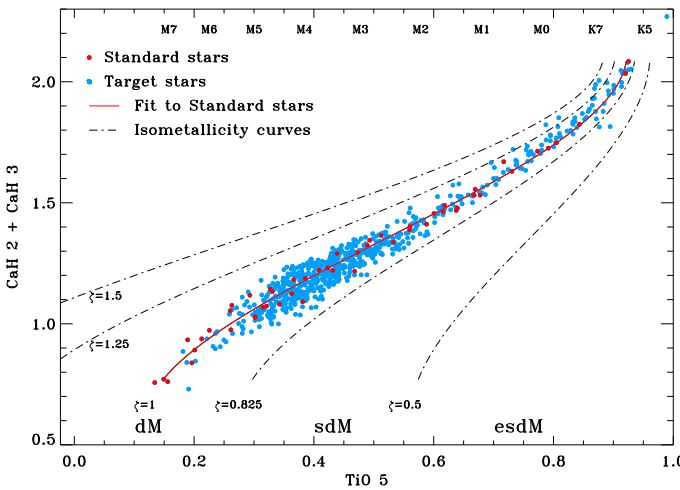


Fig. 7. CaH 2 + CaH 3 vs. TiO 5 index-index diagram of our CAFOS stars, after discarding giants. The spectral types at the top are indicative, but follow the TiO 5 fit given in Table 5. The solid and dash-dotted lines are iso-metallicity curves of the ζ index.

2012; Mann et al. 2014; Newton et al. 2014), or in both wavelength ranges (Mann et al. 2013, 2015).

- High-resolution spectroscopy in the optical (from spectral synthesis: Woolf & Wallerstein 2005; from spectral indices: Woolf & Wallerstein 2006 and Bean et al. 2006; from the measurement of pseudo-equivalent widths: Neves et al. 2013, 2014), in the near-infrared (Shulyak et al. 2011 in the Y band; Önehag et al. 2012 in the J band; Tsuji & Nakajima 2014 in the K band), or in the optical and near-infrared simultaneously (Gaidos & Mann 2014). The novel mid-resolution spectroscopy study in the optical aided with spectral synthesis by Zboril & Byrne (1998) also belongs in this item.

For the 753 CAFOS stars, we computed the $\zeta_{\text{TiO/CaH}}$ metallicity parameter (denoted ζ for short) described by Lépine et al. (2007):

$$\zeta = \frac{1 - \text{TiO } 5}{1 - [\text{TiO } 5]_{Z_\odot}}, \quad (1)$$

where $[\text{TiO } 5]_{Z_\odot} = 0.571 - 1.697\text{CaH} + 1.841\text{CaH}^2 - 0.454\text{CaH}^3$ is a third-order fit of $\text{CaH} = \text{CaH } 2 + \text{CaH } 3$ for *our* standard stars, and TiO 5, CaH 2, and CaH 3 are the spectral indices of Reid et al. (1995) (see also Gizis & Reid 1997 and Lépine et al. 2003). The ζ index is correlated with metallicity in metal-poor M subdwarfs (Woolf et al. 2009) and metal-rich dwarfs (Lépine et al. 2007; Mann et al. 2014). For completeness, we also tabulate the ζ index for our 25 giants, but they are not useful for a comparison. We made the same assumption of standard stars having solar metallicity ($\zeta \approx 1$) as in Lépine et al. (2007), which was later justified by the small dispersion of the data points.

We looked for M dwarfs (and subdwarfs) in our sample with abnormal metallicity, which could be spotted in a CaH 2 + CaH 3 vs. TiO 5 index-index diagram as in Fig. 7. Lépine et al. (2007) defined the classes subdwarf (sd), $0.5 < \zeta < 0.825$, and extreme subdwarf (esd), $\zeta < 0.5$. All our non-giant stars except two have ζ values greater than 0.825, which is the empirical boundary between dwarfs and subdwarfs. The spectra of the two exceptions

show shallower molecular bands and lines than M dwarfs of the same spectral type.

One of our two subdwarf candidates is J19346+045 (sdM1; $\zeta = 0.775$ – HD 184489). Some authors have reported features of low metallicity (e.g., Maldonado et al. 2010), but none had classified it as a subdwarf (but see Sandage & Kowal 1986). Its low effective temperature has prevented spectral synthesis analyses on high-resolution spectra.

The other new subdwarf candidate is J16354–039 (sdM0; $\zeta = 0.664$ – HD 149414 B, BD–03 3968B). Giclas et al. (1959) discovered it and associated it with the G5 Ve single-line spectroscopic binary HD 149414 Aa,Ab. Afterwards, its membership in the very wide system has been investigated by Poveda et al. (1994), Tokovinin (2008), and Dhital et al. (2010), for example, and confirmed and quantified by Caballero (2009). The projected physical separation between Aa,Ab and B amounts to 53 000 au (about a quarter of a parsec). Remarkably, the primary is a halo binary of low metallicity ($[\text{Fe}/\text{H}] \sim -1.4$ – Strom & Strom 1967; Sandage 1969; Cayrel de Strobel et al. 1997; Holmberg et al. 2009). This explains the low ζ metallicity index of J16354–039 for its spectral type and the wide separation of the system (due to gravitational disruption by the Galactic gravitational potential or to common origin and ejection from the same cluster; cf. Caballero 2009 and references therein).

In addition, J12025+084 (M1.5 V; $\zeta = 0.898$ – LHS 320) was classified by Gizis (1997) as an sdM2.0 star and was investigated extensively afterwards with high-resolution imagers (Gizis & Reid 2000; Riaz et al. 2008; Jao et al. 2009; Lodieu et al. 2009). However, we failed to detect any subdwarf signpost in our high signal-to-noise spectrum, which is partly consistent with the metallicity $[\text{Fe}/\text{H}] = -0.6 \pm 0.3$ measured by Rajpurohit et al. (2014).

No CAFOS star showed a very high metallicity index greater than $\zeta = 1.5$. In spite of the dispersion of the ζ index around unity, we considered that all our 726 dwarfs (753 stars in total minus the 25 giants and the two subdwarfs) *approximately* have solar metallicity ($[\text{Fe}/\text{H}] \approx 0.0$). This assumption is relevant for instance to derive the mass from absolute magnitudes, the spectral types, and theoretical models that need metallicity as an input.

4.4. Activity

Chromospheric activity is one of the main relevant parameters for exoplanet detection around M dwarfs. The heterogeneities on the stellar surface of the almost-fully convective, rotating, M dwarfs, such as dark spots, may induce spurious radial-velocity variations at visible wavelengths (Bonfils et al. 2007; Reiners et al. 2010; Barnes et al. 2011; Andersen & Korhonen 2015; Robertson et al. 2015). Near-infrared observations are expected to improve the precision of radial-velocity measurements with respect to the visible for stars cooler than M3, and CARMENES will cover the wavelength range from 0.55 to $1.70\mu\text{m}$. In spite of this, we plan to identify the least active stars for our exoplanet search. Moreover, several authors have identified significant differences between colours and spectral indices of active and inactive stars of similar properties that may affect the spectral typing of M dwarfs (Stauffer & Hartmann 1986; Hawley et al. 1996; Bochanski et al. 2007; Morales et al. 2008).

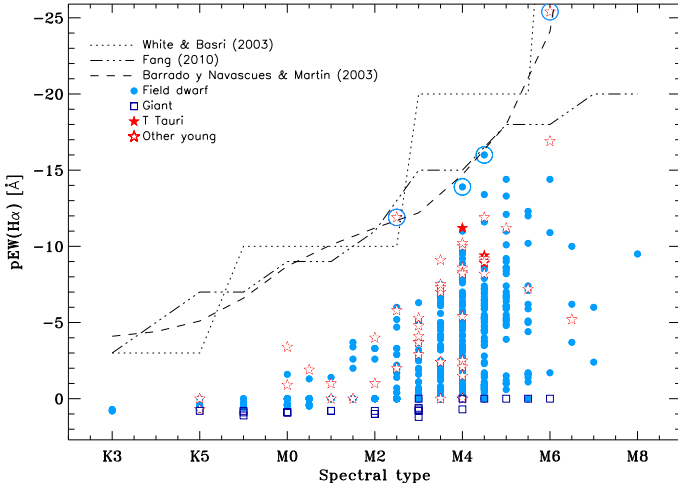


Fig. 8. Pseudo-equivalent width of $H\alpha$ line vs. spectral type diagram. Measurement errors are 0.5 subtypes for the spectral type and are of the order of 10 % with a minimum of 0.1 Å for $pEW(H\alpha)$ (but scatter due to variability is probably larger than 10 %). Dotted, dash-dotted, and dashed lines indicate the boundaries between chromospheric and accretion emission for different authors. Giants, plotted with open squares, have filled $H\alpha$ lines or in absorption. None of the young stars, plotted with open and filled stars, show accretion emission. The four stars at the accretion boundary discussed in the text are encircled.

4.4.1. $H\alpha$ emission

The $H\alpha$ index (Reid et al. 1995) was one of the 31 indices measured on our CAFOS spectra (Table 4). For a better reliability on the activity determination and comparison with other works, we also measured the pseudo-equivalent width of the $H\alpha$ line, $pEW(H\alpha)$, of all the CAFOS stars (Table A.2). We here used $pEW(H\alpha)$ as the proxy for activity (we used the pseudo-equivalent width of the line measured with respect to a local pseudo-continuum instead of the equivalent width because in M-and L, T, and Y-dwarfs the spectral continuum is not observable – e.g. Tsuji & Nakajima 2014).

We plot in Fig. 8 the $pEW(H\alpha)$ vs. spectral type diagram for the whole sample. M dwarfs with late spectral types tend to show the $H\alpha$ line in (strong) emission more often than earlier stars (see e.g. Hawley et al. 1996, West et al. 2004, or Reiners et al. 2013). There is a significant number of M4.0 V stars and later, however, that show very low $H\alpha$ emission below 5 Å (in absolute values).

A few stars stand out in the $pEW(H\alpha)$ vs. spectral type diagram in Fig. 8. Four of them lie at the boundary between chromospheric and accretion emission, as defined by Barrado y Navascués & Martín (2003), White & Basri (2003), and Fang (2010). Their high activity led us to investigate them in detail.

- J04290+186 (M2.5 V, $pEW(H\alpha) = -11.9^{+0.5}_{-0.3}$ Å, V1103 Tau). It is a member of the 600 Ma-old Hyades cluster (Johnson et al. 1962; Griffin et al. 1988; Stauffer et al. 1991; Reid 1992).
- J04544+650 (M4.0 V, $pEW(H\alpha) = -13.9^{+0.8}_{-0.5}$ Å, 1RXS J045430.9+650451). It is an anonymous Tycho-2 star (TYC 4087–1172–1; Lépine & Gaidos 2011) that we cross-matched with an aperiodic, variable, X-ray source identified by Fuhrmeister & Schmitt (2003). This X-ray

variability and the presence of $\text{He I } \lambda 5875.6$ Å in emission indicates that J04544+650 was flaring during our observations.

- J01567+305 (M4.5 V, $pEW(H\alpha) = -16.0 \pm 0.4$ Å, NLTT 6496, Koenigstuhl 4 A). It forms a loosely bound common-proper-motion pair together with the M6.5:V star NLTT 6491 (Koenigstuhl 4 B), and is associated with an X-ray source (Caballero 2012). Interestingly, Aberasturi et al. (2014) collected low-resolution spectroscopy for J01567+305 just two months earlier, for which they determined a spectral type identical to ours within the uncertainties, but measured $pEW(H\alpha) = -9.3 \pm 0.3$ Å, which is significantly lower than our measurement. Our CAFOS spectrum also shows He I in emission, so the mid-M dwarf likely underwent a flare during our observations.
- J07523+162 (M6.0 V, $pEW(H\alpha) = -25.4^{+1.4}_{-1.0}$ Å, LP 423–031). It has also been classified as a single M7 Ve star from optical spectra (Cruz et al. 2003; Reid et al. 2003; Gatewood & Coban 2009; Reiners & Basri 2009), but as an M6 V with surface gravity consistent with normal field dwarfs from near-infrared spectra (Allers & Liu 2013). From high-resolution spectroscopy ($pEW(H\alpha) = -22.3$ Å) and *ROSAT* X-ray count rates, Shkolnik et al. (2009) assigned J07523+162 an age of about 100 Ma, younger than the Pleiades. However, Reiners & Basri (2010) observed flaring activity in a J07523+162 spectrum ($pEW(H\alpha) = -44.4$ Å) and Gagné et al. (2014) and Klutsch et al. (2014) were not able to determine membership in any known stellar kinematic group.

There is an additional fifth active dwarf that stands out among the remaining stars in Fig. 8. It is J03332+462 (M0.0 V, $pEW(H\alpha) = -3.4^{+0.5}_{-0.3}$ Å, V577 Per B), a confirmed member of the ~70 Ma-old AB Doradus moving group (Zuckerman et al. 2004; da Silva et al. 2009; Schlieder et al. 2012a). Its relatively bright primary at about 9 arcsec is a young K2 V star with strong ultraviolet and X-ray emission and lithium in absorption (Pounds et al. 1993; Jeffries 1995; Montes et al. 2001; Zuckerman & Song 2004; Xing & Xing 2012).

4.4.2. Young (and very young) stars

The identification of one open cluster member, one moving group member, and one purported young star in the field among five M dwarfs led us to examine the bibliography for other young star candidates in our CAFOS sample. The result of this bibliographic search is summarised in Table 7. In total, 49 spectroscopically investigated stars in this work have been reported to belong to the Taurus-Auriga star-forming region (~1–10 Ma, three stars), β Pictoris moving group (~12–22 Ma, five stars), Carina or Columba associations (~15–50 Ma, two stars), Argus association (~40 Ma, one star), AB Doradus moving group (~70–120 Ma, five stars), Pleiades cluster (~120 Ma, one star – with a relatively early K5 V spectral type), IC 2391 super-cluster (~100–200 Ma, one star), Hercules-Lyra moving group (~200–300 Ma, four stars – note the question marks), Castor moving group (~200–300 Ma, six stars), Ursa Major moving group (~300–500 Ma, one star), and Hyades cluster and super-cluster (~600 Ma, 14 and 2 stars, respectively), and four to the young ($\tau \lesssim 600$ Ma) field star population in the solar neighbourhood. See Zuckerman & Song (2004) and Torres et al. (2008) for reviews on young moving groups.

The actual existence of some of the entities above (e.g., Hercules-Lyra and Castor moving groups, and IC 2391 and

Table 7. Reported young stars in our sample.

Karmn	Moving group / association / cluster / star-forming region	Ref. ^a
J03332+462	AB Dor MG	See text
J03466+243 AB	Pleiades	vMa45
J03473-019	AB Dor MG	Zuc04
J03548+163 AB	Hyades	Gic62
J04123+162 AB	Hyades	Gic62
J04177+136 AB	Hyades	Gic62
J04206+272	Taurus	Sce07
J04207+152 AB	Hyades	Gic62
J04227+205	Hyades	Reid93
J04238+149 AB	Hyades	Gic62
J04238+092 AB	Hyades	Gic62
J04252+172 ABC	Hyades	Gic62
J04290+186	Hyades	Gic62
J04313+241 AB	Taurus	HR72
J04360+188	Hyades	Pels75
J04366+186	Hyades	See text
J04373+193	Hyades	Reid93
J04393+335	Taurus	Wic96
J04425+204 AB	Hyades	Reid93
J04430+187 AB	Hyades	Gic62
J05019+011	β Pic MG	Sch12
J05062+046	β Pic MG	Sch12
J05256-091 AB	AB Dor MG	Shk12
J05320-030	β Pic MG	daS09
J05415+534	Her-Lyr MG?	Eis13
J05457-223	UMa MG	Tab15
J06075+472	AB Dor MG	Sch12
J06246+234	Young	Mon01
J07319+362N	Castor MG	Cab10
J07319+362S AB	Castor MG	Cab10
J07361-031	Castor MG	Cab10
J07523+162	Young	See text
J08298+267	Castor MG	Cab10
J09328+269	Her-Lyr MG	Eis13
J09362+375	Young	Malo14
J10196+198 AB	Castor MG	Cab10
J10359+288	β Pic MG	Sch12
J10508+068	Her-Lyr MG?	Eis13
J11046-042S AB	Her-Lyr MG	Eis13
J13143+133 AB	Young	Sch14
J15079+762	IC 2391 MG	Mon01
J17198+265	Hyades SC	Klu14
J17199+265	Hyades SC	Klu14
J18313+649	AB Dor	Sch12
J21376+016	β Pic MG	Sch12
J22160+546	Her-Lyr MG?	Eis13
J22234+324 AB	AB Dor MG	Malo14
J23194+790	Carina/Columba Ass.	Klu
J23209-017 AB	Argus Ass.	Malo14
J23228+787	Carina/Columba Ass.	Klu

^a References – vMa45: van Maanen 1945; Gic62: Giclas et al. 1962; HR72: Herbig & Rao 1972; Pels75: Pels et al. 1975; Reid93: Reid 1993; Wic96: Wichmann et al. 1996; Mon01: Montes et al. 2001; Zuc04: Zuckerman et al. 2004; Sce07: Scelsi et al. 2007; daS09: da Silva et al. 2009; Cab10: Caballero 2010; Sch12: Schlieder et al. 2012a; Shk12: Shkolnik et al. 2012; Eis13: Eisenbeiss et al. 2013; Klu14: Klutsch et al. 2014; Malo14: Malo et al. 2014; Sch14: Schlieder et al. 2014; Tab14: Tabernero et al. 2015; Klu: Klutsch, priv. comm. Part of the content of this table was extracted from Hidalgo (2014).

Hyades superclusters) is questioned by several authors. Three of the five stars with the lowest $H\alpha$ emission for their spectral type belong to the hypothetical Castor moving group (Barrado y Navascués 1998; Montes et al. 2001; Ribas 2003; Caballero 2010; Mamajek 2013; Zuckerman et al. 2013), and the other two to the Hyades (super-) cluster (van Altena 1966; Hanson 1975; Leggett & Hawkins 1988; Hawley et al. 1996; Stauffer et al. 1997; Montes et al. 2001; Klutsch et al. 2014). However, the extreme youth of some targets is confirmed by detection of lithium in absorption, X-ray in emission, and common proper-motion to bona fide primaries in nearby young moving groups.

Eleven of the 16 Hyads are known to be binaries. The relatively large number and (apparent) high binary frequency is a natural consequence of the Malmquist bias, which leads to the preferential detection of intrinsically bright objects. Equal-mass binaries are brighter than single stars of the same spectral type (by up to 0.75 mag) and, thus, the frequency of binarity in our magnitude-limited sample is higher than in a bias-free, volume-limited sample. While most of our targets lie at 20–30 pc (Cortés-Contreras et al. 2015), the overbrightness of binary Hyads makes them to look as if they were located roughly at 30 pc instead at the nominal distance of the Hyades at about 46 pc. We suggest to investigate the actual multiplicity status of the five remaining *single* M dwarfs with a mid-resolution spectroscopic monitoring.

At $d \sim 140$ pc, the three Taurus stars in Table 7 are *not* in the solar neighbourhood. Since they are still on the Hayashi track of contraction, their radii are larger than those of dwarfs of the same effective temperature. As a result, they are also much more luminous, which explains why we were able to observe them even though they are located an order of magnitude farther away than the rest of our dwarf targets. As expected from their extreme youth, the three T Tauri stars have $H\alpha$ emissions in the highest quartile ($pEW(H\alpha)$ s between -9 and -11 Å, and spectral types between M4.0 and M4.5) and have been investigated spectroscopically earlier (Herbig & Rao 1972; Mathieu 1994; Wichmann et al. 1996; Kenyon et al. 1998; Scelsi et al. 2008; Sestito et al. 2008). The three of them displayed not only $H\alpha$ in emission, but also $H\beta$ and $H\gamma$ (we used one of them, J04393+335, in Fig. 3 to illustrate best the discarded wavelength ranges that are contaminated by activity in Sect. 3.2.2).

A large radius also translates into low gravity. Indeed, the brightest of the trio of T Tauri stars, J04313+241 AB (V927 Tau AB, $J = 9.73$ mag) was the only non-giant target with spectral index Ratio C < 1.07 (Fig. 6) and the only one to which we did not assign a luminosity class in Table A.3. Its optical spectrum is intermediate between those of giants and dwarfs of the same spectral type (M4.0:). Something similar is true for the other two T Tauri stars, which also have very low Ratio C indices for their spectral type (but all giant stars in our sample display $H\alpha$ in absorption). Although T Tauri stars are not natural targets for radial-velocity searches of low-mass exoplanets and none of the trio satisfies our criteria to be considered in the CARMENES sample (Table 1), a monitoring of bright, young, M dwarfs could shed light on the process of exoplanet formation (e.g., Crockett et al. 2012). Furthermore, young, nearby, very late stars are also ideal targets for direct-imaging surveys for Jupiter-like planetary companions at wide separations (Masciadri et al. 2005; Daemgen et al. 2007; Chauvin et al. 2010; Biller et al. 2013; Delorme et al. 2013, and references therein). Some of these targets are J13143+733 AB (NLTT 33370, M6.0 V in AB Doradus) and J09328+269 (DX Leo B, M5.5 V in Hercules-Lyra).

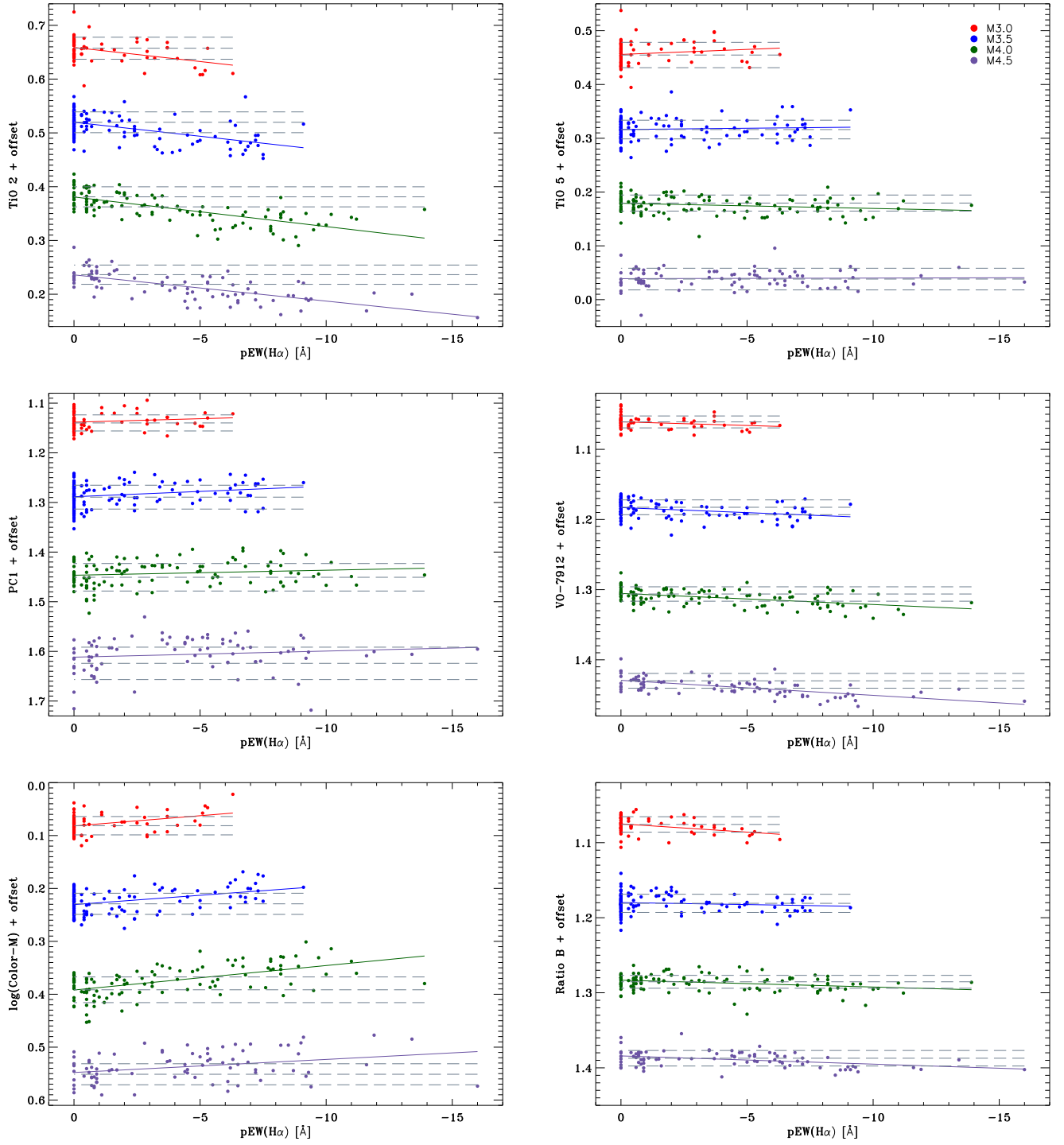


Fig. 9. Spectral-typing indices TiO 2, TiO 5 (top), PC1, VO-7912 (middle), Color-M, and Ratio B (bottom) as a function of H α pseudo-equivalent width for spectral types M3.0 V, M3.5 V, M4.0 V, and M4.5 V, from top to bottom. For clarity, the indices are offset in steps of 0.1 in the vertical axis. Solid lines are linear fits of the indices as a function of $pEWH(\alpha)$. Dashed lines indicate the mean and $\pm 1\sigma$ index at quiescence ($pEWH(\alpha) > -1 \text{ \AA}$).

4.4.3. Effect of activity on spectral typing

As pointed out above, chromospheric activity could affect spectral typing. To study the validity of our results, we plot in Fig. 9 four of the five indices that we used for spectral typing as a function of $pEW(H\alpha)$. We investigated the four spectral type intervals with the largest number of stars (in parenthesis): M3.0 V (72), M3.5 V (134), M4.0 V (113), and M4.5 V (84). Grouping

by spectral type minimised the natural variation of the spectral index with effective temperature. The effect of activity on the TiO 5 and PC1 indices is not significant. However, strong activity in the largest quartile of $pEW(H\alpha)$ has an appreciable effect on the indices VO-7912 and Color-M (not shown), but they fortuitously compensate each other because of the opposite slopes in their index vs. $pEW(H\alpha)$ relations. The effect of activ-

ity on the TiO 2 index is more appreciable in the top left panel of Fig. 9, which agrees with the results shown by Hawley et al. (1996), who found that active M dwarfs tended to have lower values of TiO 2 (more absorption) than inactive dwarfs with the same TiO 5 indices (spectral types). However, this level of activity translates into a variation in spectral type of less than 0.8 subtypes for the most active stars, after using the coefficients in Table 5. In the end, the counter-weighting combination of five spectral indices and, especially, the use of the χ^2 and best-match methods guarantee that our adopted spectral types are free from the effect of chromospheric activity (for the investigated interval of $pEW(H\alpha)$).

Our results on quantifying the variation of some spectral types as a function of activity are seemingly in contrast to some previous works, such as Morales et al. (2008). However, a direct comparison should be avoided because they grouped the stars by absolute magnitude, for which a determination of the distance is needed. A specific work on activity in M dwarfs will be another item of this series of papers on the science preparation of the CARMENES sample. It will be supported on one hand by new measurements of the emission of H α , H β , and the Ca II H & K doublet and near-infrared triplet from high-resolution spectra and on the other hand by a comprehensive parallax distance compilation and accurate spectro-photometric distance determination.

5. Summary

CARMENES, the new spectrograph at the 3.5 m Calar Alto telescope, will spectroscopically monitor a sample of M dwarfs to detect exoplanets with the radial-velocity method. We are selecting the best planet host star candidates. For that, we are compiling a comprehensive list of dwarf stars coming from existing spectroscopic and photometric catalogues, as well as from late-type star studies. Currently, we are gathering all available information and determine fundamental properties from observations for approximately 2200 targets. Here we presented the first paper of a series that explains in detail the characterisation of our sample of targets for the CARMENES survey. This paper detailed optical low-resolution spectroscopy.

One of the key stellar astrophysical parameters that we need for each target is its spectral type. From the spectral type we estimate the stellar mass and infer planet detectability thresholds, and we ensure that we collate an even sampling of early-, mid-, and late-M dwarfs. Here, we undertook low-resolution spectroscopic observations of 753 targets with the CAFOS spectrograph on the 2.2 m Calar Alto telescope. This CAFOS sample contained M-dwarf candidates with poorly constrained spectral types, cool stars in multiple systems, and numerous comparison and standard stars. We classified our targets using both least-squares fitting techniques and 31 spectral indices, of which we chose five indices with small dispersion to empirically calibrate spectral types (TiO 2, TiO 5, PC1, VO-7912 and Color-M).

Additionally, we investigated the relation of spectral indices with surface gravity. We classified 25 of the observed targets as giant stars using the CaH series of related spectral indices, which are useful indicators to segregate giant stars from dwarfs. Metallicity was estimated through the ζ parameters (Lépine et al. 2007). We concluded that all our field dwarf stars except two new subdwarf candidates have solar metallicity. We identified 49 late-type stars as young dwarfs in star-forming regions or moving groups already reported in the bibliography.

Finally, we also computed stellar activity indicators. Stellar activity is a fundamental property for the CARMENES survey

because activity features, such as photospheric spots, can mimic the signature of exoplanets or increase the stellar intrinsic jitter that can mask real exoplanet signals. We computed the pseudo-equivalent width of the H α line of each target as an activity indicator, and analysed the effect of activity on spectral typing through indices. Although we have identified significant trends for some indices, the spectral type variation due to stellar activity is below one subtype level.

In summary, from the 753 targets that we observed with CAFOS, we obtained for the first time spectral types for 305 stars and improved it for 448 stars. We estimated gravity, metallicity, and activity indices for all targets. We identified 683 M dwarfs, of which 520 fulfill the CARMENES requirements and, therefore, will be included in the list of input targets. A more detailed investigation of these targets with high-resolution spectroscopic and imaging observations to select the best candidates for the CARMENES survey will produce the largest compilation of fully characterised M-type stars.

Acknowledgements. CARMENES is funded by the German Max-Planck-Gesellschaft (MPG), the Spanish Consejo Superior de Investigaciones Científicas (CSIC), the European Union through European Regional Fund (FEDER/ERF), the Spanish Ministry of Economy and Competitiveness, the state of Baden-Württemberg, the German Science Foundation (DFG), and the Junta de Andalucía, with additional contributions by the members of the CARMENES Consortium (Max-Planck-Institut für Astronomie, Instituto de Astrofísica de Andalucía, Landessternwarte Königstuhl, Institut de Ciències de l’Espai, Institut für Astrophysik Göttingen, Universidad Complutense de Madrid, Thüringer Landessternwarte Tautenburg, Instituto de Astrofísica de Canarias, Hamburger Sternwarte, Centro de Astrobiología, and the Centro Astronómico Hispano-Alemán). Financial support was also provided by the Universidad Complutense de Madrid, the Comunidad Autónoma de Madrid, the Spanish Ministerios de Ciencia e Innovación and of Economía y Competitividad, and the Fondo Europeo de Desarrollo Regional (FEDER/ERF) under grants AP2009-0187, SP2009/ESP-1496, AYA2011-30147-C03-01, -02, and -03, AYA2012-39612-C03-01, and ESP2013-48391-C4-1-R. Based on observations collected at the Centro Astronómico Hispano Alemán (CAHA) at Calar Alto, operated jointly by the Max-Planck Institut für Astronomie and the Instituto de Astrofísica de Andalucía. This research made use of the SIMBAD, operated at Centre de Données astronomiques de Strasbourg, France, the NASA’s Astrophysics Data System, the RECONS project database (<http://www.recons.org>), the M, L, T, and Y dwarf compendium housed at <http://dwarfarchives.org> maintained by C. Gelino, J. D. Kirkpatrick and A. Burgasser, and the Washington Double Star Catalog maintained at the U.S. Naval Observatory. We thank S. Lépine and E. Gaidos for sharing unpublished data with us, J. I. González-Hernández, E. W. Guenther, A. Hatzes, and M. R. Zapatero Osorio of the CARMENES Consortium for helpful comments, and the anonymous referee for the quick and encouraging report.

References

- Aberasturi, M., Caballero, J. A., Montesinos, B., et al. 2014, AJ, 148, 36
- Adibekyan, V. Zh., Sousa, S. G., Santos, N. C., et al. 2012, A&A, 545, A32
- Allard, F., Homeier, D., & Freytag, B. 2011, ASPC, 448, 91
- Allers, K. N., & Liu, M. C. 2013, ApJ, 772, 79
- Alonso-Floriano, F. J., Caballero, J. A., & Montes, D. 2013a, Highlights of Spanish Astrophysics VII, 431
- Alonso-Floriano, F. J., Montes, D., Jeffers, S. V., et al. 2013b, Protostars and Planets VI, 2K021
- Amado, P. J., Quirrenbach, A., Caballero, J. A., et al. 2013, Highlights of Spanish Astrophysics VII, 842
- Andersen, J. M., & Korhonen, H. 2015, MNRAS, in press (eprint arXiv:1501.01302)
- Appenzeller, I., Thiering, I., Zickgraf, F.-J., et al. 1998, ApJS, 117, 319
- Artigau, É., Kouach, D., Donati, J.-F., et al. 2014, Proc. SPIE, 9147, E15
- Avenhaus, H., Schmidt, H.M., & Meyer, M.R. 2012, A&A, 548A, 105
- Baraffe, I., Chabrier, G., Allard, F., & Hauschildt, P. H. 1998, A&A, 337, 403
- Barnes, J. R., Jeffers, S. V., & Jones, H. R. A. 2011, MNRAS, 412, 1599
- Barrado y Navascués, D. 1998, A&A, 339, 831
- Barrado y Navascués, D., & Martín, E.L. 2003, AJ, 126, 2997
- Bean, J. L., Sneden, C., Hauschildt, P. H., Johns-Krull, C. M., & Benedict, G. F. 2006, ApJ, 652, 1604
- Bean, J. L., Seifahrt, A., Hartman, H., et al. 2010, ApJ, 713, 410

- Béjar, V. J. S., Gauza, B., Caballero, J. A. et al. 2012, 17th Cambridge Workshop on Cool Stars, Stellar Systems and the Sun, published on-line at <http://www.coolstars17.net>
- Bender, C. F. & Simon, M. 2008, ApJ, 689, 416
- Bensby, T., Feltzing, S., & Oey, M. S. 2014, A&A, 562, A71
- Bergfors, C., Brandner, W., Janson, M., et al. 2010, A&A, 520, A54
- Bidelman, W. P. 1985, ApJS, 59, 197
- Biller, B. A., Liu, M. C., Wahhaj, Z., et al. 2013, ApJ, 777, 160
- Bochanski, J. J., Hawley, S. L., Reid, I. N., et al. 2005, AJ, 130, 1871
- Bochanski, J. J., West, A. A., Hawley, S. L., & Covey, K. R. 2007, AJ, 133, 531
- Bonfils, X., Delfosse, X., Udry, S., et al. 2005, A&A, 442, 635
- Bonfils, X., Mayor, M., Delfosse, X., et al. 2007, A&A, 474, 293
- Bonfils, X., Delfosse, X., Udry, S., et al. 2013, A&A, 549, 109
- Boyd, M. R., Winters, J. G., Henry, T. J., et al. 2011, AJ, 142, 10
- Caballero, J. A. 2007, ApJ, 667, 520
- Caballero, J. A. 2009, A&A, 507, 251
- Caballero, J. A. 2010, A&A, 514, A98
- Caballero, J. A. 2012, The Observatory, 132, 1
- Caballero, J. A., Montes, D., Klutsch, A., et al. 2010, A&A, 520, A91
- Caballero, J. A., Cortés-Conteras, M., López-Santiago, J., et al. 2013, Highlights of Spanish Astrophysics VII, 645
- Casagrande, L., Flynn, C., & Bessell, M. 2008, MNRAS, 389, 585
- Cayrel de Strobel, G., Soubiran, C., Friel, E. D., Ralite, N., & Francois, P. 1997, A&AS, 124, 299
- Chabrier, G., Baraffe, I., Allard, F., & Hauschildt, P. 2000, ApJ, 542, 464
- Chauvin, G., Lagrange, A.-M., Bonavita, M. et al. 2010, A&A, 509, A52
- Cortés-Conteras, M., Caballero, J. A., Alonso-Floriano, F. J., et al. 2013, Highlights of Spanish Astrophysics VII, 646
- Cortés-Conteras, M., Caballero, J. A., & Montes, D. 2014, The Observatory, 134, 348
- Cortés-Conteras, M., Béjar, V. J. S., Caballero, J. A., et al. 2015, 18th Cambridge Workshop on Cool Stars, Stellar Systems and the Sun, in press
- Crifo, F., Phan-Bao, N., Delfosse, X., et al. 2005, A&A, 441, 653
- Crockett, C. J., Mahmud, N. I., Prato, L., et al. 2012, ApJ, 761, 164
- Crossfield, I. J. M. 2014, A&A, 566, A130
- Cruz, K. L., & Reid, I. N. 2002, AJ, 123, 2828
- Cruz, K. L., Reid, I. N., Liebert, J., Kirkpatrick, J. D., & Lowrance, P. J. 2003, AJ, 126, 2421
- Cruz, K. L., Reid, I. N., Kirkpatrick, J. D., et al. 2007, AJ, 133, 439
- Cutispoto, G., Pastori, L., Guerrero, A., et al. 2000, A&A, 364, 205
- Daemgen, S., Siegler, N., Reid, I. N., & Close, L. M. 2007, ApJ, 654, 558
- da Silva, L., Torres, C. A. O., de La Reza, R., et al. 2009, A&A, 508, 833
- Deacon, N. R., Liu, M. C., Magnier, E. A., et al. 2012, ApJ, 757, 100
- Delfosse, X., Forveille, T., Beuzit, J.-L. et al. 1999, A&A, 344, 897
- Delorme, P., Gagné, J., Girard, J. H., et al. 2013, A&A, 553, L5
- Dhital, S., West, A. A., Stassun, K. G., & Bochanski, J. J. 2010, AJ, 139, 2566
- Dhital, S., West, A. A., Stassun, K. G., et al. 2012, AJ, 143, 67
- Dieterich, S. B., Henry, T. J., Jao, W.-C., et al. 2014, AJ, 147, 94
- Dressing, C. D., & Charbonneau, D. 2013, ApJ, 767, 95
- Dressing, C. D., & Charbonneau, D. 2015, ApJ, submitted (eprint arXiv:1501.01623)
- Ehrenreich, D., Lagrange, A.-M., Montagnier, G., et al. 2010, A&A, 523, A73
- Eisenbeiss, T., Seifahrt, A., Mugrauer, M., et al., AN, 328, 521
- Eisenbeiss, T., Ammler-von Eiff, M., Roell, T., et al. 2013, A&A, 556, A53
- Fang, M. 2000, PhD thesis, Universität Heidelberg, Germany
- Frith, J., Pinfield, D. J., Jones, H. R. A., et al. 2013, MNRAS, 435, 2161
- Fuhrmeister, B., & Schmitt, J. H. M. M. 2003, A&A, 403, 247
- Gagné, J., Lafrenière, D., Doyon, R., Malo, L., & Artigau, É. 2014, ApJ, 783, 121
- Gaidos, E., & Mann, A. W. 2014, ApJ, 791, 54
- Gaidos, E., Mann, A. W., Lépine, S., et al. 2014, MNRAS, 443, 2561
- García, B. 1989, Bulletin d'Information du Centre de Données Stellaires, 36, 27
- Gatewood, G., & Coban, L. 2009, AJ, 137, 402
- Giclas, H. L., Slaughter, C. D., & Burnham, R. 1959, Lowell Observatory Bulletin, 4, 136
- Giclas, H. L., Burnham, R., & Thomas, N. G. 1962, Lowell Observatory Bulletin, 5, 257
- Gigoyan, K. S., Hambaryan, V. V., & Azzopardi, M. 1998, Astrophysics, 41, 356
- Gizis, J. E. 1997, AJ, 113, 806
- Gizis, J. E. & Reid, I. N. 1997, PASP, 109, 1233
- Gizis, J. E., & Reid, I. N. 2000, PASP, 112, 610
- Gizis, J. E., Monet, D. G., Reid, I. N., et al. 2000a, MNRAS, 311, 385
- Gizis, J. E., Monet, D. G., Reid, I. N., et al. 2000b, AJ, 120, 1085
- Gizis, J. E., Reid, I. N., & Hawley, S. L. 2002, AJ, 123, 3356
- Gliese, W., & Jahreiss, H. 1991, *Preliminary Version of the Third Catalogue of Nearby Stars*, NASA/Astronomical Data Center, Goddard Space Flight Center, Greenbelt
- González, G. 1997, MNRAS, 285, 403
- González Hernández, J. I., Rebolo, R., Israelian, G., et al. 2004, ApJ, 609, 988
- Gould, A., & Chanamé, J. 2004, ApJS, 150, 455
- Gray, R. O., Corbally, C. J., Garrison, R. F., McFadden, M. T., & Robinson, P. E. 2003, AJ, 126, 2048
- Gray, R. O., Corbally, C. J., Garrison, R. F., et al. 2006, AJ, 132, 161
- Gray, R. O., & Corbally, C. J. 2009, *Stellar Spectral Classification*, Princeton University Press
- Griffin, R. F., Griffin, R. E. M., Gunn, J. E., & Zimmerman, B. A. 1988, AJ, 96, 172
- Guenther, E. W., & Wuchterl, G. 2003, A&A, 401, 677
- Guenther, E. W., & Tal-Or, L. 2010, A&A, 521, A83
- Hanson, R. B. 1975, AJ, 80, 379
- Hawley, S. L., Gizis, J. E., & Reid, I. N. 1996, AJ, 112, 2799
- Hawley, S. L., Covey, K. R., Knapp, G. R., et al. 2002, AJ, 123, 3409
- Heintz, W.D. 1986, A&AS, 64, 1
- Henry, T. J., Kirkpatrick, J. D., & Simons, D. A. 1994, AJ, 108, 1437
- Henry, T. J., Walkowicz, L. M., Barto, T. C., & Goliowski, D. A. 2002, AJ, 123, 2002
- Henry, T. J., Jao, W.-C., Subasavage, J. P., et al. 2006, AJ, 132, 2360
- Herbig, G. H., & Rao, N. K. 1972, ApJ, 174, 401
- Hidalgo, D. 2014, MSc thesis, Universidad Complutense de Madrid, Spain
- Holmberg, J., Nordström, B., & Andersen, J. 2009, A&A, 501, 941
- Howard, A. W., Marcy, G. W., Bryson, S. T., et al. 2012, ApJS, 201, 15
- Irwin, J., Berta, Z. K., Burke, C. J., et al. 2011, ApJ, 727, 56
- Jacoby, G. H., Hunter, D. A., & Christian, C. A. 1984, ApJS, 56, 257
- Jahreiß, H., Meusinger, H., Scholz, R.-D., & Stecklum, B. 2008, A&A, 484, 575
- Jao, W.-C., Mason, B. D., Hartkopf, W. I., Henry, T. J., & Ramos, S. N. 2009, AJ, 137, 3800
- Jao, W.-C., Henry, T. J., Subasavage, J. P. et al. 2011, AJ, 141, 117
- Janson, M., Hormuth, F., Bergfors, C., et al. 2012, ApJ, 754, 44
- Janson, M., Bergfors, C., Brandner, W., et al. 2014, ApJ, 789, 102
- Jeffries, R. D. 1995, MNRAS, 273, 559
- Jiménez-Esteban, F. M., Caballero, J. A., Dorda, R., Miles-Páez, P. A., & Solano, E. 2012, A&A, 539, A86
- Jódar, E., Pérez-Garrido, A., Díaz-Sánchez, A., et al. 2013, MNRAS, 429, 859
- Johnson, H. L., & Morgan, W. W. 1953, ApJ, 117, 313
- Johnson, J. A., Aller, K. M., Howard, A. W., & Crepp, J. R. 2010, PASP, 122, 905
- Jones, H. R. A., Rayner, J., Ramsey, L., et al. 2008, Proc. SPIE, 7014, E0Y
- Joshi, M. M., Haberle, R. M., & Reynolds, R. T. 1997, Icarus, 129, 450
- Joy, A. H., & Abt, H. A. 1974, ApJS, 28, 1
- Kasting, J. F., Whitmire, D. P., & Reynolds, R. T. 1993, Icarus, 101, 108
- Keenan, P. C., & McNeil, R. C. 1989, ApJS, 71, 245
- Kenyon, S. J., Brown, D. I., Tout, C. A., & Berlind, P. 1998, AJ, 115, 2491
- Kirkpatrick, J. D., Henry, T. J., & McCarthy, D. W., Jr. 1991, ApJS, 77, 417
- Kirkpatrick, J. D., Henry, T. J., & Simons, D. A. 1995, AJ, 109, 797
- Kirkpatrick, J. D., Reid, I. N., Liebert, J., et al. 1999, ApJ, 519, 802
- Kirkpatrick, J. D. 2005, ARA&A, 43, 195
- Klutsch, A., Alonso-Floriano, F. J., Caballero, J. A., et al. 2012, SF2A-2012: Proceedings of the Annual meeting of the French Society of Astronomy and Astrophysics, 357
- Klutsch, A., Freire Ferrero, R., Guillout, P., et al. 2014, A&A, 567, A52
- Kopparapu, R. K. 2013, ApJ, 767, L8
- Kopparapu, R. K., Ramirez, R., Kasting, J. F., et al. 2013, ApJ, 765, 131
- Kotani, T., Tamura, M., Suto, H., et al. 2014, Proc. SPIE, 9147, E14
- Krisciunas, K., Aspin, C., Geballe, T. R., et al. 1993, MNRAS, 263, 781
- Kubas, D., Beaulieu, J. P., Bennett, D. P., et al. 2012, A&A, 540, A78
- Lalitha, S., Czesla, S., Schmitt, J. H. M. M. et al. 2012, 17th Cambridge Workshop on Cool Stars, Stellar Systems and the Sun, published on-line at <http://www.coolstars17.net>
- Lamert, A. 2014, MSc thesis, Georg-August-Universität Göttingen, Germany
- Lammer, H., Lichtenegger, H. I. M., Kulikov, Y. N., et al. 2007, Astrobiology, 7, 185
- Law, N. M., Hodgkin, S. T., & Mackay, C. D. 2008, MNRAS, 384, 150
- Lee, S.-G. 1984, AJ, 89, 702
- Léger, A., Rouan, D., Schneider, J., et al. 2009, A&A, 506, 287
- Leggett, S. K., & Hawkins, M. R. S. 1988, MNRAS, 234, 1065
- Lépine, S., & Shara, M. M. 2005, AJ, 129, 1483
- Lépine, S., & Gaidos, E. 2011, AJ, 142, 138
- Lépine, S., Rich, R. M., & Shara, M. M. 2003, AJ, 125, 1598
- Lépine, S., Rich, R. M., Shara, M. M., 2007, 669, 1235
- Lépine, S., Thorstensen, J. R., Shara, M. M., & Rich, R. M. 2009, AJ, 137, 4109
- Lépine, S., Hilton, E. J., Mann, A. W., et al. 2013, AJ, 145, 102
- Li, J. Z., Hu, J. Y., & Chen, W. P. 2000, A&A, 356, 157
- Lissauer, J. J., Ragozzine, D., Fabrycky, D. C., et al. 2011, ApJS, 197, 8
- Lodieu, N., Scholz, R.-D., McCaughey, M. J., et al. 2005, A&A, 440, 1061
- Lodieu, N., Zapatero Osorio, M. R., & Martín, E. L. 2009, A&A, 499, 729

- López-Corredoira, M., Gutiérrez, C. M., Mohan, V., Gunthardt, G. I., & Alonso, M. S. 2008, A&A, 480, 61
- Magrini, L., Randich, S., Zoccali, M., et al. 2010, A&A, 523, A11
- Mahadevan, S., Ramsey, L. W., Terrien, R., et al. 2014, Proc. SPIE, 9147, E1G
- Maldonado, J., Martínez-Arnáiz, R. M., Eiroa, C., Montes, D., & Montesinos, B. 2010, A&A, 521, A12
- Malo, L., Doyon, R., Lafrenière, D., et al. 2013, ApJ, 762, 88
- Malo, L., Doyon, R., Feiden, G. A. et al. 2014, ApJ, 792, 37
- Mamajek, E. E., Bartlett, J. L., Seifahrt, A., et al. 2013, AJ, 146, 154
- Mann, A. W., Brewer, J. M., Gaidos, E., Lépine, S., & Hilton, E. J. 2013, AJ, 145, 52
- Mann, A. W., Deacon, N. R., Gaidos, E., et al. 2014, AJ, 147, 160
- Mann, A. W., Feiden, G. A., Gaidos, E., & Boyajian, T. 2015, ApJ, submitted (eprint arXiv:1501.01635)
- Martín, E. L., Rebolo, R., & Magazzù, A. 1994, ApJ, 436, 262
- Martín, E. L., & Kun, M. 1996, A&AS, 116, 467
- Martín, E. L., Rebolo, R., & Zapatero Osorio, M. R. 1996, ApJ, 469, 706
- Martín, E. L., Delfosse, X., Basri, G., et al. 1999, AJ, 118, 2466
- Martín, E. L., Guenther, E., del Burgo, C., et al. 2010, ASPC, 430, 181
- Masciadri, E., Mundt, R., Henning, T., Álvarez, C., & Barrado y Navascués, D. 2005, ApJ, 625, 1004
- Mason, K. O., Hassall, B. J. M., Bromage, G. E., et al. 1995, MNRAS, 274, 1194
- Mathieu, R. D. 1994, ARA&A, 32, 465
- McWilliam, A. 1990, ApJS, 74, 1075
- Meisenheimer, K. 1994, Sterne und Weltraum, 33, 516
- Mochnacki, S. W., Gladders, M. D., Thomson, J. R., et al. 2002, AJ, 124, 2868
- Montagnier, G., Ségransan, D., Beuzit, J.-L., et al. 2006, A&A, 460, L19
- Montes, D., López-Santiago, J., Gálvez, M. C., et al. 2001, MNRAS, 328, 45
- Montes, D., Alonso-Floriano, F. J., Tabernero, H. M., et al. 2013, Protostars and Planets VI, 2K022
- Montes, D., Caballero, J. A., Alonso-Floriano, A. F. et al. 2015, 18th Cambridge Workshop on Cool Stars, Stellar Systems and the Sun, in press
- Moore, J. H., & Paddock, G. F. 1950, ApJ, 112, 48
- Morales, J. C., Ribas, I., Caballero, J. A., et al. 2013, Highlights of Spanish Astrophysics VII, 664
- Morales, J. C., Ribas, I., & Jordi, C. 2008, A&A, 478, 507
- Motch, C., Guillout, P., Haberl, F., et al. 1997, A&A, 318, 111
- Motch, C., Guillout, P., Haberl, F., et al. 1998, A&AS, 132, 341
- Mundt, R., Alonso-Floriano, F. J., Caballero, J. A. et al. 2013, Protostars and Planets VI, 2K055
- Neves, V., Bonfils, X., Santos, N. C., et al. 2012, A&A, 538, A25
- Neves, V., Bonfils, X., Santos, N. C., et al. 2013, A&A, 551, A36
- Neves, V., Bonfils, X., Santos, N. C., et al. 2014, A&A, 568, A121
- Newton, E. R., Charbonneau, D., Irwin, J., et al. 2014, AJ, 147, 20
- Önehag, A., Heiter, U., Gustafsson, B., et al. 2012, A&A, 542, A33
- Passegger, V.-M.. Wende, S., Reiners, A. et al. 2014, Towards other Earths II: the star-planet connection, in press
- Pels, G., Oort, J. H., & Pels-Kluyver, H. A. 1975, A&A, 43, 423
- Phan-Bao, N., & Bessell, M. S. 2006, A&A, 446, 515
- Pickles, A. & Depagne, E. 2010, PASP, 122, 1437
- Pounds, K. A., Allan, D. J., Barber, C., et al. 1993, MNRAS, 260, 77
- Poveda, A., Herrera, M. A., Allen, C., Cordero, G., & Lavallee, C. 1994, RMxAA, 28, 43
- Quirrenbach, A., Amado, P. J., Mandel, H., et al. 2010, Proc. SPIE, 7735, E13
- Quirrenbach, A., Amado, P. J., Seifert, W., et al. 2012, Proc. SPIE, 8446, E0R
- Quirrenbach, A., Amado, P. J., Caballero, J. A., et al. 2014, Proc. SPIE, 9147, E1F
- Rajpurohit, A. S., Reylé, C., Allard, F., et al. 2013, A&A, 556, A15
- Rajpurohit, A. S., Reylé, C., Allard, F., et al. 2014, A&A, 564, A90
- Recio-Blanco, A., Bijaoui, A., & de Laverny, P. 2006, MNRAS, 370, 141
- Reid, N. 1992, MNRAS, 257, 257
- Reid, N. 1993, MNRAS, 265, 785
- Reid, I. N., Hawley, S. L., & Gizis, J. E. 1995, AJ, 110, 1838
- Reid, I. N., Gizis, J. E., & Hawley, S. L. 2002, AJ, 124, 2721
- Reid, I. N., Cruz, K. L., Allen, P., et al. 2003, AJ, 126, 3007
- Reid, I. N., Cruz, K. L., Allen, P., et al. 2004, AJ, 128, 463
- Reid, I. N., Cruz, K. L., & Allen, P. 2007, AJ, 133, 2825
- Reid, I. N., Cruz, K. L., Kirkpatrick, J. D., et al. 2008, AJ, 136, 1290
- Reiners, A., & Basri, G. 2009, ApJ, 705, 1416
- Reiners, A., & Basri, G. 2010, ApJ, 710, 924
- Reiners, A., Bean, J. L., Huber, K. F., et al. 2010, ApJ, 710, 432
- Reiners, A., Shulyak, D., Anglada-Escudé, G., et al. 2013, A&A, 552, A103
- Reyes-Sánchez, K. P. 2014, MSc thesis, Universidad Internacional de Valencia, Spain
- Reylé, C., Scholz, R.-D., Schultheis, M., Robin, A. C., & Irwin, M. 2006, MNRAS, 373, 705
- Riaz, B., Gizis, J. E., & Harvin, J. 2006, AJ, 132, 866
- Riaz, B., Gizis, J. E., & Samaddar, D. 2008, ApJ, 672, 115
- Ribas, I. 2003, A&A, 400, 297
- Riddick, F. C., Roche, P. F., & Lucas, P. W. 2007, MNRAS, 381, 1067
- Ridgway, S. T., Joyce, R. R., White, N. M., & Wing, R. F. 1980, ApJ, 235, 126
- Riedel, A. R., Finch, C. T., Henry, T. J., et al. 2014, AJ, 147, 85
- Robertson, P., Endl, M., Henry, G. W., et al. 2015, ApJ, in press (arXiv:1501.02807)
- Rodríguez-López, C., Anglada-Escudé, G., Amado, P. J., et al. 2014, Highlights of Spanish Astrophysics VIII, in press
- Rojas-Ayala, B., Covey, K. R., Muirhead, P. S., & Lloyd, J. P. 2010, ApJ, 720, L113
- Rojas-Ayala, B., Covey, K. R., Muirhead, P. S., & Lloyd, J. P. 2012, ApJ, 748, 93
- Sánchez, S. F., Acciutto, J., Thiele, U., Pérez-Ramírez, D., & Alves, J. 2007, PASP, 119, 118
- Sánchez, S. F., Thiele, U., Aceituno, J., et al. 2008, PASP, 120, 1244
- Sánchez-Blázquez, P., Peletier, R. F., Jiménez-Vicente, J., et al. 2006, MNRAS, 371, 703
- Sandage, A. 1969, ApJ, 158, 1115
- Sandage, A., & Kowal, C. 1986, AJ, 91, 1140
- Sanduleak, N. & Pesch, P. 1988, ApJS, 66, 387
- Scalo, J., Kaltenegger, L., Segura, A. G., et al. 2007, Astrobiology, 7, 85
- Scelsi, L., Maggio, A., Michela, G., et al. 2007, A&A, 468, 405
- Scelsi, L., Sacco, G., Affer, L., et al. 2008, A&A, 490, 601
- Schlaufman, K. C., & Laughlin, G. 2010, A&A, 519, A105
- Schlieder, J. E., Lépine, S., & Simon, M. 2012a, AJ, 143, 80
- Schlieder, J., Lépine, S., Rice, E., et al. 2012b, AJ, 143, 114
- Schlieder, J., Bonnefoy, M., Herbst, T. M., et al. 2014, ApJ, 783, 27
- Scholz, R.-D., Meusinger, H., & Jahreß, H. 2005, A&A, 442, 211
- Seeliger, M., Neuhäuser, R., & Eisenbeiss, T. 2011, AN, 332, 821
- Seifert, W., Sánchez Carrasco, M. A., Xu, W., et al. 2012, Proc. SPIE, 8446, E33
- Sestito, P., Palla, F., & Randich, S. 2008, A&A, 487, 965
- Shkolnik, E., Liu, M. C., & Reid, I. N. 2009, ApJ, 699, 649
- Shkolnik, E. L., Hebb, L., Liu, M. C., Reid, I. N., & Collier Cameron, A. 2010, ApJ, 716, 1522
- Shkolnik, E. L., Anglada-Escudé, G., Liu, M. C., et al. 2012, ApJ, 758, 56
- Shulyak, D., Seifahrt, A., Reiners, A., Kochukhov, O., & Piskunov, N. 2011, MNRAS, 418, 2548
- Skrutskie, M. F., Cutri, R. M., Stiening, R., et al. 2006, AJ, 131, 1163
- Sousa, S. G., Santos, N. C., Mayor, M., et al. 2008, A&A, 487, 373
- Sousa, S. G., Santos, N. C., Israelián, G., Mayor, M., & Udry, S. 2011, A&A, 533, A141
- Stauffer, J. R., & Hartmann, L. W. 1986, ApJS, 61, 531
- Stauffer, J. R., Giampapa, M. S., Herbst, W., et al. 1991, ApJ, 374, 142
- Stephenson, C. B. 1986, AJ, 91, 144
- Strom, S. E., & Strom, K. M. 1967, ApJ, 150, 501
- Tabernero, H. M., Montes, D., & González Hernández, J. I. 2012, A&A, 547, A13
- Tabernero, H. M., Montes, D., González Hernández, J. I., & Ammler-von Eiff, M., 2015, A&A, in press (eprint arXiv:1409.2348)
- Tarter, J. C., Backus, P. R., Mancinelli, R. L., et al. 2007, Astrobiology, 7, 30
- Teegarden, B. J., Pravdo, S. H., Hicks, M., et al. 2003, ApJ, 589, L51
- Terrien, R. C., Mahadevan, S., Bender, C. F., et al. 2012, ApJ, 747, L38
- Tokovinin, A. 2008, MNRAS, 389, 925
- Torres, C. A. O., Quast, G. R., Melo, C. H. F., & Sterzik, M. F. 2008, *Handbook of Star Forming Regions*, Volume II, 757
- Tsuji, T., & Nakajima, T. 2014, PASJ, 66, 98
- Valenti, J. A., & Piskunov, N. 1996, A&AS, 118, 595
- Valenti, J. A., & Fischer, D. A. 2005, ApJS, 159, 141
- van Altena, W. F. 1966, AJ, 71, 482
- van Maanen, A. 1945, ApJ, 102, 26
- Vysotsky, A. N. 1956, AJ, 61, 201
- West, A. A., Hawley, S. L., Walkowicz, L. M., et al. 2004, AJ, 128, 426
- West, A. A., Morgan, D. P., Bochanski, J. J., et al. 2011, AJ, 141, 97
- White, R., & Basri, G. 2003, ApJ, 582, 1109
- Wichmann, R., Krautter, J., Schmitt, J. H. M. M., et al. 1996, A&A, 312, 439
- Wilking, B. A., Meyer, M. R., Robinson, J. G., & Greene, T. P. 2005, AJ, 130, 1733
- Winters, J. G., Henry, T. J., Lurie, J. C., et al. 2014, AJ, 149, 5
- Woolf, V. M., & Wallerstein, G. 2005, MNRAS, 356, 963
- Woolf, V. M., & Wallerstein, G. 2006, PASP, 118, 218
- Woolf, V. M., Lépine, S., & Wallerstein, G. 2009, PASP, 121, 117
- Xing, L.-F., & Xing, Q.-F. 2012, A&A, 537, A91
- Yi, Z., Luo, A., Song, Y., et al. 2014, AJ, 147, 33
- Zboril, M., & Byrne, P. B. 1998, MNRAS, 299, 753
- Zechmeister, M., Kürster, M., & Endl, M. 2009, A&A, 505, 859
- Zechmeister, M., Kürster, M., Endl, M., et al. 2013, A&A, 552, A78
- Zuckerman, B., & Song, I. 2004, ARA&A, 42, 685
- Zuckerman, B., Song, I., & Bessell, M. S. 2004, ApJ, 613, L65

Zuckerman, B., Vican, L., Song, I., & Schneider, A. 2013, ApJ, 778, 5

Appendix A: Long tables

^a **References to Table A.3** – PMSU: Palomar/Michigan State University survey (see text); Simbad: spectral type as reported by Simbad; MP50: Moore & Paddock 1950; Vys56: Vyssotsky 1956; JM53: Johnson & Morgan 1953; Lee84: Lee 1984; Bid85: Bidelman 1985; Ste86: Stephenson 1986; SP88: Sanduleak & Pesch 1988; Gar89: García 1989; KMc89: Keenan & McNeil et al. 1989; Kir91: Kirkpatrick et al. 1991; Kri93: Krisciunas et al. 1993; Hen94: Henry et al. 1994; Jac94: Jacoby et al. 1994; Mar94: Martín et al. 1994; Giz97: Gizis 1997; GR97: Gizis & Reid 1997; Mot97: Motch et al. 1997; App98: Appenzeller et al. 1998; Gig98: Gigoyan et al. 1998; Mot98: Motch et al. 1998; Cut00: Cutispoto et al. 2000; Giz00: Gizis et al. 2000a; Li00: Li et al. 2000; CrRe02: Cruz & Reid 2002; Gray03: Gray et al. 2003; Lep03: Lépine et al. 2003; Reid03: Reid et al. 2003; Tee03: Teegarden et al. 2003; Reid04: Reid et al. 2004; Boc05: Bochanski et al. 2005; Scho05: Scholz et al. 2005; Gray06: Gray et al. 2006; Mon06: Montagnier et al. 2006; Riaz06: Riaz et al. 2006; SB06: Sánchez-Blázquez et al. 2006; Dae07: Daemgen et al. 2007; Eis07: Eisenbeiss et al. 2007; Reid07: Reid et al. 2007; BS08: Bender & Simon 2008; Jah08: Jahreiß et al. 2008; Law08: Law et al. 2008; LC08: López-Corredoira et al. 2008; Sce08: Scelsi et al. 2008; Cab09: Caballero 2009; Shk09: Shkolnik et al. 2009; Cab10: Caballero et al. 2010; Shk10: Shkolnik et al. 2010; LG11: Lépine & Gaidos 2011; Jan12: Janson et al. 2012; JE12: Jiménez-Esteban et al. 2012; RA12: Rojas-Ayala et al. 2012; Fri13: Frith et al. 2013; Lep13: Lépine et al. 2013; Mann13: Mann et al. 2013; Abe14: Aberasturi et al. 2014; Lam14: Lamert 2014; New14: Newton et al. 2014; RS14: Reyes-Sánchez 2014.

Table A.1. Observed stars: identification, common name, Gliese number, 2MASS coordinates and *J* magnitude, observing date, and exposure time.

No.	Karmn	Name	Gl/GJ	α (J2000)	δ (J2000)	<i>J</i> [mag]	Observation date	$N \times t_{\text{exp}}$ [s]
1	J00066–070 AB	2MASS J00063925–0705354	...	00:06:39.20	−07:05:35.3	9.83	04 Aug 2012	1 × 1000
2	J00077+603 AB	G 217–032	...	00:07:42.60	+60:22:54.3	8.91	24 Sep 2012	1 × 600
3	J00115+591	LSR J0011+5908	...	00:11:51.82	+59:08:40.0	9.95	11 Jan 2012	2 × 700
4	J00118+229	LP 348–40	...	00:11:53.03	+22:59:04.7	8.86	07 Dec 2011	1 × 250
5	J00119+330	G 130–053	...	00:11:56.54	+33:03:17.8	9.07	07 Dec 2011	1 × 220
6	J00122+304	IRXS J001213.6+302906	...	00:12:13.41	+30:28:44.3	10.24	12 Nov 2011	1 × 600
7	J00133+275	[ACM2014] J0013+2733	...	00:13:19.52	+27:33:31.1	10.43	12 Nov 2011	1 × 900
8	J00136+806	G 242–048	3014 A	00:13:38.71	+80:39:56.8	7.76	01 Sep 2012	1 × 300
9	J00146+202	χ Peg	...	00:14:36.16	+20:12:24.1	1.76	11 Jan 2012	1 × 1
10	J00152+530	G 217–040	...	00:15:14.53	+53:04:45.7	10.82	14 Feb 2013	1 × 800
11	J00162+198W	EZ Psc	1006 A	00:16:14.63	+19:51:37.6	7.88	22 Sep 2012	1 × 100
12	J00162+198E	LP 404–062	1006 B	00:16:16.08	+19:51:51.5	8.89	22 Sep 2012	1 × 180
13	J00183+440	GX And	15 A	00:18:22.57	+44:01:22.2	5.25	11 Nov 2011	1 × 40
14	J00228–164	PM 100228–1627	...	00:22:50.20	−16:27:44.3	10.25	02 Aug 2012	3 × 500
15	J00240+264	LSPM J0024+2626	...	00:24:03.77	+26:26:29.9	10.22	12 Nov 2011	1 × 700
16	J00253+235	LP 349–017	...	00:25:19.60	+23:32:51.2	9.79	08 Dec 2011	1 × 800
17	J00297+012	LP 585–038	...	00:29:43.22	+01:12:38.5	9.15	08 Dec 2011	1 × 700
18	J00313+336	G 130–073	...	00:31:20.10	+33:37:37.5	8.75	08 Dec 2011	1 × 700
19	J00313+001	LP 585–046	...	00:31:21.50	+00:09:29.4	9.76	03 Aug 2012	1 × 650
20	J00322+544	G 217–056	...	00:32:15.74	+54:29:02.7	9.39	08 Dec 2011	1 × 350
21	J00328–045 AB	GR* 50	...	00:32:53.14	−04:34:06.8	9.28	08 Dec 2011	1 × 350
22	J00358+526	NLTT 1920	...	00:35:53.22	+52:41:12.4	8.93	01 Sep 2012	1 × 350
23	J00367+444	V428 And	...	00:36:46.44	+44:29:18.9	2.26	11 Jan 2012	1 × 4
24	J00380+169	PM I00380+1656	...	00:38:03.86	+16:56:02.9	9.38	08 Dec 2011	1 × 800
25	J00389+306	Wolf 1056	26	00:38:58.79	+30:36:58.4	7.45	22 Sep 2012	1 × 30
26	J00395+149S	LP 465–061	...	00:39:33.49	+14:54:18.9	9.96	07 Dec 2011	1 × 700
27	J00395+149N	LP 465–062	...	00:39:33.74	+14:54:34.8	9.83	09 Jan 2012	1 × 700
28	J00452+002 AB	HD 4271 BC	...	00:45:13.59	+00:15:51.0	10.11	04 Sep 2012	1 × 800
29	J00464+506	G 172–022	...	00:46:29.90	+50:38:38.9	9.96	03 Jan 2012	1 × 800
30	J00467–044	HD 4449 B	...	00:46:43.36	−04:24:45.5	11.20	02 Sep 2012	2 × 800
31	J00484+753	LSPM J0048+7518	...	00:48:29.71	+75:18:48.0	9.49	03 Jan 2012	1 × 300
32	J00490+657	PM I00490+6544	...	00:49:04.77	+65:44:37.8	9.30	03 Jan 2012	1 × 300
33	J00490+578	η Cas B	34 B	00:49:05.20	+57:49:03.8	7.17	04 Aug 2012	1 × 25
34	J00502+601	HD 236547	...	00:50:16.44	+60:07:55.8	5.50	11 Jan 2012	1 × 40
35	J00502+086	RX J0050.2+0837	...	00:50:17.53	+08:37:34.1	9.75	10 Jan 2012	1 × 750
36	J00540+691	Ross 317	...	00:54:00.49	+69:11:01.3	9.46	07 Dec 2011	1 × 300
37	J00548+275	G 069–032	...	00:54:48.03	+27:31:03.6	10.34	24 Sep 2012	2 × 600
38	J00580+393	IRXS J005802.4+391912	...	00:58:01.16	+39:19:11.2	9.56	09 Jan 2012	1 × 800
39	J01009–044	LP 646–077	1025	01:00:56.44	−04:26:56.1	9.04	22 Sep 2012	1 × 200
40	J01012+571	1RXS J011212.8+570839	...	01:01:13.46	+57:08:44.4	10.05	11 Jan 2012	1 × 700
41	J01014–010	LP 586–043	...	01:01:24.60	−01:05:58.6	9.27	03 Aug 2012	1 × 210
42	J01014+188	G 033–032	...	01:01:26.70	+18:53:10.0	9.63	08 Dec 2011	1 × 400
43	J01026+623	BD+61 195	49 A	01:02:38.96	+62:20:42.2	6.23	02 Sep 2012	1 × 80
44	J01028+189	RX J0102.8+1857	...	01:02:51.00	+18:56:54.2	9.51	03 Aug 2012	1 × 600
45	J01028+470	G 172–035	...	01:02:53.50	+47:03:03.0	9.35	03 Aug 2012	1 × 600
46	J01032+712	LP 29–70	...	01:03:14.50	+71:13:12.7	9.69	03 Jan 2012	1 × 600
47	J01033+623	V388 Cas	51 B	01:03:19.72	+62:21:55.7	8.61	10 Feb 2012	1 × 700
48	J01055+153	HD 6440 B	9038 B	01:05:29.75	+15:23:18.6	7.15	15 Feb 2013	2 × 150
49	J01069+804	NLTT 3583	...	01:06:54.74	+80:27:24.4	9.35	03 Jan 2012	1 × 500
50	J01074–025	RAVE J010727.5–023326	...	01:07:27.50	−02:33:26.4	10.38	25 Sep 2012	3 × 900
51	J01076+229E	HD 6660 B	53.1 B	01:07:38.50	+22:57:21.9	9.53	04 Sep 2012	1 × 300
52	J01097+356	Mirach	53.3	01:09:43.92	+35:37:14.0	−0.96	11 Jan 2012	1 × 0.3
53	J01186–008	HD 7895 B	56.3 B	01:18:40.18	−00:52:27.6	8.01	04 Sep 2012	1 × 100
54	J01214+313	BD+30 206 B	...	01:21:27.40	+31:20:32.7	9.98	04 Sep 2012	1 × 500
55	J01226+127	BD+12 168	...	01:22:36.60	+12:45:03.4	7.86	12 Feb 2013	1 × 400
								+ 1 × 300
56	J01342–015	LP 588–009	...	01:34:12.35	−01:34:26.0	11.72	04 Sep 2012	2 × 700
57	J01356–200 AB	G 272–050	...	01:35:39.90	−20:03:42.6	8.99	24 Sep 2012	3 × 600
58	J01390–179 AB	BL Cet + UV Cet	65 AB	01:39:01.20	−17:57:02.7	6.28	11 Nov 2011	1 × 900
59	J01406–081	PM I01406–0808	...	01:40:39.60	−08:05:44.4	10.37	25 Sep 2012	1 × 900
60	J01431+210	RX J0143.1+2101	...	01:43:11.90	+21:01:10.6	9.25	03 Aug 2012	1 × 450
61	J01541–156	LP 768–670	...	01:54:08.00	−15:36:22.3	9.81	01 Sep 2012	1 × 600
62	J01551–162	PM I01551–1615	...	01:55:06.60	−16:15:52.3	9.94	10 Jan 2012	1 × 700
63	J01562+001	RX J0156.2+0006	...	01:56:14.90	+00:06:08.9	9.49	03 Aug 2012	1 × 700
64	J01567+305	Koenigstuhl 4 A	...	01:56:45.71	+30:33:28.8	10.32	12 Nov 2011	1 × 900
65	J01571–102	HD 11964 B	81.1 B	01:57:11.00	−10:14:53.3	8.41	04 Sep 2012	1 × 150
66	J02000+135 AB	LP 469–041 AB	...	02:00:02.30	+13:34:50.7	9.31	03 Aug 2012	1 × 300
67	J02002+130	TZ Ari	83.1	02:00:12.79	+13:03:11.2	7.51	11 Nov 2011	1 × 500
68	J02019+342	PM I02019+3413	...	02:01:58.70	+34:13:45.0	9.51	07 Dec 2011	1 × 900
69	J02022+103	LP 469–067	3128	02:02:16.21	+10:20:13.7	9.84	03 Aug 2012	1 × 1200
70	J02023+012	LP 589–023	...	02:02:22.40	+01:15:42.8	9.81	07 Dec 2011	1 × 600
71	J02100–088	LP 709–043	...	02:10:03.70	−08:52:59.7	8.95	14 Feb 2013	1 × 400
72	J02133+368 AB	EUVE J0213+36.8	...	02:13:20.62	+36:48:50.7	9.37	07 Dec 2011	1 × 400
73	J02142–039	LP 649–072	...	02:14:12.51	−03:57:43.4	10.48	04 Aug 2012	3 × 900
74	J02159–094 ABC	EUVE J0215–09.5	...	02:15:58.90	−09:29:12.2	8.43	14 Feb 2013	1 × 150
75	J02274+031	PM I02274+0310	...	02:27:27.56	+03:10:54.8	9.98	10 Jan 2012	1 × 800
76	J02285–200	HD 15468 C	100 C	02:28:31.89	−20:02:26.5	9.18	12 Nov 2011	1 × 300
77	J02291+228	BD+22 353B	...	02:29:06.99	+22:52:01.9	8.73	12 Feb 2013	1 × 300
78	J02362+068	BX Cet	105 B	02:36:15.36	+06:52:19.1	7.33	12 Nov 2011	1 × 300

Table A.1. Observed stars: identification, common name, Gliese number, 2MASS coordinates and J magnitude, observing date, and exposure time (cont.).

No.	Karmn	Name	Gl/GJ	α (J2000)	δ (J2000)	J [mag]	Observation date	$N \times t_{\text{exp}}$ [s]
79	J02367+226	G 036-026	...	02:36:44.13	+22:40:26.5	10.08	22 Sep 2012	2 × 600
80	J02412-045	G 075-035	...	02:41:15.11	-04:32:17.7	9.20	08 Dec 2011	1 × 400
81	J02441+492	θ Per B	107 B	02:44:10.25	+49:13:54.1	6.69	12 Nov 2011	1 × 120
82	J02456+449	G 078-004	3178 A	02:45:39.63	+44:56:55.7	7.82	22 Sep 2012	1 × 30
83	J02479-124	Z Eri	...	02:47:55.92	-12:27:38.3	1.59	09 Feb 2012	1 × 2
84	J02502+628	G 246-012	...	02:50:16.44	+62:51:19.8	9.37	08 Dec 2011	1 × 400
85	J02530+168	Teegarden's star	...	02:53:00.85	+16:52:53.3	8.39	22 Sep 2012	2 × 500
86	J02555+268	HD 18143 C	118.2 C	02:55:35.73	+26:52:20.9	9.56	09 Jan 2012	1 × 500
87	J02558+183	ρ ⁰² Ari	...	02:55:48.50	+18:19:53.9	0.23	08 Dec 2011	1 × 2
88	J02562+239	LSPM J0256+2359	...	02:56:13.96	+23:59:10.5	9.98	08 Dec 2011	1 × 900
89	J03026-181	LP 771-72	121.1	03:02:38.01	-18:09:58.7	8.21	22 Sep 2012	1 × 50
90	J03033-080	StM 20	...	03:03:21.32	-08:05:15.4	9.12	08 Dec 2011	1 × 200
91	J03047+617	HD 18757 B	3195 B	03:04:43.35	+61:44:09.7	8.88	09 Jan 2012	1 × 300
92	J03110-046	LP 652-062	...	03:11:04.89	-04:36:35.8	9.41	08 Dec 2011	1 × 250
93	J03147+114	RX J0314.7+1127	...	03:14:47.02	+11:27:27.2	9.35	03 Jan 2012	1 × 250
94	J03154+578	G 246-030	...	03:15:29.44	+57:51:33.0	11.12	01 Sep 2012	1 × 800
95	J03162+581S	Ross 370 A	130.1 A	03:16:13.82	+58:10:02.4	7.34	01 Sep 2012	1 × 300
96	J03162+581N	Ross 370 B	130.1 B	03:16:13.90	+58:10:07.3	7.50	01 Sep 2012	1 × 300
97	J03167+389	HAT 168-01565	...	03:16:46.13	+38:55:27.4	9.16	03 Jan 2012	1 × 210
98	J03174-011	LP 592-031	...	03:17:28.12	-01:07:29.7	9.73	14 Feb 2013	1 × 300
99	J03179-010	G 077-042	...	03:17:55.33	-01:05:44.2	10.81	14 Feb 2013	1 × 900
100	J03181+426	Wolf 140	...	03:18:07.01	+42:40:09.1	9.25	09 Jan 2012	1 × 300
101	J03194+619	G 246-033	...	03:19:28.80	+61:56:04.4	9.51	07 Dec 2011	1 × 650
102	J03236+476	Koenig 33	...	03:23:37.70	+47:37:26.5	9.48	07 Dec 2011	1 × 750
103	J03236+056	1RXS J032338.7+054117	...	03:23:39.16	+05:41:15.3	9.87	10 Jan 2012	1 × 800
104	J03263+171	TYC 1237-889-1	...	03:26:23.62	+17:09:30.9	9.77	08 Dec 2011	1 × 650
105	J03275+222	[ACM2014] J0327+2212	...	03:27:30.84	+22:12:38.3	10.04	09 Jan 2012	1 × 800
106	J03294+117	PM 103294+1142	...	03:29:25.20	+11:42:11.3	9.34	03 Aug 2012	1 × 300
107	J03303+346	1RXS J033021.4+340444	...	03:30:23.32	+34:40:32.6	10.00	06 Mar 2012	1 × 650
108	J03309+706	LP 031-368	...	03:30:54.74	+70:41:14.6	9.49	03 Jan 2012	1 × 500
109	J03319+492	TYC 3320-337-1	...	03:31:57.00	+49:12:58.4	9.00	12 Feb 2013	1 × 300
110	J03320+436	HD 21727 B	...	03:32:05.99	+43:40:01.0	9.24	12 Feb 2013	1 × 500
111	J03325+287 ABC	RX J0332.6+2843	...	03:32:35.79	+28:43:55.5	9.36	07 Dec 2011	1 × 400
112	J03332+462	V577 Per B	...	03:33:14.04	+46:15:19.4	8.38	04 Sep 2012	1 × 150
113	J03354+428	HD 22122 B	...	03:35:28.52	+42:53:35.0	10.83	12 Feb 2013	1 × 700
114	J03356-084	LP 653-013	...	03:35:38.50	-08:29:22.4	10.38	01 Sep 2012	3 × 600
115	J03361+313	[GBM90] Per 49	...	03:36:08.68	+31:18:39.8	9.19	03 Jan 2012	1 × 600
116	J03375+288	PM 103375+2852	...	03:37:30.30	+28:52:28.3	9.47	07 Dec 2011	1 × 250
117	J03375+178N AB	LP 413-018	3239 A	03:37:33.32	+17:51:14.6	9.10	24 Sep 2012	1 × 120
118	J03375+178S AB	LP 413-019	3240 B	03:37:33.87	+17:51:00.5	9.19	24 Sep 2012	1 × 200
119	J03392+565 AB	G 175-002	...	03:39:15.30	+56:32:05.9	9.99	07 Dec 2011	1 × 1100
120	J03430+459	NLTT 11633	...	03:43:02.07	+45:54:18.2	9.67	03 Jan 2012	1 × 600
121	J03466+243 AB	V642 Tau	...	03:46:37.30	+24:20:36.6	10.12	03 Jan 2012	1 × 500
122	J03473-019	G 080-021	...	03:47:23.30	-01:58:19.8	7.80	14 Feb 2013	1 × 90
123	J03480+405	HD 23596 B	...	03:48:05.88	+40:32:22.6	9.35	25 Sep 2012	1 × 300
124	J03510+142	PM 103510+1413 A	...	03:51:00.79	+14:13:39.9	9.44	06 Mar 2012	1 × 400
125	J03519+397	HDE 275867 B	...	03:51:58.14	+39:46:56.7	8.28	15 Feb 2013	1 × 150
126	J03548+163 AB	HG 7-33	...	03:54:53.20	+16:18:56.4	9.96	04 Jan 2012	1 × 800
127	J03556+522	HD 24421 B	...	03:55:36.89	+52:14:29.1	10.89	12 Feb 2013	1 × 1500
128	J03565+319	1RXS J035632.5+315746	...	03:56:33.08	+31:57:24.8	9.80	04 Jan 2012	1 × 600
129	J03566+507	43 Per B	...	03:56:40.57	+50:42:48.1	8.15	25 Sep 2012	1 × 300
130	J03574-011 AB	HD 24916 BC	157 BC	03:57:28.92	-01:09:23.4	7.77	10 Feb 2012	1 × 220
131	J03588+125	G 007-014	...	03:58:49.06	+12:30:24.2	9.76	04 Jan 2012	1 × 700
132	J04041+307	G 038-024	...	04:04:06.16	+30:42:45.5	9.26	13 Dec 2011	1 × 300
133	J04061-055	2MASS J04060688-0534444	...	04:06:06.88	-05:34:44.4	9.13	13 Dec 2011	1 × 300
134	J04079+142	HDE 286475 B	...	04:07:54.80	+14:13:00.7	9.22	10 Jan 2012	1 × 300
135	J04081+743	LP 032-016	...	04:08:11.01	+74:23:01.8	9.25	09 Jan 2012	1 × 400
136	J04083+691	LP 031-433	...	04:08:23.72	+69:10:59.3	10.26	11 Jan 2012	2 × 500
137	J04123+162 AB	HG 7-124	...	04:12:21.73	+16:15:03.3	9.74	09 Jan 2012	1 × 700
138	J04153-076	o ⁰² Eri C	166 C	04:15:21.73	-07:39:17.4	6.75	09 Feb 2012	1 × 200
139	J04177+410	LSPM J0417+4103	...	04:17:44.31	+41:03:13.8	9.24	11 Jan 2012	1 × 300
140	J04177+136 AB	HG 7-153	...	04:17:47.70	+13:39:42.3	9.41	07 Dec 2011	1 × 300
141	J04191-074	LP 654-039	...	04:19:06.60	-07:27:44.8	9.97	07 Dec 2011	1 × 700
142	J04191+097	PM 104191+0944	...	04:19:08.09	+09:44:48.2	9.99	04 Jan 2012	1 × 700
143	J04205+815	PM 104205+8131	...	04:20:35.05	+81:31:55.6	9.48	11 Jan 2012	1 × 400
144	J04206+272	XEST 16-045	...	04:20:39.18	+27:17:31.7	10.50	02 Sep 2012	2 × 600
145	J04206-168	DG Eri	...	04:20:41.35	-16:49:47.9	2.99	13 Dec 2011	1 × 10
146	J04207+152 AB	HG 7-172	...	04:20:47.96	+15:14:09.2	9.49	04 Jan 2012	1 × 600
147	J04224+036	RX J0422.4+0337	...	04:22:25.04	+03:37:08.2	9.86	07 Dec 2011	1 × 900
148	J04227+205	LP 415-030	...	04:22:42.84	+20:34:12.5	10.46	11 Jan 2012	3 × 700
149	J04229+259	G 008-031	...	04:22:59.26	+25:59:14.8	9.65	11 Jan 2012	1 × 700
150	J04234+809	1RXS J042323.2+805511	...	04:23:29.05	+80:55:10.2	9.41	06 Mar 2012	1 × 450
151	J04238+149 AB	IN Tau	...	04:23:50.33	+14:55:17.4	9.29	04 Jan 2012	1 × 400
152	J04238+092 AB	HG 7-192	...	04:23:50.70	+09:12:19.4	9.12	06 Mar 2012	1 × 220
153	J04247-067 ABC	1RXS J042441.9-064725	...	04:24:42.60	-06:47:31.3	9.57	06 Aug 2012	1 × 700
154	J04252+172 ABC	V805 Tau	...	04:25:13.53	+17:16:05.6	9.15	09 Jan 2012	1 × 300
155	J04290+186	V1103 Tau	...	04:29:01.00	+18:40:25.4	9.57	04 Jan 2012	1 × 500
156	J04308-088	Koenigstuhl 2 A	...	04:30:52.03	-08:49:19.3	9.85	02 Sep 2012	1 × 800
157	J04310+367	1RXS J043100.0+364800	...	04:31:00.10	+36:47:54.8	9.45	04 Jan 2012	1 × 800
158	J04313+241 AB	V927 Tau	...	04:31:23.82	+24:10:52.9	9.73	24 Sep 2012	1 × 350

Table A.1. Observed stars: identification, common name, Gliese number, 2MASS coordinates and *J* magnitude, observing date, and exposure time (cont.).

No.	Karmn	Name	Gl/GJ	α (J2000)	δ (J2000)	<i>J</i> [mag]	Observation date	$N \times t_{\text{exp}}$ [s]
159	J04329+001S	LP 595–023	...	04:32:56.24	+00:06:15.9	8.42	04 Sep 2012	1 × 250
160	J04347–004	G 082–033	...	04:34:45.32	-00:26:46.4	9.31	10 Jan 2012	1 × 300
161	J04360+188	LP 415–1582	...	04:36:04.17	+18:53:18.9	9.77	03 Jan 2012	1 × 500
162	J04366+186	LP 415–1619	...	04:36:38.90	+18:36:56.8	9.78	09 Feb 2012	1 × 568
163	J04373+193	LP 415–1644	...	04:37:21.89	+19:21:17.5	10.18	03 Jan 2012	1 × 500
164	J04386–115	LP 715–039	...	04:38:37.20	-11:30:14.8	8.67	14 Feb 2013	1 × 200
165	J04388+217	NLTT 13673	...	04:38:53.53	+21:47:54.9	9.55	10 Jan 2012	1 × 600
166	J04393+335	V583 Aur B	...	04:39:23.20	+33:31:49.4	9.92	10 Jan 2012	1 × 700
167	J04398+251	2MASS J04394898+2509262	...	04:39:48.98	+25:09:26.2	9.64	09 Feb 2012	1 × 450
168	J04413+327	NLTT 13733	...	04:41:23.88	+32:42:22.8	9.46	11 Jan 2012	1 × 500
169	J04425+204 AB	LP 415–345	...	04:42:30.30	+20:27:11.4	9.40	01 Sep 2012	1 × 500
170	J04430+187 AB	HD 285970	...	04:43:01.43	+18:42:41.9	7.75	25 Sep 2012	1 × 150
171	J04458–144	PM 104458–1426	...	04:45:52.70	-14:26:25.8	9.09	02 Sep 2012	1 × 300
172	J04468–112 AB	1RXS J044652.0–111658	...	04:46:51.70	-11:16:47.7	8.14	14 Feb 2013	1 × 150
173	J04472+206	RX J0447.2+2038	...	04:47:12.25	+20:38:10.9	9.38	10 Sep 2012	1 × 1200
174	J04494+484 AB	G 081–034	...	04:49:29.47	+48:28:45.9	9.06	10 Feb 2012	1 × 431
175	J04496–153	2MASS J04455273–1426259	...	04:49:37.00	-15:22:52.6	10.32	24 Sep 2012	4 × 900
176	J04499+711	NLTT 13933	...	04:49:55.70	+71:09:47.0	9.63	09 Jan 2012	1 × 500
177	J04536+623	G 247–039	...	04:53:40.12	+62:19:03.9	9.23	04 Jan 2012	1 × 800
178	J04538+158	LSPM J0453+1549	...	04:53:50.05	+15:49:15.6	9.43	09 Feb 2012	1 × 327
179	J04544+650	1RXS J045430.9+650451	...	04:54:29.82	+65:04:41.1	9.67	13 Dec 2011	1 × 700
180	J04559+046	HD 31412 B	9169 B	04:55:54.46	+04:40:16.4	5.97	09 Feb 2012	1 × 150
181	J04560+432	G 096–010	...	04:56:03.54	+43:13:55.6	9.30	10 Feb 2012	1 × 358
182	J05003+251 AB	HD 31867 B	...	05:00:19.52	+25:07:51.0	9.41	15 Feb 2013	1 × 250
183	J05019+011	1RXS J050156.7+010845	...	05:01:56.70	+01:08:42.9	8.53	24 Sep 2012	1 × 180
184	J05030+213 AB	HDE 285190 BC	...	05:03:05.63	+21:22:36.2	9.75	07 Dec 2011	1 × 1100
185	J05032+213	HDE 285190 A	...	05:03:16.08	+21:23:56.4	7.45	02 Sep 2012	1 × 300
186	J05050+442	PM 105050+4414	...	05:05:09.92	+44:14:03.8	9.83	07 Dec 2011	1 × 800
187	J05062+046	RX J0506.2+0439	...	05:06:12.90	+04:39:27.2	8.91	24 Sep 2012	1 × 280
188	J05068+516	9 Aur C	187.2 C	05:06:49.19	+51:36:35.3	7.34	25 Sep 2012	1 × 200
189	J05072+375	1RXS J050714.8+373103	...	05:07:14.49	+37:30:42.1	10.28	04 Jan 2012	3 × 700
190	J05083+756	LP 015–315	...	05:08:18.41	+75:38:15.5	9.39	07 Dec 2011	1 × 600
191	J05151–073	LHS 1747	3340	05:15:08.05	-07:20:48.6	8.36	25 Sep 2012	1 × 700
192	J05152+236	[ACM2004] J0515+2336	...	05:15:17.54	+23:36:26.1	10.19	09 Jan 2012	1 × 1000
193	J05173+321	G 086–037	...	05:17:19.96	+32:07:35.0	9.24	11 feb 2012	1 × 250
194	J05175+487	HAT 94–03592	...	05:17:33.60	+48:46:14.5	9.97	08 Dec 2011	1 × 500
195	J05187+464	PM 105187+4629	...	05:18:44.56	+46:29:59.5	9.96	13 Dec 2011	1 × 900
196	J05187–213	HD 34751 B	199 B	05:18:47.54	-21:23:36.5	7.85	15 Feb 2013	1 × 250
197	J05195+649	IRXS J051929.3+645435	...	05:19:31.20	+64:54:33.8	8.95	24 Sep 2012	1 × 300
198	J05200–229	PM 105200–2257	...	05:20:03.50	-22:57:03.3	9.17	02 Sep 2012	1 × 200
199	J05223+305	PM 105223+3031	...	05:22:20.53	+30:31:09.7	9.41	10 Feb 2012	1 × 350
200	J05256–091 AB	LP 717–036	...	05:25:41.70	-09:09:12.5	8.45	14 Feb 2013	1 × 160
201	J05289+125	HD 35956 B	3348	05:28:56.50	+12:31:53.9	9.65	10 Feb 2012	1 × 600
202	J05294+155E	LP 417–212	2043 A	05:29:27.04	+15:34:38.4	7.56	24 Sep 2012	1 × 60
203	J05295–113	PM 105295–1119	...	05:29:32.90	-11:19:57.3	10.13	04 Jan 2012	1 × 900
204	J05300+121W	AHD 19 B	...	05:30:01.70	+12:07:26.5	9.65	03 Jan 2012	1 × 700
205	J05300+121E	AHD 19 A	...	05:30:02.30	+12:07:34.8	10.25	03 Jan 2012	1 × 700
206	J05314–036	HD 36395	205	05:31:27.35	-03:40:35.7	5.00	14 Dec 2011	1 × 300
207	J05320–030 AB	V1311 Ori	...	05:32:04.50	-03:05:29.4	7.88	14 Feb 2013	1 × 160
208	J05324–072	BD–07 1110	...	05:32:26.90	-07:14:19.0	7.95	14 Feb 2013	1 × 90
209	J05328+338	LHS 5108	...	05:32:51.95	+33:49:47.5	9.39	03 Jan 2012	1 × 300
210	J05342+103S	Ross 45 B	3353	05:34:15.08	+10:19:09.2	9.19	02 Sep 2012	1 × 300
211	J05342+103N	Ross 45 A	3354	05:34:15.14	+10:19:14.2	8.56	02 Sep 2012	1 × 300
212	J05394+747	NLTT 15320	...	05:39:25.41	+74:46:04.9	9.33	03 Jan 2012	1 × 350
213	J05415+534	HD 37394 B	212 B	05:41:30.73	+53:29:23.3	6.59	10 Feb 2012	1 × 90
214	J05421+124	V1352 Ori	213	05:42:08.98	+12:29:25.3	7.12	11 Jan 2012	1 × 300
215	J05424+506	LP 159–15	...	05:42:25.00	+50:38:41.4	9.91	03 Jan 2012	1 × 650
216	J05425+154	1RXS J05423.1+152459	...	05:42:31.78	+15:25:01.6	9.44	10 Jan 2012	1 × 300
217	J05427+026	HD 38014 B	...	05:42:45.50	+02:41:41.5	9.45	09 Feb 2012	1 × 300
218	J05455–119	PM 105455–1158	...	05:45:31.98	-11:58:03.5	9.59	11 feb 2012	1 × 600
219	J05456+729	PM 105456+7255	...	05:45:38.80	+72:55:12.7	9.4	13 Dec 2011	1 × 1200
220	J05456+111	PM 105456+1107	...	05:45:41.60	+11:07:48.5	9.90	09 Jan 2012	1 × 1200
221	J05457–223	γ Lep C (VB 1)	216 C	05:45:43.22	-22:20:03.5	11.13	12 Feb 2013	1 × 1200
222	J05458+729	PM 105458+7254	...	05:45:49.74	+72:54:07.2	9.34	02 Jan 2012	1 × 300
223	J05463+012	HD 38529 B	...	05:46:19.38	+01:12:47.2	9.72	09 Feb 2012	1 × 300
224	J05501+051	IRXS J055009.0+051154	...	05:50:08.60	+05:11:53.7	9.37	11 Jan 2012	1 × 300
225	J05511+122	PM 105511+1216	...	05:51:10.40	+12:16:10.2	9.45	11 feb 2012	1 × 350
226	J05566–103	IRXS J055641.0–101837	...	05:56:40.66	-10:18:37.9	9.07	11 feb 2012	1 × 350
227	J05582–046	HD 40397 C	3377 C	05:58:17.17	-04:38:01.3	11.11	14 Feb 2013	4 × 800
228	J05588+213	LHS 6097	...	05:58:53.33	+21:21:01.1	9.97	09 Jan 2012	3 × 600
229	J05596+585	EG Cam	3371 A	05:59:37.75	+58:35:35.1	7.07	22 Sep 2012	1 × 150
230	J06024+663	LP 057–046	...	06:02:25.54	+66:20:40.4	9.86	08 Dec 2011	1 × 1000
231	J06024+498	G 192–015	3380	06:02:29.18	+49:51:56.2	9.35	06 Mar 2012	1 × 800
232	J06035+168	IRXS J060334.8+165128	...	06:03:34.62	+16:51:45.7	9.39	09 Feb 2012	1 × 358
233	J06035+155	TYC 1313–1482–1	...	06:03:34.80	+15:31:30.9	8.2	08 Dec 2011	1 × 1000
234	J06054+608	LP 086–173	...	06:05:29.36	+60:49:23.2	9.10	13 Dec 2011	1 × 300
235	J06065+045	vB 2	...	06:06:30.57	+04:30:32.7	11.16	15 Feb 2013	2 × 500
236	J06066+465	PM 106066+4633	...	06:06:37.89	+46:33:46.3	9.23	14 Dec 2011	1 × 300
237	J06075+472	EUVE J0607+47.2	...	06:07:31.85	+47:12:26.6	9.72	14 Dec 2011	1 × 900
238	J06102+225	2E 1607	...	06:10:17.76	+22:34:19.9	9.88	01 Jan 2012	1 × 683
239	J06103+722	LSPM J0610+7212	...	06:10:18.26	+72:12:00.6	9.27	04 Jan 2012	1 × 600

Table A.1. Observed stars: identification, common name, Gliese number, 2MASS coordinates and J magnitude, observing date, and exposure time (cont.).

No.	Karmn	Name	Gl/GJ	α (J2000)	δ (J2000)	J [mag]	Observation date	$N \times t_{\text{exp}}$ [s]
240	J06145+025	LP 564-051	...	06:14:34.91	+02:30:27.4	9.30	07 Dec 2011	1 × 650
241	J06151-164	LP 779-034	...	06:15:11.99	-16:26:15.2	9.28	06 Mar 2012	1 × 520
242	J06171+051 AB	HD 43587 BC	231.1 BC	06:17:10.65	+05:07:02.4	9.09	10 Feb 2012	1 × 300
243	J06185+250	NLTT 16348	...	06:18:34.80	+25:03:06.4	9.95	09 Jan 2012	1 × 700
244	J06236-096 AB	LP 720-010	...	06:23:38.50	-09:38:51.7	9.82	10 Jan 2012	1 × 700
245	J06238+456	LP 160-022	...	06:23:51.24	+45:40:05.1	10.35	01 Jan 2012	3 × 750
246	J06246+234	Ross 64	232	06:24:41.32	+23:25:58.6	8.66	24 Sep 2012	1 × 650
247	J06298-027 AB	G 108-004	...	06:29:50.28	-02:47:45.5	9.47	03 Jan 2012	1 × 250
248	J06307+397	PM I06307+3947	...	06:30:47.42	+39:47:37.1	9.41	03 Jan 2012	1 × 250
249	J06313+006	HDE 291725 B	...	06:31:23.74	+00:36:44.5	11.08	12 feb 2013	1 × 1500
250	J06314-016	G 106-054	...	06:31:28.52	-01:41:20.8	10.55	15 Feb 2013	1 × 500
251	J06323-097	PM 106323-0943	...	06:32:20.29	-09:43:29.0	9.85	13 Dec 2011	1 × 500
252	J06325+641	LP 057-192	...	06:32:30.61	+64:06:20.7	9.81	03 Jan 2012	1 × 600
253	J06332+054	HD 46375 B	...	06:33:12.09	+05:27:53.2	8.70	09 Feb 2012	1 × 220
254	J06354-040 AB	IRXS J06351.2-040314	...	06:35:29.87	-04:03:18.5	9.27	11 Feb 2012	1 × 500
255	J06361+201	LP 420-004	...	06:36:11.93	+20:08:14.2	9.43	03 Jan 2012	1 × 250
256	J06367+378	BD+37 1545B	...	06:36:43.22	+37:51:37.1	11.44	14 Feb 2013	3 × 800
257	J06401-164	LP 780-023	...	06:40:08.61	-16:27:26.9	9.12	03 Jan 2012	1 × 200
258	J06435+166	G 110-014	...	06:43:34.77	+16:41:34.9	9.78	04 Jan 2012	1 × 1000
259	J06461+325	HDE 263175 B	3409	06:46:07.50	+32:33:14.9	8.99	09 Feb 2012	1 × 250
260	J06474+054	G 108-027	...	06:47:27.51	+05:24:28.2	9.45	09 Feb 2012	1 × 272
261	J06489+211	IRXS J064855.9+210754	...	06:48:55.22	+21:08:03.9	9.37	03 Jan 2012	1 × 250
262	J06509-091	LP 661-002	...	06:50:59.48	-09:10:50.6	9.40	09 Feb 2012	1 × 250
263	J06522+627	G 250-025	...	06:52:16.60	+62:46:58.5	9.42	03 Jan 2012	1 × 350
264	J06522+179	PM 06522+1756	...	06:52:16.80	+17:56:19.5	9.68	13 Dec 2011	1 × 350
265	J06523-051S AB	HD 50281 B	250 B	06:52:18.04	-05:11:24.1	6.58	14 Nov 2011	1 × 200
266	J06523-051N	HD 50281 A	250 A	06:52:18.05	-05:10:25.4	5.01	14 Nov 2011	1 × 200
267	J06548+332	HDE 265866	251	06:54:49.03	+33:16:05.9	6.10	06 Mar 2012	1 × 60
268	J06565+440	G 107-036	...	06:56:30.94	+44:01:56.8	9.92	13 Dec 2011	1 × 700
269	J07001-190	IRXS J070005.1-190115	...	07:00:06.83	-19:01:23.6	9.03	06 Mar 2012	1 × 900
270	J07009-023	PM I07009-0221	...	07:00:59.78	-02:21:33.0	9.30	13 Dec 2011	1 × 300
271	J07031+836	HD 48974 B	...	07:03:10.98	+83:38:58.9	11.11	15 Feb 2013	3 × 450
272	J07051-101	IRXS J070511.2-100801	...	07:05:11.95	-10:07:52.8	10.20	03 Jan 2012	3 × 500
273	J07105-087	IRXS J071032.6-084232	...	07:10:31.47	-08:42:48.5	9.05	10 Jan 2012	1 × 350
274	J07105+283	StKM 1-629	...	07:10:34.20	+28:22:41.9	8.92	13 Dec 2011	1 × 300
275	J07111-035	PM 10711-0334	...	07:11:09.00	-03:34:11.7	9.10	14 Dec 2011	3 × 700
276	J07111+434 AB	LP 206-011	...	07:11:11.38	+43:29:59.0	9.98	01 Jan 2012	3 × 700
277	J07172-050	SCR J0717-0501	...	07:17:17.10	-05:01:03.1	8.87	14 Feb 2013	1 × 500
278	J07182+137	PM 107182+1342	...	07:18:12.91	+13:42:16.7	9.36	13 Dec 2011	1 × 300
279	J07191+667	HD 55745 B	...	07:19:09.18	+66:44:29.8	8.88	12 Feb 2013	1 × 600
280	J07195+328	BD+33 1505	270	07:19:31.28	+32:49:48.3	7.18	03 Mar 2012	1 × 150
281	J07219-222	PM I07219-2216	...	07:21:57.50	-22:16:38.4	10.00	10 Jan 2012	1 × 800
282	J07274+052	Luyten's star	273	07:27:24.50	+05:13:32.9	5.71	12 Nov 2011	1 × 180
283	J07310+460	IRXS J073101.9+460030	...	07:31:01.29	+46:00:26.6	9.95	13 Dec 2011	1 × 700
284	J07319+362N	BL Lyn	277 B	07:31:57.35	+36:13:47.8	7.57	06 Mar 2012	1 × 200
285	J07319+362S AB	VV Lyn	277 A	07:31:57.74	+36:13:10.2	6.77	06 Mar 2012	1 × 200
286	J07321-088	HD 59984 B	3450	07:32:07.26	-08:53:01.7	8.03	12 Feb 2013	1 × 200
287	J07324-130	PM I07324-1304	...	07:32:28.40	-13:04:09.0	9.89	04 Jan 2012	1 × 1200
288	J07359+785	LP 017-066	...	07:35:58.15	+78:32:52.9	9.21	03 Jan 2012	1 × 210
289	J07361-031	HD 61606 C	282 C	07:36:07.10	-03:06:38.7	6.79	13 Dec 2011	1 × 300
290	J07365-006	PM 107365-0039	...	07:36:30.27	-00:39:35.2	9.42	10 Jan 2012	1 × 500
291	J07366+440	G 111-020	...	07:36:39.28	+44:04:48.9	9.96	13 Dec 2011	1 × 500
292	J07420+142	NZ Gem	...	07:42:02.22	+14:12:30.6	1.59	07 Dec 2011	1 × 8
293	J07429-107	PM I07429-1043	...	07:42:55.70	-10:43:45.2	9.52	10 Jan 2012	1 × 500
294	J07467+574	G 193-065	...	07:46:42.03	+57:26:53.4	9.70	14 Dec 2011	1 × 600
295	J07470+760	LP 017-075	...	07:47:05.83	+76:03:19.6	9.98	03 Jan 2012	1 × 700
296	J07497-033	2MASS J07494215-0320338	...	07:49:42.10	-03:20:33.9	8.89	14 Feb 2013	1 × 220
297	J07498-032	IRXS J074948.5-031712	...	07:49:50.90	-03:17:19.5	8.04	14 Feb 2013	1 × 120
298	J07523+162	LP 423-031	...	07:52:23.90	+16:12:15.7	10.88	22 Sep 2012	3 × 900
299	J07545-096	PM 107545-0941	...	07:54:32.73	-09:41:47.8	9.70	09 Feb 2012	1 × 623
300	J07545+085	LSPM J0754+0832	...	07:54:34.12	+08:32:25.3	8.54	14 Dec 2011	1 × 800
301	J07558+833	LP 005-088	1101	07:55:53.97	+83:23:05.0	8.74	19 Mar 2011	2 × 1000
302	J07591+173	IRXS J075908.2+171957	...	07:59:07.19	+17:19:47.4	9.47	01 Jan 2012	1 × 327
303	J08025-130	LP 724-016	...	08:02:32.91	-13:05:29.1	9.42	13 Dec 2011	1 × 300
304	J08031+203 AB	2MASS J08031018+2022154	...	08:03:10.18	+20:22:15.5	9.24	07 Dec 2011	1 × 300
305	J08069+422	G 111-056	...	08:06:55.32	+42:17:33.4	9.72	07 Dec 2011	1 × 550
306	J08082+211N	BD+21 1764A	3481	08:08:13.18	+21:06:18.2	6.86	09 Jan 2012	1 × 200
307	J08082+211S AB	BD+21 1764B	3482	08:08:13.59	+21:06:09.4	7.34	10 Feb 2012	1 × 200
308	J08104-111	TYC 5430-1154-1	...	08:10:26.50	-11:09:37.0	8.29	14 Feb 2013	1 × 120
309	J08105-138 AB	18 Pup B	297.2 B	08:10:34.29	-13:48:51.4	8.28	09 Feb 2012	1 × 220
310	J08117+531	G 194-014	...	08:11:47.60	+53:11:51.3	9.29	07 Dec 2011	1 × 350
311	J08143+630	HD 67850 B	...	08:14:18.97	+63:04:39.8	9.91	15 Feb 2013	1 × 250
312	J08161+013	GJ 2066	2066	08:16:07.98	+01:18:09.2	6.63	03 Mar 2012	1 × 100
313	J08283+553	PM 108283+5522	...	08:28:18.81	+55:22:42.4	9.24	01 Jan 2012	1 × 248
314	J08286+660	2E 1987	...	08:28:41.22	+66:02:23.9	9.20	07 Dec 2011	1 × 400
315	J08298+267	DX Cnc	1111	08:29:49.50	+26:46:34.8	8.24	14 Nov 2011	1 × 1200
316	J08353+141	LSPM J0835+1408	...	08:35:19.93	+14:08:33.4	9.16	07 Dec 2011	1 × 450
317	J08375+035	LSPM J0837+0333	...	08:37:30.21	+03:33:45.8	9.85	13 Dec 2011	1 × 700
318	J08386-028	GWP 1056 A	...	08:38:37.31	-02:48:59.4	10.57	14 Feb 2013	1 × 120
319	J08394-028	GWP 1056 B	...	08:39:24.54	-02:49:11.4	12.14	14 Feb 2013	3 × 600
320	J08423-048	G 114-014	...	08:42:23.20	-04:53:55.1	9.05	13 Dec 2011	1 × 900

Table A.1. Observed stars: identification, common name, Gliese number, 2MASS coordinates and J magnitude, observing date, and exposure time (cont.).

No.	Karmn	Name	Gl/GJ	α (J2000)	δ (J2000)	J [mag]	Observation date	$N \times t_{\text{exp}}$ [s]
321	J08449–066 AB	2MASS J08445566–0637259	...	08:44:55.67	−06:37:25.9	9.33	14 Dec 2011	1 × 350
322	J08526+283	ρ Cnc B	324 B	08:52:40.85	+28:18:58.9	8.56	09 Feb 2012	1 × 300
323	J08531–202	RAVE J085310.9–201717	...	08:53:10.91	−20:17:17.3	9.32	13 Dec 2011	1 × 300
324	J08563–044	LP 666–044	...	08:56:18.80	−04:24:55.2	9.78	13 Dec 2011	1 × 900
325	J08572+194	LP 426–035	...	08:57:15.41	+19:24:17.8	9.45	02 Jan 2012	1 × 350
326	J08590+364	G 115–039	...	08:59:05.40	+36:26:31.9	8.85	08 Dec 2011	1 × 1000
327	J08595+537	G 194–047	...	08:59:35.93	+53:43:50.5	9.01	01 Jan 2012	1 × 226
328	J08599+042	PM 108599+0417	...	08:59:57.60	+04:17:55.3	9.93	14 Dec 2011	1 × 600
329	J09003+218	LP 368–128	...	09:00:23.59	+21:50:05.4	9.44	06 Mar 2012	3 × 800
330	J09008+237	HD 77052 B	...	09:00:53.23	+23:46:58.5	11.40	15 Feb 2013	3 × 500
331	J09023+177	2MASS J09022307+1746326	...	09:02:23.08	+17:46:32.6	9.65	03 Jan 2012	1 × 500
332	J09028+060	BD+06 2091B	...	09:02:53.20	+06:02:09.6	11.26	14 Feb 2013	1 × 900
333	J09040–159	IRXS J090406.8–155512	...	09:04:05.55	−15:55:18.4	9.16	03 Jan 2012	1 × 210
334	J09045+164 AB	BD+16 1895	...	09:04:31.00	+16:25:01.6	9.10	03 Jan 2012	1 × 300
335	J09058+555	HD 77599 B	...	09:05:51.18	+55:32:18.4	11.49	15 Feb 2013	3 × 450
336	J09091+227	[ACM2004] J0909+2247	...	09:09:07.99	+22:47:41.3	10.47	09 Jan 2012	3 × 450
337	J09115+126	LP 487–010	...	09:11:31.95	+12:37:23.7	9.41	01 Jan 2012	1 × 226
338	J09143+526	HD 79210	338 A	09:14:22.98	+52:41:12.5	4.89	10 Feb 2012	1 × 30
339	J09144+526	HD 79211	338 B	09:14:24.86	+52:41:11.8	4.78	10 Feb 2012	1 × 30
340	J09151+233	HD 79498 B	...	09:15:10.12	+23:21:33.1	9.14	14 Feb 2013	1 × 300
341	J09156–105 AB	G 161–007	...	09:15:36.40	−10:35:47.2	8.61	14 Feb 2013	1 × 500
342	J09201+037	IRXS J092010.8+034731	...	09:20:10.87	+03:47:25.8	9.31	09 Jan 2012	1 × 300
343	J09206–169	PM I09206–1654	...	09:20:40.00	−16:54:58.4	9.57	10 Jan 2012	1 × 600
344	J09212+603	BD+61 1116B	...	09:21:17.62	+60:21:46.7	9.13	15 Feb 2013	1 × 250
345	J09218–023	RAVE J09218.1–021943	...	09:21:48.13	−02:19:43.4	8.44	13 Dec 2011	1 × 700
346	J09243+063	HD 81212 C	...	09:24:23.86	+06:22:41.8	10.60	14 Feb 2013	1 × 600
347	J09248+306	RX J0924.8+3041	...	09:24:50.83	+30:41:37.3	9.49	14 Dec 2011	1 × 400
348	J09256+634	G 235–025	...	09:25:40.33	+63:29:19.7	9.82	14 Dec 2011	1 × 900
349	J09301–009	LP 607–057	...	09:30:08.60	−00:57:58.8	8.76	13 Dec 2011	1 × 350
350	J09308+024	IRXS J093051.2+022741	...	09:30:50.85	+02:27:20.2	9.42	04 Jan 2012	1 × 700
351	J09328+269	DX Leo B	354.1 B	09:32:48.27	+26:59:44.3	10.36	09 Jan 2012	1 × 1000
352	J09351–103	HD 83008 B	...	09:35:11.84	−10:18:34.0	9.08	15 Feb 2013	1 × 220
353	J09362+375	HD 89239 B	9303	09:36:15.91	+37:31:45.5	8.09	15 Feb 2013	1 × 150
354	J09394+146	NLTT 22280	...	09:39:29.94	+14:38:49.8	9.39	03 Jan 2012	1 × 300
355	J09449–123	G 161–071	...	09:44:54.20	−12:20:54.4	8.50	13 Feb 2013	1 × 600
356	J09488+156	G 043–002	...	09:48:50.20	+15:38:44.9	9.30	03 Jan 2012	1 × 300
357	J09526–156	LP 728–071	...	09:52:41.77	−15:36:13.8	9.32	03 Mar 2012	1 × 700
358	J09538–073	TYC 4902–210–1	...	09:53:51.70	−07:20:07.9	7.83	13 Feb 2013	1 × 180
359	J09589+059	NLTT 23096	...	09:58:56.51	+05:58:00.1	9.94	02 Jan 2012	1 × 1100
360	J09597+721	Pul–3 620285	...	09:59:45.35	+72:11:59.8	9.06	03 Jan 2012	1 × 200
361	J10008+319	20 LMi B	376 B	10:00:50.31	+31:55:46.0	10.26	14 Feb 2013	3 × 700
362	J10020+697	LP 037–057	...	10:02:05.81	+69:45:29.4	9.77	03 Jan 2012	1 × 800
363	J10028+484	G 195–055	...	10:02:49.36	+48:27:33.4	9.96	03 Jan 2012	1 × 500
364	J10063–064	GWP 1102 A	...	10:06:20.56	−06:26:10.2	13.26	14 Feb 2013	3 × 700
365	J10068–127	2MASS J10065210–1246543	...	10:06:52.11	−12:46:54.3	9.75	10 Jan 2012	1 × 1200
366	J10098–007	BPM 73854	...	10:09:51.20	−00:46:18.9	9.01	10 Jan 2012	1 × 600
367	J10120–026 AB	LP 609–71	381 AB	10:12:04.66	−02:41:04.5	7.02	14 Nov 2011	1 × 300
368	J10130+233	G 054–018	...	10:13:00.26	+23:20:50.5	9.19	03 Jan 2012	1 × 250
369	J10148+213	G 054–019	...	10:14:53.15	+21:23:46.4	9.73	10 Jan 2012	1 × 900
370	J10155–164	WT 1774	...	10:15:35.40	−16:28:23.6	9.36	11 Jan 2012	1 × 400
371	J10196+198 AB	AD Leo	388 AB	10:19:36.35	+19:52:12.2	5.45	06 Mar 2012	1 × 40
372	J10200+289	G 118–051	...	10:20:00.88	+28:57:13.1	9.16	04 Jan 2012	1 × 400
373	J10238+438	LP 212–062	...	10:23:51.85	+43:53:33.2	10.04	04 Jan 2012	1 × 900
374	J10240+366	2MASS J10240507+3639326	...	10:24:05.07	+36:39:32.6	9.43	09 Jan 2012	1 × 400
375	J10278+028	LHS 5171	...	10:27:49.67	+02:51:36.9	9.44	11 Jan 2012	1 × 300
376	J10304+559	36 UMa B	394	10:30:25.31	+55:59:56.8	6.12	13 Feb 2013	1 × 120
377	J10359+288	RX J1035.9+2853	...	10:35:57.25	+28:53:31.7	9.25	10 Jan 2012	1 × 300
378	J10368+509	LP 127–502	...	10:36:48.12	+50:55:04.1	9.87	04 Jan 2012	1 × 900
379	J10430–092 AB	WT 1827	...	10:43:02.93	−09:12:41.1	9.67	09 Jan 2012	1 × 500
380	J10443+124	LP 490–063	...	10:44:18.82	+12:25:11.7	9.42	10 Jan 2012	1 × 400
381	J10482–113	LP 731–058	3622	10:48:12.58	−11:20:08.2	8.86	06 Mar 2012	2 × 900
382	J10508+068	EE Leo	402	10:50:52.01	+06:48:29.3	7.32	06 Mar 2012	1 × 200
383	J10546–073	LP 671–008	...	10:54:42.00	−07:18:33.1	8.88	13 Feb 2013	1 × 600
384	J10560+061	56 Leo	...	10:56:01.47	+06:11:07.3	0.43	08 Dec 2011	1 × 3
385	J10563+042	PM 110563+0415	...	10:56:22.25	+04:15:45.9	9.18	10 Jan 2012	1 × 300
386	J10564+070	CN Leo	406	10:56:28.86	+07:00:52.8	7.09	02 Jan 2012	1 × 600
387	J10584–107	BD–10 3166B	...	10:58:28.00	−10:46:30.5	9.51	04 Jan 2012	1 × 900
388	J11018–024	p^2 Leo	...	11:01:49.67	−02:29:04.5	1.78	13 Dec 2011	1 × 1
389	J11030+037	Wolf 360	...	11:03:04.27	+03:44:22.6	9.31	10 Jan 2012	1 × 300
390	J11033+359	HD 95735	411	11:03:20.24	+35:58:11.8	4.20	18 Mar 2011	1 × 10
391	J11046–042S AB	HH Leo BC	...	11:04:40.98	−04:13:24.7	7.27	06 Mar 2012	1 × 100
392	J11054+435	BD+44 2051A	412 A	11:05:29.03	+43:31:35.7	5.54	11 Feb 2012	1 × 50
393	J11055+435	BD+44 2051B (WX UMa)	412 B	11:05:31.33	+43:31:17.1	8.74	03 Mar 2012	1 × 900
394	J11075+437	HAT 141–00828	...	11:07:32.08	+43:45:56.4	9.94	09 Jan 2012	1 × 800
395	J11151+734N	HD 97584 B	420 B	11:15:11.06	+73:28:36.0	7.88	11 Jan 2012	1 × 220
396	J11151+734S	HD 97584 A	420 A	11:15:11.90	+73:28:30.7	5.78	11 Jan 2012	1 × 220
397	J11201–104 AB	LP 733–099	...	11:20:06.10	−10:29:46.8	7.81	13 Feb 2013	1 × 120
398	J11201+301	HD 98500	...	11:20:11.18	+30:07:13.7	4.34	19 Mar 2011	1 × 10
399	J11214–204S	SZ Crt A	425 A	11:21:26.56	−20:27:09.5	6.64	11 Jan 2012	1 × 200
400	J11214–204N	SZ Crt B	425 B	11:21:26.66	−20:27:13.6	6.10	11 Jan 2012	1 × 200

Table A.1. Observed stars: identification, common name, Gliese number, 2MASS coordinates and J magnitude, observing date, and exposure time (cont.).

No.	Karmn	Name	Gl/GJ	α (J2000)	δ (J2000)	J [mag]	Observation date	$N \times t_{\text{exp}}$ [s]
401	J11218+181	HD 98736 B	426 B	11:21:49.13	+18:11:28.0	7.65	12 Feb 2013	1 × 400
402	J11240+381	RX J1124.1+3808	...	11:24:04.35	+38:08:10.9	9.93	04 Jan 2012	1 × 900
403	J11306-080	LP 672-042	...	11:30:41.80	-08:05:43.1	8.03	13 Feb 2013	1 × 300
404	J11312+631	BD+63 695	430	11:31:13.09	+63:09:27.1	7.40	06 Mar 2012	1 × 60
405	J11378+418	BD+42 2230B	...	11:37:49.92	+41:49:59.5	11.04	15 Feb 2013	1 × 500
406	J11403+095	BD+10 2321B	...	11:40:20.84	+09:30:45.4	10.12	15 Feb 2013	1 × 400
407	J11421+267	Ross 905	436	11:42:10.55	+26:42:30.5	6.90	14 Nov 2011	1 × 200
408	J11451+183	LP 433-047	...	11:45:11.92	+18:02:58.7	9.16	10 Jan 2012	1 × 300
409	J11458+065	ν Vir	...	11:45:51.56	+06:31:45.7	1.18	14 Dec 2011	1 × 1
410	J11472+770	HD 102326 B	...	11:47:12.68	+77:02:35.9	9.20	15 Feb 2013	1 × 300
411	J11474+667	IRXS J114728.8+664405	...	11:47:28.57	+66:44:02.6	9.68	04 Jan 2012	1 × 1100
412	J11485+076	G 010-052	...	11:48:35.59	+07:41:40.4	9.48	10 Jan 2012	1 × 400
413	J11511+352	BD+36 2219	450	11:51:07.34	+35:16:19.2	6.42	11 Feb 2012	1 × 60
414	J11522+100	HD 103112 B	3690	11:52:17.93	+10:00:39.2	11.42	11 Feb 2012	2 × 900
415	J11549-021	PM I11549-0206	...	11:54:56.93	-02:06:09.2	9.55	10 Jan 2012	1 × 600
416	J12025+084	LHS 320	...	12:02:33.65	+08:25:50.6	10.74	03 Jan 2012	1 × 600
417	J12049+174	HD 104923 B	...	12:04:56.11	+17:28:11.9	9.79	12 Feb 2013	1 × 600
418	J12069+058	HD 105219 B	...	12:06:56.94	+05:48:09.3	8.58	15 Feb 2013	1 × 300
419	J12088+217	BD+22 2442B	...	12:08:55.41	+21:47:31.6	11.15	13 Feb 2013	1 × 1800
420	J12093+210	StM 165	...	12:09:21.81	+21:03:07.7	9.47	04 Jan 2012	1 × 600
421	J12104-131	NLTT 29827	...	12:10:28.34	-13:10:23.5	9.29	10 Jan 2012	1 × 400
422	J12124+121	PM I12124+1211	...	12:12:26.06	+12:11:38.1	9.39	10 Jan 2012	1 × 300
423	J12162+508	RX J1216.2+5053	...	12:16:15.06	+50:53:37.7	9.29	09 Jan 2012	1 × 400
424	J12228-040	G 013-033	...	12:22:50.62	-04:04:46.2	9.66	10 Jan 2012	1 × 600
425	J12322+454	BW CVn	...	12:32:14.37	+45:29:50.4	4.81	19 Mar 2011	1 × 30
426	J12349+322	PM I12349+3214	...	12:34:54.01	+32:14:27.9	9.46	04 Jan 2012	1 × 600
427	J12364+352	G 123-045	...	12:36:28.70	+35:12:00.8	9.11	09 Jan 2012	1 × 350
428	J12368-019	RAVE J123652.2-015901	...	12:36:52.15	-01:59:00.7	9.44	10 Jan 2012	1 × 300
429	J12372+358	BD+36 2288B	...	12:37:15.47	+35:49:17.7	11.35	15 Feb 2013	1 × 1100
430	J12417+567	RX J1241.7+5645	...	12:41:47.37	+56:45:13.8	9.48	04 Jan 2012	1 × 600
431	J12440-111	LP 735-029	...	12:44:00.76	-11:10:30.2	9.52	10 Jan 2012	1 × 500
432	J12456+271	HD 110964	...	12:45:36.99	+27:07:44.3	5.09	06 Mar 2012	1 × 30
433	J12470+466	Ross 991	3748	12:47:01.02	+46:37:33.4	8.10	06 Mar 2012	1 × 200
434	J12488+120	HD 111398 B	...	12:48:53.45	+12:04:32.7	11.40	14 Feb 2013	3 × 1000
435	J12533-053	LP 676-026	...	12:53:19.40	-05:19:52.5	8.92	13 Feb 2013	1 × 400
436	J12533+466	BZ CVn	...	12:53:20.02	+46:39:22.9	3.36	19 Mar 2011	1 × 15
437	J12549-063	BD-05 3596B	488.2 B	12:54:55.12	-06:20:03.9	11.38	09 Feb 2012	3 × 800
438	J12593-001	LP 616-056	...	12:59:18.20	-00:10:33.4	8.79	14 Feb 2013	1 × 300
439	J13027+415	G 123-084	...	13:02:47.52	+41:31:09.9	9.03	10 Jan 2012	1 × 200
440	J13088-015	LP 617-004	...	13:08:51.20	-01:31:07.6	8.92	14 Feb 2013	1 × 300
441	J13102+477	G 177-025	...	13:10:12.69	+47:45:19.0	9.58	09 Jan 2012	1 × 1200
442	J13113+096	HD 114606 B	9431 B	13:11:22.44	+09:36:13.2	9.68	15 Feb 2013	1 × 400
443	J13143+133 AB	NLTT 33370	...	13:14:20.39	+13:20:01.2	9.75	09 Jan 2012	2 × 800
444	J13167-123	LP 737-014	...	13:16:45.46	-12:20:20.4	9.49	11 Jan 2012	1 × 300
445	J13168+170	HD 115404 B	505 B	13:16:51.54	+17:00:59.9	6.53	09 Feb 2012	1 × 60
446	J13179+362	GJ 1170	1170	13:17:58.40	+36:17:56.9	8.11	18 Mar 2011	1 × 800
447	J13182+733	PM I13182+7322	...	13:18:13.52	+73:22:07.4	9.54	11 Jan 2012	1 × 500
448	J13247-050	G 014-052	...	13:24:46.48	-05:04:19.4	9.47	11 Feb 2012	1 × 300
449	J13251-114	PM I13251-1126	...	13:25:11.72	-11:26:36.8	9.16	11 Jan 2012	1 × 250
450	J13253+426	BD+43 2328B	...	13:25:23.50	+42:41:29.6	9.08	15 Feb 2013	1 × 300
451	J13260+275	IRXS J132601.9+273449	...	13:26:02.68	+27:35:02.1	9.25	11 Jan 2012	1 × 250
452	J13294-143	IRXS J132923.9-142206	...	13:29:24.08	-14:22:12.3	9.06	11 Jan 2012	1 × 200
453	J13312+589	PM I13312+5857	...	13:31:12.50	+58:57:19.0	10.95	18 Apr 2013	2 × 500
454	J13314-079	HD 117579 B	...	13:31:29.79	-07:59:54.9	9.60	15 Feb 2013	1 × 400
455	J13321-112	HD 117676 B	...	13:32:06.86	-11:16:40.8	9.45	15 Feb 2013	1 × 300
456	J13326+309	LP 323-169	...	13:32:39.08	+30:59:06.5	9.62	11 Jan 2012	1 × 900
457	J13335+704	2MASS J1333371+7029412	...	13:33:33.72	+70:29:41.3	9.23	11 Jan 2012	1 × 300
458	J13386-115	IRXS J133841.3-113137	...	13:38:40.87	-11:32:07.8	9.71	11 Jan 2012	1 × 600
459	J13394+461 AB	BD+46 1889	521 AB	13:39:24.10	+46:11:11.4	7.05	06 Mar 2012	1 × 90
460	J13413-091	PM I13413-0907	...	13:41:21.22	-09:07:17.1	9.44	11 Jan 2012	1 × 300
461	J13414+489	StM 186	...	13:41:27.70	+48:54:45.9	9.00	12 Feb 2013	1 × 500
462	J13474+063	HD 120066 B	...	13:47:28.80	+06:18:56.4	7.76	12 Feb 2013	1 × 200
463	J13503-216	LP 798-041	...	13:50:23.77	-21:37:19.3	9.46	09 Feb 2012	1 × 272
464	J13537+521 AB	IRXS J135348.0+521036	...	13:53:45.89	+52:10:29.9	9.13	11 Jan 2012	1 × 300
465	J13551-079	BPM 76486	...	13:55:10.80	-07:56:59.2	8.73	14 Feb 2013	1 × 250
466	J13555-073	G 064-028	...	13:55:35.10	-07:23:16.6	8.81	14 Feb 2013	1 × 150
467	J13582-120	LP 739-002	...	13:58:16.22	-12:02:59.2	9.73	11 Jan 2012	1 × 600
468	J13583-132	LP 739-003	...	13:58:19.56	-13:16:24.8	9.49	09 Feb 2012	1 × 518
469	J13587+465	HD 122132	...	13:58:45.70	+46:35:46.5	4.12	19 Mar 2011	1 × 10
470	J14019+432	PM I14019+4316	...	14:01:58.79	+43:16:42.7	9.28	09 Feb 2012	1 × 226
471	J14102-180	IRXS J141553.4-110227	...	14:10:12.70	-18:01:16.3	10.03	11 Feb 2012	3 × 500
472	J14159-110	PM I14159-1102	...	14:15:54.20	-11:02:44.6	9.00	12 Feb 2013	1 × 400
473	J14171+088	PM I14171+0851	...	14:17:07.31	+08:51:36.3	9.11	09 Feb 2012	1 × 431
474	J14175+025	RX J1417.5+0233	...	14:17:30.21	+02:33:43.6	9.27	11 Feb 2012	1 × 220
475	J14194+029	NLTT 36959	...	14:19:29.58	+02:54:36.5	9.95	09 Feb 2012	3 × 450
476	J14195-051	HD 125455 B	544 B	14:19:35.85	-05:09:08.0	10.49	12 Feb 2013	1 × 900
477	J14215-079	PM I14215-0755	...	14:21:34.06	-07:55:16.6	9.46	11 Feb 2012	1 × 327
478	J14227+164	NLTT 37131	...	14:22:43.41	+16:24:46.4	10.30	09 Feb 2012	3 × 600
479	J14244+602	BD+60 1536B	...	14:24:27.44	+60:15:17.0	9.73	12 Feb 2013	1 × 1500
480	J14251+518	θ Boo B	549 B	14:25:11.61	+51:49:53.5	7.88	11 Feb 2012	1 × 200
481	J14255-118	LP 740-010	...	14:25:34.13	-11:48:51.5	9.35	11 Feb 2012	1 × 327

Table A.1. Observed stars: identification, common name, Gliese number, 2MASS coordinates and J magnitude, observing date, and exposure time (cont.).

No.	Karmn	Name	Gl/GJ	α (J2000)	δ (J2000)	J [mag]	Observation date	$N \times t_{\text{exp}}$ [s]
482	J14312+754	LSPM J1431+7526	...	14:31:13.49	+75:26:42.4	9.79	09 Feb 2012	1 \times 568
483	J14336+093	HD 127871 B	...	14:33:39.86	+09:20:09.5	10.23	18 Apr 2013	1 \times 700
484	J14415+136	HD 129290 B	...	14:41:30.25	+13:37:36.2	10.35	12 Feb 2013	1 \times 800
485	J14446-222	HD 129715 B	3865	14:44:40.13	-22:14:45.5	10.57	12 Feb 2013	1 \times 600
486	J14472+570	RX J1447.2+5701	...	14:47:13.54	+57:01:55.1	9.91	09 Feb 2012	1 \times 623
487	J14480+384	BD+39 2801	563.1	14:48:01.43	+38:27:58.4	7.23	18 Mar 2011	1 \times 340
488	J14485+101	G 066-027	...	14:48:33.16	+10:06:57.4	9.48	09 Feb 2012	1 \times 272
489	J14492+498	PM I14492+4949	...	14:49:14.77	+49:49:39.1	10.24	18 Apr 2013	1 \times 450
490	J14501+323	LP 326-034	...	14:50:11.12	+32:18:17.3	9.14	09 Feb 2012	1 \times 206
491	J14544+161 ABC	CE Boo	569	14:54:29.23	+16:06:04.0	6.63	06 Mar 2012	1 \times 90
492	J14595+454	HD 132830 B	...	14:59:30.59	+45:26:52.9	8.10	15 Feb 2013	1 \times 200
493	J15079+762	HD 135363 B	...	15:07:57.24	+76:13:59.0	9.24	11 Feb 2012	1 \times 500
494	J15081+623	LSPM J1508+6221	...	15:08:11.93	+62:21:53.6	9.30	11 Feb 2012	1 \times 300
495	J15118+395	HD 135144 B	...	15:11:51.45	+39:33:02.4	9.87	12 Feb 2013	1 \times 1200
496	J15131+181	PM I15131+1808N	...	15:13:06.62	+18:08:44.2	11.02	18 Apr 2013	1 \times 700
497	J15142-099	PM I15142-0958	...	15:14:16.90	-09:58:38.8	9.67	12 Feb 2013	1 \times 1200
498	J15147+645	G 224-057	...	15:14:46.81	+64:33:43.9	9.79	11 Feb 2012	1 \times 700
499	J15151+333	LP 272-063	...	15:15:07.06	+33:18:03.3	9.21	11 Feb 2012	1 \times 200
500	J15157-074	LTT 6084	...	15:15:43.70	-07:25:21.1	8.57	14 Feb 2013	1 \times 120
501	J15164+167	HD 135792 B	...	15:16:25.29	+16:47:41.5	7.82	15 Feb 2013	1 \times 300
502	J15197+046	PM I15197+0439	...	15:19:45.85	+04:39:34.5	9.55	11 Feb 2012	1 \times 500
503	J15204+001	HD 136378 B	...	15:20:28.30	+00:11:26.9	9.43	14 Feb 2013	1 \times 300
504	J15210+255	HD 136655 B	...	15:21:04.80	+25:33:30.2	8.46	15 Feb 2013	1 \times 220
505	J15238+584	G 224-065	...	15:23:51.44	+58:28:06.4	9.91	11 Feb 2012	1 \times 650
506	J15277-090	HD 137763 C	586 C	15:27:45.03	-09:01:32.8	10.55	14 Feb 2013	3 \times 500
507	J15290+467 AB	RX J1529.0+4646	...	15:29:02.97	+46:46:24.0	9.94	09 Feb 2012	3 \times 450
508	J15291+574	HD 138367 B	...	15:29:09.36	+57:24:41.8	8.83	14 Feb 2013	1 \times 300
509	J15305+094	NLTT 40406	...	15:30:30.33	+09:26:01.4	9.57	11 Feb 2012	3 \times 450
510	J15340+513	LP 135-414	...	15:34:03.87	+51:22:02.4	9.37	11 Feb 2012	1 \times 500
511	J15386+371	G 179-042	...	15:38:37.08	+37:07:24.7	9.98	11 Feb 2012	1 \times 700
512	J15430-130	PM I15430-1302	...	15:43:05.68	-13:02:52.0	10.24	18 Apr 2013	1 \times 300
513	J15474+451	LP 177-102	...	15:47:27.44	+45:07:51.2	9.08	11 Feb 2012	1 \times 300
514	J15476+226	LSPM J1547+2241	...	15:47:40.71	+22:41:16.5	9.54	11 Feb 2012	1 \times 600
515	J15480+043	RX J1548.0+0421	...	15:48:02.80	+04:21:39.3	9.06	11 Feb 2012	1 \times 188
516	J15481+015	V382 Ser B	3917 B	15:48:09.30	+01:34:36.0	9.30	10 Feb 2012	1 \times 500
517	J15499+796	G 256-025	...	15:49:55.18	+79:39:51.7	9.72	11 Feb 2012	1 \times 900
518	J15552-101	RAVE J155514.5-101023	...	15:55:14.50	-10:10:23.1	8.48	13 Feb 2013	1 \times 200
519	J15557-103	IRXS J155542.1-102012	...	15:55:42.30	-10:20:01.6	9.40	12 Feb 2013	1 \times 600
520	J15558-118	LP 743-053	...	15:55:52.20	-11:54:19.6	8.98	13 Feb 2013	1 \times 400
521	J15569+376	RX J1556.9+37381	...	15:56:58.24	+37:38:13.8	9.42	11 Feb 2012	1 \times 250
522	J15578+090	LSPM J1557+0901	...	15:57:48.27	+09:01:09.9	9.28	11 Feb 2012	1 \times 327
523	J16023+036	HD 143809 B	...	16:02:16.91	+03:38:41.2	10.35	10 Feb 2012	1 \times 600
524	J16042+235	LSPM J1604+2331	...	16:04:13.20	+23:31:38.7	9.97	02 Aug 2012	3 \times 350
525	J16048+391	HD 144579 B	611 B	16:04:50.93	+39:09:36.0	9.90	12 Feb 2013	1 \times 1200
526	J16120+033N	IRXS J161204.8+031850	...	16:12:05.00	+03:18:53.3	9.96	23 Sep 2012	1 \times 900
527	J16139+337 AB	σ CrB C	615.2 C	16:13:56.27	+33:46:24.3	8.60	12 Feb 2013	1 \times 400
528	J16148+606 AB	HD 146868 B	...	16:14:52.97	+60:38:27.8	9.82	12 Feb 2013	1 \times 1500
529	J16157+586	G 225-054	...	16:16:42.20	+58:39:43.1	10.18	04 Aug 2012	1 \times 750
530	J16167+672S	HD 147379	617 A	16:16:42.80	+67:14:19.7	5.78	18 Mar 2011	1 \times 40
531	J16183+757	η UMi B	3951 B	16:18:20.95	+75:43:08.1	10.84	18 Apr 2013	3 \times 500
532	J16243+199	RX J1624.3+1959	...	16:24:22.70	+19:59:22.6	9.32	06 Aug 2012	1 \times 400
533	J16254+543	GJ 625	625	16:25:24.59	+54:18:14.9	6.61	02 Sep 2012	1 \times 120
534	J16269+149	2E 3693	...	16:26:54.40	+14:57:50.2	9.75	23 Sep 2012	1 \times 900
535	J16276-035 AB	MCC 765	...	16:27:39.20	-03:35:03.4	8.54	13 Feb 2013	1 \times 400
536	J16299+048	PM I16299+0453	...	16:29:54.70	+04:53:25.4	9.15	03 Aug 2012	1 \times 200
537	J16314+471	LSPM J1631+4710	...	16:31:28.10	+47:10:21.3	9.40	06 Aug 2012	1 \times 500
538	J16330+031	HD 149162 C	9566 C	16:33:02.79	+03:11:37.2	10.63	18 Apr 2013	1 \times 500
539	J16354-039	BD-03 3968B	629.2 B	16:35:29.11	-03:57:58.6	11.09	18 Apr 2013	1 \times 350
540	J16365+287	G 169-019	...	16:36:30.30	+28:46:42.3	9.45	04 Sep 2012	1 \times 330
541	J16459+609	LP 101-126	...	16:45:55.00	+60:57:04.1	9.39	06 Aug 2012	1 \times 600
542	J16465+345	LP 276-022	...	16:46:31.55	+34:34:55.5	10.53	03 Aug 2012	3 \times 900
543	J16480+453	RX J1648.0+4522	...	16:48:04.50	+45:22:43.0	9.35	06 Aug 2012	1 \times 800
544	J16528+610	LSPM J1652+6304	...	16:52:49.50	+63:04:38.9	9.59	23 Sep 2012	1 \times 900
545	J16536+560	G 226-033	...	16:53:39.20	+56:03:27.3	9.86	04 Sep 2012	1 \times 600
546	J16543+256	LP 387-019	...	16:54:19.10	+25:37:36.5	9.39	25 Sep 2012	1 \times 300
547	J16555-083	V1054 Oph D (vB 8)	644 C	16:55:35.29	-08:23:40.1	9.78	02 Aug 2012	2 \times 1200 + 1 \times 900
548	J17011+555	LP 138-020	...	17:01:11.60	+55:35:00.3	9.15	05 Aug 2012	1 \times 240
549	J17017+741	LP 043-292	...	17:01:45.90	+74:11:51.3	9.44	04 Sep 2012	1 \times 400
550	J17052-050	HD 154363 B	654	17:05:13.78	-05:05:39.2	6.78	18 Apr 2013	1 \times 100
551	J17062+646	G 240-044	...	17:06:17.70	+64:38:09.1	9.38	05 Aug 2012	1 \times 250
552	J17094+391	Wolf 648	...	17:09:26.00	+39:09:37.4	9.84	23 Sep 2012	1 \times 900
553	J17126-099	Ruber 7	...	17:12:40.72	-09:54:12.1	6.19	19 Mar 2011	1 \times 200
554	J17140+176	LP 447-021	...	17:14:01.50	+17:38:55.0	9.28	25 Sep 2012	1 \times 250
555	J17154+308	G 181-032	...	17:15:28.00	+30:52:22.0	9.45	25 Sep 2012	1 \times 250
556	J17163-053	LP 687-017	...	17:16:20.60	-05:23:51.4	8.70	13 Feb 2013	1 \times 300
557	J17167+115	LSPM J1716+1133	...	17:16:47.80	+11:33:52.3	9.80	04 Sep 2012	1 \times 600
558	J17176+524	HD 156985 B	...	17:17:38.60	+52:24:22.4	9.77	05 Aug 2012	1 \times 700
559	J17198+265	V639 Her	669 B	17:19:52.98	+26:30:02.6	8.23	06 Aug 2012	1 \times 800
560	J17199+265	V647 Her	669 A	17:19:54.20	+26:30:03.1	7.27	06 Aug 2012	1 \times 600
561	J17199+242	V475 Her	...	17:19:59.50	+24:12:05.4	9.75	25 Sep 2012	1 \times 570

Table A.1. Observed stars: identification, common name, Gliese number, 2MASS coordinates and J magnitude, observing date, and exposure time (cont.).

No.	Karmn	Name	Gl/GJ	α (J2000)	δ (J2000)	J [mag]	Observation date	$N \times t_{\text{exp}}$ [s]
562	J17216–171	TYC 6238–480–1	...	17:21:39.95	–17:11:29.5	6.15	19 Mar 2011	1 × 100
563	J17239+136	LSPM J1723+1338	...	17:23:56.80	+13:38:20.2	9.50	25 Sep 2012	1 × 500 + 1 × 400
564	J17246+617	LSPM J1724+6147	...	17:24:39.90	+61:47:50.8	9.45	05 Aug 2012	1 × 250
565	J17265–227	IRXS J172635.8–224359	...	17:26:35.40	–22:44:02.2	9.56	25 Sep 2012	1 × 600
566	J17267–050	PM I17267–0500	...	17:26:46.80	–05:00:35.6	9.48	18 Apr 2013	1 × 280
567	J17270+422	HD 158415 B	...	17:27:03.09	+42:14:07.8	8.50	18 Apr 2013	1 × 160
568	J17281–017	SCR J1728–0143	...	17:28:11.10	–01:43:57.0	9.89	18 Apr 2013	1 × 700
569	J17299–209	LP 807–018	...	17:29:58.60	–20:59:24.6	9.78	25 Sep 2012	1 × 900
570	J17301+546	LSPM J1730+5439	...	17:30:06.10	+54:39:32.2	9.04	05 Aug 2012	1 × 210
571	J17304+337	LSPM J1730+3344	...	17:30:26.70	+33:44:52.5	9.46	04 Sep 2012	1 × 300
572	J17364+683	BD+68 946	687	17:36:25.94	+68:20:22.0	5.34	11 Nov 2011	1 × 60
573	J17412+724	G 258–17	...	17:41:16.12	+72:26:32.0	10.28	18 Apr 2013	3 × 450
574	J17426+756	LP 024–054	...	17:42:41.60	+75:37:18.8	9.68	23 Sep 2012	1 × 900
575	J17428+167	BD+16 3268B	...	17:42:52.04	+16:43:47.9	10.40	14 Feb 2013	1 × 450
576	J17464+277 AB	μ Her BC	695 BC	17:46:25.08	+27:43:01.4	5.77	23 Sep 2012	1 × 180
577	J17477+277	BD+27 2891B	...	17:47:44.32	+27:47:07.4	11.42	14 Feb 2013	2 × 500
578	J17520+566	RX J1752.0+5636	...	17:52:02.90	+56:36:27.8	9.23	23 Sep 2012	1 × 500
579	J17559+294	PM I17559+2926	...	17:55:58.00	+29:26:09.8	9.76	24 Sep 2012	2 × 900
580	J17578+046	Barnard's star	699	17:57:48.49	+04:41:40.5	5.24	04 Aug 2012	1 × 80
581	J17578+465	G 204–039	4040 A	17:57:50.96	+46:35:18.2	7.85	19 Mar 2011	1 × 100
582	J18006+685	BD+68 971B	...	18:00:36.96	+68:32:54.0	9.67	18 Apr 2013	1 × 250
583	J18007+295	HD 164595 B	...	18:00:45.44	+29:33:56.7	9.06	12 Nov 2011	1 × 300
584	J18019+001	PM I18019+0007	...	18:01:58.30	+00:07:50.2	10.13	05 Aug 2012	3 × 500
585	J18022+642	LP 071–082	...	18:02:16.60	+64:15:44.3	8.54	24 Sep 2012	1 × 500
586	J18028–030	PM I18028–0300	...	18:02:49.40	–03:00:02.6	9.44	25 Sep 2012	1 × 250
587	J18036–189	G 154–043	...	18:03:36.10	–18:58:50.5	9.13	25 Sep 2012	1 × 400
588	J18041+838	LSPM J1804+8350	...	18:04:10.60	+83:50:28.1	9.02	24 Sep 2012	1 × 700
589	J18046+139	LSPM J1804+1354	...	18:04:38.70	+13:54:14.3	9.47	18 Apr 2013	1 × 300
590	J18054+015	G 140–036	...	18:05:29.10	+01:32:36.0	9.11	18 Apr 2013	1 × 350
591	J18057–143	PM I18057–1422	...	18:05:44.70	–14:22:42.4	9.78	02 Sep 2012	3 × 500
592	J18068+177	LP 449–010	...	18:06:48.60	+17:20:47.2	9.49	24 Sep 2012	1 × 900
593	J18090+241	HD 166301 B	...	18:09:01.93	+24:09:04.2	9.30	18 Apr 2013	1 × 240
594	J18112–010	IRXS J181115.2–010111	...	18:11:14.90	–01:01:11.7	10.19	04 Aug 2012	4 × 600
595	J18130+414	HD 167389 B	...	18:13:00.02	+41:29:19.6	10.21	15 Feb 2013	1 × 500
596	J18131+260 AB	LP 390–016	4044 AB	18:13:06.57	+26:01:51.9	8.90	23 Sep 2012	1 × 240
597	J18135+055	NLTT 46124	...	18:13:33.20	+05:32:12.0	9.70	25 Sep 2012	1 × 600 + 1 × 520
598	J18149+196	Wolf 832	...	18:14:59.90	+19:39:26.0	9.44	06 Aug 2012	1 × 500
599	J18162+686	BD+68 986B	...	18:16:14.75	+68:40:27.8	11.53	15 Feb 2013	3 × 500
600	J18224+620	LP 103–305	1227	18:22:27.19	+62:03:02.5	8.64	18 Mar 2011	1 × 700
601	J18253+186	PM I18252+1839	...	18:25:18.00	+18:39:09.1	9.57	06 Aug 2012	1 × 900
602	J18306–039	PM I18306–0356	...	18:30:39.50	–03:56:19.0	9.72	25 Sep 2012	1 × 700
603	J18313+649	RX J1831.3+6454	...	18:31:21.80	+64:54:13.3	9.36	06 Aug 2012	1 × 500
604	J18338+194	NLTT 46663	...	18:33:50.10	+19:26:11.2	9.16	25 Sep 2012	1 × 400
605	J18353+457	BD+45 2743	720 A	18:35:18.33	+45:44:37.9	6.88	11 Nov 2011	1 × 90
606	J18354+457	BD+45 2743B (vB 9)	720 B	18:35:27.23	+45:45:40.3	8.89	11 Nov 2011	1 × 500
607	J18400+726	LP 044–334	...	18:40:02.38	+72:40:54.0	10.97	02 Aug 2012	3 × 1200
608	J18409+315	BD+31 3330B	...	18:40:54.98	+31:32:04.8	6.80	15 Feb 2013	1 × 220
609	J18423–013	Ruber 8	...	18:42:20.54	–01:20:15.2	6.18	19 Mar 2011	1 × 150
610	J18427+596N	HD 173739	725 A	18:42:46.66	+59:37:49.9	5.19	12 Nov 2011	1 × 180
611	J18427+596S	HD 173740	725 B	18:42:46.88	+59:37:37.4	5.72	12 Nov 2011	1 × 180
612	J18453+188	G 184–024	...	18:45:22.90	+18:51:58.5	9.27	25 Sep 2012	1 × 500
613	J18467+007	IRXS J184646.9+004320	...	18:46:46.80	+00:43:26.1	9.59	04 Sep 2012	1 × 500
614	J18482+076	G 141–036	...	18:48:17.50	+07:41:21.1	8.85	25 Sep 2012	1 × 800
615	J18491–032	PM I18491–0315	...	18:49:06.40	–03:15:17.5	9.61	02 Sep 2012	1 × 900
616	J18499+186	G 184–031	...	18:49:54.49	+18:40:29.5	9.38	02 Sep 2012	1 × 300
617	J18542+109	PM I18542+1058	...	18:54:17.10	+10:58:09.2	9.38	04 Sep 2012	1 × 300
618	J18550+429	IRXS J185504.7+425952	...	18:55:04.50	+42:59:51.0	9.78	06 Aug 2012	1 × 900
619	J18570+473	G 205–048	...	18:57:00.50	+47:20:28.8	9.42	06 Aug 2012	1 × 400
620	J19052+387	2MASS J1901335+3845050	...	19:05:13.40	+38:45:05.3	9.35	04 Aug 2012	1 × 400
621	J19060–074	SCR J1906–0729	...	19:06:02.60	–07:29:41.2	9.50	05 Aug 2012	1 × 300
622	J19070+208	HD 349726	745 A	19:07:05.56	+20:53:16.8	7.30	02 Sep 2012	1 × 150
623	J19072+442	LP 230–029	...	19:07:12.70	+44:16:07.3	10.45	05 Aug 2012	3 × 660
624	J19105–075	PM I19105–0734	...	19:10:33.30	–07:34:04.3	9.88	04 Sep 2012	1 × 450
625	J19164+842	PM I19164+8413	...	19:16:24.80	+84:13:41.1	9.98	06 Aug 2012	3 × 600
626	J19168+003	IRXS J191650.3+002341	...	19:16:48.80	+00:23:32.1	9.96	02 Sep 2012	1 × 650
627	J19169+051N	V1428 Aql	752 A	19:16:55.26	+05:10:08.6	5.58	05 Aug 2012	1 × 70
628	J19169+051S	V1298 Aql (vB 10)	752 B	19:16:57.62	+05:09:02.2	9.91	03 Aug 2012	3 × 1200 + 1 × 900
629	J19243+426	PM I19243+4237	...	19:24:21.00	+42:37:25.6	9.34	05 Aug 2012	1 × 300
630	J19260+244	G 185–023	...	19:26:01.60	+24:26:17.2	9.63	05 Aug 2012	1 × 1000
631	J19271+770	NLTT 478944	...	19:27:09.10	+77:04:32.8	9.24	06 Aug 2012	1 × 400
632	J19282–001	PM I19282–0009	...	19:28:13.70	–00:09:51.9	9.72	04 Sep 2012	1 × 700
633	J19312+361 AB	G 125–015	...	19:31:12.60	+36:07:29.9	9.61	05 Aug 2012	1 × 500
634	J19316–069	PM J19316–0658	...	19:31:38.70	–06:58:25.3	9.48	04 Sep 2012	1 × 360
635	J19327–068	SCR J1932–0652	...	19:32:46.30	–06:52:18.1	9.94	04 Sep 2012	1 × 500
636	J19346+045	HD 184489	763	19:34:39.84	+04:34:57.0	6.71	11 Nov 2011	1 × 60
637	J19390+338	PM I19390+3352	...	19:39:05.60	+33:52:02.1	9.39	05 Aug 2012	1 × 300
638	J19393+148	PM I19393+1448	...	19:39:22.10	+14:48:16.0	9.94	05 Aug 2012	1 × 600
639	J19421+656	G 260–031	...	19:42:10.00	+65:38:30.0	9.35	05 Aug 2012	1 × 240

Table A.1. Observed stars: identification, common name, Gliese number, 2MASS coordinates and J magnitude, observing date, and exposure time (cont.).

No.	Karmn	Name	Gl/GJ	α (J2000)	δ (J2000)	J [mag]	Observation date	$N \times t_{\text{exp}}$ [s]
640	J19430+102	G 142-046	...	19:43:02.70	+10:12:39.6	9.25	23 Sep 2012	1 × 500
641	J19439-057	IRXS J194354.7-054634	...	19:43:54.30	-05:46:36.4	9.75	04 Sep 2012	1 × 450
642	J19452+407	TYC 3140-883-1	...	19:45:12.50	+40:43:18.4	8.96	25 Sep 2012	1 × 450
643	J19519+141	LSPM J1951+1408	...	19:51:55.50	+14:08:23.4	9.42	03 Aug 2012	1 × 250
644	J19524+603	PM I19524+6022	...	19:52:24.50	+60:22:14.5	9.79	03 Aug 2012	1 × 700
645	J19539+444W AB	V1581 Cyg	1245 AB	19:53:54.43	+44:24:54.2	7.79	02 Aug 2012	1 × 800
646	J19539+444E	G 208-045	1245 C	19:53:55.09	+44:24:55.0	8.28	02 Aug 2012	1 × 1000
647	J19547+844	IRXS J195446.2+842937	...	19:54:47.20	+84:29:29.6	9.51	24 Sep 2012	1 × 900
648	J19564+591	BD+58 2015B	9677 B	19:56:24.90	+59:09:21.7	9.65	23 Sep 2012	1 × 600
649	J19565+591	BD+58 2015A	9677 A	19:56:34.01	+59:09:42.1	7.42	23 Sep 2012	1 × 200
650	J19578-108	LP 754-008	...	19:57:52.00	-10:53:05.0	9.73	02 Sep 2012	1 × 900
651	J20021+130 AB	PM I20021+1300	...	20:02:10.60	+13:00:31.5	9.73	05 Aug 2012	1 × 600
652	J20033+672	G 262-003	...	20:03:23.30	+67:16:48.8	9.45	05 Aug 2012	1 × 500
653	J20034+298	HD 190360 B	777 B	20:03:26.52	+29:52:00.1	9.55	12 Nov 2011	1 × 600
654	J20047+512	Wolf 1129	...	20:04:47.40	+51:13:16.9	9.49	05 Aug 2012	2 × 300
655	J20065+159	G 143-029	...	20:06:31.10	+15:59:17.1	9.74	05 Aug 2012	1 × 500
656	J20077+189	Wolf 869	...	20:07:42.70	+18:59:00.4	9.43	04 Sep 2012	1 × 350
657	J20093-012	SCR J2009-0113	...	20:09:18.20	-01:13:38.2	9.40	02 Sep 2012	1 × 497
658	J20108+772	HD 193202	786	20:10:52.42	+77:14:20.3	6.41	04 Aug 2012	1 × 120
659	J20112+161	HD 191785 B	783.2 B	20:11:13.29	+16:11:07.5	9.63	12 Nov 2011	1 × 350
660	J20123-126	ξ Cap B	4139 B	20:12:20.30	-12:37:06.0	...	23 Sep 2012	1 × 600
661	J20177+059	LSPM J2017+0559	...	20:17:43.30	+05:59:17.3	9.32	04 Sep 2012	1 × 250
662	J20182-202	NLTT 49012	...	20:18:14.60	-20:12:47.7	9.46	04 Sep 2012	1 × 250
663	J20216-199	LP 815-004	...	20:21:41.10	-19:57:18.0	9.47	02 Sep 2012	1 × 300
664	J20254-198	PM I20254-1948	...	20:25:27.10	-19:48:03.4	10.04	04 Aug 2012	3 × 600
665	J20283+617	LP 106-101	...	20:28:19.20	+61:43:47.9	9.32	03 Aug 2012	1 × 450
666	J20300+003 AB	PM I20300+0023	...	20:30:01.90	+00:23:55.3	9.91	04 Sep 2012	1 × 700
667	J20332+283	G 210-026	...	20:33:15.80	+28:23:44.5	9.96	04 Aug 2012	1 × 1000
668	J20336+365	G 209-036	...	20:33:41.80	+36:35:58.7	9.42	02 Sep 2012	1 × 400
669	J20382+231	IRXS J203813.6+230750	...	20:38:14.40	+23:07:52.4	9.20	04 Aug 2012	1 × 240
670	J20405+154	G 144-25	1256	20:40:33.64	+15:29:57.2	8.64	31 Aug 2012	1 × 1000
								+ 1 × 800
671	J20407+199 AB	HD 197076 B	797 B	20:40:44.50	+19:54:02.3	8.16	12 Nov 2011	1 × 300
672	J20439+231	Wolf 1361	...	20:43:54.10	+23:07:13.7	9.28	02 Sep 2012	1 × 300
673	J20467-118	LP 756-003	...	20:46:43.60	-11:48:13.3	9.35	04 Aug 2012	1 × 360
674	J20510+399	G 210-038	...	20:51:01.60	+39:55:43.3	9.06	03 Aug 2012	1 × 200
675	J20540+603	IRXS J205405.4+601811	...	20:54:05.10	+60:18:04.1	10.10	04 Aug 2012	3 × 450
676	J20581+401 AB	HD 200007 B	...	20:58:11.47	+40:11:29.0	8.14	23 Sep 2012	1 × 400
677	J20583+425	G 212-012	...	20:58:23.10	+42:35:03.4	9.49	04 Aug 2012	1 × 360
678	J20593+530 AB	LSPM J2059+5303	...	20:59:20.40	+53:03:04.9	9.91	03 Aug 2012	1 × 600
679	J21009+510	G 231-024	...	21:00:59.80	+51:03:14.7	9.88	07 Dec 2011	1 × 400
680	J21019-063	Wolf 906	816	21:01:58.66	-06:19:07.1	7.56	02 Sep 2012	1 × 400
681	J21027+349	G 211-009	...	21:02:46.06	+34:54:36.0	9.85	07 Dec 2011	1 × 600
682	J21053+208	G 144-063	...	21:05:22.20	+20:51:34.2	9.42	03 Aug 2012	1 × 350
683	J21057+502W	PM I21057+5015W	...	21:05:42.40	+50:15:57.7	9.97	02 Aug 2012	1 × 749
684	J21057+502E	PM I21057+5015E	...	21:05:45.38	+50:15:43.6	9.54	07 Dec 2011	1 × 750
685	J21068+387	61 Cyg A	820 A	21:06:53.42	+38:44:53.0	3.11	11 Nov 2011	1 × 4
686	J21069+387	61 Cyg B	820 B	21:06:54.74	+38:44:26.64	3.55	11 Nov 2011	1 × 10
687	J21074+198	LP 456-039	...	21:07:24.44	+19:50:52.3	9.18	07 Dec 2011	1 × 300
688	J21074+468	PM I21074+4651	...	21:07:28.10	+46:51:53.8	9.49	07 Dec 2011	1 × 300
689	J21109+469	G 212-027	...	21:10:58.80	+46:57:32.1	9.88	02 Aug 2012	3 × 600
690	J21114+658	LSPM J2111+6553	...	21:11:27.40	+65:53:26.5	9.48	03 Aug 2012	1 × 350
691	J21127-073	PM I21127-0719	...	21:12:45.60	-07:19:55.8	9.90	07 Dec 2011	1 × 1100
692	J21147+160	G 145-029	...	21:14:47.50	+16:04:49.7	9.22	03 Aug 2012	1 × 250
693	J21245+400	LSR J2124+4003	...	21:24:32.34	+40:04:00.0	10.34	02 Aug 2012	3 × 900
694	J21376+016	2E 4498	...	21:37:40.20	+01:37:13.8	8.80	24 Sep 2012	1 × 300
695	J21414+207	IRXS J214127.5+204302	...	21:41:26.60	+20:43:10.8	9.43	03 Aug 2012	1 × 250
696	J21466+668	G 264-012	...	21:46:40.20	+66:48:10.6	8.84	24 Sep 2012	1 × 480
697	J21467-212	LP 874-062	...	21:46:45.50	-21:17:46.9	9.29	04 Sep 2012	1 × 280
698	J21472-047	PM I21472-0444	...	21:47:17.50	-04:44:40.6	9.42	02 Aug 2012	1 × 749
699	J21554+596 AB	RX J2155.3+5938	...	21:55:24.40	+59:38:37.2	9.18	02 Aug 2012	1 × 431
700	J22021+014	HD 209290	846	22:02:10.27	+01:24:00.8	6.20	05 Aug 2012	1 × 60
701	J22035+036 AB	IRXS J220330.8+034001	...	22:03:33.38	+03:40:23.6	9.74	04 Jan 2012	1 × 700
702	J22088+117	PM I22088+1144	...	22:08:50.35	+11:44:13.2	9.90	03 Jan 2012	1 × 750
703	J22089-177	HD 210190 B	...	22:08:54.18	-17:47:52.2	11.97	04 Sep 2012	1 × 800
704	J22095+118	LP 519-038	...	22:09:31.68	+11:52:53.7	9.90	10 Jan 2012	1 × 650
705	J22114+409	IRXS J221124.3+410000	...	22:11:24.17	+40:59:58.7	9.73	03 Jan 2012	3 × 600
706	J22160+546	V447 Per B	4269 B	22:16:02.59	+54:39:59.5	9.72	05 Aug 2012	1 × 900
706	J22202+067	Wolf 1034	...	22:20:13.27	+06:43:32.1	9.50	10 Jan 2012	1 × 300
708	J22234+324 AB	Wolf 1225	856 AB	22:23:29.05	+32:27:33.4	6.90	23 Sep 2012	1 × 80
709	J22264+583	PM I22264+5823	...	22:26:24.98	+58:23:05.1	9.46	03 Jan 2012	1 × 300
710	J22300+488 AB	2E 4617	...	22:30:04.19	+48:51:34.7	9.52	04 Jan 2012	1 × 450
711	J22386+567	V416 Lac	...	22:38:37.92	+56:47:44.3	1.09	04 Jan 2012	1 × 2
712	J22387+252	G 127-042	...	22:38:44.26	+25:13:30.5	9.77	09 Jan 2012	1 × 700
713	J22396-125	NV Aqr C	867.1 C	22:39:41.59	-12:35:20.4	10.57	04 Aug 2012	1 × 1000
714	J22415+260	IRXS J224134.7+260210	...	22:41:35.78	+26:02:12.9	9.04	10 Jan 2012	1 × 250
715	J22437+192	RX J2243.7+1916	...	22:43:43.78	+19:16:54.5	9.24	10 Jan 2012	1 × 300
716	J22476+184	LP 461-011	...	22:47:38.84	+18:26:36.5	9.10	10 Jan 2012	1 × 200
717	J22489+183	PM J22489+1819	...	22:48:54.59	+18:19:59.3	9.96	10 Jan 2012	1 × 1000
718	J22509+499	IRXS J225056.4+495906	...	22:50:55.05	+49:59:13.2	9.80	03 Jan 2012	1 × 850
719	J22524+099 AB	σ Peg B	9801 B	22:52:29.77	+09:54:04.3	9.66	04 Sep 2012	1 × 360

Table A.1. Observed stars: identification, common name, Gliese number, 2MASS coordinates and *J* magnitude, observing date, and exposure time (cont.).

No.	Karmn	Name	Gl/GJ	α (J2000)	δ (J2000)	<i>J</i> [mag]	Observation date	$N \times t_{\text{exp}}$ [s]
720	J22526+750	NLTT 55174	...	22:52:39.64	+75:04:19.0	9.09	07 Dec 2011	1 × 200
721	J22582–110	IRXS J225817.2–110434	...	22:58:16.40	−11:04:17.1	9.07	03 Aug 2012	1 × 200
722	J22588+690	BD+68 1345B	...	22:58:50.60	+69:01:37.1	10.59	04 Sep 2012	2 × 800
723	J23006+036	LP 641–057	...	23:00:36.10	+03:38:17.0	9.59	06 Aug 2012	1 × 600
724	J23028+436	LSPM J2302+4338	...	23:02:52.51	+43:38:15.7	9.32	08 Dec 2011	1 × 400
725	J23036–072	LP 701–066	...	23:03:36.40	−07:16:30.2	9.48	05 Aug 2012	2 × 400
726	J23036+097	PM 123036+0942	...	23:03:37.45	+09:42:58.5	9.99	08 Dec 2011	1 × 300
727	J23051+519	PM 123051+5159	...	23:05:06.32	+51:59:13.3	9.68	08 Dec 2011	1 × 250
728	J23051+452	LSPM J2305+4517	...	23:05:08.71	+45:17:31.8	9.30	03 Jan 2012	1 × 210
729	J23070+094	55 Peg	...	23:07:00.26	+09:24:34.2	1.58	07 Dec 2011	1 × 1
730	J23177+490	8 And	...	23:17:44.65	+49:00:55.1	1.62	11 Jan 2012	1 × 1
731	J23182+795	LP 012–069	...	23:18:17.06	+79:34:47.4	9.71	03 Jan 2012	1 × 520
732	J23194+790	V368 Cep B	...	23:19:24.47	+79:00:03.7	8.04	11 Feb 2012	1 × 250
733	J23209–017 AB	LP 642–048	...	23:20:57.70	−01:47:37.3	9.36	06 Aug 2012	1 × 400
734	J23220+569	G 217–006	...	23:22:00.71	+56:59:19.9	9.47	08 Dec 2011	1 × 400
735	J23228+787	NLTT 56725	...	23:22:53.85	+78:47:38.6	10.42	11 Feb 2012	3 × 800
736	J23235+457	HD 220445 B	...	23:23:30.68	+45:47:18.6	7.38	04 Sep 2012	1 × 60
737	J23261+170 AB	2MASS J23261182+1700082	...	23:26:11.82	+17:00:08.3	9.36	10 Jan 2012	1 × 300
738	J23266+453	2MASS J23263798+4521054	...	23:26:37.98	+45:21:05.5	8.20	04 Sep 2012	1 × 60
739	J23306+466	Ross 247	...	23:30:41.80	+46:39:56.2	9.97	08 Dec 2011	1 × 700
740	J23317–064	2MASS J23314763–0625502	...	23:31:47.60	−06:25:50.4	9.84	05 Aug 2012	1 × 900
741	J23376+163	LP 463–023	...	23:37:36.00	+16:22:03.2	10.48	24 Sep 2012	3 × 900
742	J23416–065	LP 703–042	...	23:41:39.30	−06:35:50.4	10.32	06 Aug 2012	3 × 700
743	J23417–059 AB	HD 222582 B	...	23:41:45.15	−05:58:14.7	10.39	12 Nov 2011	1 × 600
744	J23419+441	HH And	905	23:41:54.99	+44:10:40.8	6.88	11 Nov 2011	1 × 400
745	J23423+349	PM 123423+3458	...	23:42:22.11	+34:58:27.7	9.32	04 Jan 2012	1 × 350
746	J23425+392	LP 291–007	...	23:42:33.50	+39:14:23.3	9.64	09 Jan 2012	1 × 1000
747	J23438+610	G 217–018	...	23:43:53.10	+61:02:15.7	9.39	04 Jan 2012	1 × 500
748	J23490–086	G 273–144	...	23:49:02.30	−08:24:30.9	9.50	02 Aug 2012	1 × 272
749	J23559–133	NLTT 58441	...	23:55:55.20	−13:21:23.8	9.26	02 Sep 2012	1 × 250
750	J23560+150	LP 523–078	...	23:56:00.29	+15:01:40.9	9.38	07 Dec 2011	1 × 250
751	J23569+230	G 129–045	...	23:56:55.10	+23:05:02.7	9.15	07 Dec 2011	1 × 300
752	J23585+242	G 131–006	...	23:58:30.21	+24:12:04.8	9.13	04 Sep 2012	1 × 90
753	J23590+208	G 129–051	...	23:59:00.42	+20:51:38.8	9.07	07 Dec 2011	1 × 180

Table A.2. Seven representative spectral indices, ζ metallicity index, and H α pseudo-equivalent width.

Karmn	PC1	TiO 2	TiO 5	VO-7912	Color-M	CaH 2	CaH 3	ζ	$pEW(H\alpha)$ [Å]
J00066-070 AB	1.269	0.492	0.317	1.148	1.778	0.404	0.654	0.973	-2.3 $^{+0.3}_{-0.5}$
J00077+603 AB	1.198	0.532	0.369	1.111	1.405	0.408	0.631	0.883	-6.7 $^{+0.3}_{-0.4}$
J00115+591	1.511	0.378	0.202	1.222	2.902	0.281	0.564	0.970	-1.6 $^{+0.2}_{-0.4}$
J00118+229	1.215	0.606	0.405	1.090	1.404	0.492	0.751	1.052	-0.5 $^{+0.2}_{-0.2}$
J00119+330	1.167	0.634	0.427	1.072	1.293	0.503	0.748	1.023	-0.3 $^{+0.1}_{-0.2}$
J00122+304	1.296	0.497	0.354	1.154	1.755	0.427	0.685	0.972	-8.7 $^{+0.4}_{-0.5}$
J00133+275	1.296	0.512	0.339	1.144	1.805	0.425	0.686	0.994	-4.0 $^{+0.2}_{-0.4}$
J00136+806	1.027	0.770	0.601	1.012	0.901	0.644	0.812	1.002	+0.0 $^{+0.2}_{-0.2}$
J00146+202	0.955	0.729	0.520	1.005	0.643	0.839	0.946	2.754	+0.8 $^{+0.1}_{-0.1}$
J00152+530	1.090	0.728	0.540	1.031	1.076	0.575	0.787	0.975	+0.0 $^{+0.2}_{-0.2}$
J00162+198E	1.271	0.559	0.367	1.121	1.663	0.451	0.731	1.032	-0.5 $^{+0.1}_{-0.2}$
J00162+198W	1.260	0.553	0.363	1.122	1.553	0.450	0.708	1.010	-4.5 $^{+0.4}_{-0.4}$
J00183+440	0.990	0.810	0.638	1.004	0.892	0.651	0.818	0.932	+0.0 $^{+0.2}_{-0.2}$
J00228-164	1.229	0.564	0.378	1.105	1.478	0.443	0.691	0.960	-2.7 $^{+0.3}_{-0.3}$
J00240+264	1.266	0.539	0.350	1.132	1.705	0.447	0.710	1.030	-1.9 $^{+0.3}_{-0.3}$
J00253+235	1.006	0.811	0.644	1.011	0.934	0.672	0.840	1.001	+0.0 $^{+0.4}_{-0.4}$
J00297+012	0.997	0.819	0.665	1.002	0.877	0.684	0.844	0.975	+0.0 $^{+0.2}_{-0.2}$
J00313+336	0.945	0.882	0.778	0.988	0.779	0.809	0.895	1.001	+0.0 $^{+0.2}_{-0.2}$
J00313+001	1.138	0.658	0.474	1.061	1.183	0.530	0.758	0.991	-0.4 $^{+0.1}_{-0.1}$
J00322+544	1.338	0.554	0.349	1.129	1.798	0.452	0.738	1.072	-0.4 $^{+0.1}_{-0.2}$
J00328-045 AB	1.293	0.561	0.358	1.131	1.748	0.451	0.723	1.038	-1.5 $^{+0.7}_{-0.1}$
J00358+526	1.080	0.706	0.510	1.035	1.059	0.565	0.777	1.004	+0.0 $^{+0.4}_{-0.4}$
J00367+444	0.993	0.751	0.546	1.013	0.758	0.854	0.963	2.888	+0.8 $^{+0.1}_{-0.1}$
J00380+169	1.124	0.672	0.471	1.057	1.189	0.509	0.742	0.945	+0.0 $^{+0.2}_{-0.2}$
J00389+306	1.090	0.715	0.526	1.035	1.079	0.570	0.790	1.001	+0.0 $^{+0.2}_{-0.2}$
J00395+149N	1.321	0.503	0.344	1.153	1.749	0.416	0.672	0.963	-7.2 $^{+0.2}_{-0.3}$
J00395+149S	1.237	0.590	0.399	1.100	1.487	0.467	0.722	0.989	-1.7 $^{+0.2}_{-0.2}$
J00452+002 AB	1.227	0.584	0.392	1.104	1.437	0.424	0.713	0.942	-3.1 $^{+0.2}_{-0.3}$
J00464+506	1.256	0.559	0.371	1.116	1.554	0.478	0.753	1.092	-0.5 $^{+0.1}_{-0.2}$
J00467-044	1.274	0.546	0.359	1.112	1.593	0.450	0.711	1.022	-0.8 $^{+0.2}_{-0.3}$
J00484+753	1.121	0.665	0.475	1.058	1.138	0.534	0.762	1.000	-1.1 $^{+0.3}_{-0.2}$
J00490+578	0.904	0.920	0.843	0.972	0.683	0.897	0.927	1.017	+0.3 $^{+0.1}_{-0.1}$
J00490+657	1.108	0.707	0.517	1.043	1.118	0.564	0.784	0.998	+0.0 $^{+0.2}_{-0.2}$
J00502+086	1.294	0.501	0.343	1.145	1.609	0.437	0.701	1.019	-6.7 $^{+0.2}_{-0.3}$
J00502+601	1.154	0.747	0.559	1.034	1.068	0.793	0.915	2.017	+0.8 $^{+0.1}_{-0.2}$
J00540+691	1.066	0.740	0.542	1.033	1.096	0.548	0.759	0.887	+0.0 $^{+0.2}_{-0.2}$
J00548+275	1.294	0.521	0.353	1.145	1.682	0.429	0.691	0.983	-5.3 $^{+5.3}_{-0.2}$
J00580+393	1.285	0.531	0.352	1.141	1.688	0.417	0.667	0.947	-3.7 $^{+0.3}_{-0.2}$
J01009-044	1.212	0.605	0.378	1.090	1.492	0.429	0.677	0.931	+0.0 $^{+0.2}_{-0.2}$
J01012+571	1.123	0.842	0.703	1.019	1.087	0.893	0.947	2.021	+1.1 $^{+0.2}_{-0.2}$
J01014+188	1.067	0.710	0.513	1.033	1.018	0.580	0.794	1.052	+0.0 $^{+0.2}_{-0.2}$
J01014-010	1.215	0.613	0.415	1.102	1.386	0.485	0.731	0.997	+0.0 $^{+0.2}_{-0.2}$
J01026+623	1.043	0.778	0.615	1.017	0.960	0.643	0.820	0.979	+0.0 $^{+0.2}_{-0.2}$
J01028+189	1.244	0.529	0.349	1.124	1.352	0.450	0.712	1.038	-9.7 $^{+0.3}_{-0.3}$
J01028+470	0.999	0.760	0.578	1.013	0.855	0.621	0.806	1.001	+0.0 $^{+0.2}_{-0.2}$
J01032+712	1.323	0.589	0.395	1.108	1.785	0.453	0.719	0.975	-0.6 $^{+0.2}_{-0.4}$
J01033+623	1.394	0.438	0.302	1.176	1.959	0.385	0.644	0.968	-10.1 $^{+0.4}_{-0.1}$
J01055+153	0.865	0.918	0.836	0.965	0.579	0.916	0.935	1.160	+0.4 $^{+0.1}_{-0.1}$
J01069+804	1.321	0.490	0.332	1.150	1.770	0.408	0.668	0.970	-7.2 $^{+0.3}_{-0.2}$
J01074-025	0.860	0.937	0.876	0.981	0.603	1.027	0.979	1.386	+0.7 $^{+0.4}_{-0.2}$
J01076+229E	1.189	0.569	0.393	1.097	1.355	0.508	0.743	1.084	+2.2 $^{+0.8}_{-0.4}$
J01097+356	0.943	0.826	0.652	0.992	0.662	0.937	0.965	2.902	+0.9 $^{+0.3}_{-0.3}$
J01186-008	0.903	0.917	0.810	0.970	0.674	0.869	0.917	1.093	+0.5 $^{+0.1}_{-0.2}$
J01214+313	1.160	0.606	0.421	1.078	1.277	0.510	0.742	1.035	+0.0 $^{+0.2}_{-0.2}$
J01226+127	0.886	0.896	0.795	0.973	0.635	0.863	0.918	1.162	+0.4 $^{+0.1}_{-0.1}$
J01342-015	0.989	0.797	0.628	0.998	0.849	0.679	0.849	1.086	+0.0 $^{+0.2}_{-0.2}$
J01356-200 AB	1.082	0.706	0.520	1.039	1.049	0.582	0.796	1.045	+0.0 $^{+0.2}_{-0.2}$
J01390-179 AB	1.336	0.429	0.313	1.198	2.326	0.410	0.638	0.970	-4.8 $^{+0.4}_{-0.2}$

Table A.2. Seven representative spectral indices, ζ metallicity index, and H α pseudo-equivalent width (cont.).

Karmn	PC1	TiO 2	TiO 5	VO-7912	Color-M	CaH 2	CaH 3	ζ	$pEW(H\alpha)$ [Å]
J01406-081	0.882	0.940	0.892	0.972	0.641	0.996	0.966	1.082	+0.7 ^{+0.2} _{-0.2}
J01431+210	1.240	0.509	0.351	1.130	1.425	0.465	0.723	1.066	-4.9 ^{+0.2} _{-0.2}
J01541-156	1.236	0.572	0.356	1.127	1.612	0.449	0.688	0.997	-1.3 ^{+0.2} _{-0.3}
J01551-162	0.896	0.923	0.865	0.979	0.668	0.955	0.948	1.128	+0.5 ^{+0.2} _{-0.2}
J01562+001	1.120	0.616	0.460	1.063	1.107	0.500	0.713	0.917	-5.2 ^{+0.3} _{-0.2}
J01567+305	1.295	0.457	0.333	1.159	1.878	0.397	0.630	0.925	-16.0 ^{+0.4} _{-0.4}
J01571-102	0.944	0.869	0.758	0.981	0.745	0.809	0.889	1.073	+0.4 ^{+0.1} _{-0.1}
J02000+135 AB	1.169	0.618	0.417	1.076	1.244	0.505	0.749	1.046	+0.0 ^{+0.2} _{-0.2}
J02002+130	1.154	0.658	0.486	1.122	1.498	0.557	0.800	1.080	-2.0 ^{+0.2} _{-0.3}
J02019+342	0.964	0.861	0.738	0.990	0.821	0.774	0.882	1.037	+0.4 ^{+0.2} _{-0.2}
J02022+103	1.491	0.387	0.213	1.216	2.583	0.319	0.619	1.015	-1.6 ^{+0.5} _{-0.3}
J02023+012	1.082	0.751	0.565	1.027	1.092	0.574	0.783	0.912	+0.0 ^{+0.2} _{-0.2}
J02100-088	1.145	0.588	0.395	1.073	1.107	0.501	0.763	1.101	-0.4 ^{+0.1} _{-0.1}
J02133+368 AB	1.279	0.476	0.330	1.149	1.735	0.381	0.617	0.906	-6.2 ^{+0.4} _{-0.2}
J02142-039	1.558	0.350	0.236	1.240	2.800	0.335	0.625	1.002	-12.3 ^{+0.9} _{-0.7}
J02159-094 ABC	1.090	0.668	0.504	1.061	1.013	0.564	0.754	0.979	-6.0 ^{+0.4} _{-0.4}
J02274+031	1.205	0.556	0.384	1.111	1.432	0.440	0.676	0.933	-4.2 ^{+0.4} _{-0.3}
J02285-200	1.070	0.719	0.512	1.043	1.068	0.537	0.752	0.921	+0.0 ^{+0.2} _{-0.2}
J02291+228	0.899	0.935	0.865	0.976	0.680	0.968	0.962	1.229	+0.6 ^{+0.2} _{-0.2}
J02362+068	1.202	0.602	0.385	1.108	1.506	0.464	0.739	1.030	-0.5 ^{+0.2} _{-0.2}
J02367+226	1.406	0.428	0.280	1.178	2.158	0.361	0.627	0.964	-5.5 ^{+0.5} _{-0.4}
J02412-045	1.272	0.507	0.352	1.136	1.682	0.405	0.651	0.921	-3.8 ^{+0.3} _{-0.4}
J02441+492	1.017	0.782	0.607	1.011	0.932	0.634	0.821	0.983	+0.0 ^{+0.2} _{-0.2}
J02456+449	0.968	0.873	0.716	0.991	0.838	0.745	0.881	1.040	+0.4 ^{+0.1} _{-0.2}
J02479-124	1.382	0.747	0.459	1.227	2.418	0.779	1.455	5.825	+0.0 ^{+0.2} _{-0.2}
J02502+628	1.125	0.680	0.489	1.048	1.187	0.532	0.759	0.967	+0.0 ^{+0.2} _{-0.2}
J02530+168	1.823	0.256	0.134	1.292	4.540	0.224	0.533	1.012	-2.4 ^{+0.6} _{-0.8}
J02555+268	1.273	0.567	0.369	1.112	1.621	0.465	0.728	1.044	-0.5 ^{+0.2} _{-0.2}
J02558+183	1.573	1.008	0.415	1.222	2.599	0.453	0.855	1.134	+0.0 ^{+0.2} _{-0.2}
J02562+239	1.357	0.478	0.328	1.156	1.896	0.402	0.679	0.980	-6.6 ^{+0.4} _{-0.2}
J03026-181	1.098	0.711	0.520	1.040	1.068	0.566	0.785	0.996	+0.0 ^{+0.2} _{-0.2}
J03033-080	1.138	0.634	0.444	1.072	1.187	0.536	0.776	1.085	-1.9 ^{+0.2} _{-0.2}
J03047+617	1.139	0.660	0.455	1.062	1.203	0.530	0.783	1.067	-0.4 ^{+0.1} _{-0.1}
J03110-046	1.133	0.676	0.480	1.059	1.171	0.534	0.765	0.997	-0.4 ^{+0.1} _{-0.1}
J03147+114	1.038	0.716	0.565	1.041	0.989	0.614	0.800	1.010	-3.3 ^{+0.5} _{-0.4}
J03154+578	1.141	0.608	0.437	1.065	1.265	0.473	0.710	0.920	+0.0 ^{+0.2} _{-0.2}
J03162+581N	1.059	0.752	0.560	1.021	0.993	0.595	0.794	0.975	+0.0 ^{+0.2} _{-0.2}
J03162+581S	1.069	0.761	0.588	1.024	1.028	0.611	0.800	0.951	+0.0 ^{+0.2} _{-0.2}
J03167+389	1.191	0.612	0.413	1.089	1.395	0.494	0.750	1.038	+0.0 ^{+0.2} _{-0.2}
J03174-011	0.954	0.820	0.682	0.990	0.760	0.710	0.855	1.007	+0.0 ^{+0.2} _{-0.2}
J03179-010	1.039	0.733	0.531	1.019	0.939	0.546	0.763	0.912	+0.0 ^{+0.2} _{-0.2}
J03181+426	1.224	0.605	0.401	1.092	1.442	0.494	0.757	1.069	+0.0 ^{+0.2} _{-0.2}
J03194+619	1.262	0.523	0.363	1.132	1.537	0.428	0.666	0.941	-7.0 ^{+0.4} _{-0.3}
J03236+056	1.354	0.488	0.320	1.164	1.755	0.417	0.693	1.022	-7.9 ^{+0.2} _{-0.3}
J03236+476	0.971	0.858	0.738	0.996	0.839	0.775	0.882	1.041	+0.4 ^{+0.2} _{-0.2}
J03263+171	1.227	0.603	0.390	1.101	1.503	0.491	0.760	1.091	-0.8 ^{+0.2} _{-0.2}
J03275+222	1.309	0.533	0.344	1.140	1.670	0.433	0.707	1.019	-5.4 ^{+0.4} _{-0.3}
J03294+117	1.064	0.684	0.474	1.055	0.981	0.561	0.777	1.071	+0.0 ^{+0.4} _{-0.4}
J03303+346	1.260	0.542	0.383	1.123	1.451	0.459	0.708	0.989	-8.2 ^{+0.3} _{-0.3}
J03309+706	1.157	0.625	0.429	1.074	1.345	0.477	0.714	0.942	+0.0 ^{+0.3} _{-0.3}
J03319+492	0.907	0.979	0.939	0.997	0.707	1.073	1.010	0.772	+1.2 ^{+0.1} _{-0.2}
J03320+436	0.906	0.913	0.832	0.972	0.699	0.902	0.932	1.125	+0.4 ^{+0.2} _{-0.2}
J03325+287 ABC	1.292	0.523	0.345	1.136	1.564	0.436	0.705	1.019	-7.0 ^{+0.4} _{-0.2}
J03332+462	0.919	0.866	0.789	0.995	0.705	0.875	0.903	1.182	-3.4 ^{+0.5} _{-0.3}
J03354+428	0.966	0.870	0.744	0.992	0.816	0.762	0.882	0.981	+0.0 ^{+0.4} _{-0.4}
J03356-084	1.443	0.424	0.238	1.182	2.405	0.339	0.628	1.003	+0.0 ^{+0.3} _{-0.3}
J03361+313	1.320	0.476	0.325	1.152	1.832	0.396	0.652	0.953	-7.4 ^{+0.6} _{-0.3}
J03375+288	0.944	0.869	0.756	0.981	0.769	0.820	0.914	1.200	+0.0 ^{+0.4} _{-0.4}
J03375+178N AB	1.085	0.728	0.542	1.045	1.099	0.573	0.784	0.962	-1.4 ^{+0.4} _{-0.2}

Table A.2. Seven representative spectral indices, ζ metallicity index, and H α pseudo-equivalent width (cont.).

Karmn	PC1	TiO 2	TiO 5	VO-7912	Color-M	CaH 2	CaH 3	ζ	$pEW(H\alpha)$ [Å]
J03375+178S AB	1.145	0.667	0.459	1.109	1.309	0.517	0.777	1.029	-6.8 $^{+0.6}_{-0.5}$
J03392+565 AB	1.141	0.673	0.479	1.058	1.185	0.556	0.795	1.084	-0.4 $^{+0.1}_{-0.1}$
J03430+459	1.209	0.566	0.373	1.099	1.485	0.443	0.694	0.971	-0.7 $^{+0.2}_{-0.3}$
J03466+243 AB	0.882	0.949	0.890	0.975	0.627	1.014	0.973	1.172	+0.0 $^{+0.5}_{-0.5}$
J03473-019	1.129	0.658	0.498	1.047	1.124	0.532	0.747	0.933	-3.7 $^{+0.4}_{-0.2}$
J03480+405	1.026	0.774	0.615	1.026	0.933	0.669	0.819	1.030	-2.6 $^{+0.5}_{-0.4}$
J03510+142	1.306	0.500	0.360	1.142	1.530	0.439	0.692	0.984	-13.4 $^{+0.6}_{-0.6}$
J03519+397	0.936	0.898	0.800	0.977	0.727	0.831	0.900	0.975	+0.0 $^{+0.4}_{-0.4}$
J03548+163 AB	1.242	0.539	0.376	1.120	1.516	0.442	0.684	0.954	-8.6 $^{+0.7}_{-0.4}$
J03556+522	1.075	0.717	0.514	1.033	1.059	0.536	0.751	0.913	+0.0 $^{+0.2}_{-0.2}$
J03565+319	1.202	0.579	0.405	1.098	1.409	0.473	0.719	0.983	-4.7 $^{+0.6}_{-0.3}$
J03566+507	0.879	0.948	0.893	0.971	0.648	0.985	0.961	1.025	+0.4 $^{+0.2}_{-0.2}$
J03574-011 AB	1.082	0.722	0.543	1.037	1.053	0.566	0.761	0.915	-2.2 $^{+0.2}_{-0.2}$
J03588+125	1.298	0.557	0.362	1.130	1.734	0.472	0.754	1.101	-0.5 $^{+0.2}_{-0.3}$
J04041+307	1.027	0.769	0.585	1.019	0.998	0.581	0.783	0.880	+0.0 $^{+0.4}_{-0.4}$
J04061-055	1.199	0.619	0.407	1.081	1.442	0.465	0.715	0.966	-0.4 $^{+0.1}_{-0.1}$
J04079+142	1.132	0.668	0.470	1.062	1.213	0.541	0.781	1.052	+0.0 $^{+0.3}_{-0.3}$
J04081+743	1.181	0.640	0.436	1.076	1.389	0.477	0.719	0.937	-0.4 $^{+0.2}_{-0.2}$
J04083+691	1.279	0.528	0.330	1.140	1.804	0.397	0.667	0.960	-0.8 $^{+0.3}_{-0.2}$
J04123+162 AB	1.211	0.584	0.402	1.099	1.434	0.472	0.724	0.993	-2.5 $^{+0.3}_{-0.3}$
J04153-076	1.297	0.475	0.315	1.133	1.653	0.402	0.666	0.986	-5.0 $^{+0.6}_{-0.5}$
J04177+410	1.165	0.614	0.458	1.074	1.212	0.489	0.708	0.900	-6.4 $^{+0.4}_{-0.3}$
J04177+136 AB	1.051	0.795	0.647	1.009	0.997	0.666	0.829	0.958	+0.0 $^{+0.2}_{-0.2}$
J04191-074	1.228	0.566	0.364	1.112	1.428	0.489	0.748	1.115	-0.4 $^{+0.1}_{-0.1}$
J04191+097	1.150	0.657	0.440	1.065	1.315	0.494	0.734	0.970	-0.3 $^{+0.1}_{-0.2}$
J04205+815	1.120	0.725	0.537	1.043	1.194	0.551	0.768	0.913	+0.0 $^{+0.3}_{-0.3}$
J04206+272	1.366	0.524	0.334	1.152	1.632	0.463	0.776	1.170	-8.9 $^{+0.6}_{-0.3}$
J04206-168	1.325	1.042	0.546	1.071	1.416	0.571	0.893	1.160	+0.0 $^{+0.5}_{-0.5}$
J04207+152 AB	1.231	0.563	0.387	1.105	1.512	0.468	0.729	1.020	-1.5 $^{+0.2}_{-0.3}$
J04224+036	1.160	0.560	0.404	1.096	1.171	0.479	0.706	0.976	-6.7 $^{+0.5}_{-0.4}$
J04227+205	1.269	0.547	0.378	1.125	1.538	0.455	0.703	0.986	-5.4 $^{+0.3}_{-0.4}$
J04229+259	1.282	0.564	0.361	1.129	1.680	0.452	0.717	1.027	-0.6 $^{+0.3}_{-0.2}$
J04234+809	1.227	0.580	0.409	1.097	1.399	0.460	0.687	0.925	-8.2 $^{+0.8}_{-0.5}$
J04238+149 AB	1.160	0.616	0.453	1.078	1.252	0.511	0.729	0.963	-9.1 $^{+0.4}_{-0.3}$
J04238+092 AB	1.166	0.668	0.497	1.053	1.238	0.527	0.749	0.931	-3.7 $^{+0.3}_{-0.2}$
J04247-067 ABC	1.237	0.553	0.364	1.090	1.314	0.450	0.689	0.986	-5.0 $^{+0.6}_{-0.4}$
J04252+172 ABC	1.186	0.581	0.416	1.102	1.260	0.486	0.712	0.973	-7.0 $^{+0.4}_{-0.4}$
J04290+186	1.096	0.693	0.526	1.056	1.061	0.570	0.765	0.960	-11.9 $^{+0.5}_{-0.3}$
J04308-088	1.267	0.564	0.363	1.109	1.581	0.437	0.686	0.972	-1.5 $^{+0.5}_{-0.4}$
J04310+367	1.134	0.639	0.460	1.067	1.240	0.501	0.728	0.936	-3.2 $^{+0.4}_{-0.2}$
J04313+241 AB	1.418	0.491	0.315	1.166	1.884	0.433	0.750	1.118	-9.4 $^{+0.6}_{-0.5}$
J04329+001S	0.957	0.825	0.669	0.992	0.757	0.711	0.845	1.024	+0.0 $^{+0.3}_{-0.3}$
J04347-004	1.213	0.588	0.391	1.105	1.517	0.443	0.691	0.940	-2.0 $^{+0.2}_{-0.4}$
J04360+188	1.107	0.645	0.488	1.060	1.113	0.541	0.750	0.968	-5.8 $^{+0.4}_{-0.4}$
J04366+186	1.077	0.722	0.540	1.033	1.049	0.582	0.790	0.989	-1.0 $^{+0.2}_{-0.3}$
J04373+193	1.269	0.501	0.350	1.131	1.594	0.428	0.670	0.964	-8.3 $^{+0.6}_{-0.2}$
J04386-115	1.193	0.643	0.432	1.070	1.282	0.504	0.769	1.046	+0.0 $^{+0.3}_{-0.3}$
J04388+217	1.175	0.624	0.422	1.087	1.349	0.499	0.748	1.026	-0.6 $^{+0.1}_{-0.2}$
J04393+335	1.266	0.540	0.384	1.135	1.447	0.470	0.718	1.014	-11.2 $^{+0.5}_{-0.4}$
J04398+251	1.168	0.625	0.422	1.081	1.317	0.480	0.726	0.972	+0.0 $^{+0.4}_{-0.4}$
J04413+327	1.252	0.599	0.403	1.103	1.571	0.490	0.758	1.062	-0.4 $^{+0.2}_{-0.1}$
J04425+204 AB	1.140	0.621	0.443	1.074	1.182	0.514	0.731	0.987	-4.8 $^{+0.3}_{-0.3}$
J04430+187 AB	0.875	0.934	0.868	0.985	0.631	1.005	0.967	1.351	+0.7 $^{+0.2}_{-0.2}$
J04458-144	1.268	0.582	0.384	1.108	1.487	0.488	0.753	1.085	-0.5 $^{+0.2}_{-0.2}$
J04468-112 AB	1.147	0.608	0.431	1.076	1.142	0.483	0.712	0.943	-5.1 $^{+0.4}_{-0.2}$
J04472+206	1.349	0.440	0.302	1.181	1.773	0.394	0.654	0.985	-14.4 $^{+1.0}_{-0.5}$
J04494+484 AB	1.252	0.538	0.378	1.107	1.500	0.440	0.680	0.944	-5.5 $^{+0.5}_{-0.5}$
J04496-153	0.867	0.957	0.914	0.966	0.614	1.019	0.979	0.945	+0.5 $^{+0.1}_{-0.2}$
J04499+711	1.223	0.612	0.420	1.084	1.475	0.486	0.745	1.009	-0.3 $^{+0.1}_{-0.2}$

Table A.2. Seven representative spectral indices, ζ metallicity index, and H α pseudo-equivalent width (cont.).

Karmn	PC1	TiO 2	TiO 5	VO-7912	Color-M	CaH 2	CaH 3	ζ	$pEW(H\alpha)$ [Å]
J04536+623	1.195	0.619	0.408	1.089	1.445	0.474	0.731	0.994	+0.0 ^{+0.2} -0.2
J04538+158	1.113	0.691	0.490	1.044	1.159	0.535	0.768	0.981	-0.4 ^{+0.1} -0.1
J04544+650	1.246	0.558	0.375	1.119	1.513	0.434	0.681	0.943	-13.9 ^{+0.8} -0.5
J04559+046	1.057	0.736	0.570	1.028	0.996	0.603	0.788	0.958	-3.3 ^{+0.3} -0.2
J04560+432	1.228	0.597	0.386	1.104	1.479	0.462	0.718	1.001	-0.5 ^{+0.2} -0.4
J05003+251 AB	1.006	0.800	0.644	0.999	0.883	0.677	0.847	1.025	+0.0 ^{+0.3} -0.3
J05019+011	1.261	0.547	0.370	1.125	1.423	0.454	0.716	1.014	-8.2 ^{+0.5} -0.3
J05030+213 AB	1.406	0.475	0.323	1.172	2.130	0.386	0.649	0.944	-5.3 ^{+0.7} -0.5
J05032+213	1.025	0.743	0.561	1.022	0.901	0.610	0.799	1.008	+0.0 ^{+0.2} -0.2
J05050+442	1.410	0.502	0.293	1.166	2.133	0.388	0.681	1.019	-1.0 ^{+0.4} -0.2
J05062+046	1.267	0.529	0.353	1.141	1.453	0.437	0.696	0.997	-10.0 ^{+0.6} -0.2
J05068+516	0.853	0.963	0.920	0.968	0.598	1.051	0.994	0.969	+0.6 ^{+0.1} -0.2
J05072+375	1.319	0.442	0.296	1.174	1.957	0.360	0.606	0.927	-9.0 ^{+0.6} -0.5
J05083+756	1.312	0.531	0.336	1.130	1.810	0.421	0.694	1.003	-0.7 ^{+0.4} -0.3
J05151-073	0.990	0.821	0.667	1.000	0.880	0.687	0.844	0.975	+0.0 ^{+0.3} -0.3
J05152+236	1.361	0.447	0.309	1.179	1.969	0.390	0.647	0.966	-8.4 ^{+0.9} -0.8
J05173+321	1.173	0.639	0.437	1.073	1.317	0.507	0.764	1.033	-1.2 ^{+0.5} -0.5
J05175+487	0.932	0.910	0.804	0.983	0.752	0.834	0.915	1.011	+0.0 ^{+0.4} -0.4
J05187+464	1.309	0.469	0.329	1.153	1.711	0.403	0.648	0.950	-11.6 ^{+0.8} -0.8
J05187-213	1.169	0.607	0.421	1.082	1.268	0.480	0.716	0.962	-3.4 ^{+0.5} -0.7
J05195+649	1.163	0.593	0.388	1.100	1.266	0.465	0.710	0.991	-2.0 ^{+0.2} -0.3
J05200-229	1.047	0.706	0.524	1.026	0.935	0.566	0.766	0.960	+0.0 ^{+0.3} -0.3
J05223+305	1.165	0.648	0.441	1.059	1.243	0.516	0.759	1.034	+0.0 ^{+0.3} -0.3
J05256-091 AB	1.162	0.596	0.420	1.071	1.185	0.464	0.701	0.928	-7.3 ^{+0.4} -0.3
J05289+125	1.224	0.604	0.394	1.097	1.469	0.448	0.699	0.948	-1.8 ^{+0.6} -0.3
J05294+155E	0.891	0.845	0.701	0.984	0.652	0.764	0.882	1.152	+0.0 ^{+0.4} -0.4
J05295-113	1.187	0.618	0.411	1.090	1.363	0.493	0.755	1.048	+0.0 ^{+0.2} -0.2
J05300+121E	0.934	0.861	0.738	0.990	0.762	0.787	0.884	1.081	+0.0 ^{+0.4} -0.4
J05300+121W	0.862	0.951	0.901	0.971	0.611	1.012	0.973	1.058	+0.6 ^{+0.2} -0.3
J05314-036	1.040	0.784	0.618	1.018	0.989	0.655	0.834	1.023	+0.0 ^{+0.3} -0.3
J05320-030	1.040	0.729	0.569	1.040	0.918	0.632	0.803	1.039	-4.0 ^{+0.3} -0.4
J05324-072	0.916	0.852	0.725	0.983	0.680	0.763	0.874	1.040	+0.0 ^{+0.2} -0.2
J05328+338	1.144	0.642	0.431	1.067	1.320	0.467	0.703	0.916	+0.0 ^{+0.2} -0.2
J05342+103N	1.145	0.647	0.446	1.056	1.139	0.531	0.771	1.065	+0.0 ^{+0.2} -0.2
J05342+103S	1.382	0.587	0.383	1.116	1.870	0.456	0.722	1.003	+0.0 ^{+0.2} -0.2
J05394+747	1.171	0.643	0.436	1.072	1.316	0.496	0.740	0.988	+0.0 ^{+0.2} -0.2
J05415+534	0.995	0.825	0.677	0.998	0.867	0.697	0.846	0.972	+0.0 ^{+0.2} -0.2
J05421+124	1.241	0.576	0.366	1.113	1.568	0.457	0.726	1.035	-0.5 ^{+0.5} -0.3
J05424+506	1.143	0.646	0.434	1.070	1.258	0.501	0.748	1.008	-0.3 ^{+0.3} -0.2
J05425+154	1.158	0.596	0.419	1.093	1.306	0.468	0.703	0.935	-4.5 ^{+0.5} -0.2
J05427+026	1.161	0.647	0.440	1.067	1.259	0.520	0.775	1.065	-0.3 ^{+0.1} -0.2
J05455-119	1.319	0.553	0.358	1.129	1.769	0.458	0.742	1.072	-0.6 ^{+0.3} -0.5
J05456+111	0.895	0.886	0.788	0.980	0.678	0.850	0.910	1.128	+0.4 ^{+0.1} -0.2
J05456+729	1.132	0.675	0.476	1.057	1.228	0.527	0.763	0.991	+0.0 ^{+0.2} -0.2
J05457-223	1.178	0.640	0.397	1.064	1.285	0.450	0.705	0.953	+0.0 ^{+0.4} -0.4
J05458+729	1.092	0.685	0.486	1.044	1.011	0.549	0.776	1.026	+0.0 ^{+0.3} -0.3
J05463+012	1.123	0.701	0.504	1.043	1.132	0.558	0.781	1.011	+0.0 ^{+0.3} -0.3
J05501+051	1.015	0.781	0.646	1.022	0.896	0.692	0.833	1.023	-3.4 ^{+0.4} -0.1
J05511+122	1.251	0.600	0.391	1.098	1.552	0.472	0.737	1.030	-0.6 ^{+0.3} -0.2
J05566-103	1.194	0.589	0.411	1.091	1.390	0.451	0.685	0.910	-3.4 ^{+0.6} -0.4
J05582-046	1.351	0.495	0.271	1.143	1.890	0.387	0.680	1.048	-0.8 ^{+0.4} -0.2
J05588+213	1.380	0.456	0.284	1.167	2.246	0.393	0.685	1.040	-1.5 ^{+0.5} -0.4
J05596+585	0.953	0.805	0.642	0.997	0.772	0.691	0.836	1.041	+0.0 ^{+0.3} -0.3
J06024+663	1.349	0.529	0.332	1.143	1.872	0.443	0.723	1.071	-0.7 ^{+0.3} -0.3
J06024+498	1.397	0.473	0.280	1.165	2.206	0.374	0.665	1.007	-0.6 ^{+0.2} -0.3
J06035+168	1.229	0.547	0.381	1.109	1.518	0.421	0.650	0.893	-5.0 ^{+0.3} -0.2
J06035+155	0.944	0.885	0.805	0.992	0.758	0.862	0.905	1.064	+0.0 ^{+0.6} -0.6
J06054+608	1.301	0.488	0.355	1.158	1.769	0.457	0.710	1.033	-9.3 ^{+0.6} -0.4
J06065+045	1.151	0.642	0.415	1.066	1.186	0.499	0.757	1.054	+0.0 ^{+0.2} -0.2

Table A.2. Seven representative spectral indices, ζ metallicity index, and H α pseudo-equivalent width (cont.).

Karmn	PC1	TiO 2	TiO 5	VO-7912	Color-M	CaH 2	CaH 3	ζ	$pEW(H\alpha)$ [Å]
J06066+465	1.153	0.658	0.464	1.062	1.286	0.518	0.763	0.998	-0.5 ^{+0.1} _{-0.2}
J06075+472	1.314	0.492	0.341	1.150	1.799	0.415	0.666	0.961	-9.2 ^{+0.8} _{-0.9}
J06102+225	1.277	0.512	0.372	1.126	1.421	0.451	0.672	0.958	-7.9 ^{+0.6} _{-0.4}
J06103+722	1.086	0.674	0.467	1.054	1.076	0.552	0.795	1.103	+0.0 ^{+0.4} _{-0.4}
J06145+025	1.143	0.626	0.428	1.071	1.172	0.515	0.760	1.058	+0.0 ^{+0.4} _{-0.4}
J06151-164	1.267	0.583	0.384	1.100	1.609	0.462	0.698	0.979	+0.0 ^{+0.3} _{-0.3}
J06171+051 AB	1.188	0.643	0.419	1.082	1.395	0.479	0.737	0.990	+0.0 ^{+0.4} _{-0.4}
J06185+250	1.244	0.576	0.387	1.110	1.505	0.486	0.757	1.084	+0.0 ^{+0.4} _{-0.4}
J06236-096 AB	1.160	0.624	0.437	1.075	1.302	0.477	0.710	0.924	-2.2 ^{+0.5} _{-0.5}
J06238+456	1.397	0.459	0.298	1.170	2.084	0.382	0.655	0.981	-6.1 ^{+0.9} _{-0.6}
J06246+234	1.214	0.559	0.342	1.103	1.489	0.412	0.669	0.959	+0.0 ^{+0.4} _{-0.4}
J06298-027 AB	1.250	0.502	0.352	1.123	1.487	0.457	0.724	1.056	-5.7 ^{+0.5} _{-0.5}
J06307+397	1.055	0.742	0.556	1.027	1.041	0.573	0.782	0.928	+0.0 ^{+0.2} _{-0.2}
J06313+006	1.022	0.806	0.631	1.014	0.931	0.657	0.838	1.000	+0.0 ^{+0.2} _{-0.2}
J06314-016	0.986	0.760	0.561	1.017	0.812	0.635	0.844	1.152	+0.0 ^{+0.2} _{-0.2}
J06323-097	1.290	0.543	0.349	1.127	1.743	0.437	0.704	1.012	-0.9 ^{+0.3} _{-0.1}
J06325+641	1.259	0.572	0.377	1.117	1.573	0.479	0.759	1.094	-0.5 ^{+0.2} _{-0.1}
J06332+054	1.070	0.734	0.551	1.030	1.037	0.608	0.815	1.058	+0.0 ^{+0.3} _{-0.3}
J06354-040 AB	1.467	0.418	0.283	1.183	2.351	0.364	0.647	0.980	-7.1 ^{+0.7} _{-0.5}
J06361+201	1.084	0.693	0.492	1.044	1.102	0.539	0.769	0.987	+0.0 ^{+0.4} _{-0.4}
J06367+378	1.219	0.568	0.396	1.110	1.336	0.475	0.718	1.000	-6.8 ^{+0.4} _{-0.3}
J06401-164	1.070	0.663	0.458	1.045	1.019	0.527	0.757	1.015	+0.0 ^{+0.4} _{-0.4}
J06435+166	1.288	0.538	0.340	1.130	1.730	0.445	0.723	1.060	-0.7 ^{+0.2} _{-0.4}
J06461+325	0.998	0.833	0.686	0.997	0.893	0.692	0.842	0.925	+0.0 ^{+0.3} _{-0.3}
J06474+054	1.266	0.587	0.382	1.109	1.567	0.486	0.758	1.094	-0.3 ^{+0.1} _{-0.2}
J06489+211	1.086	0.689	0.525	1.051	1.097	0.561	0.765	0.949	-1.9 ^{+0.1} _{-0.3}
J06509-091	1.187	0.632	0.429	1.068	1.330	0.498	0.748	1.013	-0.3 ^{+0.1} _{-0.3}
J06522+179	0.937	0.916	0.833	0.978	0.761	0.862	0.922	0.958	+0.4 ^{+0.1} _{-0.2}
J06522+627	1.205	0.604	0.426	1.087	1.436	0.467	0.703	0.924	-2.4 ^{+0.5} _{-0.3}
J06523-051S AB	1.065	0.744	0.554	1.032	1.054	0.583	0.791	0.964	+0.0 ^{+0.3} _{-0.3}
J06523-051N	0.840	0.972	0.925	0.969	0.553	1.079	1.005	0.953	+0.8 ^{+0.1} _{-0.4}
J06548+332	1.156	0.662	0.458	1.061	1.277	0.514	0.753	0.990	+0.0 ^{+0.3} _{-0.3}
J06565+440	1.299	0.559	0.357	1.128	1.740	0.462	0.744	1.082	-0.5 ^{+0.2} _{-0.5}
J07001-190	1.388	0.476	0.327	1.170	1.941	0.435	0.713	1.054	-8.6 ^{+0.7} _{-0.5}
J07009-023	1.136	0.671	0.482	1.058	1.218	0.535	0.769	0.999	+0.0 ^{+0.3} _{-0.3}
J07031+836	1.170	0.621	0.417	1.066	1.273	0.468	0.711	0.948	+0.0 ^{+0.3} _{-0.3}
J07051-101	1.330	0.476	0.323	1.150	1.908	0.389	0.648	0.946	-6.0 ^{+0.4} _{-0.7}
J07105-087	1.203	0.613	0.423	1.088	1.421	0.480	0.727	0.972	-1.7 ^{+0.5} _{-0.5}
J07105+283	0.930	0.885	0.780	0.984	0.760	0.822	0.896	1.033	+0.4 ^{+0.1} _{-0.2}
J07111-035	0.979	0.871	0.748	0.992	0.848	0.762	0.879	0.960	+0.0 ^{+0.3} _{-0.3}
J07111+434 AB	1.577	0.350	0.181	1.229	2.971	0.289	0.597	1.019	-1.4 ^{+0.4} _{-0.5}
J07172-050	1.158	0.563	0.383	1.093	1.255	0.436	0.674	0.927	-3.5 ^{+0.5} _{-0.5}
J07182+137	1.211	0.608	0.421	1.088	1.439	0.499	0.755	1.038	+0.0 ^{+0.4} _{-0.4}
J07191+667	0.931	0.883	0.795	0.983	0.748	0.848	0.908	1.080	+0.4 ^{+0.1} _{-0.2}
J07195+328	0.932	0.873	0.773	0.980	0.749	0.813	0.900	1.051	+0.0 ^{+0.4} _{-0.4}
J07219-222	1.220	0.620	0.408	1.085	1.412	0.491	0.747	1.037	-0.5 ^{+0.2} _{-0.2}
J07274+052	1.176	0.612	0.408	1.091	1.393	0.481	0.740	1.015	-0.5 ^{+0.2} _{-0.2}
J07310+460	1.249	0.520	0.365	1.126	1.559	0.431	0.669	0.943	-9.5 ^{+0.6} _{-0.5}
J07319+362N	1.217	0.595	0.404	1.102	1.438	0.471	0.719	0.982	-2.4 ^{+0.3} _{-0.2}
J07319+362S AB	1.103	0.672	0.487	1.057	1.109	0.551	0.773	1.020	-2.0 ^{+2.0} _{-0.2}
J07321-088	0.845	0.979	0.926	0.956	0.543	1.050	1.000	0.911	+0.6 ^{+0.2} _{-0.2}
J07324-130	0.900	0.880	0.759	0.980	0.686	0.812	0.892	1.090	+0.0 ^{+0.4} _{-0.4}
J07359+785	1.151	0.635	0.430	1.069	1.253	0.511	0.763	1.052	+0.0 ^{+0.5} _{-0.5}
J07361-031	0.979	0.833	0.704	1.004	0.875	0.724	0.851	0.960	-1.0 ^{+0.3} _{-0.2}
J07365-006	1.192	0.638	0.436	1.079	1.376	0.490	0.731	0.967	-1.5 ^{+0.4} _{-0.3}
J07366+440	1.175	0.654	0.453	1.071	1.315	0.525	0.766	1.035	+0.0 ^{+0.4} _{-0.4}
J07420+142	1.176	0.922	0.649	1.049	1.240	0.966	1.249	3.966	+0.8 ^{+0.2} _{-0.4}
J07429-107	1.104	0.677	0.493	1.061	1.150	0.547	0.766	0.993	-2.0 ^{+0.4} _{-0.2}
J07467+574	1.323	0.496	0.337	1.159	1.921	0.407	0.684	0.976	-6.1 ^{+0.8} _{-0.6}

Table A.2. Seven representative spectral indices, ζ metallicity index, and H α pseudo-equivalent width (cont.).

Karmn	PC1	TiO 2	TiO 5	VO-7912	Color-M	CaH 2	CaH 3	ζ	$pEW(H\alpha)$ [Å]
J07470+760	1.219	0.598	0.397	1.096	1.479	0.467	0.728	1.001	+0.0 ^{+0.3} -0.3
J07497-033	1.170	0.605	0.404	1.078	1.275	0.459	0.708	0.956	-1.4 ^{+0.4} -0.4
J07498-032	1.153	0.553	0.387	1.094	1.192	0.447	0.677	0.936	-7.5 ^{+0.4} -0.6
J07523+162	1.605	0.359	0.260	1.247	2.785	0.360	0.694	1.050	-25.4 ^{+1.4} -1.0
J07545+085	1.103	0.699	0.502	1.044	1.166	0.532	0.755	0.938	+0.0 ^{+0.3} -0.3
J07545-096	1.176	0.642	0.448	1.069	1.290	0.501	0.734	0.965	-0.8 ^{+0.2} -0.5
J07558+833	1.451	0.572	0.404	1.129	2.212	0.409	0.661	0.860	-5.2 ^{+0.6} -0.2
J07591+173	1.205	0.550	0.388	1.101	1.262	0.449	0.671	0.930	-9.2 ^{+0.8} -0.5
J08025-130	1.122	0.676	0.489	1.057	1.176	0.535	0.762	0.976	+0.0 ^{+0.4} -0.4
J08031+203 AB	1.165	0.586	0.425	1.089	1.232	0.467	0.687	0.907	-7.2 ^{+0.5} -0.3
J08069+422	1.284	0.550	0.367	1.124	1.658	0.439	0.699	0.981	-2.5 ^{+0.3} -0.4
J08082+211N	0.901	0.924	0.852	0.975	0.700	0.908	0.937	1.025	+0.5 ^{+0.1} -0.2
J08082+211S AB	1.128	0.658	0.481	1.060	1.159	0.518	0.738	0.934	-3.7 ^{+0.4} -0.5
J08104-111	0.956	0.741	0.539	1.013	0.743	0.613	0.810	1.087	+0.0 ^{+0.3} -0.3
J08105-138 AB	1.093	0.722	0.532	1.033	1.108	0.570	0.784	0.977	+0.0 ^{+0.3} -0.3
J08117+531	1.109	0.646	0.446	1.060	1.137	0.535	0.788	1.101	+0.0 ^{+0.3} -0.3
J08143+630	1.024	0.784	0.618	1.007	0.890	0.647	0.828	0.995	+0.0 ^{+0.3} -0.3
J08161+013	1.056	0.752	0.561	1.025	1.023	0.598	0.804	0.997	+0.0 ^{+0.3} -0.3
J08283+553	1.131	0.684	0.480	1.051	1.151	0.537	0.767	1.002	+0.0 ^{+0.3} -0.3
J08286+660	1.228	0.557	0.386	1.113	1.414	0.438	0.682	0.934	-7.7 ^{+0.3} -0.3
J08298+267	1.680	0.299	0.196	1.298	4.578	0.270	0.568	0.974	-5.2 ^{+0.9} -1.1
J08353+141	1.277	0.522	0.341	1.133	1.608	0.440	0.715	1.041	-3.5 ^{+0.5} -0.5
J08375+035	1.258	0.565	0.367	1.114	1.674	0.445	0.719	1.012	+0.0 ^{+0.6} -0.6
J08386-028	0.815	0.952	0.930	0.961	0.506	1.054	0.999	0.858	+0.4 ^{+0.1} -0.1
J08394-028	0.954	0.817	0.642	0.999	0.771	0.705	0.873	1.167	+0.0 ^{+0.3} -0.3
J08423-048	1.132	0.678	0.476	1.058	1.234	0.532	0.773	1.012	+0.0 ^{+0.4} -0.4
J08449-066 AB	1.164	0.631	0.421	1.075	1.331	0.466	0.699	0.926	+0.0 ^{+0.3} -0.3
J08526+283	1.329	0.543	0.357	1.124	1.806	0.456	0.737	1.065	-0.7 ^{+0.2} -0.3
J08531-202	1.135	0.654	0.457	1.065	1.213	0.512	0.752	0.987	+0.0 ^{+0.4} -0.4
J08563-044	0.996	0.824	0.680	1.001	0.896	0.694	0.847	0.959	+0.0 ^{+0.4} -0.4
J08572+194	1.183	0.636	0.425	1.073	1.294	0.500	0.746	1.020	+0.0 ^{+0.4} -0.4
J08590+364	0.957	0.846	0.696	0.992	0.807	0.769	0.897	1.238	+0.0 ^{+0.4} -0.4
J08595+537	1.195	0.586	0.412	1.092	1.368	0.444	0.669	0.886	-5.0 ^{+0.4} -0.2
J08599+042	0.996	0.840	0.689	0.997	0.884	0.713	0.860	1.002	+0.0 ^{+0.4} -0.4
J09003+218	1.737	0.307	0.201	1.269	4.123	0.293	0.598	0.998	-10.0 ^{+0.8} -0.8
J09008+237	1.123	0.668	0.456	1.061	1.137	0.522	0.760	1.016	+0.0 ^{+0.3} -0.3
J09023+177	1.210	0.588	0.393	1.092	1.458	0.470	0.736	1.021	+0.0 ^{+0.6} -0.6
J09028+060	1.031	0.780	0.613	1.005	0.952	0.646	0.827	1.004	+0.0 ^{+0.3} -0.3
J09040-159	1.077	0.709	0.536	1.039	1.052	0.563	0.768	0.934	-2.9 ^{+0.2} -0.2
J09045+164 AB	0.844	0.970	0.923	0.972	0.568	1.076	1.003	0.974	+0.7 ^{+0.1} -0.2
J09058+555	1.182	0.624	0.414	1.078	1.281	0.473	0.715	0.963	+0.0 ^{+0.4} -0.4
J09091+227	1.314	0.527	0.332	1.139	1.932	0.416	0.688	0.997	+0.0 ^{+0.2} -1.0
J09115+126	1.105	0.696	0.504	1.050	1.124	0.566	0.796	1.050	+0.0 ^{+0.2} -0.2
J09143+526	0.941	0.902	0.805	0.981	0.750	0.839	0.909	1.001	+0.0 ^{+0.3} -0.3
J09144+526	0.943	0.896	0.791	0.978	0.759	0.822	0.904	1.003	+0.0 ^{+0.3} -0.3
J09151+233	0.938	0.879	0.767	0.979	0.750	0.803	0.896	1.040	+0.0 ^{+0.3} -0.3
J09156-105 AB	1.369	0.431	0.280	1.174	1.981	0.351	0.609	0.943	-3.9 ^{+0.5} -0.3
J09201+037	1.196	0.622	0.427	1.083	1.407	0.477	0.723	0.957	-1.4 ^{+0.5} -0.6
J09206-169	0.922	0.908	0.811	0.981	0.735	0.855	0.917	1.042	+0.0 ^{+0.4} -0.4
J09212+603	1.029	0.781	0.612	1.012	0.911	0.651	0.832	1.026	+0.0 ^{+0.4} -0.4
J09218-023	1.051	0.723	0.531	1.033	1.065	0.537	0.751	0.883	+0.0 ^{+0.3} -0.3
J09243+063	1.222	0.561	0.375	1.111	1.366	0.465	0.727	1.033	-6.1 ^{+0.4} -0.3
J09248+306	1.162	0.595	0.435	1.085	1.316	0.476	0.696	0.912	-7.2 ^{+0.5} -0.4
J09256+634	1.272	0.534	0.347	1.135	1.715	0.413	0.670	0.953	-5.1 ^{+0.4} -0.7
J09301-009	0.947	0.864	0.732	0.993	0.789	0.810	0.910	1.267	+0.4 ^{+0.1} -0.1
J09308+024	1.230	0.562	0.384	1.110	1.572	0.437	0.684	0.936	-3.5 ^{+0.3} -0.3
J09328+269	1.479	0.415	0.257	1.216	2.454	0.356	0.660	1.019	-7.2 ^{+0.6} -0.6
J09351-103	0.804	0.940	0.870	0.949	0.467	1.018	0.971	1.392	+0.6 ^{+0.1} -0.2
J09362+375	0.940	0.859	0.744	0.983	0.738	0.773	0.878	0.999	-0.9 ^{+0.2} -0.3

Table A.2. Seven representative spectral indices, ζ metallicity index, and H α pseudo-equivalent width (cont.).

Karmn	PC1	TiO 2	TiO 5	VO-7912	Color-M	CaH 2	CaH 3	ζ	$pEW(H\alpha)$ [Å]
J09394+146	1.151	0.631	0.442	1.073	1.310	0.478	0.705	0.912	-1.8 $^{+0.6}_{-0.4}$
J09449-123	1.416	0.403	0.274	1.190	1.839	0.369	0.632	0.983	-13.3 $^{+1.0}_{-1.0}$
J09488+156	1.094	0.673	0.479	1.060	1.197	0.491	0.712	0.872	-2.9 $^{+0.4}_{-0.3}$
J09526-156	1.146	0.629	0.418	1.085	1.246	0.487	0.728	0.991	+0.0 $^{+0.3}_{-0.3}$
J09538-073	0.966	0.899	0.754	0.989	0.748	0.765	0.868	0.922	-1.3 $^{+0.2}_{-0.2}$
J09589+059	1.320	0.502	0.332	1.144	1.773	0.390	0.641	0.928	-4.5 $^{+0.7}_{-0.6}$
J09597+721	1.185	0.636	0.431	1.082	1.374	0.485	0.734	0.974	+0.0 $^{+0.3}_{-0.3}$
J10008+319	1.613	0.333	0.221	1.252	3.106	0.316	0.622	1.003	-14.4 $^{+1.2}_{-1.8}$
J10020+697	1.263	0.557	0.356	1.121	1.671	0.437	0.698	0.995	-0.8 $^{+0.2}_{-0.2}$
J10028+484	1.448	0.380	0.264	1.223	2.463	0.349	0.611	0.964	-12.0 $^{+0.6}_{-0.6}$
J10063-064	1.415	0.521	0.312	1.099	1.704	0.456	0.724	1.120	+0.0 $^{+0.4}_{-0.4}$
J10068-127	1.285	0.487	0.327	1.145	1.763	0.390	0.630	0.926	-4.4 $^{+0.5}_{-0.6}$
J10098-007	0.862	0.943	0.889	0.984	0.604	1.023	0.973	1.209	+0.6 $^{+0.1}_{-0.2}$
J10120-026 AB	1.087	0.726	0.532	1.041	1.140	0.560	0.777	0.950	+0.0 $^{+0.3}_{-0.3}$
J10130+233	1.197	0.595	0.398	1.093	1.405	0.485	0.755	1.059	+0.0 $^{+0.3}_{-0.3}$
J10148+213	1.276	0.500	0.329	1.144	1.696	0.395	0.643	0.938	-5.9 $^{+0.5}_{-0.9}$
J10155-164	1.226	0.583	0.391	1.102	1.400	0.483	0.745	1.054	-3.5 $^{+0.3}_{-0.5}$
J10196+198 AB	1.141	0.638	0.466	1.066	1.204	0.506	0.732	0.937	-4.1 $^{+0.3}_{-0.4}$
J10200+289	1.111	0.678	0.479	1.056	1.216	0.514	0.742	0.938	+0.0 $^{+0.4}_{-0.4}$
J10238+438	1.407	0.435	0.288	1.185	2.299	0.396	0.696	1.050	-5.1 $^{+0.5}_{-0.5}$
J10240+366	1.184	0.623	0.423	1.095	1.382	0.487	0.735	0.991	-1.9 $^{+0.2}_{-0.3}$
J10278+028	1.222	0.607	0.401	1.089	1.413	0.494	0.758	1.072	+0.0 $^{+0.6}_{-0.6}$
J10304+559	0.891	0.942	0.883	0.971	0.663	0.931	0.947	0.902	+0.5 $^{+0.1}_{-0.2}$
J10359+288	1.142	0.640	0.460	1.080	1.265	0.506	0.736	0.952	-2.9 $^{+0.6}_{-0.4}$
J10368+509	1.271	0.510	0.347	1.138	1.747	0.413	0.665	0.948	-4.5 $^{+0.3}_{-0.3}$
J10430-092 AB	1.471	0.439	0.259	1.190	2.546	0.363	0.677	1.038	-1.7 $^{+0.4}_{-0.5}$
J10443+124	1.217	0.610	0.407	1.092	1.417	0.501	0.763	1.078	+0.0 $^{+0.6}_{-0.6}$
J10482-113	1.787	0.266	0.149	1.307	4.604	0.237	0.534	0.999	-3.7 $^{+0.6}_{-1.0}$
J10508+068	1.261	0.586	0.385	1.110	1.670	0.461	0.727	1.010	+0.0 $^{+0.4}_{-0.4}$
J10546-073	1.256	0.609	0.380	1.106	1.540	0.466	0.752	1.061	+0.0 $^{+0.4}_{-0.4}$
J10560+061	1.448	0.668	0.414	1.297	3.074	0.683	1.373	7.230	+0.0 $^{+0.4}_{-0.4}$
J10563+042	1.102	0.699	0.510	1.046	1.137	0.551	0.772	0.973	+0.0 $^{+0.4}_{-0.4}$
J10564+070	1.662	0.328	0.226	1.244	3.418	0.327	0.645	1.025	-10.9 $^{+0.9}_{-0.2}$
J10584-107	1.324	0.445	0.312	1.156	1.933	0.387	0.635	0.948	-6.1 $^{+0.4}_{-0.7}$
J11018-024	1.001	0.842	0.690	1.002	0.769	0.927	0.953	2.412	+0.9 $^{+0.3}_{-0.1}$
J11030+037	1.112	0.698	0.501	1.052	1.165	0.540	0.770	0.972	+0.0 $^{+0.3}_{-0.3}$
J11033+359	1.042	0.773	0.570	1.018	0.991	0.616	0.823	1.042	+0.0 $^{+0.3}_{-0.3}$
J11046-042S AB	0.959	0.862	0.763	0.989	0.792	0.794	0.879	0.984	-1.9 $^{+0.2}_{-0.1}$
J11054+435	0.978	0.829	0.678	0.995	0.853	0.687	0.845	0.947	+0.0 $^{+0.3}_{-0.3}$
J11055+435	1.472	0.299	0.191	1.232	2.560	0.257	0.473	0.937	-10.2 $^{+1.2}_{-1.9}$
J11075+437	1.135	0.651	0.468	1.068	1.256	0.488	0.713	0.891	-2.9 $^{+0.4}_{-0.4}$
J11151+734N	1.097	0.707	0.517	1.043	1.120	0.555	0.774	0.968	+0.0 $^{+0.3}_{-0.3}$
J11151+734S	0.809	0.987	0.913	0.987	0.560	1.087	1.018	1.125	+0.8 $^{+0.2}_{-0.2}$
J11201-104 AB	1.057	0.755	0.566	1.020	0.886	0.611	0.773	0.954	-3.3 $^{+0.2}_{-0.2}$
J11201+301	1.001	0.802	0.646	0.999	0.795	0.897	0.948	2.449	+0.9 $^{+0.2}_{-0.3}$
J11214-204N	0.902	0.938	0.870	0.973	0.676	0.934	0.943	0.998	+0.0 $^{+0.3}_{-0.3}$
J11214-204S	1.124	0.697	0.535	1.053	1.211	0.552	0.757	0.904	-3.3 $^{+0.2}_{-0.2}$
J11218+181	0.943	0.859	0.737	0.993	0.774	0.788	0.888	1.099	+0.0 $^{+0.4}_{-0.4}$
J11240+381	1.259	0.510	0.352	1.136	1.693	0.405	0.649	0.921	-6.9 $^{+0.4}_{-0.3}$
J11306-080	1.189	0.651	0.434	1.067	1.300	0.487	0.738	0.976	+0.0 $^{+0.3}_{-0.3}$
J11312+631	0.907	0.934	0.855	0.974	0.696	0.912	0.941	1.029	+0.3 $^{+0.2}_{-0.1}$
J11378+418	1.071	0.731	0.523	1.032	1.011	0.586	0.817	1.084	+0.0 $^{+0.3}_{-0.3}$
J11403+095	1.006	0.804	0.628	1.015	0.881	0.647	0.824	0.961	+0.0 $^{+0.3}_{-0.3}$
J11421+267	1.090	0.697	0.489	1.046	1.136	0.545	0.779	1.017	+0.0 $^{+0.3}_{-0.3}$
J11451+183	1.246	0.576	0.389	1.107	1.492	0.488	0.759	1.086	+0.0 $^{+0.3}_{-0.3}$
J11458+065	0.974	0.804	0.636	0.990	0.722	0.896	0.967	2.677	+0.8 $^{+0.1}_{-0.2}$
J11472+770	0.893	0.902	0.807	0.970	0.650	0.888	0.927	1.212	+0.4 $^{+0.1}_{-0.2}$
J11474+667	1.338	0.444	0.307	1.170	1.971	0.398	0.657	0.986	-9.2 $^{+0.6}_{-0.6}$
J11485+076	1.171	0.570	0.408	1.100	1.369	0.440	0.663	0.883	-6.2 $^{+0.5}_{-0.5}$

Table A.2. Seven representative spectral indices, ζ metallicity index, and H α pseudo-equivalent width (cont.).

Karmn	PC1	TiO 2	TiO 5	VO-7912	Color-M	CaH 2	CaH 3	ζ	$pEW(H\alpha)$ [Å]
J11511+352	1.015	0.802	0.640	1.004	0.930	0.650	0.828	0.945	+0.0 ^{+0.3} -0.3
J11522+100	1.297	0.571	0.374	1.112	1.635	0.470	0.739	1.057	-0.8 ^{+0.4} -0.2
J11549-021	1.130	0.668	0.464	1.056	1.239	0.512	0.747	0.967	+0.0 ^{+0.3} -0.3
J12025+084	1.011	0.769	0.589	1.012	0.949	0.590	0.790	0.898	+0.0 ^{+0.3} -0.3
J12049+174	1.143	0.622	0.440	1.075	1.229	0.475	0.701	0.907	-6.2 ^{+0.2} -0.2
J12069+058	0.874	0.956	0.901	0.966	0.624	0.999	0.971	1.011	+0.5 ^{+0.1} -0.1
J12088+217	0.971	0.860	0.737	0.997	0.819	0.766	0.890	1.040	+0.0 ^{+0.3} -0.3
J12093+210	1.131	0.661	0.472	1.066	1.230	0.527	0.758	0.989	-0.7 ^{+0.3} -0.3
J12104-131	1.263	0.516	0.352	1.123	1.619	0.424	0.679	0.967	-3.5 ^{+0.5} -0.5
J12124+121	1.053	0.746	0.560	1.022	1.027	0.599	0.798	0.989	+0.0 ^{+0.3} -0.3
J12162+508	1.280	0.544	0.374	1.120	1.540	0.446	0.697	0.976	-7.6 ^{+0.4} -0.4
J12228-040	1.288	0.488	0.335	1.152	1.709	0.402	0.651	0.943	-6.5 ^{+0.5} -0.4
J12322+454	1.147	1.023	0.641	1.100	1.338	0.996	1.470	1.593	+0.8 ^{+0.1} -0.2
J12349+322	1.157	0.649	0.439	1.078	1.330	0.497	0.741	0.985	+0.0 ^{+0.3} -0.3
J12364+352	1.296	0.546	0.363	1.131	1.750	0.432	0.703	0.984	-1.7 ^{+0.3} -0.3
J12368-019	1.226	0.603	0.400	1.103	1.444	0.490	0.758	1.067	+0.0 ^{+0.3} -0.3
J12372+358	1.028	0.754	0.583	1.019	0.937	0.620	0.810	0.995	+0.0 ^{+0.3} -0.3
J12417+567	1.155	0.604	0.433	1.083	1.327	0.469	0.694	0.905	-5.0 ^{+0.3} -0.3
J12440-111	1.282	0.523	0.346	1.136	1.709	0.416	0.672	0.960	-4.4 ^{+0.4} -0.3
J12456+271	1.211	0.872	0.542	1.114	1.521	0.859	1.346	5.309	+0.7 ^{+0.2} -0.2
J12470+466	1.125	0.691	0.499	1.049	1.168	0.560	0.791	1.042	+0.0 ^{+0.3} -0.3
J12488+120	1.303	0.539	0.331	1.119	1.718	0.424	0.710	1.032	+0.0 ^{+0.3} -0.3
J12533-053	1.118	0.654	0.436	1.062	1.092	0.513	0.771	1.056	+0.0 ^{+0.3} -0.3
J12533+466	1.145	0.913	0.601	1.098	1.630	0.945	1.329	3.775	+0.7 ^{+0.2} -0.1
J12549-063	1.331	0.495	0.341	1.141	1.868	0.381	0.619	0.891	-5.5 ^{+0.6} -0.4
J12593-001	1.241	0.603	0.398	1.091	1.443	0.483	0.757	1.059	+0.0 ^{+0.3} -0.3
J13027+415	1.184	0.638	0.432	1.088	1.327	0.505	0.758	1.033	+0.0 ^{+0.3} -0.3
J13088-015	1.141	0.640	0.454	1.060	1.191	0.514	0.759	1.007	+0.0 ^{+0.3} -0.3
J13102+477	1.348	0.478	0.306	1.165	1.921	0.390	0.655	0.978	-5.9 ^{+0.5} -0.8
J13113+096	0.912	0.898	0.787	0.981	0.688	0.880	0.942	1.372	+0.5 ^{+0.2} -0.2
J13143+133 AB	1.587	0.336	0.221	1.282	2.931	0.322	0.618	1.006	-16.9 ^{+1.4} -1.1
J13167-123	1.195	0.617	0.415	1.084	1.374	0.469	0.712	0.953	+0.0 ^{+0.4} -0.4
J13168+170	0.964	0.845	0.700	0.990	0.806	0.736	0.864	1.032	+0.0 ^{+0.3} -0.3
J13179+362	0.986	0.806	0.632	1.005	0.861	0.703	0.870	1.186	+0.0 ^{+0.3} -0.3
J13182+733	1.200	0.600	0.393	1.099	1.367	0.489	0.752	1.069	+0.0 ^{+0.4} -0.4
J13247-050	1.260	0.571	0.377	1.112	1.643	0.457	0.721	1.014	-1.2 ^{+0.5} -0.6
J13251-114	1.120	0.655	0.466	1.065	1.206	0.516	0.746	0.969	-1.6 ^{+0.4} -0.2
J13253+426	0.887	0.959	0.900	0.965	0.648	0.982	0.970	0.970	+0.5 ^{+0.1} -0.1
J13260+275	1.105	0.644	0.476	1.071	1.187	0.502	0.735	0.918	-2.0 ^{+0.4} -0.4
J13294-143	1.181	0.583	0.426	1.092	1.251	0.473	0.688	0.913	-6.1 ^{+0.4} -0.5
J13312+589	1.080	0.723	0.539	1.036	1.077	0.548	0.765	0.903	+0.0 ^{+0.3} -0.3
J13314-079	0.928	0.879	0.754	0.978	0.709	0.812	0.906	1.157	+0.4 ^{+0.2} -0.1
J13321-112	0.913	0.899	0.795	0.975	0.701	0.862	0.914	1.146	+0.4 ^{+0.2} -0.1
J13326+309	1.266	0.508	0.346	1.135	1.630	0.415	0.664	0.952	-5.3 ^{+0.3} -0.4
J13335+704	1.221	0.615	0.411	1.089	1.436	0.485	0.746	1.024	+0.0 ^{+0.4} -0.4
J13386-115	1.263	0.499	0.348	1.133	1.565	0.411	0.648	0.930	-6.4 ^{+0.5} -0.5
J13394+461 AB	1.024	0.780	0.606	1.011	0.928	0.671	0.854	1.139	+0.0 ^{+0.3} -0.3
J13413-091	1.117	0.682	0.476	1.058	1.161	0.521	0.750	0.962	+0.0 ^{+0.3} -0.3
J13414+489	1.169	0.667	0.451	1.069	1.327	0.498	0.742	0.965	+0.0 ^{+0.3} -0.3
J13474+063	0.881	0.957	0.914	0.967	0.641	1.007	0.974	0.907	+0.6 ^{+0.1} -0.1
J13503-216	1.212	0.612	0.400	1.085	1.442	0.479	0.735	1.019	+0.0 ^{+0.3} -0.3
J13537+521 AB	1.160	0.600	0.422	1.081	1.271	0.507	0.746	1.036	+0.0 ^{+0.6} -0.6
J13551-079	0.915	0.892	0.780	0.976	0.694	0.834	0.905	1.098	+0.3 ^{+0.2} -0.1
J13555-073	1.132	0.673	0.477	1.039	1.166	0.530	0.761	0.991	+0.0 ^{+0.3} -0.3
J13582-120	1.295	0.533	0.338	1.142	1.705	0.442	0.715	1.050	+0.0 ^{+0.6} -0.6
J13583-132	1.243	0.565	0.377	1.110	1.574	0.440	0.697	0.965	-1.9 ^{+0.4} -0.3
J13587+465	1.085	0.732	0.558	1.012	0.927	0.827	0.941	2.414	+1.0 ^{+0.1} -0.1
J14019+432	1.087	0.686	0.487	1.042	1.052	0.541	0.767	0.995	+0.0 ^{+0.3} -0.3
J14102-180	1.125	0.690	0.498	1.049	1.160	0.571	0.801	1.081	+0.0 ^{+0.3} -0.3

Table A.2. Seven representative spectral indices, ζ metallicity index, and H α pseudo-equivalent width (cont.).

Karmn	PC1	TiO 2	TiO 5	VO-7912	Color-M	CaH 2	CaH 3	ζ	$pEW(H\alpha)$ [Å]
J14159–110	1.032	0.757	0.602	1.012	0.892	0.625	0.794	0.931	-2.0 ^{+0.2} _{-0.3}
J14171+088	1.273	0.524	0.326	1.122	1.627	0.427	0.703	1.036	-1.0 ^{+0.3} _{-0.4}
J14175+025	1.121	0.669	0.483	1.059	1.192	0.512	0.731	0.915	-2.5 ^{+0.5} _{-0.3}
J14194+029	1.372	0.471	0.309	1.166	1.942	0.394	0.671	0.992	-7.4 ^{+0.5} _{-0.7}
J14195–051	1.217	0.576	0.370	1.107	1.494	0.446	0.687	0.972	+0.0 ^{+0.3} _{-0.3}
J14215–079	1.240	0.609	0.401	1.094	1.504	0.480	0.755	1.046	+0.0 ^{+0.3} _{-0.3}
J14227+164	1.342	0.476	0.326	1.147	1.857	0.399	0.652	0.954	-6.4 ^{+0.4} _{-0.6}
J14244+602	1.073	0.751	0.569	1.020	0.989	0.610	0.807	1.004	+0.0 ^{+0.3} _{-0.3}
J14251+518	1.083	0.707	0.511	1.034	1.063	0.558	0.780	0.995	+0.0 ^{+0.3} _{-0.3}
J14255–118	1.239	0.585	0.400	1.100	1.491	0.475	0.734	1.012	-2.0 ^{+0.4} _{-0.4}
J14312+754	1.194	0.548	0.377	1.100	1.436	0.406	0.630	0.870	-4.7 ^{+0.5} _{-0.6}
J14336+093	1.167	0.649	0.432	1.071	1.286	0.501	0.750	1.015	+0.0 ^{+0.3} _{-0.3}
J14415+136	1.008	0.810	0.658	1.004	0.868	0.693	0.839	1.006	+0.0 ^{+0.3} _{-0.3}
J14446–222	1.315	0.540	0.350	1.116	1.654	0.468	0.755	1.119	+0.0 ^{+0.3} _{-0.3}
J14472+570	1.192	0.547	0.386	1.103	1.353	0.436	0.659	0.908	-6.7 ^{+0.5} _{-0.3}
J14480+384	0.880	0.937	0.858	0.972	0.639	0.932	0.945	1.092	+0.4 ^{+0.1} _{-0.1}
J14485+101	1.209	0.618	0.426	1.079	1.361	0.505	0.759	1.045	+0.0 ^{+0.3} _{-0.3}
J14492+498	1.020	0.779	0.611	1.021	0.920	0.648	0.821	1.000	+0.0 ^{+0.3} _{-0.3}
J14501+323	1.188	0.633	0.429	1.074	1.305	0.516	0.774	1.080	+0.0 ^{+0.3} _{-0.3}
J14544+161 ABC	0.981	0.748	0.570	1.006	0.802	0.619	0.798	1.002	-1.4 ^{+0.3} _{-0.2}
J14595+454	0.887	0.946	0.885	0.960	0.641	0.956	0.954	0.985	+0.5 ^{+0.1} _{-0.1}
J15079+762	1.268	0.469	0.322	1.149	1.556	0.412	0.667	0.986	-9.0 ^{+0.5} _{-0.3}
J15081+623	1.229	0.623	0.416	1.098	1.462	0.477	0.728	0.980	+0.0 ^{+0.3} _{-0.3}
J15118+395	1.107	0.701	0.504	1.045	1.130	0.537	0.759	0.946	+0.0 ^{+0.3} _{-0.3}
J15131+181	1.052	0.751	0.571	1.027	0.981	0.602	0.800	0.973	+0.0 ^{+0.3} _{-0.3}
J15142–099	1.226	0.538	0.355	1.109	1.414	0.428	0.674	0.960	-3.8 ^{+0.6} _{-0.4}
J15147+645	1.156	0.626	0.414	1.066	1.354	0.433	0.668	0.872	-0.5 ^{+0.2} _{-0.1}
J15151+333	1.064	0.734	0.529	1.023	1.039	0.562	0.774	0.957	+0.0 ^{+0.3} _{-0.3}
J15157–074	1.207	0.566	0.384	1.103	1.390	0.440	0.690	0.946	-3.3 ^{+0.4} _{-0.2}
J15164+167	0.880	0.936	0.868	0.965	0.645	0.963	0.969	1.203	+0.6 ^{+0.1} _{-0.1}
J15197+046	1.238	0.588	0.400	1.099	1.585	0.444	0.692	0.927	-1.8 ^{+0.3} _{-0.3}
J15204+001	0.899	0.921	0.829	0.972	0.673	0.872	0.927	1.026	+0.4 ^{+0.2} _{-0.1}
J15210+255	0.888	0.937	0.860	0.975	0.647	0.939	0.947	1.110	+0.4 ^{+0.2} _{-0.1}
J15238+584	1.197	0.549	0.381	1.105	1.345	0.432	0.660	0.913	-8.2 ^{+0.3} _{-0.3}
J15277–090	1.345	0.513	0.331	1.146	1.901	0.427	0.713	1.038	+0.0 ^{+0.4} _{-0.4}
J15290+467 AB	1.308	0.490	0.323	1.141	1.808	0.389	0.640	0.939	-4.8 ^{+0.5} _{-0.4}
J15291+574	0.981	0.838	0.708	0.991	0.840	0.729	0.867	0.995	+0.0 ^{+0.3} _{-0.3}
J15305+094	1.482	0.380	0.244	1.216	2.570	0.319	0.586	0.953	-7.4 ^{+0.8} _{-0.8}
J15340+513	1.337	0.551	0.348	1.119	1.848	0.446	0.730	1.057	-0.9 ^{+0.4} _{-0.3}
J15386+371	1.184	0.640	0.425	1.081	1.336	0.493	0.751	1.017	+0.0 ^{+0.4} _{-0.4}
J15430–130	1.015	0.788	0.617	1.018	0.922	0.644	0.818	0.973	+0.0 ^{+0.3} _{-0.3}
J15474+451	1.232	0.564	0.366	1.100	1.485	0.441	0.708	0.996	-4.1 ^{+0.7} _{-0.5}
J15476+226	1.276	0.504	0.338	1.134	1.630	0.417	0.672	0.973	-4.7 ^{+0.4} _{-0.2}
J15480+043	1.122	0.668	0.499	1.047	1.137	0.526	0.745	0.922	-4.7 ^{+0.3} _{-0.2}
J15481+015	1.132	0.682	0.495	1.052	1.241	0.533	0.751	0.946	+0.0 ^{+0.4} _{-0.4}
J15499+796	1.375	0.462	0.302	1.171	1.969	0.379	0.635	0.956	-6.7 ^{+0.6} _{-0.9}
J15552–101	1.107	0.672	0.466	1.045	1.029	0.544	0.785	1.072	+0.0 ^{+0.3} _{-0.3}
J15557–103	1.178	0.584	0.412	1.092	1.272	0.464	0.689	0.927	-4.9 ^{+0.5} _{-0.4}
J15558–118	1.157	0.671	0.454	1.060	1.163	0.515	0.765	1.018	+0.0 ^{+0.3} _{-0.3}
J15569+376	1.083	0.654	0.489	1.058	1.043	0.541	0.744	0.957	-5.2 ^{+0.3} _{-0.3}
J15578+090	1.280	0.581	0.373	1.106	1.629	0.463	0.740	1.051	+0.0 ^{+0.3} _{-0.3}
J16023+036	1.022	0.778	0.637	1.023	0.911	0.670	0.812	0.960	-3.7 ^{+0.3} _{-0.3}
J16042+235	1.398	0.455	0.302	1.165	2.058	0.380	0.645	0.966	-6.8 ^{+0.8} _{-0.8}
J16048+391	1.210	0.590	0.361	1.099	1.460	0.408	0.661	0.921	-1.7 ^{+0.3} _{-0.5}
J16120+033N	1.195	0.573	0.376	1.098	1.365	0.454	0.705	0.991	-1.8 ^{+0.6} _{-1.0}
J16139+337 AB	1.113	0.700	0.510	1.043	1.128	0.548	0.769	0.963	+0.0 ^{+0.3} _{-0.3}
J16148+606 AB	1.109	0.655	0.454	1.057	1.151	0.481	0.708	0.899	-1.1 ^{+0.3} _{-0.6}
J16157+586	1.360	0.464	0.309	1.154	1.871	0.401	0.655	0.983	-7.0 ^{+0.9} _{-0.6}
J16167+672S	0.931	0.877	0.762	0.982	0.738	0.813	0.899	1.099	+0.0 ^{+0.4} _{-0.4}

Table A.2. Seven representative spectral indices, ζ metallicity index, and H α pseudo-equivalent width (cont.).

Karmn	PC1	TiO 2	TiO 5	VO-7912	Color-M	CaH 2	CaH 3	ζ	$pEW(H\alpha)$ [Å]
J16183+757	1.266	0.561	0.368	1.113	1.604	0.440	0.700	0.982	-1.0 ^{+0.5} _{-0.6}
J16243+199	1.121	0.610	0.456	1.066	1.052	0.482	0.697	0.885	-6.3 ^{+0.6} _{-0.4}
J16254+543	1.014	0.768	0.591	1.016	0.920	0.592	0.777	0.878	+0.0 ^{+0.3} _{-0.3}
J16269+149	1.259	0.507	0.354	1.123	1.342	0.423	0.643	0.927	-8.8 ^{+0.7} _{-0.9}
J16276-035 AB	0.856	0.964	0.919	0.962	0.578	1.043	0.989	0.961	+0.0 ^{+0.5} _{-0.5}
J16299+048	1.144	0.646	0.450	1.071	1.239	0.503	0.738	0.969	+0.0 ^{+0.3} _{-0.3}
J16314+471	1.175	0.564	0.389	1.094	1.273	0.445	0.689	0.942	-3.9 ^{+0.3} _{-0.4}
J16330+031	1.172	0.648	0.440	1.064	1.265	0.511	0.756	1.022	+0.0 ^{+0.3} _{-0.3}
J16354-039	0.925	0.958	0.895	0.977	0.722	0.889	0.926	0.664	+0.0 ^{+0.4} _{-0.4}
J16365+287	1.214	0.602	0.407	1.088	1.353	0.500	0.757	1.069	+0.0 ^{+0.3} _{-0.3}
J16459+609	1.171	0.627	0.416	1.085	1.288	0.480	0.736	0.994	+0.0 ^{+0.4} _{-0.4}
J16465+345	1.658	0.354	0.189	1.238	3.594	0.300	0.634	1.042	-1.7 ^{+0.7} _{-0.7}
J16480+453	1.239	0.521	0.365	1.121	1.360	0.435	0.667	0.947	-7.8 ^{+0.3} _{-0.4}
J16528+610	1.333	0.526	0.327	1.138	1.828	0.431	0.713	1.050	+0.0 ^{+0.5} _{-0.5}
J16536+560	1.172	0.583	0.377	1.085	1.271	0.476	0.737	1.059	+0.0 ^{+0.3} _{-0.3}
J16543+256	1.138	0.645	0.433	1.066	1.187	0.521	0.769	1.070	+0.0 ^{+0.3} _{-0.3}
J16555-083	1.864	0.239	0.156	1.318	4.955	0.242	0.519	0.987	-6.0 ^{+1.0} _{-1.1}
J17011+555	1.098	0.721	0.512	1.038	1.109	0.536	0.757	0.926	+0.0 ^{+0.3} _{-0.3}
J17017+741	1.163	0.612	0.404	1.075	1.290	0.467	0.713	0.970	+0.0 ^{+0.3} _{-0.3}
J17052-050	1.028	0.747	0.559	1.019	0.928	0.631	0.828	1.113	+0.0 ^{+0.3} _{-0.3}
J17062+646	1.107	0.673	0.474	1.047	1.154	0.504	0.741	0.930	+0.0 ^{+0.3} _{-0.3}
J17094+391	1.103	0.663	0.448	1.051	1.121	0.499	0.728	0.954	+0.0 ^{+0.3} _{-0.3}
J17126-099	1.321	0.610	0.450	1.050	1.476	0.673	0.904	1.788	+0.8 ^{+0.1} _{-0.1}
J17140+176	1.104	0.693	0.486	1.046	1.110	0.547	0.784	1.033	+0.0 ^{+0.3} _{-0.3}
J17154+308	1.098	0.708	0.518	1.045	1.108	0.560	0.772	0.973	+0.0 ^{+0.3} _{-0.3}
J17163-053	1.282	0.552	0.317	1.112	1.506	0.427	0.668	1.009	-3.1 ^{+0.4} _{-0.2}
J17167+115	1.269	0.566	0.364	1.110	1.528	0.468	0.736	1.067	+0.0 ^{+0.3} _{-0.3}
J17176+524	1.197	0.616	0.404	1.091	1.387	0.467	0.708	0.965	+0.0 ^{+0.6} _{-0.6}
J17198+265	1.303	0.462	0.321	1.159	1.572	0.414	0.659	0.982	-8.2 ^{+0.8} _{-0.7}
J17199+242	1.273	0.521	0.362	1.136	1.518	0.431	0.673	0.953	-9.1 ^{+0.5} _{-0.8}
J17199+265	1.191	0.612	0.423	1.087	1.307	0.495	0.736	1.003	-2.4 ^{+0.2} _{-0.2}
J17216-171	1.150	1.101	0.724	1.084	1.384	1.062	1.502	0.840	+0.6 ^{+0.2} _{-0.2}
J17239+136	1.227	0.579	0.395	1.100	1.457	0.449	0.690	0.939	-3.2 ^{+0.4} _{-0.3}
J17246+617	1.160	0.610	0.441	1.062	1.163	0.499	0.721	0.957	-2.8 ^{+0.6} _{-0.3}
J17265-227	1.072	0.676	0.477	1.046	1.026	0.534	0.750	0.980	+0.0 ^{+0.4} _{-0.4}
J17267-050	1.087	0.698	0.520	1.036	1.057	0.577	0.790	1.026	+0.0 ^{+0.4} _{-0.4}
J17270+422	0.858	0.962	0.915	0.967	0.593	1.048	0.988	1.012	+0.6 ^{+0.1} _{-0.2}
J17281-017	1.259	0.546	0.365	1.120	1.572	0.439	0.688	0.973	-2.6 ^{+0.5} _{-0.6}
J17299-209	1.151	0.646	0.431	1.078	1.199	0.525	0.787	1.112	+0.0 ^{+0.4} _{-0.4}
J17301+546	1.205	0.628	0.414	1.089	1.333	0.503	0.755	1.056	+0.0 ^{+0.4} _{-0.4}
J17304+337	1.139	0.607	0.432	1.076	1.192	0.487	0.719	0.955	-2.4 ^{+0.4} _{-0.4}
J17364+683	1.141	0.652	0.439	1.063	1.209	0.520	0.770	1.061	+0.0 ^{+0.4} _{-0.4}
J17412+724	1.230	0.566	0.367	1.113	1.516	0.430	0.680	0.951	-2.8 ^{+0.6} _{-0.4}
J17426+756	1.275	0.544	0.344	1.132	1.634	0.422	0.703	1.002	-1.6 ^{+0.4} _{-0.4}
J17428+167	1.027	0.768	0.602	1.014	0.943	0.624	0.818	0.973	+0.0 ^{+0.4} _{-0.4}
J17464+277 AB	1.190	0.640	0.431	1.076	1.302	0.514	0.762	1.053	+0.0 ^{+0.4} _{-0.4}
J17477+277	1.020	0.778	0.608	1.005	0.936	0.645	0.833	1.029	+0.0 ^{+0.4} _{-0.4}
J17520+566	1.219	0.577	0.427	1.089	1.273	0.477	0.705	0.936	-7.3 ^{+0.6} _{-0.7}
J17559+294	1.188	0.590	0.399	1.093	1.331	0.468	0.715	0.983	+0.0 ^{+0.4} _{-0.4}
J17578+046	1.168	0.596	0.382	1.088	1.384	0.426	0.666	0.912	+0.0 ^{+0.3} _{-0.3}
J17578+465	1.135	0.679	0.464	1.064	1.205	0.523	0.766	1.011	+0.0 ^{+0.4} _{-0.4}
J18006+685	0.927	0.903	0.834	0.963	0.696	0.871	0.916	0.959	+0.0 ^{+0.4} _{-0.4}
J18007+295	1.067	0.734	0.557	1.033	1.069	0.584	0.792	0.959	+0.0 ^{+0.4} _{-0.4}
J18019+001	1.191	0.596	0.402	1.092	1.393	0.438	0.673	0.900	-2.5 ^{+0.6} _{-0.5}
J18022+642	1.344	0.447	0.309	1.166	1.865	0.376	0.612	0.926	-5.2 ^{+0.7} _{-0.6}
J18028-030	1.215	0.612	0.396	1.098	1.412	0.498	0.770	1.105	-0.7 ^{+0.4} _{-0.3}
J18036-189	1.354	0.459	0.308	1.159	1.894	0.381	0.636	0.950	-8.2 ^{+0.7} _{-0.6}
J18041+838	1.233	0.622	0.420	1.093	1.431	0.490	0.744	1.012	+0.0 ^{+0.4} _{-0.4}
J18046+139	1.085	0.695	0.503	1.055	1.131	0.518	0.736	0.892	+0.0 ^{+0.4} _{-0.4}

Table A.2. Seven representative spectral indices, ζ metallicity index, and H α pseudo-equivalent width (cont.).

Karmn	PC1	TiO 2	TiO 5	VO-7912	Color-M	CaH 2	CaH 3	ζ	$pEW(H\alpha)$ [Å]
J18054+015	1.183	0.632	0.426	1.075	1.322	0.503	0.751	1.030	+0.0 ^{+0.4} -0.4
J18057-143	1.463	0.378	0.235	1.207	2.391	0.320	0.577	0.959	-5.9 ^{+0.9} -0.5
J18068+177	1.215	0.589	0.382	1.094	1.452	0.446	0.681	0.946	+0.0 ^{+0.4} -0.4
J18090+241	1.008	0.805	0.645	1.005	0.895	0.679	0.843	1.021	+0.0 ^{+0.4} -0.4
J18112-010	1.182	0.593	0.406	1.103	1.280	0.457	0.691	0.932	-5.6 ^{+0.7} -0.5
J18130+414	1.187	0.601	0.398	1.083	1.390	0.447	0.694	0.935	-2.0 ^{+0.5} -0.5
J18131+260 AB	1.242	0.526	0.368	1.109	1.373	0.432	0.656	0.929	-7.8 ^{+1.2} -0.7
J18135+055	1.250	0.611	0.410	1.076	1.487	0.492	0.740	1.027	+0.0 ^{+0.4} -0.4
J18149+196	1.036	0.738	0.550	1.024	0.957	0.556	0.757	0.879	+0.0 ^{+0.4} -0.4
J18162+686	1.009	0.755	0.616	1.011	0.878	0.633	0.817	0.954	+0.0 ^{+0.4} -0.4
J18224+620	1.295	0.553	0.379	1.120	1.791	0.477	0.711	1.022	-0.5 ^{+0.2} -0.3
J18253+186	1.184	0.621	0.420	1.072	1.289	0.486	0.724	0.981	+0.0 ^{+0.4} -0.4
J18306-039	1.382	0.530	0.333	1.130	1.951	0.396	0.678	0.965	-2.4 ^{+0.5} -0.4
J18313+649	1.144	0.574	0.416	1.081	1.235	0.455	0.684	0.906	-3.2 ^{+0.5} -0.4
J18338+194	1.149	0.697	0.502	1.056	1.199	0.545	0.758	0.960	-0.6 ^{+0.1} -0.2
J18353+457	0.938	0.855	0.717	0.986	0.744	0.780	0.889	1.163	+0.0 ^{+0.4} -0.4
J18354+457	1.139	0.651	0.464	1.069	1.246	0.561	0.765	1.072	+0.0 ^{+0.4} -0.4
J18400+726	1.726	0.275	0.188	1.317	4.112	0.279	0.562	0.985	-6.2 ^{+2.1} -1.8
J18409+315	0.999	0.816	0.665	0.997	0.880	0.668	0.832	0.921	+0.0 ^{+0.4} -0.4
J18423-013	1.200	0.894	0.837	1.015	1.354	0.908	0.960	1.215	+0.9 ^{+0.3} -0.2
J18427+596N	1.117	0.682	0.473	1.054	1.200	0.526	0.769	1.003	+0.0 ^{+0.4} -0.4
J18427+596S	1.149	0.640	0.431	1.071	1.330	0.484	0.736	0.974	+0.0 ^{+0.4} -0.4
J18453+188	1.229	0.553	0.384	1.110	1.457	0.433	0.668	0.916	-6.8 ^{+0.5} -0.4
J18467+007	1.211	0.524	0.368	1.112	1.398	0.428	0.652	0.920	-6.3 ^{+0.7} -0.7
J18482+076	1.426	0.433	0.276	1.173	2.280	0.377	0.666	1.018	-4.9 ^{+0.7} -0.6
J18491-032	1.311	0.536	0.338	1.125	1.693	0.444	0.714	1.050	-0.6 ^{+0.3} -0.3
J18499+186	1.293	0.537	0.349	1.141	1.756	0.423	0.696	0.989	-1.4 ^{+0.6} -0.4
J18542+109	1.256	0.569	0.367	1.104	1.499	0.471	0.743	1.075	+0.0 ^{+0.4} -0.4
J18550+429	1.215	0.528	0.361	1.122	1.366	0.426	0.657	0.934	-6.4 ^{+0.5} -0.4
J18570+473	1.091	0.690	0.476	1.047	1.060	0.534	0.761	0.998	+0.0 ^{+0.4} -0.4
J19052+387	1.216	0.621	0.401	1.089	1.433	0.461	0.708	0.961	+0.0 ^{+0.6} -0.6
J19060-074	1.105	0.704	0.509	1.038	1.094	0.570	0.798	1.051	+0.0 ^{+0.4} -0.4
J19070+208	1.035	0.764	0.577	1.016	0.978	0.588	0.784	0.909	+0.0 ^{+0.4} -0.4
J19072+442	1.308	0.529	0.334	1.132	1.782	0.430	0.713	1.038	-0.9 ^{+0.6} -0.3
J19105-075	1.165	0.636	0.430	1.074	1.260	0.512	0.766	1.058	-0.5 ^{+0.2} -0.2
J19164+842	1.379	0.486	0.300	1.153	1.959	0.396	0.681	1.017	-1.2 ^{+0.5} -0.4
J19168+003	1.186	0.575	0.412	1.083	1.259	0.460	0.675	0.908	-6.9 ^{+0.5} -0.3
J19169+051N	1.093	0.704	0.512	1.042	1.082	0.574	0.791	1.038	+0.0 ^{+0.4} -0.4
J19169+051S	1.983	0.344	0.261	1.292	6.103	0.334	0.641	0.979	-9.5 ^{+1.1} -1.0
J19243+426	1.237	0.597	0.403	1.093	1.447	0.487	0.743	1.036	+0.0 ^{+0.4} -0.4
J19260+244	1.305	0.517	0.353	1.146	1.671	0.433	0.692	0.988	-6.3 ^{+0.6} -0.5
J19271+770	1.054	0.682	0.463	1.043	0.991	0.517	0.737	0.964	+0.0 ^{+0.4} -0.4
J19282-001	1.450	0.452	0.280	1.188	2.061	0.399	0.711	1.082	-11.0 ^{+1.0} -0.9
J19312+361	1.300	0.498	0.322	1.154	1.571	0.423	0.695	1.028	-8.5 ^{+0.8} -0.5
J19316-069	1.107	0.686	0.485	1.050	1.087	0.547	0.774	1.018	+0.0 ^{+0.4} -0.4
J19327-068	1.209	0.596	0.395	1.093	1.344	0.493	0.754	1.075	+0.0 ^{+0.4} -0.4
J19346+045	1.024	0.949	0.876	0.978	0.908	0.883	0.930	0.775	+0.0 ^{+0.4} -0.4
J19390+338	1.253	0.590	0.392	1.093	1.447	0.487	0.753	1.070	+0.0 ^{+0.4} -0.4
J19393+148	1.141	0.656	0.468	1.059	1.180	0.532	0.766	1.017	+0.0 ^{+0.4} -0.4
J19421+656	1.160	0.642	0.442	1.061	1.249	0.491	0.719	0.943	+0.0 ^{+0.4} -0.4
J19430+102	1.066	0.721	0.545	1.035	0.999	0.583	0.787	0.977	+0.0 ^{+0.5} -0.5
J19439-057	1.196	0.558	0.391	1.108	1.305	0.462	0.680	0.948	-6.2 ^{+0.3} -0.2
J19452+407	0.957	0.877	0.757	0.988	0.802	0.786	0.884	1.002	+0.0 ^{+0.4} -0.4
J19519+141	0.971	0.833	0.705	0.991	0.828	0.735	0.866	1.017	+0.0 ^{+0.4} -0.4
J19524+603	1.148	0.669	0.452	1.069	1.260	0.503	0.730	0.955	+0.0 ^{+0.4} -0.4
J19539+444W AB	1.438	0.388	0.253	1.214	2.548	0.332	0.594	0.954	-5.1 ^{+1.0} -0.9
J19539+444E	1.489	0.372	0.232	1.230	2.677	0.315	0.592	0.969	-4.4 ^{+1.0} -1.0
J19547+844	1.249	0.543	0.369	1.128	1.373	0.439	0.680	0.958	-11.0 ^{+1.2} -0.8
J19564+591	1.172	0.640	0.427	1.075	1.245	0.504	0.760	1.043	+0.0 ^{+0.4} -0.4

Table A.2. Seven representative spectral indices, ζ metallicity index, and H α pseudo-equivalent width (cont.).

Karmn	PC1	TiO 2	TiO 5	VO-7912	Color-M	CaH 2	CaH 3	ζ	$pEW(H\alpha)$ [Å]
J19565+591	0.910	0.890	0.809	0.984	0.692	0.914	0.937	1.352	+0.5 ^{+0.1} _{-0.1}
J19578-108	1.284	0.531	0.354	1.132	1.582	0.423	0.678	0.961	-5.9 ^{+0.7} _{-0.6}
J20021+130	1.186	0.628	0.436	1.079	1.322	0.504	0.758	1.024	+0.0 ^{+0.4} _{-0.4}
J20033+672	1.129	0.665	0.466	1.037	1.158	0.530	0.753	1.000	+0.0 ^{+0.4} _{-0.4}
J20034+298	1.325	0.511	0.325	1.149	1.951	0.433	0.723	1.067	-1.1 ^{+0.4} _{-0.3}
J20047+512	1.154	0.653	0.433	1.080	1.270	0.520	0.763	1.061	+0.0 ^{+0.4} _{-0.4}
J20065+159	1.061	0.741	0.549	1.023	1.024	0.565	0.775	0.921	+0.0 ^{+0.4} _{-0.4}
J20077+189	1.219	0.586	0.380	1.107	1.406	0.486	0.746	1.080	+0.0 ^{+0.4} _{-0.4}
J20093-012	1.375	0.432	0.282	1.179	1.944	0.363	0.616	0.955	-8.6 ^{+1.2} _{-0.7}
J20108+772	0.884	0.916	0.848	0.974	0.636	0.934	0.935	1.136	+0.5 ^{+0.3} _{-0.2}
J20112+161	1.235	0.575	0.380	1.118	1.563	0.461	0.741	1.036	-0.9 ^{+0.5} _{-0.5}
J20123-126	0.823	1.031	0.989	0.980	0.533	1.188	1.081	0.103	+2.0 ^{+0.2} _{-0.5}
J20177+059	1.133	0.668	0.465	1.048	1.143	0.533	0.766	1.025	+0.0 ^{+0.4} _{-0.4}
J20182-202	1.130	0.658	0.463	1.046	1.116	0.544	0.771	1.054	+0.0 ^{+0.4} _{-0.4}
J20216-199	1.041	0.764	0.584	1.009	0.964	0.613	0.803	0.969	+0.0 ^{+0.4} _{-0.4}
J20254-198	1.403	0.452	0.290	1.185	1.748	0.426	0.706	1.092	-12.1 ^{+0.8} _{-1.0}
J20283+617	1.106	0.688	0.493	1.050	1.157	0.528	0.763	0.960	+0.0 ^{+0.4} _{-0.4}
J20300+003 AB	1.231	0.504	0.329	1.118	1.558	0.384	0.621	0.912	-2.8 ^{+0.8} _{-0.6}
J20332+283	1.287	0.574	0.363	1.117	1.637	0.465	0.739	1.069	-0.8 ^{+0.3} _{-0.4}
J20336+365	1.205	0.602	0.393	1.094	1.409	0.459	0.708	0.973	-0.4 ^{+0.2} _{-0.4}
J20382+231	1.061	0.722	0.558	1.031	0.981	0.573	0.759	0.892	-2.6 ^{+0.4} _{-0.4}
J20405+154	1.335	0.513	0.331	1.136	1.817	0.428	0.706	1.032	-0.9 ^{+0.4} _{-0.5}
J20407+199 AB	1.082	0.698	0.498	1.042	1.093	0.540	0.758	0.961	+0.0 ^{+0.4} _{-0.4}
J20439+231	1.181	0.623	0.434	1.075	1.263	0.515	0.753	1.036	+0.0 ^{+0.4} _{-0.4}
J20467-118	1.220	0.518	0.371	1.117	1.426	0.437	0.667	0.939	-7.8 ^{+0.7} _{-1.0}
J20510+399	1.152	0.655	0.458	1.062	1.222	0.541	0.788	1.087	+0.0 ^{+0.4} _{-0.4}
J20540+603	1.102	0.690	0.506	1.037	1.086	0.545	0.760	0.955	-1.7 ^{+0.3} _{-0.3}
J20581+401 AB	0.911	0.915	0.832	0.975	0.698	0.896	0.929	1.091	+0.4 ^{+0.1} _{-0.2}
J20583+425	1.128	0.669	0.468	1.058	1.172	0.530	0.759	1.003	+0.0 ^{+0.4} _{-0.4}
J20593+530 AB	1.198	0.569	0.397	1.111	1.413	0.457	0.693	0.948	-3.3 ^{+0.4} _{-0.4}
J21009+510	1.088	0.646	0.467	1.051	1.054	0.519	0.743	0.967	-3.3 ^{+0.7} _{-0.7}
J21019-063	1.106	0.696	0.493	1.045	1.094	0.561	0.784	1.044	+0.0 ^{+0.4} _{-0.4}
J21027+349	1.273	0.474	0.313	1.146	1.570	0.424	0.695	1.043	-4.5 ^{+0.6} _{-0.7}
J21053+208	1.110	0.675	0.482	1.050	1.158	0.514	0.737	0.925	+0.0 ^{+0.4} _{-0.4}
J21057+502E	1.230	0.593	0.395	1.098	1.401	0.499	0.762	1.097	+0.0 ^{+0.4} _{-0.4}
J21057+502W	1.255	0.553	0.364	1.116	1.502	0.478	0.748	1.097	+0.0 ^{+0.4} _{-0.4}
J21068+387	0.848	0.964	0.920	0.963	0.572	1.044	0.991	0.947	+0.7 ^{+0.1} _{-0.2}
J21069+387	0.960	0.944	0.871	0.977	0.790	0.904	0.942	0.895	+0.5 ^{+0.2} _{-0.2}
J21074+198	0.960	0.751	0.566	1.008	0.783	0.631	0.813	1.063	+0.0 ^{+0.4} _{-0.4}
J21074+468	1.085	0.703	0.519	1.040	1.040	0.584	0.795	1.048	+0.0 ^{+0.4} _{-0.4}
J21109+469	1.168	0.623	0.428	1.076	1.256	0.518	0.760	1.062	+0.0 ^{+0.4} _{-0.4}
J21114+658	1.057	0.739	0.541	1.039	1.039	0.554	0.757	0.895	+0.0 ^{+0.4} _{-0.4}
J21127-073	1.202	0.617	0.407	1.078	1.237	0.501	0.757	1.069	+0.0 ^{+0.4} _{-0.4}
J21147+160	1.219	0.591	0.407	1.092	1.407	0.492	0.753	1.050	+0.0 ^{+0.4} _{-0.4}
J21245+400	1.538	0.429	0.263	1.192	2.820	0.375	0.701	1.069	-1.1 ^{+0.6} _{-0.5}
J21376+016	1.301	0.502	0.344	1.146	1.504	0.434	0.688	0.998	-11.9 ^{+1.3} _{-0.8}
J21414+207	1.146	0.608	0.442	1.072	1.203	0.491	0.706	0.928	-5.0 ^{+0.7} _{-0.4}
J21466+668	1.253	0.582	0.380	1.103	1.547	0.471	0.739	1.049	+0.0 ^{+0.4} _{-0.4}
J21467-212	1.229	0.563	0.389	1.108	1.408	0.438	0.671	0.918	-5.1 ^{+1.0} _{-0.5}
J21472-047	1.277	0.530	0.316	1.134	1.618	0.415	0.683	1.015	+0.0 ^{+0.4} _{-0.4}
J21554+596 AB	1.203	0.553	0.389	1.100	1.349	0.438	0.665	0.911	-8.3 ^{+0.8} _{-0.5}
J22021+014	0.958	0.858	0.731	0.990	0.798	0.758	0.871	0.998	+0.0 ^{+0.4} _{-0.4}
J22035+036 AB	1.245	0.520	0.352	1.123	1.529	0.412	0.645	0.922	-5.6 ^{+0.8} _{-0.8}
J22088+117	1.357	0.484	0.327	1.145	1.875	0.413	0.682	0.996	-6.5 ^{+0.5} _{-0.5}
J22089-177	1.104	0.696	0.489	1.047	1.104	0.497	0.705	0.856	+0.0 ^{+0.4} _{-0.4}
J22095+118	1.136	0.681	0.483	1.057	1.180	0.543	0.780	1.028	+0.0 ^{+0.4} _{-0.4}
J22114+409	1.468	0.399	0.264	1.192	2.486	0.375	0.685	1.051	-5.0 ^{+0.5} _{-0.5}
J22160+546	1.236	0.578	0.390	1.109	1.511	0.446	0.701	0.955	-2.1 ^{+0.5} _{-0.5}
J22202+067	1.100	0.694	0.485	1.043	1.142	0.512	0.736	0.916	+0.0 ^{+0.4} _{-0.4}

Table A.2. Seven representative spectral indices, ζ metallicity index, and H α pseudo-equivalent width (cont.).

Karmn	PC1	TiO 2	TiO 5	VO-7912	Color-M	CaH 2	CaH 3	ζ	$pEW(H\alpha)$ [Å]
J22234+324 AB	1.130	0.657	0.470	1.062	1.115	0.516	0.727	0.936	-5.3 ^{+0.6} _{-0.3}
J22264+583	1.160	0.666	0.462	1.066	1.265	0.512	0.757	0.986	+0.0 ^{+0.4} _{-0.4}
J22300+488 AB	1.322	0.543	0.396	1.113	1.841	0.412	0.655	0.868	-6.1 ^{+0.9} _{-0.7}
J22386+567	1.390	0.960	0.598	1.136	2.184	0.884	1.446	3.081	+0.0 ^{+0.4} _{-0.4}
J22387+252	1.192	0.648	0.450	1.072	1.351	0.509	0.755	1.002	+0.0 ^{+0.4} _{-0.4}
J22396-125	1.157	0.634	0.439	1.058	1.264	0.489	0.721	0.948	-0.7 ^{+0.2} _{-0.2}
J22415+260	1.161	0.635	0.451	1.083	1.264	0.489	0.720	0.928	-4.0 ^{+0.5} _{-0.4}
J22437+192	1.111	0.676	0.483	1.056	1.113	0.536	0.758	0.984	-2.5 ^{+0.5} _{-0.4}
J22476+184	1.101	0.658	0.453	1.065	1.109	0.525	0.764	1.033	+0.0 ^{+0.4} _{-0.4}
J22489+183	1.273	0.523	0.362	1.128	1.595	0.413	0.650	0.914	-5.3 ^{+0.9} _{-0.6}
J22509+499	1.243	0.491	0.343	1.138	1.403	0.428	0.683	0.990	-8.9 ^{+0.8} _{-0.6}
J22524+099 AB	1.116	0.669	0.468	1.051	1.195	0.493	0.723	0.907	+0.0 ^{+0.4} _{-0.4}
J22526+750	1.354	0.528	0.335	1.134	1.879	0.451	0.742	1.100	-0.8 ^{+0.4} _{-0.3}
J22582-110	1.133	0.606	0.434	1.074	1.144	0.490	0.706	0.939	-2.9 ^{+0.4} _{-0.4}
J22588+690	1.146	0.639	0.436	1.070	1.213	0.512	0.746	1.017	+0.0 ^{+0.4} _{-0.4}
J23006+036	1.148	0.663	0.462	1.063	1.204	0.516	0.753	0.985	+0.0 ^{+0.4} _{-0.4}
J23028+436	1.263	0.521	0.354	1.133	1.588	0.404	0.643	0.912	-5.8 ^{+0.8} _{-0.9}
J23036-072	1.152	0.657	0.464	1.065	1.195	0.535	0.767	1.030	+0.0 ^{+0.4} _{-0.4}
J23036+097	1.173	0.633	0.441	1.080	1.304	0.519	0.786	1.080	+0.0 ^{+0.4} _{-0.4}
J23051+519	1.184	0.621	0.432	1.091	1.296	0.519	0.771	1.074	+0.0 ^{+0.4} _{-0.4}
J23051+452	1.181	0.582	0.424	1.092	1.304	0.490	0.719	0.972	-6.6 ^{+0.6} _{-0.4}
J23070+094	1.272	0.813	0.663	1.029	1.444	0.813	0.919	1.653	+0.8 ^{+0.2} _{-0.2}
J23177+490	1.160	0.698	0.501	1.026	1.005	0.772	0.930	2.244	+1.0 ^{+0.6} _{-0.3}
J23182+795	1.116	0.644	0.444	1.067	1.124	0.526	0.765	1.052	+0.0 ^{+0.4} _{-0.4}
J23194+790	1.212	0.560	0.403	1.097	1.331	0.474	0.697	0.961	-7.5 ^{+1.0} _{-0.8}
J23209-017 AB	1.221	0.548	0.397	1.106	1.300	0.459	0.685	0.941	-10.2 ^{+1.0} _{-0.7}
J23220+569	1.157	0.633	0.434	1.066	1.230	0.522	0.783	1.093	+0.0 ^{+0.4} _{-0.4}
J23228+787	1.302	0.347	0.206	1.224	1.634	0.350	0.641	1.066	-11.2 ^{+1.6} _{-1.2}
J23235+457	0.852	0.955	0.913	0.969	0.564	1.061	0.986	1.062	+0.8 ^{+0.2} _{-0.2}
J23261+170 AB	1.257	0.549	0.369	1.119	1.532	0.428	0.676	0.943	-3.1 ^{+0.8} _{-0.8}
J23266+453	1.263	0.852	0.543	1.116	1.496	0.851	1.262	5.896	+0.0 ^{+0.4} _{-0.4}
J23306+466	1.048	0.745	0.573	1.022	0.996	0.603	0.805	0.980	+0.0 ^{+0.4} _{-0.4}
J23317-064	1.362	0.539	0.355	1.139	1.846	0.472	0.763	1.127	-0.9 ^{+0.6} _{-0.6}
J23376+163	1.459	0.386	0.250	1.210	2.384	0.330	0.602	0.963	-6.2 ^{+0.7} _{-1.0}
J23416-065	1.330	0.534	0.332	1.124	1.761	0.437	0.709	1.044	+0.0 ^{+0.4} _{-0.4}
J23417-059 AB	1.165	0.605	0.416	1.072	1.297	0.473	0.719	0.965	+0.0 ^{+0.4} _{-0.4}
J23419+441	1.386	0.467	0.293	1.170	2.372	0.409	0.710	1.072	-1.0 ^{+0.4} _{-0.3}
J23423+349	1.215	0.591	0.383	1.094	1.447	0.467	0.732	1.029	-0.6 ^{+0.2} _{-0.4}
J23425+392	0.928	0.904	0.823	0.982	0.739	0.875	0.921	1.054	-1.6 ^{+0.4} _{-0.3}
J23438+610	1.110	0.641	0.434	1.059	1.176	0.492	0.731	0.974	+0.0 ^{+0.4} _{-0.4}
J23490-086	1.054	0.737	0.534	1.029	0.999	0.563	0.775	0.947	+0.0 ^{+0.4} _{-0.4}
J23559-133	1.184	0.568	0.405	1.094	1.331	0.472	0.700	0.959	-4.2 ^{+0.5} _{-0.4}
J23560+150	1.102	0.709	0.517	1.040	1.110	0.560	0.783	0.990	+0.0 ^{+0.4} _{-0.4}
J23569+230	1.012	0.801	0.640	1.007	0.914	0.680	0.848	1.045	+0.0 ^{+0.4} _{-0.4}
J23585+242	0.898	0.921	0.836	0.977	0.677	0.905	0.931	1.105	+0.5 ^{+0.3} _{-0.2}
J23590+208	1.111	0.668	0.469	1.059	1.097	0.561	0.785	1.095	+0.0 ^{+0.4} _{-0.4}

Table A.3. Spectral types of observed stars.

Karmn	Sp. type biblio.	Ref. ^a	Sp. type			Sp. type			Sp. type adopted
			Best-fit	χ^2	TiO2	TiO5	PC1	VO-7912	
J00066-070 AB	M3.5 V+m4.5:	Reid07, Jan12	4.5	4.5	4.5	4.5	4.0	4.5	4.5
J00077+603 AB	M4.5 V	Lep13	4.0	4.0	4.5	4.0	3.5	4.0	3.5
J00115+591	M5.5 V	Lep03	6.0	6.0	5.5	6.0	5.5	5.5	M5.5 V
J00118+229	M3.5 V	Reid04	3.5	3.5	3.5	3.5	4.0	4.0	3.5
J00119+330	M3.5 V	Giz97	3.5	3.0	3.5	3.5	3.5	3.5	M3.5 V
J00122+304	M5.0 V	Abe14	4.5	4.5	4.5	4.0	4.5	5.0	4.5
J00133+275	M4.5 V	Abe14	4.5	4.5	4.5	4.5	4.5	4.5	M4.5 V
J00136+806	M1.5 V	PMSU	1.5	1.5	1.5	1.5	1.5	1.5	M1.5 V
J00146+202	M2 III	Gar89, Kir91	M III
J00152+530	M2.2 V	Mann13	2.5	2.0	2.5	2.0	2.5	2.0	M2.5 V
J00162+198E	M4.0 V	PMSU	4.0	4.0	4.0	4.0	4.5	4.0	M4.0 V
J00162+198W	M4.0 V	PMSU	4.0	4.0	4.0	4.0	4.0	4.5	M4.0 V
J00183+440	M1.0 V	PMSU	1.0	1.5	1.0	1.5	1.0	1.0	M1.0 V
J00228-164	4.0	4.0	4.0	4.0	4.0	4.0	M4.0 V
J00240+264	M4.0 V	Abe14	4.0	4.5	4.0	4.0	4.0	4.5	M4.0 V
J00253+235	1.5	1.5	1.0	1.0	1.0	1.5	M1.5 V
J00297+012	1.0	1.0	1.0	1.0	1.0	1.0	M1.0 V
J00313+336	K5 V	Ste86	0.0	0.0	0.0	0.0	0.0	0.5	M0.0 V
J00313+001	m:	Simbad	3.0	3.0	3.0	3.0	3.0	3.0	M3.0 V
J00322+544	k:	Simbad	4.5	4.5	4.0	4.0	4.5	4.5	M4.5 V
J00328-045 AB	M3.5 V	Reid07	4.5	4.5	4.0	4.0	4.5	4.5	M4.5 V
J00358+526	M3.5 V	Giz97	2.5	2.0	2.5	2.5	2.5	2.0	M2.5 V
J00367+444	K5 III	Gar89, Kir91	K III
J00380+169	3.0	2.5	3.0	3.0	3.0	3.0	M3.0 V
J00389+306	M2.5 V	PMSU	2.5	2.0	2.5	2.5	2.5	2.5	M2.5 V
J00395+149N	4.5	4.5	4.5	4.5	4.5	5.0	M4.5 V
J00395+149S	4.0	4.0	4.0	3.5	4.0	4.0	M4.0 V
J00452+002 AB	M3.8 V	Mann13	3.5	3.5	4.0	4.0	4.0	4.0	M4.0 V
J00464+506	M3.5 V	Reid04	4.0	4.0	4.0	4.0	4.0	4.5	M4.0 V
J00467-044	m:	Simbad	4.0	4.0	4.0	4.0	4.5	4.0	M4.0 V
J00484+753	3.0	2.5	3.0	3.0	3.0	3.0	M3.0 V
J00490+657	2.5	2.5	2.5	2.5	2.5	2.5	M2.5 V
J00490+578	K7 V	Hen94	-1.0	-1.0	-1.0	-1.0	-0.5	-0.5	K7 V
J00502+601	K7 III	Jac84, Kir91	K III
J00502+086	4.5	4.5	4.5	4.5	4.5	4.5	M4.5 V
J00540+691	M2 V:	Bid85	2.5	2.5	2.0	2.0	2.0	2.0	M2.0 V
J00548+275	M4.6 V	Shk09	4.5	4.5	4.5	4.0	4.5	4.5	M4.5 V
J00580+393	M4.5 V	Abe14	4.5	4.5	4.5	4.0	4.5	4.5	M4.5 V
J01009-044	M3.5 V	PMSU	4.0	4.0	3.5	4.0	4.0	4.0	M4.0 V
J01012+571	M III
J01014-010	3.5	3.5	3.5	3.5	4.0	4.0	M3.5 V
J01014+188	2.0	2.0	2.5	2.5	2.0	2.0	M2.0 V
J01026+623	M1.5 V	PMSU	1.5	1.5	1.5	1.5	2.0	1.5	M1.5 V
J01028+189	M4 V	Riaz06	4.0	4.0	4.5	4.0	4.0	4.5	M4.0 V
J01028+470	m5:	LG11	1.5	1.0	2.0	2.0	1.0	1.5	M1.5 V
J01032+712	M3.5 V	Giz97	4.0	4.5	4.0	3.5	4.5	4.0	M4.0 V
J01033+623	M5.0 V	PMSU	5.0	5.0	5.0	5.0	5.0	5.0	M5.0 V
J01055+153	K7.4 V	Mann13	-1.0	-1.0	-1.0	-1.0	-1.5	-1.0	-2.0
J01069+804	4.5	5.0	4.5	4.5	4.5	5.0	M4.5 V
J01074-025	≤ -2.0	≤ -2.0	K5 V
J01076+229E	M3.0 V	PMSU	3.5	3.0	4.0	3.5	3.5	4.0	M3.5 V
J01097+356	M0 III	Gar89	K III
J01186-008	K7 V	PMSU	-1.0	-1.0	-0.5	-0.5	-0.5	-0.5	K7 V
J01214+313	M1 V:	Bid85	3.5	3.0	3.5	3.5	3.5	3.5	M3.5 V
J01226+127	K7.8 V	Mann13	-1.0	-1.0	-0.5	-0.5	-1.0	-0.5	-1.5
J01342-015	m:	Simbad	1.0	1.0	1.5	1.5	1.0	1.0	M1.0 V
J01356-200 AB	m:	Simbad	2.5	2.0	2.5	2.5	2.5	2.5	M2.5 V
J01390-179 AB	M5.5 V+M6.0	Kirk91	5.0	5.0	5.0	4.5	4.5	5.5	M5.0 V
J01406-081	≤ -2.0	≤ -2.0	K5 V
J01431+210	M4.0 V	Fri13	3.5	4.0	4.5	4.0	4.0	4.5	M4.0 V
J01541-156	M4.0 V	Reid04	4.0	4.5	4.0	4.0	4.0	4.5	M4.0 V
J01551-162	-1.0	-1.0	-1.0	-1.0	-1.0	0.0	-1.0
J01562+001	3.0	3.0	3.5	3.0	3.0	3.0	M3.0 V
J01567+305	M5.0 V	Abe14	4.5	4.5	5.0	4.5	4.5	5.0	M4.5 V
J01571-102	K7 V	PMSU	0.0	0.0	0.0	0.0	0.0	0.0	M0.0 V
J02000+135 AB	m:	Reid04	3.5	3.0	3.5	3.5	3.5	3.5	M3.5 V
J02002+130	M4.5 V	PMSU	3.5	3.5	3.0	3.0	3.0	4.5	M3.5: V
J02019+342	0.5	0.5	0.5	0.5	0.5	0.5	M0.5 V
J02022+103	M6.0 V	PMSU	5.5	5.5	5.5	6.0	5.5	5.5	M5.5 V
J02023+012	2.5	2.5	2.0	2.0	2.5	2.0	M2.5 V
J02100-088	M3.5 V	Giz97	3.0	3.0	4.0	3.5	3.0	3.5	M3.0 V
J02133+368 AB	M4.5 V	Riaz06	4.5	4.5	5.0	4.5	4.5	4.5	M4.5 V
J02142-039	M5.5 V	CrRe02	5.5	5.5	6.0	5.5	5.5	6.0	M5.5 V
J02159-094 ABC	M2.5 V	Riaz06	2.5	2.5	3.0	2.5	2.5	3.0	M2.5 V
J02274+031	4.0	4.0	4.0	4.0	3.5	4.0	M4.0 V
J02285-200	M2.9 V	Mann13	2.5	2.5	2.5	2.5	2.0	2.5	M2.5 V
J02291+228	K5.9 V	Mann13	-1.0	-1.0	-1.0	-1.0	-1.0	-0.5	K7 V
J02362+068	M4.0 V	PMSU	3.5	4.0	3.5	4.0	3.5	4.0	M4.0 V
J02367+226	M5.0 V	Reid04	5.0	5.0	5.0	5.0	5.0	5.0	M5.0 V
J02412-045	M4.0 V	CrRe02	4.5	4.5	4.5	4.0	4.5	4.5	M4.5 V

Table A.3. Spectral types of observed stars (cont.).

Karmn	Sp. type biblio.	Ref. ^a	Sp. type			Sp. type			Sp. type adopted
			Best-fit	χ^2	TiO2	TiO5	PC1	VO-7912	
J02441+492	M1.5 V	PMSU	1.5	1.5	1.5	1.5	1.5	1.5	M1.5 V
J02456+449	M0.0 V	PMSU	0.5	0.5	0.0	0.5	0.5	0.5	M0.5 V
J02479-124	M5 III	SB06	M III
J02502+628	2.5	2.5	3.0	2.5	3.0	2.5	M2.5 V
J02530+168	M6.5 V	Tee03	7.0	6.5	7.0	7.0	7.0	6.5	M7.0 V
J02555+268	M4.0 V	PMSU	4.0	4.0	4.0	4.0	4.5	4.0	M4.0 V
J02558+183	M6 III	Gar89, SB06	M III
J02562+239	M4.5 V	Reid07	5.0	5.0	5.0	4.5	5.0	5.0	M5.0 V
J03026-181	M2.0 V	PMSU	2.5	2.0	2.5	2.5	2.5	2.5	M2.5 V
J03033-080	M3.0 V	Reid07	2.5	2.5	3.5	3.0	3.0	3.5	M3.0 V
J03047+617	M3.0 V	PMSU	2.5	2.5	3.0	3.0	3.0	3.0	M3.0 V
J03110-046	M2.5 V	Sch05	2.5	2.5	3.0	3.0	3.0	3.0	M3.0 V
J03147+114	M1 V	Li00	2.0	1.5	2.5	2.0	1.5	2.5	M2.0 V
J03154+578	m:	Cab09	3.5	3.5	3.5	3.5	3.0	3.0	M3.5 V
J03162+581N	M2.0 V	PMSU	2.0	2.0	2.0	2.0	2.0	2.0	M2.0 V
J03162+581S	M2.0 V	Bid85	2.0	2.0	2.0	2.0	2.0	2.0	M2.0 V
J03167+389	3.5	3.5	3.5	3.5	3.5	3.5	M3.5 V
J03174-011	k:	Simbad	0.5	0.5	1.0	1.0	0.5	0.5	M0.5 V
J03179-010	m:	Simbad	2.0	2.0	2.0	2.5	2.0	1.5	M2.0 V
J03181+426	M4.0 V	Reid04	3.5	3.5	3.5	3.5	4.0	4.0	M3.5 V
J03194+619	M4.1 V	Shk09	4.0	4.0	4.5	4.0	4.0	4.5	M4.0 V
J03236+056	4.5	4.5	4.5	4.5	5.0	5.0	M4.5 V
J03236+476	0.5	0.5	0.5	0.5	0.5	0.5	M0.5 V
J03263+171	4.0	4.0	3.5	4.0	4.0	4.0	M4.0 V
J03275+222	M4.0 V	Abe14	4.5	4.5	4.5	4.5	4.5	4.5	M4.5 V
J03294+117	2.5	2.0	3.0	3.0	2.0	3.0	M2.5 V
J03303+346	4.0	4.0	4.0	4.0	4.0	4.5	M4.0 V
J03309+706	m5:	LG11	3.5	3.5	3.5	3.5	3.0	3.5	M3.5 V
J03319+492	m3:	LG11	K III
J03320+436	K7.3 V	Mann13	-1.0	-1.0	-0.5	-0.5	-0.5	-0.5	K7 V
J03325+287 ABC	M4.0 V	Riaz06	4.5	4.5	4.5	4.5	4.5	4.5	M4.5 V
J03332+462	M0.0 V	Lep13	-1.0	-1.0	0.0	0.0	-0.5	0.5	M0.0 V
J03354+428	M0.4 V	Mann13	0.5	0.5	0.0	0.0	0.5	0.5	M0.5 V
J03356-084	m:	Simbad	5.5	5.5	5.0	5.5	5.0	5.0	M5.5 V
J03361+313	M4.5 V	Riaz06	4.5	5.0	5.0	4.5	4.5	5.0	M4.5 V
J03375+288	0.0	0.0	0.0	0.0	0.0	0.0	M0.0 V
J03375+178N AB	M2.0 V+M3.6	PMSU, Shk10	2.5	2.0	2.5	2.0	2.5	2.5	M2.5 V
J03375+178S AB	M3.0 V+M4.3	PMSU, Shk10	3.5	3.5	3.0	3.0	3.0	4.0	M3.5 V
J03392+565 AB	m6:	LG11	2.5	2.5	3.0	3.0	3.0	3.0	M2.5 V
J03430+459	m5:	LG11	4.0	4.0	4.0	4.0	3.5	4.0	M4.0 V
J03466+243 AB	K3 V	Simbad	≤ -2.0	≤ -2.0	K5 V
J03473-019	M2.8 V	Shk09	3.0	3.0	3.0	2.5	3.0	2.5	M3.0 V
J03480+405	M2.0 V	New14	1.5	1.5	1.5	1.5	1.5	2.0	M1.5 V
J03510+142	4.5	4.5	4.5	4.0	4.5	4.5	M4.5 V
J03519+397	M0.0 V	Lep13	0.0	0.0	-0.5	-0.5	0.0	-0.5	M0.0 V
J03548+163 AB	4.0	4.0	4.0	4.0	4.0	4.5	M4.0 V
J03556+522	M2.7 V	Mann13	2.5	2.0	2.5	2.5	2.5	2.0	M2.5 V
J03565+319	M3.0 V	Reid07	4.0	3.5	4.0	3.5	3.5	4.0	M3.5 V
J03566+507	-2.0	-2.0	-1.5	-1.5	-1.0	-0.5	K7 V
J03574-011 AB	M2.0 V	PMSU	2.5	2.0	2.5	2.0	2.5	2.5	M2.5 V
J03588+125	4.0	4.0	4.0	4.0	4.5	4.5	M4.0 V
J04041+307	M1.5 V	Giz97	1.5	1.5	1.5	2.0	1.5	1.5	M1.5 V
J04061-055	M3.5 V	Reid07	3.5	4.0	3.5	3.5	3.5	3.5	M3.5 V
J04079+142	2.5	2.5	3.0	3.0	3.0	3.0	M2.5 V
J04081+743	M3.5 V	Giz97	3.5	3.5	3.5	3.5	3.5	3.5	M3.5 V
J04083+691	m4.5:	Law08	4.5	4.5	4.5	4.5	4.5	4.5	M4.5 V
J04123+162 AB	M1	BS08	4.0	3.5	4.0	3.5	4.0	4.0	M4.0 V
J04153-076	M4.5 V	PMSU	4.5	4.5	5.0	4.5	4.5	4.5	M4.5 V
J04177+410	3.5	3.5	3.5	3.0	3.5	3.5	M3.5 V
J04177+136 AB	M1 V	Simbad	1.5	1.5	1.5	1.0	2.0	1.5	M1.5 V
J04191-074	M4.0 V	Sch05	3.5	3.5	4.0	4.0	4.0	4.0	M3.5 V
J04191+097	3.5	3.0	3.0	3.0	3.0	3.0	M3.0 V
J04205+815	3.0	3.0	2.5	2.5	3.0	2.5	M3.0 V
J04206+272	M3-IV IV	Sce08	4.5	4.5	4.5	4.5	5.0	5.0	M4.5 V
J04206-168	M3III	KMc89, Gar89	M III
J04207+152 AB	m5:	LG11	4.0	4.0	4.0	4.0	4.0	4.0	M4.0 V
J04224+036	3.5	3.0	4.0	3.5	3.5	4.0	M3.5 V
J04227+205	4.0	4.0	4.0	4.0	4.0	4.5	M4.0 V
J04229+259	M4.0 V	Reid04	4.0	4.5	4.0	4.0	4.5	4.5	M4.5 V
J04234+809	4.0	4.0	4.0	3.5	4.0	4.0	M4.0 V
J04238+149 AB	M3 V	Simbad	3.5	3.0	3.5	3.0	3.5	3.5	M3.5 V
J04238+092 AB	M3 V	Simbad	3.0	3.0	3.0	2.5	3.5	3.0	M3.0 V
J04247-067 ABC	M4.5+M5.5+M5.7	Shk10	4.0	4.0	4.0	4.0	4.0	4.0	M4.0 V
J04252+172 ABC	M3 V+M3+M4:	Cut00	3.5	3.5	4.0	3.5	3.5	4.0	M3.5 V
J04290+186	2.5	2.5	2.5	2.5	2.5	3.0	M2.5 V
J04308-088	M4.0 V	Reid04	4.0	4.5	4.0	4.0	4.0	4.0	M4.0 V
J04310+367	3.0	3.0	3.5	3.0	3.0	3.0	M3.0 V
J04313+241 AB	M5.5 V	Mar94	4.5	5.0	4.5	4.5	5.0	5.0	M4.5:
J04329+001S	M0.5 V	Reid04	0.5	0.5	1.0	1.0	0.5	0.5	M0.5 V
J04347-004	m:	Simbad	4.0	4.0	4.0	4.0	4.0	4.0	M4.0 V
J04360+188	M3.5 V	Simbad	2.5	2.5	3.0	3.0	2.5	3.0	M2.5 V

Table A.3. Spectral types of observed stars (cont.).

Karmn	Sp. type biblio.	Ref. ^a	Sp. type			Sp. type			Sp. type adopted
			Best-fit	χ^2	TiO2	TiO5	PC1	VO-7912	
J04366+186	2.0	2.0	2.5	2.0	2.5	2.0	M2.0 V
J04373+193	4.0	4.5	4.5	4.0	4.0	4.5	M4.0 V
J04386-115	M3.0 V	Sch05	3.0	3.5	3.0	3.5	3.5	3.5	M3.5 V
J04388+217	M3.5 V	Reid04	3.5	3.0	3.5	3.5	3.5	3.5	M3.5 V
J04393+335	M2.5 V	Simbad	4.0	4.0	4.0	4.0	4.0	4.5	M4.0 V
J04398+251	M3.0 V	Reid07	3.5	3.5	3.5	3.5	3.5	3.5	M3.5 V
J04413+327	4.0	4.0	3.5	3.5	4.0	4.0	M4.0 V
J04425+204 AB	3.0	3.0	3.5	3.0	3.0	3.5	M3.0 V
J04430+187 AB	K8 V	Vys56	≤ 2.0	≤ 2.0	K5 V
J04458-144	M4.0 V	Reid07	4.0	4.0	4.0	4.0	4.0	4.0	M4.0 V
J04468-112 AB	M4.9 V	Shk09	3.0	3.0	3.5	3.5	3.0	3.5	M3.0 V
J04472+206	M4.5 V	Reid07	5.0	5.0	5.0	5.0	5.0	4.5	M5.0 V
J04494+484 AB	M4.0 V	Shk09	4.0	4.0	4.0	4.0	4.0	4.0	M4.0 V
J04496-153	-2.0	-2.0	K5 V
J04499+711	4.0	3.5	3.5	4.0	3.5	4.0	M3.5 V
J04536+623	3.5	3.5	3.5	3.5	3.5	3.5	M3.5 V
J04538+158	M2.5 V	Reid07	2.5	2.5	2.5	2.5	2.5	2.5	M2.5 V
J04544+650	4.0	4.0	4.0	4.0	4.0	4.0	M4.0 V
J04559+046	M3 V	New14	2.0	2.0	2.0	2.0	2.0	2.0	M2.0 V
J04560+432	4.0	4.0	3.5	4.0	4.0	4.0	M4.0 V
J05003+251 AB	1.5	1.5	1.5	1.0	1.0	1.0	M1.0 V
J05019+011	M4.5 V	Lep13	4.0	4.0	4.0	4.0	4.0	4.5	M4.0 V
J05030+213 AB	m4.5+m5.0:	Law08	5.0	5.0	5.0	4.5	5.0	5.0	M5.0 V
J05032+213	M1.5 V	Reid04	1.5	1.5	2.0	2.0	1.5	2.0	M1.5 V
J05050+442	5.0	5.0	4.5	5.0	5.0	5.0	M5.0 V
J05062+046	M4.0 V	Lep13	4.5	4.0	4.5	4.0	4.0	4.5	M4.0 V
J05068+516	k:	Kri93	-2.0	-2.0	K5 V
J05072+375	M5.0 V	Abe14	5.0	5.0	5.0	4.5	5.0	4.5	M5.0 V
J05083+756	M5.0 V	Sch05	4.5	4.5	4.5	4.5	4.5	4.5	M4.5 V
J05151-073	M0.5 V	PMSU	1.0	1.0	1.0	1.0	1.0	1.0	M1.0 V
J05152+236	M4.5 V	Abe14	5.0	5.0	5.0	4.5	5.0	4.5	M5.0 V
J05173+321	M3.5 V	Reid04	3.5	3.0	3.5	3.5	3.5	3.5	M3.5 V
J05175+487	0.0	0.0	-0.5	-0.5	0.0	0.0	M0.0 V
J05187+464	4.5	4.5	5.0	4.5	4.5	5.0	M4.5 V
J05187-213	3.5	3.5	3.5	3.5	3.5	3.5	M3.5 V
J05195+649	M4.0 V	Lep13	3.5	3.0	3.5	4.0	3.5	4.0	M3.5 V
J05200-229	2.0	2.0	2.5	2.5	2.0	2.0	M2.0 V
J05223+305	3.5	3.0	3.0	3.0	3.5	3.0	M3.0 V
J05256-091 AB	M3.5 V+M5.0	Reid04, Shk09	3.5	3.5	3.5	3.5	3.5	3.5	M3.5 V
J05289+125	M4.0 V	PMSU	4.0	4.0	3.5	3.5	4.0	4.0	M4.0 V
J05294+155E	M0.0 V:	PMSU	-1.0	-1.0	0.5	0.5	-1.0	0.0	M0.0:V
J05295-113	3.5	3.5	3.5	3.5	3.5	3.5	M3.5 V
J05300+121E	0.0	0.5	0.5	0.5	0.0	0.5	M0.5 V
J05300+121W	-2.0	-2.0	K5 V
J05314-036	M1.5 V	PMSU	1.5	1.5	1.5	1.5	2.0	1.5	M1.5 V
J05320-030 AB	M2.0 V	Riaz06	1.5	1.5	2.5	2.0	2.0	2.5	M2.0 V
J05324-072	M0-1 V	Ste86	0.5	0.5	0.5	0.5	-0.5	0.0	-0.5
J05328+338	M3.5 V	Reid04	3.5	3.5	3.5	3.5	3.0	3.0	M3.5 V
J05342+103N	M3.5 V	PMSU	3.0	3.0	3.0	3.0	3.0	3.0	M3.0 V
J05342+103S	M3.0 V	PMSU	4.5	4.5	4.0	4.0	5.0	4.0	M4.5 V
J05394+747	3.5	3.5	3.0	3.5	3.5	3.5	M3.5 V
J05415+534	M0.5 V	PMSU	1.0	1.0	1.0	1.0	1.0	1.0	M1.0 V
J05421+124	M4.0 V	PMSU	4.0	4.0	4.0	4.0	4.0	4.0	M4.0 V
J05424+506	m:	Simbad	3.0	3.0	3.0	3.5	3.0	3.5	M3.0 V
J05425+154	M5.0 V	LC08	3.5	3.5	3.5	3.5	3.5	4.0	M3.5 V
J05427+026	m:	Simbad	3.5	3.0	3.0	3.0	3.5	3.0	M3.0 V
J05455-119	4.5	4.5	4.0	4.0	4.5	4.5	M4.5 V
J05456+111	-1.0	-1.0	0.0	0.0	-1.0	0.0	-0.5
J05456+729	3.0	3.0	3.0	3.0	3.0	3.0	M3.0 V
J05457-223	m6:	Simbad	3.5	3.5	3.5	3.5	3.5	3.0	M3.5 V
J05458+729	2.5	2.5	3.0	3.0	2.5	2.5	M2.5 V
J05463+012	M1 V	New14	2.5	2.5	2.5	2.5	3.0	2.5	M2.5 V
J05501+051	1.5	1.0	1.5	1.0	1.5	2.0	M1.5 V
J05511+122	4.0	4.0	3.5	4.0	4.0	4.0	M4.0 V
J05566-103	M3.5 V	Riaz06	3.5	3.5	4.0	3.5	3.5	4.0	M3.5 V
J05582-046	M5.0 V	RA12	4.5	5.0	4.5	5.0	5.0	4.5	M4.5 V
J05588+213	M4.5 V	Reid04	5.0	5.0	5.0	5.0	5.0	5.0	M5.0 V
J05596+585	M0.5 V	PMSU	0.0	0.0	1.0	1.0	0.5	0.5	M0.5 V
J06024+663	M4.5 V	Giz97	4.5	4.5	4.5	4.5	5.0	4.5	M4.5 V
J06024+498	M5.0 V	PMSU	5.0	5.0	5.0	5.0	5.0	5.0	M5.0 V
J06035+168	4.0	4.0	4.0	4.0	4.0	4.0	M4.0 V
J06035+155	M0.0 V	Lep13	0.5	0.0	0.0	-0.5	0.0	0.5	M0.0 V
J06054+608	M4.5 V	Giz97	4.5	4.5	4.5	4.0	4.5	5.0	M4.5 V
J06065+045	m:	Simbad	3.0	3.0	3.5	3.5	3.0	3.0	M3.0 V
J06066+465	3.0	3.0	3.0	3.0	3.0	3.0	M3.0 V
J06075+472	M3.5 V	Reid07	4.5	4.5	4.5	4.5	4.5	5.0	M4.5 V
J06102+225	4.0	4.0	4.5	4.0	4.5	4.5	M4.0 V
J06103+722	2.5	2.0	3.0	3.0	2.5	3.0	M2.5 V
J06145+025	M3.0 V	Sch05	2.5	2.5	3.5	3.5	3.0	3.5	M3.0 V
J06151-164	4.0	4.0	4.0	4.0	4.0	4.0	M4.0 V
J06171+051 AB	M3.5 V	PMSU	3.5	3.5	3.0	3.5	3.5	3.5	M3.5 V

Table A.3. Spectral types of observed stars (cont.).

Karmn	Sp. type biblio.	Ref. ^a	Sp. type			Sp. type			Sp. type adopted
			Best-fit	χ^2	TiO2	TiO5	PC1	VO-7912	
J06185+250	M4.0 V	Reid04	4.0	3.5	4.0	4.0	4.0	4.0	M4.0 V
J06236-096 AB	M3.5 V	Reid04	3.5	3.5	3.5	3.5	3.5	3.5	M3.5 V
J06238+456	M5.0 V	Sch05	5.0	5.0	5.0	5.0	5.0	5.0	M5.0 V
J06246+234	M4.5 V	PMSU	4.0	4.0	4.0	4.5	4.0	4.0	M4.0 V
J06298-027 AB	M3.5 V+M6.3	Reid04, Shk10	4.0	4.0	4.5	4.0	4.0	4.5	M4.0 V
J06307+397	2.0	2.0	2.0	2.0	2.0	2.0	M2.0 V
J06313+006	1.5	1.5	1.0	1.5	1.5	1.5	M1.5 V
J06314-016	m:	Simbad	1.5	1.0	2.0	2.0	1.0	1.5	0.5
J06323-097	4.0	4.5	4.0	4.0	4.5	4.5	M4.5 V
J06325+641	M4.0 V	Giz97	4.0	4.0	4.0	4.0	4.0	4.0	M4.0 V
J06332+054	M1.0 V	New14	2.0	2.0	2.0	2.0	2.0	2.0	M2.0 V
J06354-040 AB	5.5	5.5	5.5	5.0	5.5	5.0	M5.5 V
J06361+201	M2.5 V	Reid04	2.5	2.5	2.5	2.5	2.5	2.5	M2.5 V
J06367+378	3.5	3.5	4.0	3.5	4.0	4.0	M3.5 V
J06401-164	2.5	2.5	3.0	3.0	2.0	2.5	M2.5 V
J06435+166	M4.5 V	Reid04	4.0	4.5	4.0	4.5	4.5	4.5	M4.5 V
J06461+325	M0.5 V	PMSU	1.0	1.0	1.0	1.0	1.0	0.5	M1.0 V
J06474+054	4.0	4.0	4.0	4.0	4.0	4.0	M4.0 V
J06489+211	2.5	2.5	2.5	2.5	2.5	3.0	M2.5 V
J06509-091	k:	Simbad	3.5	3.5	3.5	3.5	3.5	3.0	M3.5 V
J06522+179	m:	Simbad	0.0	0.0	-0.5	-0.5	0.0	0.0	M0.0 V
J06522+627	3.5	4.0	3.5	3.5	3.5	3.5	M3.5 V
J06523-051S AB	M2.0 V	PMSU	2.0	2.0	2.0	2.0	2.0	2.0	M2.0 V
J06523-051N	K3 V	Simbad	-4.0	<-3.0	<K5 V
J06548+332	M3.0 V	PMSU	3.0	3.0	3.0	3.0	3.0	3.0	M3.0 V
J06565+440	m:	Simbad	4.5	4.5	4.0	4.0	4.5	4.5	M4.5 V
J07001-190	5.0	5.0	5.0	4.5	5.0	5.0	M5.0 V
J07009-023	3.0	3.0	3.0	3.0	3.0	3.0	M3.0 V
J07031+836	3.0	3.5	3.5	3.5	3.5	3.0	M3.5 V
J07051-101	5.0	5.0	5.0	4.5	4.5	4.5	M5.0 V
J07105-087	3.5	3.5	3.5	3.5	3.5	3.5	M3.5 V
J07105+283	K7 V	Ste86	0.0	0.0	0.0	0.0	0.0	0.0	M0.0 V
J07111-035	1.0	0.5	0.0	0.0	1.0	0.5	M0.5 V
J07111+434 AB	M6.0 V+M7.5	Sch05, Mon06	5.5	5.5	6.0	6.5	6.0	5.5	M5.5 V
J07172-050	M4.0 V	Riaz06	3.5	3.5	4.0	4.0	3.5	4.0	M3.5 V
J07182+137	3.5	3.5	3.5	3.5	4.0	3.5	M3.5 V
J07191+667	0.0	0.0	0.0	-0.5	0.0	0.0	M0.0 V
J07195+328	K7 V	PMSU	0.0	0.0	0.0	0.0	0.0	0.0	M0.0 V
J07219-222	3.5	3.5	3.5	3.5	4.0	3.5	M3.5 V
J07274+052	M3.5 V	PMSU	3.5	3.5	3.5	3.5	3.5	4.0	M3.5 V
J07310+460	M4.0 V	Riaz06	4.0	4.0	4.5	4.0	4.0	4.5	M4.0 V
J07319+362N	M3.5 V	PMSU	4.0	3.5	3.5	3.5	4.0	4.0	M3.5 V
J07319+362S AB	M2.5 V	PMSU	2.5	2.5	3.0	3.0	2.5	3.0	M2.5 V
J07321-088	-2.0	-2.0	K5 V
J07324-130	0.0	0.0	0.0	0.0	-0.5	0.0	M0.0 V
J07359+785	M3.5 V	Reid04	3.0	3.0	3.5	3.5	3.0	3.5	M3.0 V
J07361-031	m:	Simbad	1.0	1.0	1.0	0.5	1.0	1.0	M1.0 V
J07365-006	3.5	3.5	3.5	3.5	3.5	3.5	M3.5 V
J07366+440	3.5	3.0	3.0	3.0	3.5	3.5	M3.5 V
J07420+142	M3 S	KMc89, SB06	M III
J07429-107	2.5	2.5	3.0	2.5	2.5	3.0	M2.5 V
J07467+574	5.0	5.0	4.5	4.5	4.5	5.0	M4.5 V
J07470+760	M4.0 V	Reid04	4.0	4.0	3.5	3.5	4.0	4.0	M4.0 V
J07497-033	M4.0 V	Reid07	3.5	3.5	3.5	3.5	3.5	3.0	M3.5 V
J07498-032	3.5	3.5	4.0	4.0	3.0	4.0	M3.5 V
J07523+162	M7.0 V	Reid03	6.0	6.0	6.0	5.5	6.0	6.0	M6.0 V
J07545+085	2.5	2.5	2.5	2.5	2.5	2.5	M2.5 V
J07545-096	3.5	3.0	3.5	3.0	3.5	3.5	M3.5 V
J07558+833	M3.5 V	PMSU	5.0	5.0	4.0	3.5	5.5	4.5	M4.5: V
J07591+173	3.5	4.0	4.0	4.0	3.5	4.0	M4.0 V
J08025-130	2.5	2.5	3.0	2.5	3.0	3.0	M2.5 V
J08031+203 AB	M3.3 V	Riaz06	3.5	3.5	4.0	3.5	3.5	3.0	M3.5 V
J08069+422	M4.5 V	Reid04	4.0	4.5	4.0	4.0	4.5	4.5	M4.0 V
J08082+211N	K5 V	PMSU	-1.0	-1.0	-1.0	-1.0	-0.5	-0.5	K7 V
J08082+211S AB	M2.5 V+M3.1	PMSU, Shk10	3.0	3.0	3.0	3.0	3.0	3.0	M3.0 V
J08104-111	0.5	1.0	2.0	2.0	0.5	1.5	M1.0 V
J08105-138 AB	M2.0 V	PMSU	2.5	2.5	2.5	2.5	2.5	2.0	M2.5 V
J08117+531	2.5	2.5	3.0	3.0	2.5	3.0	M2.5 V
J08143+630	1.5	1.5	1.5	1.5	1.5	1.0	M1.5 V
J08161+013	M2.0 V	PMSU	2.0	2.0	2.0	2.0	2.0	2.0	M2.0 V
J08283+553	2.5	2.5	3.0	3.0	3.0	3.0	M2.5 V
J08286+660	M0 Ve	App98	4.0	4.0	4.0	4.0	4.0	4.0	M4.0 V
J08298+267	M6.0 V	PMSU	6.5	6.5	6.5	6.0	6.0	6.5	M6.5 V
J08353+141	M4.5 V	Reid07	4.5	4.5	4.5	4.5	4.5	4.0	M4.5 V
J08375+035	4.0	4.5	4.0	4.0	4.0	4.0	M4.0 V
J08386-028	-2.0	-2.0	K5 V
J08394-028	0.5	0.5	1.0	1.0	0.5	1.0	M0.5 V
J08423-048	M2.5 V	Sch05	3.0	3.0	3.0	3.0	3.0	3.0	M3.0 V
J08449-066 AB	M3.0 V	Reid07	3.5	3.5	3.5	3.5	3.5	3.5	M3.5 V
J08526+283	M4.0 V	PMSU	4.5	4.5	4.0	4.0	4.5	4.5	M4.5 V
J08531-202	3.0	3.0	3.0	3.0	3.0	3.0	M3.0 V

Table A.3. Spectral types of observed stars (cont.).

Karmn	Sp. type biblio.	Ref. ^a	Sp. type			Sp. type			Sp. type adopted
			Best-fit	χ^2	TiO2	TiO5	PC1	VO-7912	
J08563-044	k:	Simbad	1.0	1.0	1.0	1.0	1.0	1.0	M1.0 V
J08572+194	M4.0 V	Sch05	3.5	3.5	3.5	3.5	3.5	3.5	M3.5 V
J08590+364	k:	Simbad	0.5	0.5	0.5	0.5	0.5	0.5	M0.5 V
J08595+537	3.5	4.0	4.0	3.5	3.5	4.0	M3.5 V
J08599+042	1.0	1.0	0.5	1.0	1.0	0.5	M1.0 V
J09003+218	M6.5 V	Reid03	6.5	6.5	6.5	6.0	6.5	6.0	M6.5 V
J09008+237	2.5	2.5	3.0	3.0	3.0	3.0	M2.5 V
J09023+177	M3.5 V	Reid07	4.0	3.5	4.0	4.0	4.0	4.0	M4.0 V
J09028+060	1.5	1.5	1.5	1.5	1.5	1.0	M1.5 V
J09040-159	M2.5 V	Riaz06	2.5	2.5	2.5	2.5	2.5	2.5	M2.5 V
J09045+164 AB	K5 V	Simbad	-4.0	<-3.0	<K5 V
J09058+555	3.5	3.5	3.5	3.5	3.5	3.0	M3.5 V
J09091+227	M3.0 V	Abe14	4.5	4.5	4.5	4.5	4.5	4.5	M4.5 V
J09115+126	2.5	2.5	2.5	2.5	2.5	2.5	M2.5 V
J09143+526	K7 V	Kir91	0.0	0.0	-0.5	-0.5	0.0	0.0	M0.0 V
J09144+526	M0 V	Kir91	0.0	0.0	-0.5	-0.5	0.0	0.0	M0.0 V
J09151+233	0.0	0.0	0.0	0.0	0.0	0.0	M0.0 V
J09156-105 AB	M5 V+M5	Sch05, Mon06	5.0	5.0	5.0	5.0	5.0	5.0	M5.0 V
J09201+037	3.5	3.5	3.5	3.5	3.5	3.5	M3.5 V
J09206-169	0.0	0.0	-0.5	-0.5	-0.5	0.0	M0.0 V
J09212+603	1.5	1.5	1.5	1.5	1.5	1.5	M1.5 V
J09218-023	2.5	2.0	2.5	2.5	2.0	2.0	M2.5 V
J09243+063	4.0	4.0	4.0	4.0	4.0	4.0	M4.0 V
J09248+306	3.5	3.5	3.5	3.5	3.5	3.5	M3.5 V
J09256+634 AB	4.0	4.5	4.5	4.5	4.5	4.5	M4.5 V
J09301-009	k:	Simbad	0.0	0.5	0.5	0.5	0.0	0.5	M0.5 V
J09308+024	4.0	4.0	4.0	4.0	4.0	4.0	M4.0 V
J09328+269	M5.5 V	PMSU	5.5	5.5	5.5	5.5	5.5	5.5	M5.5 V
J09351-103	m:	Simbad	-2.0	-2.0	K5 V
J09362+375	M0.5 V	Lep13	0.0	0.0	0.5	0.0	0.0	0.0	M0.0 V
J09394+146	3.5	3.5	3.5	3.0	3.0	3.5	M3.5 V
J09449-123	M5.0 V	Sch05	5.0	5.0	5.5	5.0	5.0	5.0	M5.0 V
J09488+156	M2.0 V	Shk09	3.0	3.0	3.0	3.0	2.5	3.0	M3.0 V
J09526-156	M4.0 V	Sch05	3.5	3.0	3.5	3.5	3.0	3.5	M3.5 V
J09538-073	M1 Ve	Ste86	0.5	1.0	-0.5	0.0	0.5	0.5	M0.5 V
J09589+059	m4.5:	Law08	4.5	5.0	4.5	4.5	4.5	4.5	M4.5 V
J09597+721	3.5	3.5	3.5	3.5	3.5	3.5	M3.5 V
J10008+319	M6.5 V	Giz00	6.0	6.0	6.0	6.0	6.0	6.0	M6.0 V
J10020+697	M4.5 V	Reid04	4.0	4.5	4.0	4.0	4.0	4.5	M4.0 V
J10028+484	M5.0 V	Boc05	5.5	5.5	5.5	5.5	5.5	5.5	M5.5 V
J10063-064	4.0	4.5	4.5	4.5	5.0	4.0	M4.5 V
J10068-127	M4.5 V	Reid07	4.5	4.5	4.5	4.5	4.5	4.5	M4.5 V
J10098-007	K4 V	Ste86	-2.0	-2.0	K5 V
J10120-026 AB	M2.5 V	PMSU	2.5	2.5	2.5	2.5	2.5	2.5	M2.5 V
J10130+233	M4.0 V	Sch05	3.5	3.5	3.5	3.5	3.5	4.0	M3.5 V
J10148+213	M4.5 V	Sch05	4.5	4.5	4.5	4.5	4.5	4.5	M4.5 V
J10155-164	4.0	3.5	4.0	4.0	4.0	4.0	M4.0 V
J10196+198 AB	M3.0 V	PMSU	3.0	3.0	3.5	3.0	3.0	3.0	M3.0 V
J10200+289	M3.0 V	Sch05	3.0	2.5	3.0	3.0	2.5	3.0	M3.0 V
J10238+438	M4.5 V	Reid04	5.0	5.0	5.0	5.0	5.0	5.0	M5.0 V
J10240+366	M3.0 V	Reid07	3.5	3.5	3.5	3.5	3.5	4.0	M3.5 V
J10278+028	k:	Simbad	3.5	3.5	3.5	3.5	4.0	3.5	M3.5 V
J10304+559	K7 V	Simbad	-1.0	-1.0	-1.5	-1.5	-1.0	-0.5	-1.0
J10359+288	M2.5 V	Reid07	3.0	3.0	3.5	3.0	3.0	3.5	M3.0 V
J10368+509	M3.5 V	Reid04	4.5	4.5	4.5	4.5	4.5	4.5	M4.5 V
J10430-092 AB	M5-6 V	Gig98	5.5	5.5	5.0	5.5	5.5	5.0	M5.5 V
J10443+124	M4.0 V	Sch05	3.5	3.5	3.5	3.5	4.0	4.0	M3.5 V
J10482-113	M6.5 V	PMSU	6.5	6.5	7.0	7.0	6.5	7.0	M6.5 V
J10508+068	M4.0 V	PMSU	4.0	4.5	4.0	4.0	4.0	4.0	M4.0 V
J10546-073	M4.0 V	Sch05	4.0	4.0	3.5	4.0	4.0	4.0	M4.0 V
J10560+061	M5.5 III	KMc89, Gar89	M III
J10563+042	2.5	2.5	2.5	2.5	2.5	2.5	M2.5 V
J10564+070	M5.5 V	PMSU	6.0	6.0	6.0	6.0	6.0	6.0	M6.0 V
J10584-107	M5.0 V	Sch05	5.0	5.0	5.0	4.5	4.5	5.0	M5.0 V
J11018-024	M0 III	Gar89, SB06	M III
J11030+037	2.5	2.5	2.5	2.5	2.5	3.0	M2.5 V
J11033+359	M2.0 V	PMSU	1.5	1.5	1.5	2.0	2.0	1.5	M1.5 V
J11046-042S AB	M0 Vke	Gray03	0.0	0.5	0.5	0.0	0.5	0.5	M0.5 V
J11054+435	M0.5 V	PMSU	1.0	1.0	1.0	1.0	1.0	0.5	M1.0 V
J11055+435	M6.0 V	PMSU	6.0	6.0	6.5	6.5	5.5	5.5	M5.5 V
J11075+437	3.0	3.0	3.0	3.0	3.0	3.0	M3.0 V
J11151+734N	M2 V	Bid85	2.5	2.5	2.5	2.5	2.5	2.5	M2.5 V
J11151+734S	K3 V	Bid85	...	<-3.0	<K5 V
J11201-104 AB	M2.0 V	Riaz06	2.0	2.0	2.0	2.0	2.0	1.5	M2.0 V
J11201+301	M0 III	MP50, JE12	M III
J11214-204S	M1.0 V	PMSU	2.5	2.5	2.5	2.5	3.0	3.0	M2.5 V
J11214-204N	K6 V	Gray06	-1.0	-1.0	-1.0	-1.0	-0.5	-0.5	K7 V
J11218+181	K6.5 V	Simbad	0.0	0.0	0.5	0.5	0.0	0.5	M0.0 V
J11240+381	M4.5 V	Reid07	4.5	4.5	4.5	4.0	4.0	4.5	M4.5 V
J11306-080	M3 V	Gray06	3.0	3.5	3.0	3.5	3.5	3.0	M3.5 V
J11312+631	K5 V	PMSU	-1.0	-1.0	-1.0	-1.0	-0.5	-0.5	K7 V

Table A.3. Spectral types of observed stars (cont.).

Karmn	Sp. type biblio.	Ref. ^a	Sp. type			Sp. type			Sp. type adopted
			Best-fit	χ^2	TiO2	TiO5	PC1	VO-7912	
J11378+418	2.0	2.0	2.0	2.5	2.0	2.0	M2.0 V
J11403+095	1.5	1.5	1.5	1.5	1.0	1.5	M1.5 V
J11421+267	M2.5 V	PMSU	2.5	2.5	2.5	2.5	2.5	2.5	M2.5 V
J11451+183	M4.0 V	Sch05	4.0	3.5	4.0	4.0	4.0	4.0	M4.0 V
J11458+065	M1 III	KMc89, Gar89	M III
J11472+770	0.0	-1.0	-0.5	-0.5	-1.0	-0.5	-1.0
J11474+667	M4.0 V	Reid07	5.0	5.0	5.0	4.5	4.5	5.0	M5.0 V
J11485+076	M3.5 V	Shk09	3.5	4.0	4.0	3.5	3.5	4.0	M3.5 V
J11511+352	M1.0 V	PMSU	1.5	1.5	1.5	1.5	1.5	1.0	M1.5 V
J11522+100	M4.0 V	PMSU	4.0	4.0	4.0	4.0	4.5	4.0	M4.0 V
J11549-021	3.0	3.0	3.0	3.0	3.0	3.0	M3.0 V
J12025+084	sdM2.0	Giz97	1.5	1.5	1.5	2.0	1.5	1.5	M1.5 V
J12049+174	M2.5 V	Riaz06	3.5	3.5	3.5	3.0	3.0	3.5	M3.5 V
J12069+058	-2.0	-2.0	K5 V
J12088+217	M3.0 V	New14	0.5	0.5	0.5	0.5	0.5	0.5	M0.5 V
J12093+210	M8 V:e	Ste86	2.5	2.5	3.0	3.0	3.0	3.0	M2.5 V
J12104-131	M4.5 V	Riaz06	4.5	4.5	4.5	4.0	4.0	4.5	M4.5 V
J12124+121	2.0	2.0	2.0	2.0	2.0	2.0	M2.0 V
J12162+508	4.0	4.0	4.0	4.0	4.5	4.5	M4.0 V
J12228-040	M4.5 V	Sch05	4.5	4.5	4.5	4.5	4.5	5.0	M4.5 V
J12322+454	M1 III	JE12	M III
J12349+322	3.5	3.0	3.0	3.5	3.0	3.5	M3.5 V
J12364+352	M3.5 V	Reid04	4.5	4.5	4.0	4.0	4.5	4.5	M4.5 V
J12368-019	3.5	3.5	3.5	3.5	4.0	4.0	M3.5 V
J12372+358	1.5	1.5	2.0	2.0	1.5	1.5	M1.5 V
J12417+567	M3.0 V	Riaz06	3.5	3.5	3.5	3.5	3.0	3.5	M3.5 V
J12440-111	M4.5 V	Sch05	4.5	4.5	4.5	4.5	4.5	4.5	M4.5 V
J12456+271	M4 III	Jac84, Kir91	M III
J12470+466	M2.5 V	PMSU	2.5	2.5	2.5	2.5	3.0	2.5	M2.5 V
J12488+120	M4.0 V	Reid06	4.5	4.5	4.0	4.5	4.5	4.5	M4.5 V
J12533-053	M3.0 V	Sch05	2.5	3.0	3.0	3.5	3.0	3.0	M3.0 V
J12533+466	M3 III	JE12	M III
J12549-063	M4.0 V	PMSU	5.0	5.0	4.5	4.5	4.5	4.5	M4.5 V
J12593-001	M4.0 V	Sch05	4.0	4.0	3.5	3.5	4.0	4.0	M4.0 V
J13027+415	k:	Simbad	3.5	3.0	3.5	3.5	3.5	3.5	M3.5 V
J13088-015	M3.0 V	Sch05	3.0	3.0	3.5	3.0	3.0	3.0	M3.0 V
J13102+477	M4.5 V	Riaz06	5.0	5.0	5.0	5.0	5.0	5.0	M5.0 V
J13113+096	M0.0 V	New14	-1.0	-1.0	-0.5	0.0	-0.5	0.0	-0.5
J13143+133 AB	M6-8 V	Sch14	6.0	6.0	6.0	6.0	6.0	6.5	M6.0 V
J13167-123	M3.0 V	Sch05	3.5	3.5	3.5	3.5	3.5	3.5	M3.5 V
J13168+170	M0.5 V	PMSU	0.5	0.5	0.5	0.5	0.5	0.5	M0.5 V
J13179+362	M1.0 V	PMSU	1.0	1.0	1.0	1.5	1.0	1.0	M1.0 V
J13182+733	3.5	3.5	3.5	4.0	3.5	4.0	M3.5 V
J13247-050	M4.0 V	Sch05	4.0	4.0	4.0	4.0	4.0	4.0	M4.0 V
J13251-114	3.0	2.5	3.0	3.0	3.0	3.0	M3.0 V
J13253+426	K5 V	Ste86	-1.0	-1.0	-1.5	-1.5	-1.0	-1.0	K7 V
J13260+275	3.0	3.0	3.0	3.0	2.5	3.5	M3.0 V
J13294-143	M3.0 V	Reid07	3.5	3.5	4.0	3.5	3.5	4.0	M3.5 V
J13312+589	2.5	2.5	2.5	2.0	2.5	2.5	M2.5 V
J13314-079	K7 V	Bid85	0.0	0.0	0.0	0.0	0.0	0.0	-0.5
J13321-112	0.0	0.0	-0.5	-0.5	-0.5	-0.5	M0.0 V
J13326+309	M4.5 V	Sch05	4.5	4.5	4.5	4.5	4.0	4.5	M4.5 V
J13335+704	M2.5 V	Reid07	3.5	3.5	3.5	3.5	4.0	3.5	M3.5 V
J13386-115	4.5	4.5	4.5	4.5	4.0	4.5	M4.5 V
J13394+461 AB	M1.0 V	PMSU	1.0	1.5	1.5	1.5	1.5	1.5	M1.5 V
J13413-091	2.5	2.5	3.0	3.0	3.0	3.0	M2.5 V
J13414+489	M3.5 V	Lep13	3.5	3.5	3.0	3.0	3.5	3.5	M3.5 V
J13474+063	M0 V	Bid85	-1.0	-1.0	-1.5	-1.5	-1.0	-1.0	K7 V
J13503-216	M3 V:	Bid85	4.0	3.5	3.5	3.5	4.0	3.5	M3.5 V
J13537+521 AB	M3.5 V	Reid07	3.5	3.0	3.5	3.5	3.5	3.0	M3.5 V
J13551-079	M0 V	Ste86	0.0	0.0	0.0	0.0	-0.5	-0.5	M0.0 V
J13555-073	k:	Simbad	3.0	3.0	3.0	3.0	3.0	2.5	M3.0 V
J13582-120	M4.0 V	Sch05	4.5	4.5	4.5	4.5	4.5	4.5	M4.5 V
J13583-132	M4 V	Sch05	4.0	4.0	4.0	4.0	4.0	4.0	M4.0 V
J13587+465	M2 III	MP50, JE12	M III
J14019+432	2.5	2.0	3.0	3.0	2.5	2.5	M2.5 V
J14102-180	2.5	2.5	2.5	2.5	3.0	2.5	M2.5 V
J14159-110	1.5	1.5	2.0	1.5	1.5	1.5	M1.5 V
J14171+088	4.5	4.5	4.5	4.5	4.5	4.5	M4.5 V
J14175+025	3.0	3.0	3.0	3.0	3.0	3.0	M3.0 V
J14194+029	m4.5:	Law08	5.0	5.0	5.0	4.5	5.0	5.0	M5.0 V
J14195-051	M5 V	New14	4.0	4.0	4.0	4.0	4.0	4.0	M4.0 V
J14215-079	4.0	4.0	4.0	3.5	3.5	4.0	M4.0 V
J14227+164	5.0	5.0	5.0	4.5	4.5	4.5	M5.0 V
J14244+602	2.0	2.0	2.0	2.0	2.0	1.5	M2.0 V
J14251+518	M2.5 V	PMSU	2.5	2.0	2.5	2.5	2.5	2.0	M2.5 V
J14255-118	4.0	4.0	4.0	3.5	4.0	4.0	M4.0 V
J14312+754	M4.0 V	Reid07	4.0	4.0	4.0	4.0	3.5	4.0	M4.0 V
J14336+093	M3 V:	Bid85	3.5	3.0	3.0	3.5	3.5	3.5	M3.5 V
J14415+136	M3 V:	Bid85	1.0	1.0	1.0	1.0	1.5	1.0	M1.0 V
J14446-222	M4.5 V	Reid04	4.5	4.5	4.0	4.0	4.5	4.0	M4.5 V

Table A.3. Spectral types of observed stars (cont.).

Karmn	Sp. type biblio.	Ref. ^a	Sp. type			Sp. type			Sp. type adopted
			Best-fit	χ^2	TiO2	TiO5	PC1	VO-7912	
J14472+570	3.5	4.0	4.0	4.0	3.5	4.0	3.5 M4.0 V
J14480+384	K5 V	PMSU	-1.0	-1.0	-1.0	-1.0	-0.5	-1.0	K7 V
J14485+101	3.5	3.5	3.5	3.5	4.0	3.5	M3.5 V
J14492+498	1.5	1.5	1.5	1.5	1.5	2.0	M1.5 V
J14501+323	M3.0 V	Reid04	3.5	3.0	3.5	3.5	3.5	3.5	M3.5 V
J14544+161 ABC	M2.0 V+M8.5+M9.0	PMSU, Simbad	0.5	1.0	2.0	2.0	1.0	1.0	M1.0: V
J14595+454	M0 V	Bid85	-1.0	-1.0	-1.5	-1.5	-1.0	-1.0	K7 V
J15079+762	4.5	4.5	5.0	4.5	4.0	4.5	M4.5 V
J15081+623	4.0	4.0	3.5	3.5	4.0	4.0	M4.0 V
J15118+395	2.5	2.5	2.5	2.5	2.5	2.5	M2.5 V
J15131+181	2.0	1.5	2.0	2.0	2.0	2.0	M2.0 V
J15142-099	4.0	4.0	4.0	4.0	4.0	4.0	M4.0 V
J15147+645	m:	Simbad	3.5	3.5	3.5	3.5	3.0	3.0	M3.5 V
J15151+333	M2.5 V	Reid04	2.0	2.0	2.0	2.5	2.0	2.0	M2.0 V
J15157-074	M2-3 V	Gig98	4.0	4.0	4.0	4.0	3.5	4.0	M4.0 V
J15164+167	-2.0	-2.0	K5 V
J15197+046	4.0	4.0	4.0	3.5	4.0	4.0	M4.0 V
J15204+001	K5 V	Bid85	0.0	0.0	-1.0	-0.5	-1.0	-0.5	M0.0 V
J15210+255	K8 V	Ste86	-1.0	-1.0	-1.0	-1.0	-1.0	-0.5	K7 V
J15238+584	M3.5 V	Sch05	4.0	4.0	4.0	4.0	3.5	4.0	M4.0 V
J15277-090	M4.5 V	PMSU	4.5	4.5	4.5	4.5	4.5	4.5	M4.5 V
J15290+467 AB	M4.5 V+m5.0:	Reid07, Jan12	4.5	4.5	4.5	4.5	4.5	4.5	M4.5 V
J15291+574	1.0	1.0	0.5	0.5	1.0	0.5	M1.0 V
J15305+094	5.5	5.5	5.5	5.5	5.5	5.5	M5.5 V
J15340+513	4.5	4.5	4.0	4.5	4.5	4.5	M4.5 V
J15386+371	M:	SP88	3.5	3.5	3.5	3.5	3.5	3.5	M3.5 V
J15430-130	1.5	1.5	1.5	1.5	1.5	1.5	M1.5 V
J15474+451	M4.0 V	Sch05	4.0	4.0	4.0	4.0	4.0	4.0	M4.0 V
J15476+226	M3.5 V	Abe14	4.5	4.5	4.5	4.5	4.5	4.0	M4.5 V
J15480+043	2.5	2.5	3.0	2.5	3.0	2.5	M2.5 V
J15481+015	M3.0 V	Eis07	2.5	2.5	3.0	2.5	3.0	3.0	M2.5 V
J15499+796	m4.5:	Law08	5.0	5.0	5.0	5.0	5.0	4.5	M5.0 V
J15552-101	2.5	2.5	3.0	3.0	2.5	2.5	M2.5 V
J15557-103	M3.5 V	Riaz06	3.5	3.5	4.0	3.5	3.5	4.0	M3.5 V
J15558-118	M3.0 V	Sch05	3.0	3.0	3.0	3.0	3.0	3.0	M3.0 V
J15569+376	M2.5 V	Riaz06	2.5	2.0	3.0	2.5	2.5	3.0	M2.5 V
J15578+090	4.0	4.0	4.0	4.0	4.5	4.0	M4.0 V
J16023+036	1.5	1.5	1.5	1.5	1.5	2.0	M1.5 V
J16042+235	5.0	5.0	5.0	5.0	5.0	5.0	M5.0 V
J16048+391	M4.0 V	PMSU	4.0	4.0	4.0	4.0	4.0	4.0	M4.0 V
J16120+033N	3.5	3.5	4.0	4.0	3.5	4.0	M3.5 V
J16139+337 AB	M2.5 V	PMSU	2.5	2.5	2.5	2.5	2.5	2.5	M2.5 V
J16148+606 AB	M3.5 V	Reid04	3.0	3.0	3.0	3.0	2.5	3.0	M3.0 V
J16157+586	M5.0 V	Sch05	5.0	5.0	5.0	4.5	5.0	4.5	M5.0 V
J16167+672S	M1.0 V	PMSU	0.0	0.0	0.0	0.0	0.0	0.0	M0.0 V
J16183+757	M4.0 V	PMSU	4.0	4.0	4.0	4.0	4.0	4.0	M4.0 V
J16243+199	3.0	3.0	3.5	3.0	3.0	3.0	M3.0 V
J16254+543	M2.0 V	PMSU	1.5	1.5	2.0	1.5	1.5	1.5	M1.5 V
J16269+149	4.0	4.0	4.5	4.0	4.0	4.5	M4.0 V
J16276-035 AB	K4 V	Ste86	-2.0	-2.0	K5 V
J16299+048	3.0	3.0	3.0	3.0	3.0	3.0	M3.0 V
J16314+471	3.5	3.5	4.0	4.0	3.5	4.0	M3.5 V
J16330+031	3.0	3.0	3.0	3.0	3.5	3.0	M3.0 V
J16354-039	m:	Simbad	0.0	0.0	-1.5	-1.5	0.0	-0.5	sdM0:
J16365+287	3.5	3.5	3.5	3.5	4.0	3.5	M3.5 V
J16459+609	3.5	3.5	3.5	3.5	3.5	3.5	M3.5 V
J16465+345	M6.5 V	Reid03	6.0	6.0	6.0	6.5	6.0	6.0	M6.0 V
J16480+453	M4.0 V	Riaz06	4.0	4.0	4.5	4.0	4.0	4.5	M4.0 V
J16528+610	M6 V	Simbad	4.5	4.5	4.5	4.5	4.5	4.5	M4.5 V
J16536+560	3.5	3.0	4.0	4.0	3.5	3.5	M3.5 V
J16543+256	2.5	2.5	3.0	3.5	3.0	3.0	M3.0 V
J16555-083	M7.0 V	PMSU	7.0	6.5	7.0	7.0	7.0	7.0	M7.0 V
J17011+555	2.5	2.5	2.5	2.5	2.5	2.5	M2.5 V
J17017+741	3.5	3.5	3.5	3.5	3.5	3.5	M3.5 V
J17052-050	M2.0 V	PMSU	1.5	1.5	2.0	2.0	1.5	1.5	M1.5 V
J17062+646	M2.5 V	GR97	3.0	3.0	3.0	3.0	2.5	2.5	M3.0 V
J17094+391	m:	Simbad	3.0	3.0	3.0	3.0	2.5	3.0	M3.0 V
J17126-099	M2: III	JE12	M III
J17140+176	2.5	2.5	2.5	3.0	2.5	2.5	M2.5 V
J17154+308	M2.5 V	Reid04	2.5	2.5	2.5	2.5	2.5	2.5	M2.5 V
J17163-053	4.0	4.5	4.0	4.5	4.5	4.0	M4.0 V
J17167+115	4.0	4.0	4.0	4.0	4.0	4.0	M4.0 V
J17176+524	M4.0 V	Sch05	3.5	3.5	3.5	3.5	3.5	3.5	M3.5 V
J17198+265	M4.5 V	PMSU	4.5	4.5	5.0	4.5	4.5	5.0	M4.5 V
J17199+265	M3.5 V	PMSU	3.5	3.5	3.5	3.5	3.5	3.5	M3.5 V
J17199+242	4.0	4.5	4.5	4.0	4.5	4.5	M4.5 V
J17216-171	M2 III	JE12	M III
J17239+136	M3.5 V	Reid07	4.0	4.0	4.0	3.5	4.0	4.0	M4.0 V
J17246+617	3.0	3.0	3.5	3.0	3.5	3.0	M3.0 V
J17265-227	2.5	2.5	3.0	3.0	2.0	2.5	M2.5 V
J17267-050	2.5	2.0	2.5	2.5	2.5	2.5	M2.5 V

Table A.3. Spectral types of observed stars (cont.).

Karmn	Sp. type biblio.	Ref. ^a	Sp. type			Sp. type			Sp. type adopted
			Best-fit	χ^2	TiO2	TiO5	PC1	VO-7912	
J17270+422	-2.0	-2.0	K5 V
J17281-017	4.0	4.0	4.0	4.0	4.0	4.5	M4.0 V
J17299-209	M3.5 V	Reid04	3.5	3.0	3.0	3.5	3.0	3.5	M3.0 V
J17301+546	3.5	3.5	3.5	3.5	3.5	3.5	M3.5 V
J17304+337	M3.0 V	Reid07	3.5	3.0	3.5	3.5	3.0	3.5	M3.5 V
J17364+683	M3.0 V	PMSU	3.0	3.5	3.0	3.5	3.0	3.0	M3.0 V
J17412+724	4.0	4.0	4.0	4.0	4.0	4.0	M4.0 V
J17426+756	M4.5 V	GR97	4.5	4.5	4.0	4.5	4.5	4.5	M4.5 V
J17428+167	1.5	1.5	2.0	1.5	1.5	1.5	M1.5 V
J17464+277 AB	M3.5 V	PMSU	3.5	3.5	3.5	3.5	3.5	3.5	M3.5 V
J17477+277	1.5	1.5	1.5	1.5	1.5	1.0	M1.5 V
J17520+566	M3.5 V	Riaz06	3.5	3.5	4.0	3.5	4.0	3.5	M3.5 V
J17559+294	3.5	3.5	4.0	3.5	3.5	4.0	3.5
J17578+046	M4.0 V	PMSU	3.5	3.5	3.5	4.0	3.5	3.5	M3.5 V
J17578+465	M3.0 V	PMSU	2.5	2.5	3.0	3.0	3.0	3.0	M2.5 V
J18006+685	-1.0	0.0	-1.0	-1.0	-0.5	0.0	-0.5
J18007+295	M2.0 V	Jah08	2.5	2.5	2.0	2.0	2.0	2.0	M2.0 V
J18019+001	3.5	4.0	3.5	3.5	3.5	4.0	3.5
J18022+642	M5.0 V	Riaz06	5.0	5.0	5.0	4.5	4.5	5.0	M5.0 V
J18028-030	M3.0 V	RS14	3.5	3.5	3.5	3.5	4.0	4.0	M3.5 V
J18036-189	m:	Simbad	5.0	5.0	5.0	4.5	5.0	5.0	M5.0 V
J18041+838	M4.5 V	RS14	3.5	4.0	3.5	3.5	4.0	4.0	M3.5 V
J18046+139	M2.5 V	Reid07	2.5	2.5	2.5	2.5	2.5	3.0	M2.5 V
J18054+015	M7.0 V	RS14	3.5	3.0	3.5	3.5	3.5	3.5	M3.5 V
J18057-143	5.5	5.5	5.5	5.5	5.5	5.5	M5.5 V
J18068+177	M4.0 V	Reid04	4.0	4.0	4.0	4.0	4.0	4.0	M4.0 V
J18090+241	1.0	1.0	1.0	1.0	1.5	1.0	M1.0 V
J18112-010	M3.5 V	Riaz06	3.5	3.5	3.5	3.5	3.5	4.0	M3.5 V
J18130+414	3.5	3.5	3.5	3.5	3.5	3.5	M3.5 V
J18131+260 AB	M4.0 V+M3.8:	PMSU, Shk09	4.0	4.0	4.5	4.0	4.0	4.0	M4.0 V
J18135+055	4.0	4.0	3.5	3.5	4.0	3.5	M4.0 V
J18149+196	M4.0 V	RS14	2.0	2.0	2.0	2.0	1.5	2.0	M2.0 V
J18162+686	m:	Simbad	1.5	1.5	2.0	1.5	1.5	1.5	M1.5 V
J18224+620	M4.5 V	PMSU	4.0	4.0	4.0	4.0	4.5	4.5	M4.0 V
J18253+186	3.5	3.5	3.5	3.5	3.5	3.5	M3.5 V
J18306-039	4.5	5.0	4.5	4.5	5.0	4.5	M4.5 V
J18313+649	M4.5 V	RS14	3.5	3.5	4.0	3.5	3.0	3.5	M3.5 V
J18338+194	M3.0 V	RS14	3.0	3.0	2.5	2.5	3.0	3.0	M3.0 V
J18353+457	M0.0 V	PMSU	0.5	0.5	0.5	0.5	0.0	0.0	M0.5 V
J18354+457	M3.5 V	PMSU	2.5	2.5	3.0	3.0	3.0	3.5	M2.5 V
J18400+726	M6.5 V	Reid04	7.0	6.0	6.5	6.5	6.5	7.0	M6.5 V
J18409+315	M1.5 V	Lep13	1.0	1.0	1.0	1.0	1.0	0.5	M1.0 V
J18423-013	M2 III:wk	JE12	M III
J18427+596N	M3.0 V	PMSU	3.0	3.0	3.0	3.0	3.0	3.0	M3.0 V
J18427+596S	M3.5 V	PMSU	3.5	3.5	3.5	3.5	3.0	3.5	M3.5 V
J18453+188	4.0	4.0	4.0	4.0	4.0	4.0	M4.0 V
J18467+007	4.0	4.0	4.5	4.0	4.0	4.0	M4.0 V
J18482+076	M5.0 V	Lep13	5.0	5.5	5.0	5.0	5.0	5.0	M5.0 V
J18491-032	4.5	4.5	4.5	4.5	4.5	4.5	M4.5 V
J18499+186	M4.5 V	Reid04	4.5	4.5	4.0	4.0	4.5	4.5	M4.5 V
J18542+109	4.0	4.0	4.0	4.0	4.0	4.0	M4.0 V
J18550+429	M4.0 V	Riaz06	4.0	4.0	4.5	4.0	4.0	4.5	M4.0 V
J18570+473	M2.5 V	RS14	2.5	2.5	2.5	3.0	2.5	2.5	M2.5 V
J19052+387	M3.5 V	Reid07	3.5	3.5	3.5	3.5	4.0	3.5	M3.5 V
J19060-074	M5.5 V	RS14	2.5	2.5	2.5	2.5	2.5	2.5	M2.5 V
J19070+208	M2.0 V	PMSU	2.0	2.0	2.0	2.0	1.5	1.5	M2.0 V
J19072+442	M4.5 V	Reid04	4.5	4.5	4.5	4.5	4.5	4.5	M4.5 V
J19105-075	3.5	3.0	3.5	3.5	3.5	3.5	M3.5 V
J19164+842	5.0	5.0	4.5	5.0	5.0	4.5	M5.0 V
J19168+003	3.5	3.5	4.0	3.5	3.5	3.5	M3.5 V
J19169+051N	M2.5 V	PMSU	2.5	2.0	2.5	2.5	2.5	2.5	M2.5 V
J19169+051S	M8.0 V	PMSU	8.0	>6.0	...	8.0	...	7.5	M8.0 V
J19243+426	M3.0 V	RS14	3.5	4.0	3.5	3.5	4.0	4.0	M3.5 V
J19260+244	M4.5 V	Reid04	4.5	4.5	4.5	4.0	4.5	4.5	M4.5 V
J19271+770	M4.0 V	RS14	2.5	2.5	3.0	3.0	2.0	2.5	M2.5 V
J19282-001	5.0	5.0	5.0	5.0	5.5	5.0	M5.0 V
J19312+361	M4.5 V	Cab10	4.5	4.5	4.5	4.5	4.5	4.0	M4.5 V
J19316-069	2.5	2.5	3.0	3.0	2.5	3.0	M2.5 V
J19327-068	3.5	3.5	3.5	3.5	4.0	4.0	M3.5 V
J19346+045	K5 V	PMSU	1.5	1.5	-1.5	-1.0	1.5	0.0	sdM1:
J19390+338	3.5	3.5	4.0	4.0	4.0	4.0	M3.5 V
J19393+148	3.0	3.0	3.0	3.0	3.0	3.0	M3.0 V
J19421+656	M4.0 V	RS14	3.0	3.0	3.5	3.0	3.5	3.0	M3.0 V
J19430+102	M3.0 V	RS14	2.0	2.0	2.5	2.0	2.0	2.5	M2.0 V
J19439-057	M4.0 V	Riaz06	3.5	3.5	4.0	4.0	3.5	4.0	M3.5 V
J19452+407	0.5	0.5	0.0	0.0	0.5	0.5	M0.5 V
J19519+141	M1.0 V	RS14	0.5	0.5	1.0	0.5	0.5	0.5	M0.5 V
J19524+603	3.0	3.0	3.0	3.0	3.0	3.0	M3.0 V
J19539+444W AB	M5.5 V	PMSU	5.5	5.5	5.5	5.0	5.5	5.5	M5.5 V
J19539+444E	M5.5 V	PMSU	5.5	5.5	5.5	5.5	5.5	5.5	M5.5 V
J19547+844	4.0	4.0	4.0	4.0	4.0	4.5	M4.0 V

Table A.3. Spectral types of observed stars (cont.).

Karmn	Sp. type biblio.	Ref. ^a	Sp. type			Sp. type			Sp. type adopted
			Best-fit	χ^2	TiO2	TiO5	PC1	VO-7912	
J19564+591	M3.5 V	PMSU	3.5	3.0	3.5	3.5	3.5	3.0	M3.5 V
J19565+591	M0:p V	PMSU	-1.0	-1.0	0.0	-0.5	-0.5	0.0	-0.5
J19578-108	M4.0 V	Riaz06	4.5	4.5	4.5	4.0	4.5	4.5	4.0
J20021+130 AB	3.5	3.5	3.5	3.5	3.5	3.5	M3.5 V
J20033+672	M3.0 V	RS14	3.0	2.5	3.0	3.0	3.0	2.5	M3.0 V
J20034+298	M4.5 V	PMSU	4.5	4.5	4.5	4.5	4.5	4.5	M4.5 V
J20047+512	M3.5 V	Bid85	3.5	3.0	3.0	3.5	3.0	3.5	M3.0 V
J20065+159	2.0	2.0	2.0	2.0	2.0	2.0	M2.0 V
J20077+189	M3: V	Bid85	3.5	3.5	4.0	4.0	4.0	4.0	M3.5 V
J20093-012	M5.0 V	Riaz06	5.0	5.0	5.0	5.0	5.0	5.0	M5.0 V
J20108+772	K5 V	PMSU	-1.0	-1.0	-0.5	-1.0	-1.0	-0.5	-1.5
J20112+161	M4.0 V	PMSU	4.0	4.0	4.0	4.0	4.0	4.5	4.0
J20123-126	-4.0	<-3.0	<K5 V
J20177+059	M3.0 V	RS14	2.5	2.5	3.0	3.0	3.0	2.5	M2.5 V
J20182-202	M2.5 V	Reid07	2.5	2.5	3.0	3.0	3.0	2.5	M2.5 V
J20216-199	2.0	1.5	2.0	2.0	2.0	1.5	M2.0 V
J20254-198	4.5	5.0	5.0	5.0	5.0	5.0	M5.0 V
J20283+617	2.5	2.5	3.0	2.5	2.5	2.5	M2.5 V
J20300+003 AB	4.0	4.5	4.5	4.5	4.0	4.5	M4.5 V
J20332+283	4.0	4.0	4.0	4.0	4.5	4.5	M4.0 V
J20336+365	M3.5 V	Reid04	3.5	4.0	3.5	3.5	3.5	4.0	M3.5 V
J20382+231	M4.5 V	RS14	2.0	2.0	2.5	2.0	2.0	2.0	M2.0 V
J20405+154	M4.5 V	PMSU	4.5	4.5	4.5	4.5	4.5	4.5	M4.5 V
J20407+199 AB	M2.5 V	PMSU	2.5	2.5	2.5	2.5	2.5	2.5	M2.5 V
J20439+231	M3.5 V	RS14	3.5	3.0	3.5	3.5	3.5	3.5	M3.5 V
J20467-118	M4.0 V	Sch05	4.0	4.0	4.5	4.0	4.0	4.5	M4.0 V
J20510+399	M3.0 V	RS14	3.0	3.0	3.0	3.0	3.0	3.0	M3.0 V
J20540+603	2.5	2.5	2.5	2.5	2.5	2.5	M2.5 V
J20581+401 AB	M1 V	Lee84	-1.0	-1.0	-0.5	-0.5	-0.5	-0.5	K7 V
J20583+425	M3.0 V	RS14	2.5	2.5	3.0	3.0	3.0	3.0	M2.5 V
J20593+530 AB	M3.5 Ve	Mot97	3.5	4.0	4.0	3.5	3.5	4.0	M3.5 V
J21009+510	M2.0 Ve	Mot97	2.5	2.5	3.0	3.0	2.5	3.0	M2.5 V
J21019-063	M3.0 V	PMSU	2.5	2.5	2.5	2.5	2.5	2.5	M2.5 V
J21027+349	M4.5 V	Reid04	4.5	4.5	5.0	4.5	4.5	4.5	M4.5 V
J21053+208	M2.5 V	RS14	2.5	2.5	3.0	3.0	2.5	2.5	M2.5 V
J21057+502E	3.5	3.5	3.5	3.5	4.0	4.0	M3.5 V
J21057+502W	4.0	3.5	4.0	4.0	4.0	4.0	M4.0 V
J21068+387	K5 V	Hen94	-2.0	-2.0	K5 V
J21069+387	K7 V	Hen94	0.5	0.5	-1.5	-1.0	0.5	-0.5	0.5
J21074+198	0.5	1.0	2.0	2.0	0.5	1.0	M1.0 V
J21074+468	2.0	2.0	2.5	2.5	2.5	2.5	M2.0 V
J21109+469	M2.5 V	Reid04	3.5	3.0	3.5	3.5	3.5	3.5	M3.5 V
J21114+658	M3.0 V	RS14	2.0	2.0	2.0	2.0	2.0	2.0	M2.0 V
J21127-073	3.0	3.5	3.5	3.5	3.5	3.5	M3.5 V
J21147+160	M3.5 V	RS14	3.5	3.5	4.0	3.5	4.0	3.5	M3.5 V
J21245+400	M6.5 V	Lep03	5.5	5.5	5.0	5.5	5.5	5.0	M5.5 V
J21376+016	M4.5 V	Lep13	4.5	4.5	4.5	4.5	4.5	4.5	M4.5 V
J21414+207	M4.5 V	RS14	3.0	3.0	3.5	3.0	3.0	3.5	M3.0 V
J21466+668	M4.0 V	Lep13	4.0	4.0	4.0	4.0	4.0	4.0	M4.0 V
J21467-212	4.0	4.0	4.0	4.0	4.0	4.0	M4.0 V
J21472-047	M3.0 V	Lam14	4.0	4.0	4.5	4.5	4.5	4.5	M4.5 V
J21554+596 AB	M4.0 Ve	Mot98	3.5	4.0	4.0	4.0	3.5	4.0	M4.0 V
J22021+014	M0.0 V	PMSU	0.5	0.5	0.5	0.5	0.5	0.5	M0.5 V
J22035+036 AB	4.0	4.5	4.5	4.0	4.0	4.5	M4.0 V
J22088+117	5.0	5.0	4.5	4.5	5.0	4.5	M4.5 V
J22089-177	M2.5 V	Boc05	2.5	2.5	2.5	2.5	2.5	2.5	M2.5 V
J22095+118	3.0	3.0	3.0	3.0	3.0	3.0	M3.0 V
J22114+409	M5.5 V	Abe14	5.5	5.5	5.5	5.5	5.5	5.0	M5.5 V
J22160+546	M4.0 V	PMSU	4.0	4.0	4.0	4.0	4.0	4.0	M4.0 V
J22202+067	M3 V:	Bid85	3.0	3.0	2.5	3.0	2.5	2.5	M2.5 V
J22234+324 AB	M3.0 V	PMSU	3.0	2.5	3.0	3.0	3.0	2.5	M3.0 V
J22264+583	3.0	3.5	3.0	3.0	3.5	3.0	M3.0 V
J22300+488 AB	5.0	5.0	4.0	3.5	4.5	4.0	M4.5 V
J22386+567	M4 III	Gar89, Kir91	M III
J22387+252	M3.5 V	Reid04	3.5	3.5	3.0	3.0	3.5	3.5	M3.5 V
J22396-125	M3.0 V	PMSU	3.0	3.0	3.5	3.5	3.0	3.0	M3.0 V
J22415+260	M3.0 V	Riaz06	3.5	3.5	3.5	3.0	3.5	3.5	M3.5 V
J22437+192	M3.0 V	Reid07	3.0	2.5	3.0	3.0	2.5	3.0	M3.0 V
J22476+184	M3.5 V	Reid04	2.5	2.5	3.0	3.0	2.5	3.0	M2.5 V
J22489+183	M4.0 V	Abe14	4.0	4.5	4.5	4.0	4.5	4.5	M4.5 V
J22509+499	4.0	4.0	4.5	4.5	4.0	4.5	M4.0 V
J22524+099 AB	M3.0 V	PMSU	3.0	3.0	3.0	3.0	3.0	3.0	M3.0 V
J22526+750	4.5	4.5	4.5	4.5	5.0	4.5	M4.5 V
J22582-110	M2.5 V	Reid07	2.5	2.5	3.5	3.5	3.0	3.5	M2.5 V
J22588+690	m:	Simbad	3.0	3.0	3.5	3.5	3.0	3.5	M3.0 V
J23006+036	3.0	3.0	3.0	3.0	3.0	3.0	M3.0 V
J23028+436	M4.0 V	Reid07	4.0	4.5	4.5	4.0	4.0	4.5	M4.0 V
J23036-072	k:	Simbad	2.5	2.5	3.0	3.0	3.0	3.0	M2.5 V
J23036+097	3.5	3.0	3.5	3.0	3.5	3.5	M3.5 V
J23051+519	3.5	3.0	3.5	3.5	3.5	4.0	M3.5 V
J23051+452	3.5	3.5	4.0	3.5	3.5	4.0	M3.5 V

Table A.3. Spectral types of observed stars (cont.).

Karmn	Sp. type biblio.	Ref. ^a	Sp. type			Sp. type			Sp. type adopted
			Best-fit	χ^2	TiO2	TiO5	PC1	VO-7912	
J23070+094	M1 III	JM53, Kir91	M III
J23177+490	M2 III	Gar89, SB06	M III
J23182+795	m:	Simbad	3.0	3.0	3.0	3.0	3.0	2.5	M3.0 V
J23194+790	M4.0 V	Lep13	3.5	3.5	4.0	3.5	4.0	3.5	M3.5 V
J23209-017 AB	M4.0 V+m4.0:	Riaz06, Dae07	4.0	4.0	4.0	3.5	4.0	3.5	M4.0 V
J23220+569	2.5	3.0	3.5	3.5	3.0	3.0	M3.0 V
J23228+787	m5.0	Law08	4.5	4.5	6.0	6.0	4.5	5.5	M5.0:V
J23235+457	K8 V	Simbad	-4.0	<-3.0	<K5 V
J23261+170 AB	M4.5	Reid07	4.0	4.5	4.0	4.0	4.0	4.0	M4.0 V
J23266+453	M3.5 III	Bid85	M III
J23306+466	M3 V	Bid85	1.5	1.5	2.0	2.0	2.0	2.0	M2.0 V
J23317-064	M4.5 V	Reid07	4.5	4.5	4.0	4.0	5.0	4.5	M4.5 V
J23376+163	M5.5 V	Sch05	5.5	5.5	5.5	5.5	5.5	5.5	M5.5 V
J23416-065	4.5	4.5	4.5	4.5	4.5	4.5	M4.5 V
J23417-059 AB	M3.0 V	New14	3.5	3.5	3.5	3.5	3.5	3.5	M3.5 V
J23419+441	M5.0 V	PMSU	5.0	5.0	5.0	5.0	5.0	5.0	M5.0 V
J23423+349	4.0	4.0	4.0	4.0	4.0	4.0	M4.0 V
J23425+392	0.0	0.0	-0.5	-0.5	0.0	0.0	M0.0 V
J23438+610	k:	Simbad	3.0	3.0	3.5	3.5	2.5	3.0	M3.0 V
J23490-086	M2.5 V	Reid04	2.0	2.0	2.0	2.5	2.0	2.0	M2.0 V
J23559-133	M3.0 V	Sch05	3.5	3.5	4.0	3.5	3.5	4.0	M3.5 V
J23560+150	2.5	2.5	2.5	2.5	2.5	2.5	M2.5 V
J23569+230	K7 V	Ste86	1.5	1.0	1.5	1.5	1.5	1.0	M1.5 V
J23585+242	K7 V	Lee84	-1.0	-1.0	-1.0	-1.0	-1.0	-0.5	K7 V
J23590+208	2.5	2.0	3.0	3.0	2.5	3.0	M2.5 V